Analysis and exploitation of non-linearities in passive RFID UHF systems

Gianfranco Andia Vera

UNIVERSITÉ DE GRENOBLE

THÈSE

Pour obtenir le grade de

DOCTEUR DE L'UNIVERSITÉ DE GRENOBLE

Spécialité : **Optique et Radiofréquences**

Arrêté ministériel : 7 août 2006

Présentée par

Gianfranco ANDIA VERA

Thèse dirigée par **Smail TEDJINI** et
codirigée par **Yvan DUROC**

préparée au sein du **Laboratoire LCIS**
dans **l'École Doctorale EEATS**

Analyse et Exploitation des Non Linéarités dans les Systèmes RFID UHF Passifs

Thèse soutenue publiquement le **20 Novembre 2014**
devant le jury composé de :

M. Jean-Marc LAHEURTE
Pr. Université de Marne La Vallée, Rapporteur et Président du jury
M. Cyril LUXEY
Pr. Université de Nice Sophia Antipolis, Rapporteur
M. Apostolos GEORGIADIS
Dr. Senior Researcher at CTTC Research center – Barcelone, Epagne, Examinateur
M. Pavel NIKITIN
Dr. Senior Researcher at INTERMEC – Seattle, USA, Examinateur
M. Christophe LOUSSERT
Vice-Président de Tagsys RFID, Examinateur
M. Yvan DUROC
Pr. Université Claude Bernard Lyon 1, Co-directeur
M. Smail TEDJINI
Pr. Grenoble-INP, Directeur

Acknowledgements

This thesis would never become a reality without the help and support of people surrounding me, both at work and in private. I would like to express my sincere gratitude to:

Prof. Smail Tedjini, my thesis director, for giving me the opportunity to join the LCIS. His perspective and support helped on the success of this project.

Prof. Yvan Duroc, my thesis co-director, for his valuable and constructive suggestions during the development of this thesis. Besides its technical and academic insights, I would like to express my gratitude to his generosity and amicable friendship.

Prof. Jean-Marc Laheurte, Université de Marne La Vallée, and Prof. Cyril Luxey, Université de Nice Sophia Antipolis, for accepting to review my thesis.

Dr. Apostolos Georgiadis from CTTC-Barcelona, my master thesis advisor, for showing me the paths and giving me the tools to discover the research world.

Dr. Pavel Nikitin, Intermec-Seattle, for accepting be part of the tribunal and for having made such a long trip. Thanks for his valuable insights and his enormous kindness. I won't ever forget the pleasant and friendly talks we had in Valence la ville de la fréquence.

All the friends from Tagsys RFID for their cooperation and contribution. Special thanks to: Ing. Marc Recouly for his professional support and constructive suggestions; M. Christophe Loussert for his kindness and who with I always had pleasant talks.

Ing. Christophe Medina from RFTLab for his kindness, disposability and enthusiastic mood when I needed to use its facilities to perform some measurements.

All my colleagues from LCIS and ESISAR for creating a pleasant working environment. Special thanks to Jennyfer Douverville, Carole Seyvet and Florence Galli for their amicable administrative support and Cedric for the IT support.

My colleges and friends I met during this period, for the happy hours at work and after work. Special thanks to: Jennyfer, Raji, Divya, Sanaa, Raquel, Mathieu, Tsitoha, Duy, Eduardo y el capo-técnico Marco. I will always have the valuable memories with all of you.

Y por último pero no menos importante, quiero agradecer a Mira por su paciencia y a mi familia que sin su soporte, nunca hubiese llegado hasta aquí.

Gianfranco
November 2014
Valence, France

Abstract

Powered by the exploding popularity of the Internet-of-Things (IoT), the demand for tagged devices with labels capable to ensure a reliable communication with added functions beyond the identification, such as sensing, location, health-care, among others, is growing rapidly. Certainly this growing is headed by the well established Radio Frequency Identification (RFID) technology, and the use of wireless low-cost self-powered tags, in other words passive RFID tags, is the most widespread used alternative. In the constant evolution on this field, usually new software treatments are offered at the application layer with the objective to processing data to produce some new information. Further works aimed at improving the physical layer around the tag antenna miniaturization and matching techniques. So far, little or no work had been done on the exploitation of the communication channel, and certainly none has been done on the exploitation of the non-linear behavior of RFID chips.

After presenting the RFID technology and phenomena produced by Radio Frequency (RF) non-linear devices, and leaning in some nearby works on the field, the core of this thesis starts by exposing two characterization platforms for the evaluation of non-linear phenomena presented during the reader-tag communication. One is specialized in radiating measurements considering the whole tag (antenna and chip) under test. The other is specialized in conducted measurements directly over RFID chips, allowing performing different parametric studies (power dependency, impedance, harmonic production, sensitivity). The characterization results show that harmonic signals generated from the passive RFID chip carry information.

By exploiting the characterization results and to verify the hypothesis of exploitation of non-linearities in RFID, i.e. the use of harmonic signals, the research is pursued by designing, fabricating, and measuring four different configurations of RFID tags. The new RFID tags operate at the fundamental frequency in the UHF band and at its 3^{rd} harmonic in the microwave band. Antenna design policies, fabrication details, and parametric studies on the performance of the new prototypes are presented. The parametric study takes special care in the antenna structure, kind of chip used, received power, and read range.

Finally, some alternative approaches for the exploitation of non-linear effects generated by rectifying devices are presented. Some theoretical aspects and experimental results are discussed linking the passive RFID technology to the theories of Wireless Power Transfer (WPT) and Electromagnetic Energy Harvesting (EEH). The solution takes advantage of the non-linear nature of rectifying elements in order to maximize the RF-to-dc conversion efficiency of EEH devices and increase the read range of passive RFID tags. The solution triggers on the design of a RF multi-device system. The design procedure and tests consider three non-linear phenomena: (1) the impedance power dependency, (2) the harmonic production, and (3) the rectifying dependence on the RF waveform.

Résumé

Avec l'explosion de l'Internet des Objets (IoT), de nouveaux dispositifs permettant de tagguer les objets sont nécessaires afin de permettre non seulement leur identification mais aussi d'assurer des communications fiables et de nouvelles fonctionnalités comme la détection, la localisation ou la capture d'informations. Cette tendance s'appuie sur la technologie bien établie qu'est la radiofréquence par identification (RFID) et donc l'utilisation d'étiquettes (ou tags) faibles coûts et télé-alimentés. Dans ce contexte, de nombreux travaux au niveau de la couche d'application se tournent vers la mise au point de traitements logiciels complémentaires visant à produire de nouveaux types d'information. D'autres travaux visent à améliorer la couche physique avec l'objectif de miniaturiser encore le tag mais aussi de le doter de nouvelles capacités. Jusqu'à présent, il n'existe quasiment pas de travaux concernant la transmission du signal et aucun sur l'exploitation du comportement non-linéaire des puces RFID. Cette thèse vise à étudier les phénomènes non-linéaires produits lors d'une communication RFID.

Dans la première partie, deux plateformes de mesure et de caractérisation spécifiques ont été développées : la première vise à observer les signaux au cours d'une communication RFID, et alors caractériser et analyser les effets liés aux phénomènes non linéaires ; la seconde permet d'effectuer différentes mesures directement sur les puces et les caractériser en termes d'impédance, production d'harmoniques et sensibilité. Ces plateformes ont permis : 1) de mettre en évidence que les fréquences harmoniques sont porteuses d'informations qui peuvent être exploitées et même offrir de nouvelles fonctionnalités ; 2) d'obtenir de nombreuses informations sur les propriétés des puces et d'en établir un modèle électrique précis ; 3) de déterminer des critères permettant d'évaluer la performance des tags dans le contexte étudié. Dans la deuxième partie, plusieurs nouveaux tags RFID ont été conçus, fabriqués, mesurés et évalués. Ces nouveaux tags fonctionnent non seulement dans la bande UHF mais aussi sont adaptés à la troisième harmonique dans la bande des microondes. Une méthodologie et des lignes directives d'aide à la conception de ce type de tags ont été établies et s'appuient sur les deux plateformes développées afin de caractériser les différents éléments. Dans un même temps, les effets liés à la fabrication ont aussi été étudiés et des études paramétriques ont permis de mettre en évidence l'effet sur les performances de la géométrie de l'antenne et du type de puce utilisée. Dans une troisième partie, les études se sont focalisées à exploiter les effets non-linéaires des dispositifs de redressement. L'idée générale est de coupler la RFID passive avec les dispositifs de transferts de puissance et de récupération d'énergie avec pour objectifs 1) de maximiser l'efficacité de conversion RF - continu 2) et d'augmenter la distance de lecture des tags passifs. Plusieurs prototypes ont été réalisés et leurs performances ont été démontrées.

L'ensemble de ces travaux a mis en évidence un nouveau concept de communication RFID exploitant les non-linéarités générées par les puces RFID. Ce concept ouvre la voie à de nouvelles applications et a fait l'objet d'un brevet international.

Printed in France, Valence 2014

A mi familia

Contents

List of Figures

List of Tables

Résumé étendu en français

1. Introduction

Depuis le début des années 2000, la filière industrielle autour de la RFID (Radio Frequency IDentification, en français dite radio-identification) a reçu un très fort soutien financier car le marché semblait exister grâce au code barre qui devait être remplacé par une RFID à très faible coût. Cette idée s'est cependant avérée fausse et la filière RFID s'est alors fragmentée en se consacrant à des marchés différents comme le contrôle d'accès, les passeports électroniques, la gestion d'inventaire et la sécurité. Dans un contexte économique difficile, les acteurs industriels de la RFID cherchent aujourd'hui plutôt à consolider leurs marchés laissant en l'état une technologie RFID UHF non aboutie et ne constituant pas un sujet prioritaire de valorisation. Le projet SPINNAKER dans lequel les travaux de cette thèse s'inscrivent vise au contraire à saisir cette opportunité. Et grâce à l'aide de l'état français (projet soutenu par un financement OSEO), ce projet a réuni huit laboratoires de recherche et quatre entreprises, acteurs reconnus du domaine, afin de casser les barrières actuelles de la technologie RFID UHF. Parmi ces acteurs, la société TAGSYS est le porteur du projet et le LCIS le pilote des partenaires académiques. Ainsi, le projet SPINNAKER vise à faire avancer significativement l'état de l'art actuel de la technologie RFID, en particulier celui de la RFID UHF Gen2 ($2^{ème}$ génération) qui reste immature mais à fort potentiel. Le programme vise à résoudre plusieurs défis majeurs du domaine et ainsi démocratiser les systèmes RFID au profit de notre quotidien ceci avec un déploiement complet amenant une économie de services nouveaux jusqu'à l'utilisateur final, et en particulier dans les secteurs de la distribution et de la santé. Le projet SPINNAKER présente ainsi pour objectifs principaux l'intégration et la miniaturisation, l'amélioration des performances en temps réel, et l'inter-connectivité des systèmes. Les enjeux sont multiples et extrêmement importants dans un contexte où la RFID joue et jouera un rôle prépondérant dans le développement du E-commerce, de la dématérialisation des entreprises, de l'ubiquité des points de ventes et de livraisons mais aussi de l'Internet des Objets (IoT, Internet of Things). Le sujet de la thèse présentée ici relève de l'une des tâches majeures identifiées dans ce projet et intitulée "$N^{ième}$ harmonique".

L'idée générale est d'exploiter le comportement non-linéaire des puces RFID passives ce qui constitue une idée nouvelle et encore jamais abordée dans la littérature. Dans un premier temps, l'objectif est de démontrer le potentiel de cette approche, et dans un second temps d'imaginer de nouveaux concepts et applications possibles. L'idée proposée est particulièrement originale parce que traditionnellement en ingénierie radiofréquence (RF) le type de non-linéarité ici exploité est souvent vu comme source de signaux parasites ou d'interférences qu'il faut éliminer ou au moins limiter. Au contraire comme les sections qui suivent vont le montrer, la non-linéarité générée par les puces RFID peut être source d'information et/ou source d'énergie.

En particulier, c'est l'exploitation de la $3^{ème}$ harmonique qui est mise en évidence et ouvre la voie à de nouvelles fonctionnalités et de nouvelles applications jusqu'à présent difficiles voire impossibles à réaliser.

L'objectif principal de cette thèse est donc de démontrer la possibilité d'exploiter les effets non-linéaires du tag se manifestant lors d'une communication en RFID passive. Les études proposées couvrent à la fois des aspects analytiques relatifs à la théorie du signal et des circuits micro-ondes ainsi que des aspects pratiques en s'appuyant sur des simulations, avec pour but de mettre en évidence les concepts proposés mais aussi en évaluer la performance. Pour cela, ces études s'appuient sur de la mesure et de la caractérisation (s'étendant des propriétés des signaux mis en jeu à la mesure d'impédance de puces en fonctionnement) mais aussi de la conception et de la fabrication de prototypes de tags intégrant de nouvelles capacités ou fonctionnalités. Le concept proposé offre un nouveau champ de recherche très large avec de nombreux impacts tant en recherche fondamentale qu'en termes d'applications. Dans les travaux développés, il est important de noter que l'approche suivie vise à respecter la règlementation actuelle (EPC global classe 1 Gen2) et aussi à maintenir autant que possible une faible complexité du tag.

Les sections qui suivent s'articulent de la façon suivante. La section 2 dresse un rapide état de l'art de la RFID UHF passive et de l'usage de dispositifs non-linéaires en RF, en particulier dans le domaine de la RFID. La section 3 présente les deux nouvelles plateformes de caractérisation qui ont été développées : l'une pour analyser les effets du comportement non-linéaire des puces RFID lors d'une communication RFID, l'autre pour caractériser précisément le comportement non-linéaire au sein de la puce elle-même. La section 4 vise à démontrer que la non-linéarité des puces RFID peut être exploitée avec bénéfice : 1) pour obtenir une source d'informations redondantes, constituant un nouveau canal de communication tag-lecteur ; 2) pour obtenir une source d'énergie complémentaire, constituant un nouveau moyen de récupération d'énergie électromagnétique. Dans cette section, plusieurs prototypes de nouveaux types de tags sont introduits en soulignant notamment d'une part la méthodologie de conception (qui s'appuie notamment sur les plateformes de caractérisation introduites), et d'autre part les performances obtenues. Enfin la section 5 conclut sur les études menées en soulignant les principales contributions de cette thèse et leurs nombreuses perspectives.

2. Etat de l'art

2.1 RFID UHF passive et non-linéarité

Dans un système RFID UHF passif EPCglobal classe 1 Gen-2, le tag ne contient pas de source d'énergie autonome comme une batterie, mais il est télé-alimenté via le champ électromagnétique du lecteur. Le principe de fonctionnement général d'un système RFID UHF passif est le suivant et est illustré par la figure 1[1]. 1) le lecteur génère une onde porteuse qui est transmise par son antenne. Les antennes des lecteurs sont généralement directives, à savoir, qu'elles rayonnent seulement dans un certain espace, la zone dite de lecture. 2) Si un tag est à l'intérieur de cette zone de lecture, la puissance transmise par le lecteur active ce tag et il est alors prêt à recevoir des commandes. 3) Lors de la réception d'une commande du lecteur, qui est transmise via la modulation de l'onde porteuse, le tag envoie son code d'identification ou une partie de sa mémoire. Le tag n'émet pas ces données de façon active, mais réfléchit une partie de l'onde porteuse du lecteur incident en désaccordant délibérément son adaptation d'impédance avec l'antenne. Ce principe est connu en tant que modulation par rétrodiffusion.

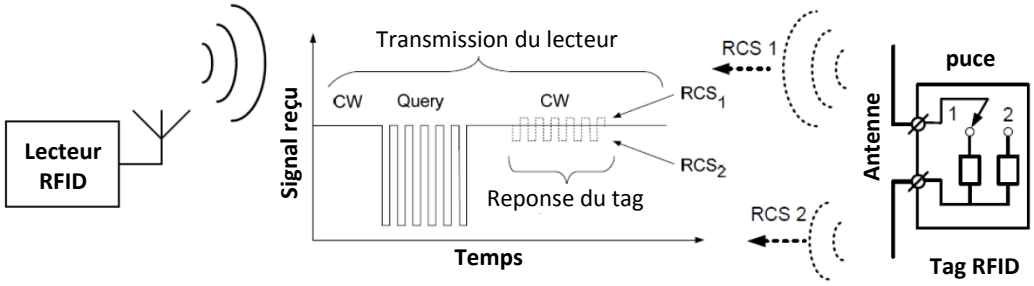

Figure 1: Principe de fonctionnement d'un système RFID UHF passif.

Selon les applications, que ce soient dans les domaines de l'optique, de l'acoustique ou de l'électronique, la distorsion introduite par une non-linéarité peut être vue comme un phénomène à combattre (onduleurs, oscillateurs, amplificateurs, filtres, etc.) mais aussi peut être considérée comme un moyen pour générer des composantes fréquentielles non présentes dans l'excitation,

[1]P.V. NIKITIN AND K.V.S. RAO. Theory and Measurement of Backscattering from RFID Tags. Antennas and Propagation Magazine, IEEE, 48(6), pages 212 – 218, dec. 2006

qui sont soit des harmoniques soit des combinaisons des fréquences d'origine (mélangeurs, modulateurs, démodulateurs, doubleurs de fréquence), ou bien pour réaliser une détection (démodulateurs non cohérents).

Dans le domaine de la RFID, l'étude des aspects non-linéaires avec notamment la génération d'harmoniques et la distorsion d'intermodulation n'est pas un sujet nouveau même si relativement peu abordé. Nikitin & al [1] ont montré pour la première fois en 2009 l'existence d'harmoniques rétrodiffusées par le tag. Plusieurs articles se sont aussi intéressés à étudier les effets non-linéaires générés par la puce, et plus particulièrement par son dispositif de redressement RF-continu. Les objectifs étaient alors soit d'obtenir un modèle plus général (champ proche et champ lointain) et plus précis des interactions lecteur-tag [2], soit d'établir à partir d'un modèle électrique des directives de conception du tag pour atténuer les harmoniques générées [3]. Dans ces différents travaux, il n'est pas question d'exploiter la non-linéarité mais de la mettre en évidence et mieux la combattre. Une seule étude à notre connaissance exploite la non-linéarité mais d'une façon détournée qui n'exploite pas la non-linéarité intrinsèque des tags. Gomes & al [4] proposent en effet d'utiliser une diode Schottky comme source non linéaire au niveau du tag afin de délivrer une nouvelle fréquence à partir de la combinaison de deux fréquences émises. Ce signal de fréquence nouvelle est alors exploité au niveau du lecteur pour déterminer le retard entre onde transmise et onde reçue, et en déduire ainsi la distance lecteur-tag. La mesure du retard s'appuie sur l'utilisation classique d'une séquence pseudo-aléatoire associée à une intercorrélation.

La non-linéarité générée par les puces RFID est donc un phénomène connu, qui a été caractérisé et qui a été modélisé sous certaines conditions, avec pour objectifs une meilleure connaissance du lien radio RFID et surtout la volonté d'atténuer au maximum les harmoniques associées. Par ailleurs, il est intéressant de noter que des approches relativement similaires en termes de modélisation peuvent se trouver dans des études qui s'intéressent à la récupération d'énergie par l'utilisation de diodes de redressement, dispositifs non-linéaires par nature, avec pour objectifs de maximiser l'efficacité de conversion RF-continu des systèmes de transfert d'énergie sans fil [5].

En résumé, l'idée d'étudier la non-linéarité générée par les puces RFID avec pour objectif d'en tirer profit est totalement nouvelle mais reste à démontrer. D'autre part, l'étude bibliographique suggère qu'il y aurait des opportunités intéressantes en associant certains des travaux portant sur la RFID, la récupération d'énergie électromagnétique et les systèmes de transfert d'énergie sans fil.

---

[1] P.V. NIKITIN, K. V. S. RAO, INTERMEC TECHNOLOGIES CORPORATION. Harmonic Scattering From Passive UHF RFID Tags. pages 222 – 225, 2009

[2] J.C. BOLOMEY, S. CAPDEVILA, L. JOFRE, J. ROMEU. Electromagnetic Modeling of RFID-Modulated Scattering Mechanism. Application to Tag Performance Evaluation. Proceedings of the IEEE, 98(9), pages 1555 – 1569, 2010.

[3] G. DE VITA AND G. IANNACCONE. Design criteria for the RF section of UHF and microwave passive RFID transponders. Microwave Theory and Techniques, IEEE Transactions on, 53(9), pages 2978 – 2990, 2005.

[4] H. C. GOMES, N. BORGES CARVALHO. RFID for Location Proposes based on the intermodulation distortion. Sensors and Transducers Journal, 106(7), pages 85 – 96, 2009.

[5] S. LADAN, K. WU. 35 GHz Harmonic Harvesting Rectifier for Wireless Power Transmission. In Microwave Symposium Digest (MTT), 2014 IEEE MTT-S International, pages 1 – 3, 2014.

3. Plateformes de caractérisation des non-linéarités en RFID UHF passive

Comme l'illustre l'état de l'art, la première étape à réaliser était d'abord de déterminer un moyen pour mettre en évidence les effets des non-linéarités produites par les puces RFID. La première plateforme développée visait cet objectif et s'est focalisée à illustrer les propriétés des signaux mis en jeu lors d'une communication RFID en fonction de différents paramètres, et en testant plusieurs types de tags et notamment des tas commerciaux différents. La seconde plateforme mis en place s'est focalisée sur la source même des non-linéarités, c'est-à-dire la puce du tag, avec pour objectif de la caractériser de façon très précise.

3.1 Effet des non-linéarités sur les propriétés des signaux mis en jeu lors d'une communication RFID

3.1.1 Description de la plateforme

La plateforme de caractérisation illustrée par la figure 2 s'appuie sur une configuration bi-statique en chambre anéchoïque. Une communication RFID type lecteur-tag est établie à l'aide d'un générateur de signaux arbitraires simulant le comportement d'un lecteur (ou d'un lecteur RFID du commerce) qui émet sur l'une des antennes. Un oscilloscope numérique rapide est connecté en réception sur la seconde antenne permettant une analyse dans le domaine temporel et dans le domaine fréquentiel du signal rétrodiffusé. Les signaux reçus sont le signal émis atténué (isolation de 48 dB) et la réponse du tag (si présent). L'ensemble est piloté par un ordinateur qui permet de configurer les signaux délivrés par le générateur et de traiter les données.

Afin d'obtenir des résultats à la fois significatifs et répétitifs, la couche physique du protocole RFID est configurée de telle sorte que la réponse renvoyée par le tag comporte une séquence de bits périodique de type 0101010...01. De plus, pour pouvoir quantifier et comparer les différents résultats obtenus le niveau de puissance du premier lobe secondaire présent dans la densité spectrale de puissance (DSP) du signal retourné par le tag est considéré. Les lobes secondaires autour de la porteuse attestent de la présence de l'information modulée et leur hauteur est liée à la profondeur de modulation qui dépend notamment de la différence d'adaptation entre les deux charges commutées.

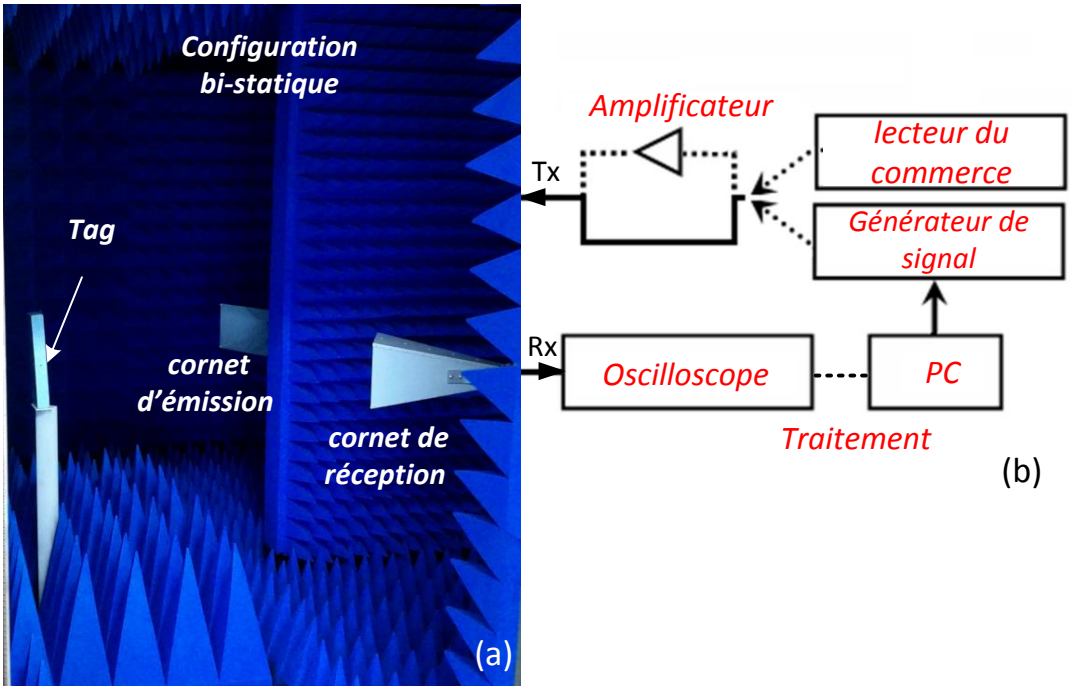

Figure 2: Plateforme de caractérisation de la réponse du tag.

3.1.2 Résultats obtenus

Les figures 3, 4 et 5 illustrent la DSP obtenue respectivement autour de la fréquence fondamentale (à 915 MHz), de la $2^{ème}$ et de la $3^{ème}$ harmonique en présence ou non d'un tag (tag commercial présenté ci-dessous et nommé T5) pour une puissance d'émission égale à $15,6$ dBm. Même si les niveaux de puissance sont faibles, il apparaît clairement que la $3^{ème}$ harmonique porte une information détectable (présence de raies autour de la fréquence porteuse à $2745\,MHz = 3 \times 915\,MHz$) et redondante puisque portée par la fréquence fondamentale. Pour cet exemple, la $2^{ème}$ harmonique ne semble pas porter d'information et si c'est le cas les raies sont noyées dans le bruit. La table 1 présente les niveaux de DSP du premier lobe secondaire

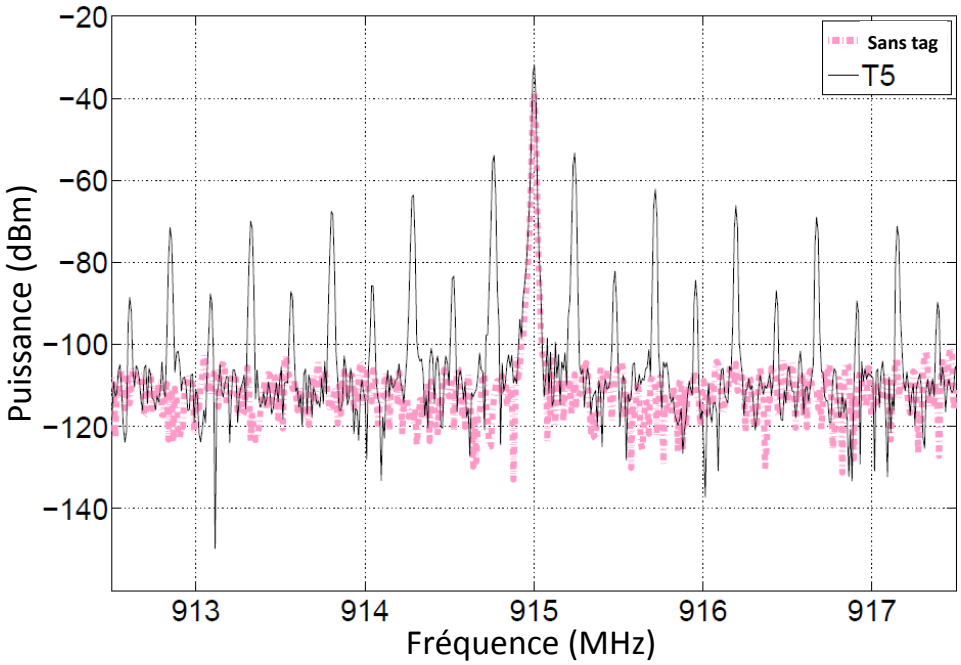

Figure 3: DSP du signal reçu à la fréquence fondamentale quand $P_{out} = 15.6$ dBm avec ou sans tag T5.

obtenus sur la $2^{ème}$ et la $3^{ème}$ harmonique, et tenant compte de la sensibilité de chaque tag, cela pour neuf tags du commerce dont les caractéristiques sont succinctement présentées. Chacun des tags testés confirme que l'information est portée par la $3^{ème}$ harmonique ; le tag T5 montrant le plus haut niveau de la DSP du lobe secondaire. Pour la $2^{ème}$ harmonique, l'information semble aussi présente mais se retrouve dans la plupart des cas noyée dans le bruit (niveau de puissance inférieur à environ - 105 dBm). Cependant dans le cas des tags T1, T2, T4 et T9 les lobes d'information sont clairement présents.

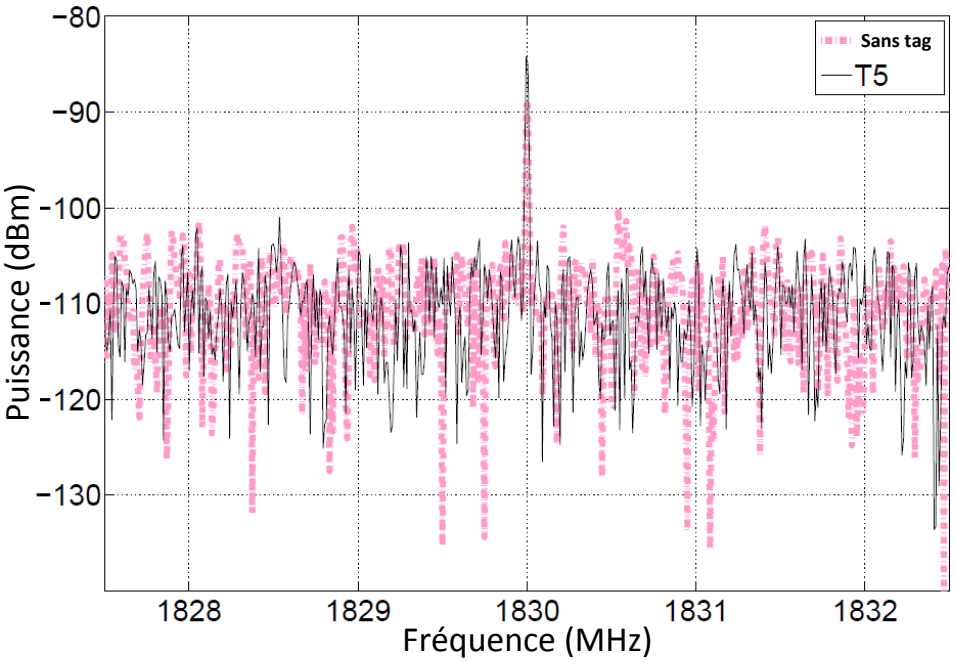

Figure 4: DSP du signal reçu à la 2ème harmonique quand $P_{out} = 15.6$ dBm avec ou sans tag T5.

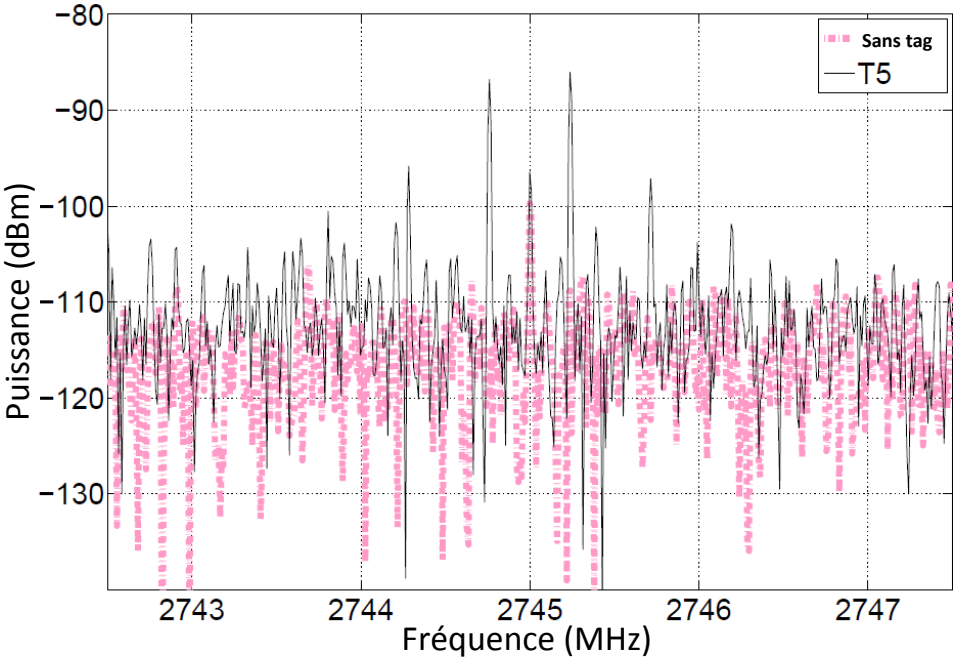

Figure 5: DSP du signal reçu à la 3ème harmonique quand $P_{out} = 15.6$ dBm avec ou sans tag T5.

Table 1: Harmoniques rétrodiffusées par le tag.

Nom	Inlay / fabricant	Sensibilité (dBm)	Zone d'opération	$2^{ème}$ harm. (dBm)	$3^{ème}$ harm. (dBm)
T1	Dogbone / UPM	-16.89	US	-98.11	-104.1
T2	Sec.Frog / UPM	-12.93	EU	-98.29	-95.08
T3	Web / UPM	-11.73	EU	-102.9	-98
T4	P9-2 / LCIS	-11.29	US	-99	-94.72
T5	MemoryStick / UPM	-12.29	US	-106	-86.03
T6	P10-1 / LCIS	-13.63	EU	-100	-92.08
T7	RapidTrack / Tagsys	-13.43	EU	-104.7	-104.5
T8	Tac.Frog / UPM	-13.15	US	-102.4	-98.24
T9	AD222 / Avery Dennison	-11.79	US	-98.39	-93.34

3.1.3 Bilan

La plateforme mis en place et la campagne de mesures effectuée montrent que l'information retournée par le tag est présente non seulement sur la fréquence fondamentale mais aussi sur les harmoniques, et notamment sur la $3^{ème}$ avec des niveaux de puissance certes faibles mais qui pourraient être détectés. Cette étude permet de valider le concept initial d'exploitation possible des harmoniques en RFID UHF passive au moins pour constituer un second canal support d'information.

3.2 Caractérisation des puces RFID tenant compte des non-linéarités

3.2.1 Description de la plateforme

Avec pour objectif de caractériser plus pleinement le phénomène de non-linéarité observé, une seconde plateforme de caractérisation a été développée se focalisant sur la puce seule. Cette plateforme assemble et étend les travaux développés par Nikitin & al [1] et Lucas & al [2]. Elle permet en mode fonctionnel (puce activée) de mesurer les puissances d'activation, les niveaux de puissance sur les harmoniques et les impédances sur une large gamme de fréquences s'étendant du fondamental jusqu'à la $4^{ème}$ harmonique. La figure 6 illustre la configuration de la plateforme développée et la figure 7 en présente une photographie. Deux parties sont soulignées : l'une est un émulateur d'impédance de l'antenne, et l'autre est nommée testeur RFID.

[1] P.V. NIKITIN, K.V.S. RAO, R. MARTINEZ, S.F. LAM. Sensitivity and Impedance Measurements of UHF RFID Chips. Microwave Theory and Techniques, IEEE Transactions on, 57(5), pages 1297 – 1302, 2009.

[2] L. W. MAYER, A. L. SCHOLTZ, Sensitivity and Impedance Measurements on UHF RFID Transponder Chips. Int EURASIP Workshop on RFID Techn, pages 1 – 10, 2007.

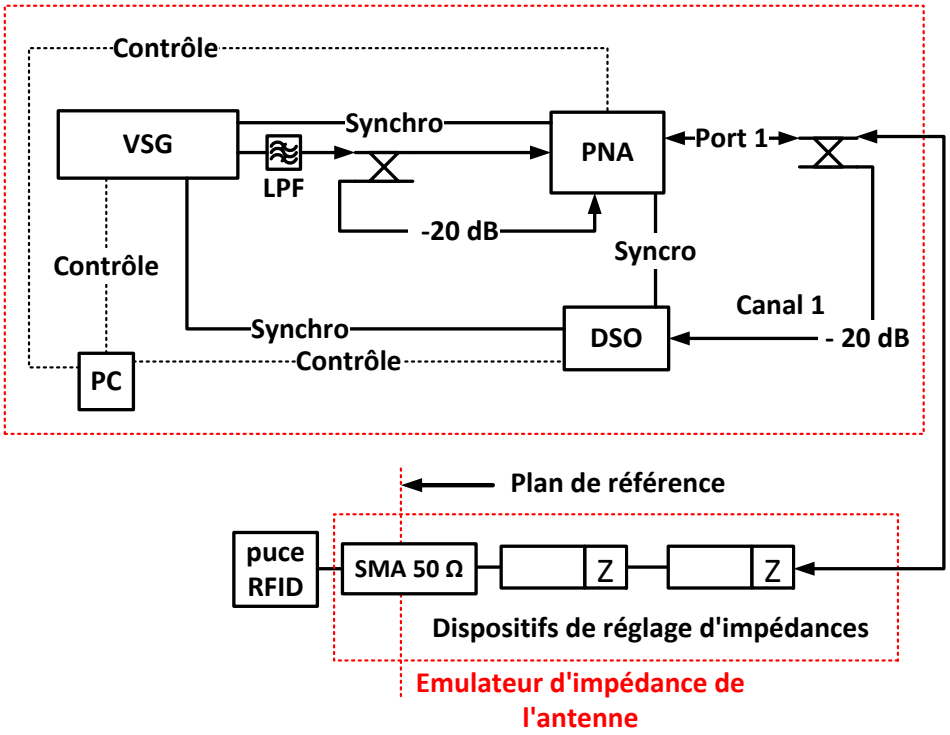

Figure 6: Plateforme de caractérisation et d'analyse du comportement non-linéaire de puces RFID.

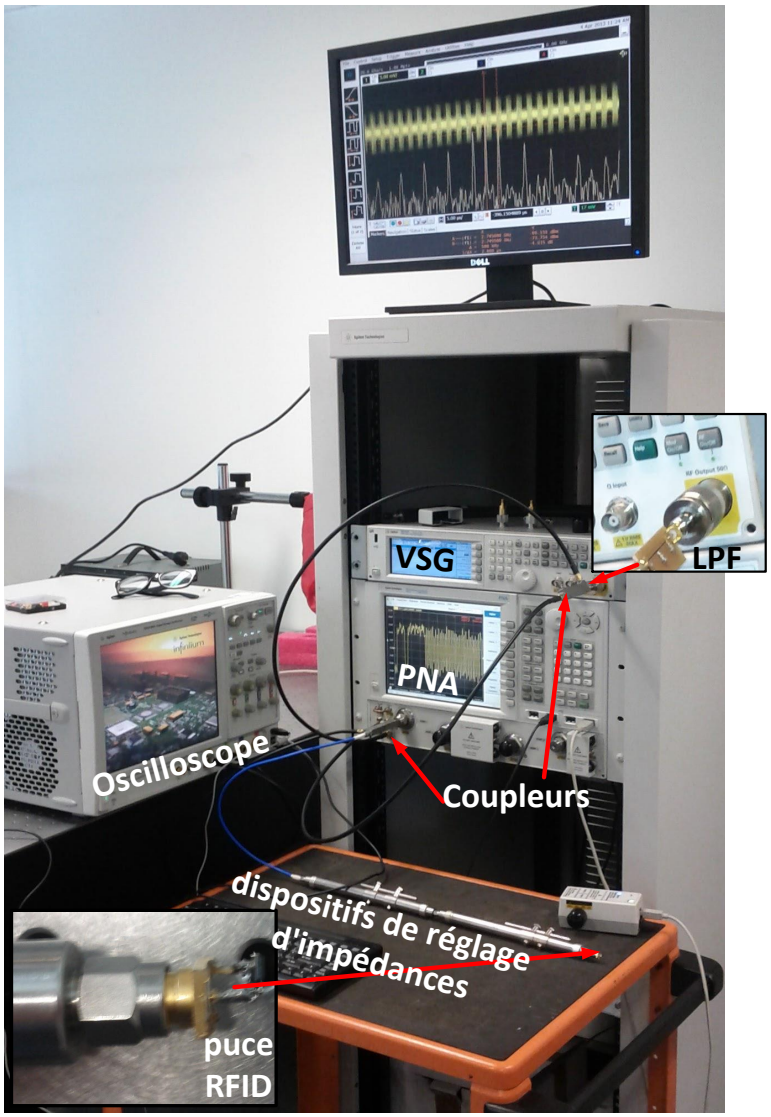

Figure 7: Photographie de la plateforme de caractérisation des puces RFID.

L'émulateur d'impédance de l'antenne est constitué de deux dispositifs de réglage d'impédances Microlab SF-30F connectés en série qui permettent de réaliser l'adaptation entre le testeur RFID 50 Ω et la puce sous test qui activée va commuter entre ses deux états de modulation. Le testeur RFID est constitué de différents éléments :

- un générateur vectoriel de signaux (VSG, Vector Signal Generator) joue le rôle du lecteur générant et envoyant les commandes ;
- un filtre passe-bas (LPF, Low Pass Filter) connecté en sortie RF du générateur permet de filtrer les harmoniques émises de façon à assurer que les harmoniques observées sont seulement dues à la puce sous test ;
- un analyseur de réseaux programmable (PNA, Programmable Network Analyzer) permet de déterminer les deux impédances (résistance et réactance : caractérisation vectorielle) de la puce sous test en fonction du temps et à la fréquence d'intérêt ;
- un oscilloscope numérique rapide permet de visualiser la réponse de la puce dans les domaines temporels et fréquentiels ;
- deux coupleurs directionnels de type C123E-20 ATM 20 dB sont utilisés pour connecter les différents éléments ;
- l'ensemble est piloté par un PC via un programme Matlab qui permet de gérer la puissance de sortie, les fréquences, les synchronisations, et d'acquérir les données.

Les puces RFID testées sont connectées à des connecteurs SMA. La figure 8 (a) montre les trois puces testées (" chip 1 " : G2XM NXP SOT505-1 ; " chip 2 " : G2XM NXP SOT1040-AA1 " chip 3 " : Impinj Monza 5) ainsi que le kit de calibration réalisé. La figure 8 (b) montre le filtre passe-bas utilisé.

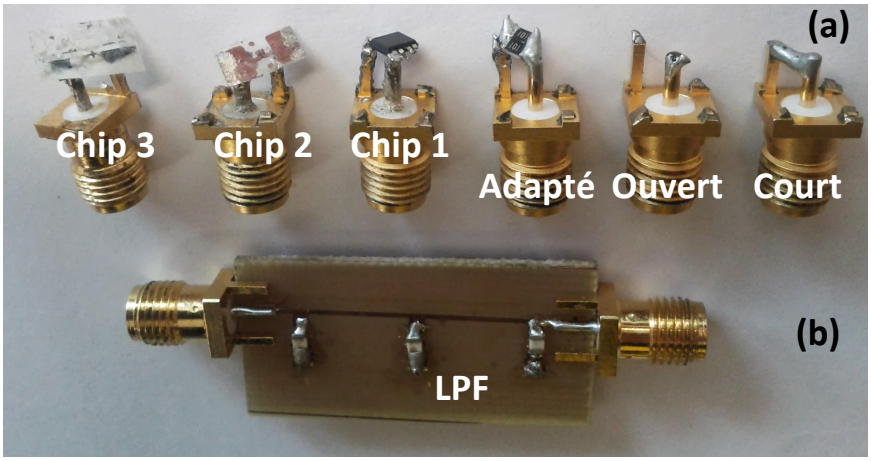

Figure 8: (a) Exemples de puces sous test et kit de calibration. (b) Filtre passe-bas filtrant les harmoniques du générateur.

3.2.2 Résultats obtenus

Relation entre puissance reçue et impédance d'entrée de la puce

Pour les deux puces "chip 1" et "chip 3", la figure 9 illustre les variations de l'impédance (résistance et réactance) d'entrée de la puce en fonction de la puissance reçue, lorsque la puce est à l'état de récupération d'énergie. Des variations significatives de la résistance et de la réactance sont observées lorsque la puissance varie et illustrent le comportement non-linéaire de la puce à travers notamment son étage de redressement. Toutefois il faut aussi remarquer qu'une fois la puce activée, pour des puissances faibles les impédances sont relativement constantes. Ce résultat est cohérent avec ce qui est attendu : performances meilleures et stables pour des puissances faibles et effet de protection aux plus hautes puissances.

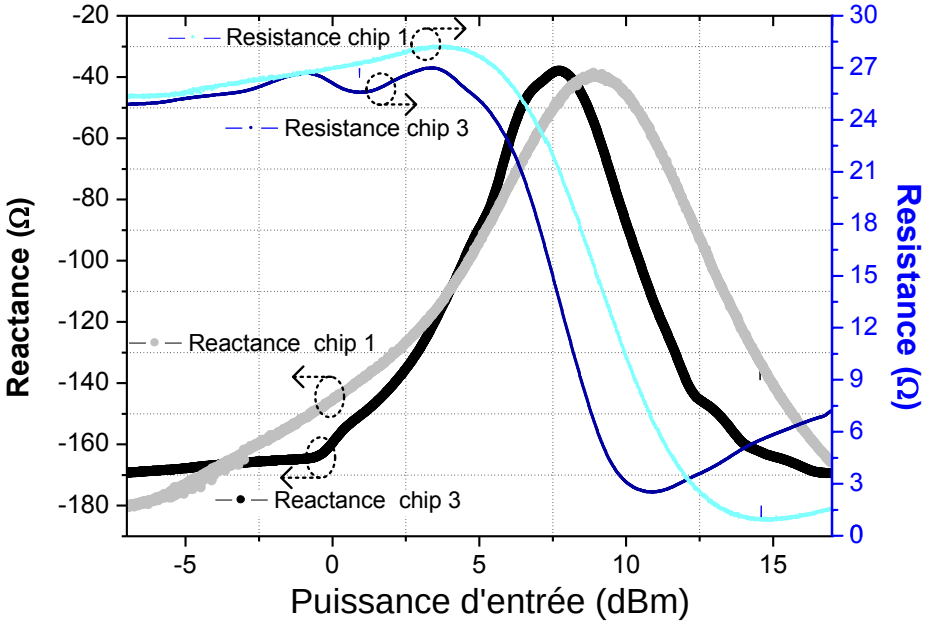

Figure 9: Impédance à l'état de récupération d'énergie en fonction de la puissance reçue pour les puces "chip 1" et "chip 3".

Réponses harmoniques

La figure 10 présente le niveau de puissance harmonique générée par la puce en fonction de la puissance d'entrée pour les trois puces, ceci de la fréquence fondamentale jusqu'à la $4^{ème}$ harmonique. Une réponse modulée est observée pour chacune des harmoniques notamment pour les puces "chip 1" et "chip 3", et d'autant plus que la puissance d'entrée devient importante. La table 2 présente les valeurs des niveaux de puissance harmonique pour les trois puces testées et tenant compte de la sensibilité de chaque puce. Pour les harmoniques, les niveaux les plus

significatifs sont observés pour l'harmonique de rang 3 ce qui est cohérent avec les résultats présentés précédemment.

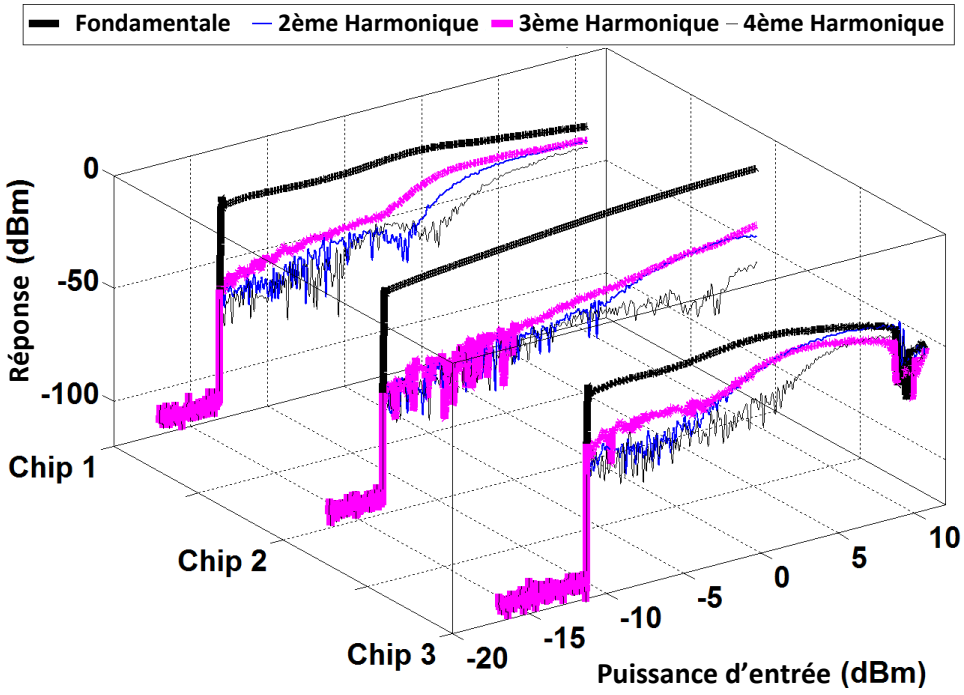

Figure 10: Niveau de puissance harmonique générée par la puce en fonction de la puissance d'entrée pour les trois puces, du fondamental jusqu'à la $4^{ème}$ harmonique.

Table 2: Harmoniques rétrodiffusées par les puces RFID passives.

Chip	**fond. (dBm)**	$2^{ème}$ **harm. (dBm)**	$3^{ème}$ **harm. (dBm)**	$4^{ème}$ **harm. (dBm)**
chip 1	-21.9	-66.7	-61.3	-76.2
chip 2	-19.9	-66.5	-61.6	-79.4
chip 3	-25.4	-60.8	-49.3	-68.5

La figure 11 illustre les impédances d'entrée (résistance et réactance) de la puce "chip 1" pour les deux états de modulation à la $3^{ème}$ harmonique. Il est notamment important de noter que la différence entre ces deux états est moins marquée que pour la fréquence fondamentale : en termes de ΔRCS (Differential Radar Cross Section), les deux états seront donc plus difficiles à discerner.

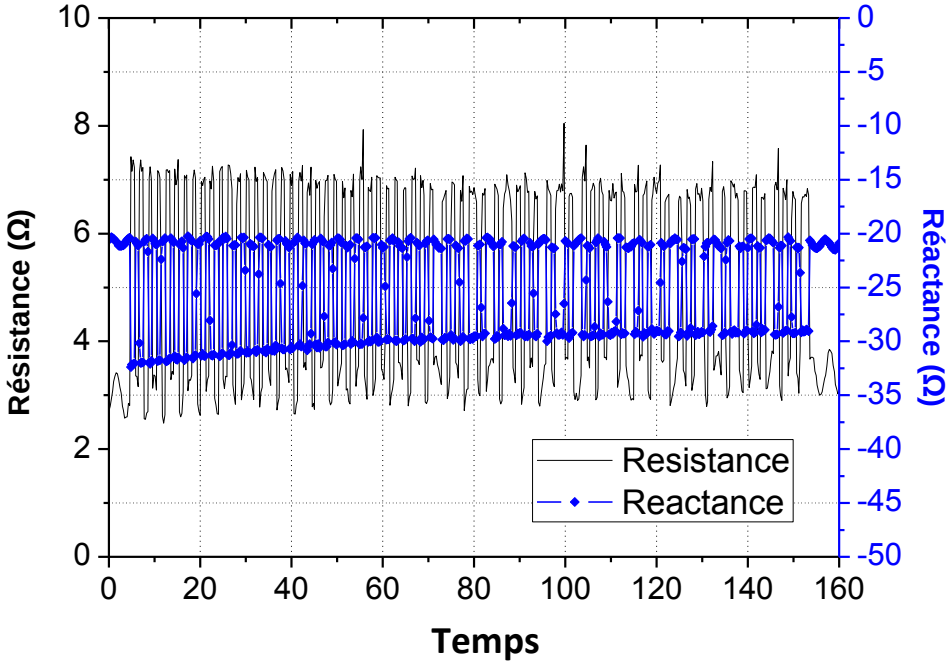

Figure 11: Impédances d'entrée de la puce "chip 1" à la $3^{ème}$ harmonique.

3.2.3 Bilan

La plateforme de caractérisation des puces qui a été développée permet de caractériser de façon très complète les puces RFID et ceci sur une large gamme de fréquences permettant de prendre en considération leur fonctionnement non-linéaire. Cette plateforme permet notamment de mesurer les impédances (résistances et réactances) des deux états de modulation des puces RFID pour différentes puissances d'activation. Les résultats présentés s'appuient sur trois types de puces mais la plateforme présentée reste plus universelle et permet de caractériser toutes sortes de puces. Enfin ces résultats renforcent encore l'idée que les non-linéarités générées par les puces pourraient être exploitées et en même temps fournissent des éléments de caractérisation très utiles pour imaginer de nouveaux types de tags, offrant de nouvelles fonctionnalités comme la section suivante va le présenter.

4. Exploitation du phénomène de non-linéarité en RFID UHF passive

Après avoir mis en évidence les effets liés aux non-linéarités des puces RFID et caractériser ce comportement non-linéaire, deux applications possibles exploitant ce phénomène de non-linéarité sont présentées : la première s'appuie sur l'idée d'obtenir un second canal porteur d'informations, informations redondantes et portées par la $3^{ème}$ harmonique ; la seconde consiste à réaliser un nouveau type de dispositif à récupération d'énergie. Dans ces deux cas, plusieurs nouveaux types de tags ont été conçus afin de démontrer les solutions envisagées et évaluer leurs performances.

4.1 Rétrodiffusion redondante en RFID UHF passive

D'après ce qui précède, il a été démontré qu'un tag du commerce renvoie une information non seulement, sur la fréquence fondamentale mais aussi ses harmoniques. Toutefois, les niveaux de puissance sur les harmoniques sont faibles et difficilement détectables même pour la $3^{ème}$ harmonique qui dans le meilleur des cas observés renvoie un niveau de puissance du premier lobe secondaire maximal égal à environ -86 dBm. L'objectif est donc de proposer de nouveaux tags, qui tout assurant leur fonction à la fréquence fondamentale avec des performances au moins égales à celles classiquement rencontrées, offrent la possibilité d'exploiter un second canal autour de la $3^{ème}$ harmonique ; autrement dit, l'objectif est de concevoir de nouvelles antennes de tags qui soient dual bande adaptées à la fréquence fondamentale et à l'harmonique de rang 3 offrant les meilleures performances possibles en termes de distance de lecture mais aussi présentant des dimensions et un coût comparables aux tags actuels du commerce.

4.1.1 Conception de tags "harmonique" dual bande

Plusieurs antennes de tags ont été conçues et sont basées sur deux types de structures : structure Yadi-Uga et structure en forme en L-F inversée, respectivement dénommées antennes HT1 et HT2 (HT signifiant Harmonic Tag). Ces structures ont été choisies car ce sont des solutions connues comme offrant des possibilités dual bande, et elles ont été modifiées pour répondre au cahier des charges énoncé. La conception de l'antenne doit prendre en compte l'impédance de la puce comme cela se fait traditionnellement. Elle s'appuie donc largement sur la plateforme de caractérisation de la puce présentée précédemment qui permet de connaître précisément les impédances à la fréquence fondamentale ainsi qu'à la $3^{ème}$ harmonique. De plus, il faut noter que

le réseau d'adaptation pour la $3^{ème}$ harmonique doit prendre en compte le caractère capacitif de la puce, ce qui permet d'utiliser les techniques d'adaptation d'impédance par boucle inductive, cas qui sont classiquement utilisés à la fréquence fondamentale.

La figure 12 présente l'un des prototypes réalisés s'appuyant sur une structure Yadi-Uda. Le résonateur à la fréquence fondamentale est un dipôle en forme de boucle qui en même temps sert d'adaptation (figure 12(b)). La structure résonante à la $3^{ème}$ harmonique est un dipôle lié à une boucle inductive permettant l'adaptation (figure 12(a)). Un réflecteur placé à l'arrière de l'antenne permet d'augmenter la directivité à la fréquence harmonique, et dans un même temps, sa position et ses dimensions permettent d'ajuster l'impédance de l'antenne (figure 12(c)). Un élément directif est placé à l'avant de l'antenne pour augmenter encore la directivité à la $3^{ème}$ harmonique (figure 12(d)).

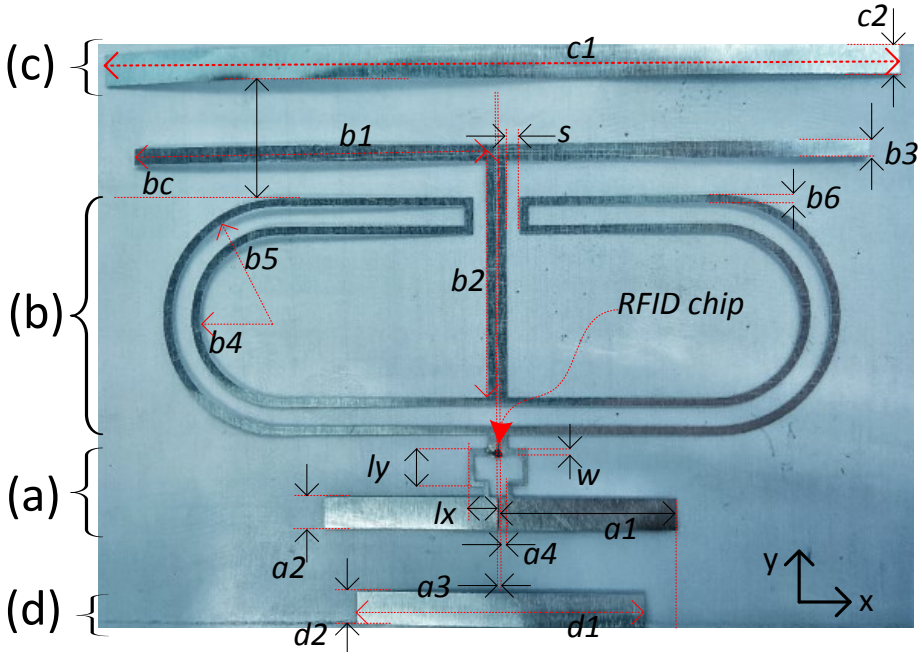

Figure 12: Prototype de tag harmonique HT1. a) résonateur à la fréquence harmonique ; b) résonateur à la fréquence fondamentale ; c) réflecteur ; d) directeur.

La figure 13 présente l'un des prototypes réalisés s'appuyant sur une structure en forme L-F inversée planaire. Les distances entre les formes L inversée et F inversée sont optimisées pour résonner aux fréquences souhaitées. De plus, les impédances capacitives vues par l'antenne à la fréquence fondamentale et son harmonique de rang 3 sont réduites en ajoutant des boucles inductives dans le plan de masse.

4.1.2 Réalisation et tests des tags HT

Les prototypes ont été réalisés sur un substrat PET (Polyethylene terephthalate) de permittivité $3,2$ et d'épaisseur $0,5$ mm. Différentes variantes ont été proposées et testées : HT1 avec ou sans

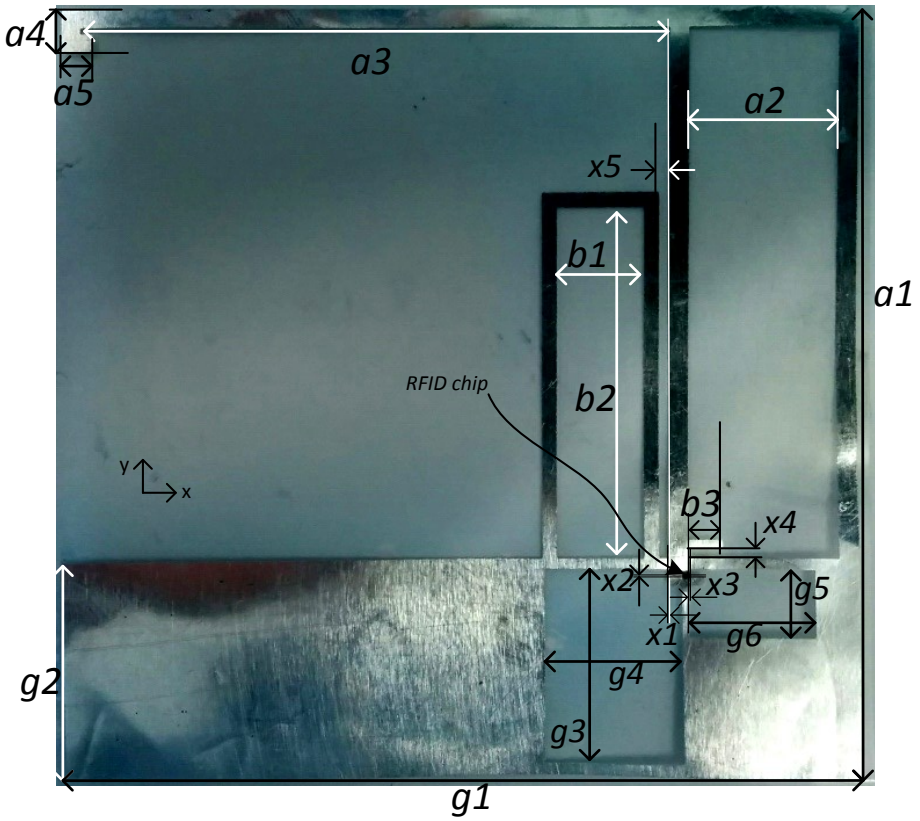

Figure 13: Prototype de tag harmonique HT2.

élément directeur, HT2 avec plusieurs types de puces différentes. Pour résumer, les figures 14 et 15 représentent les distance de lecture obtenues pour une sensibilité donnée du récepteur, et cela pour plusieurs mêmes prototypes réalisés (en parallèle, une étude de sensibilité de fabrication a aussi été réalisée ; cette étude n'est pas présentée en détail dans ce résumé ; les courbes de différentes couleur correspondent à des prototypes différents mais de même type ; les résultats les plus significatifs sont ici présentés). Pour les tags de type HT1 (figure 14), une distance de lecture supérieure à 5 mètres à la $3^{ème}$ harmonique est obtenue en faisant l'hypothèse que la sensibilité du lecteur est égale à -90 dBm (correspondant à l'ordre de grandeur du niveau de sensibilité des lecteurs RFID classiques du commerce). Dans les mêmes conditions, les tags de type HT2 présentent une distance de lecture comprise entre 3 et 4 mètres à la $3^{ème}$ harmonique (figure 15).

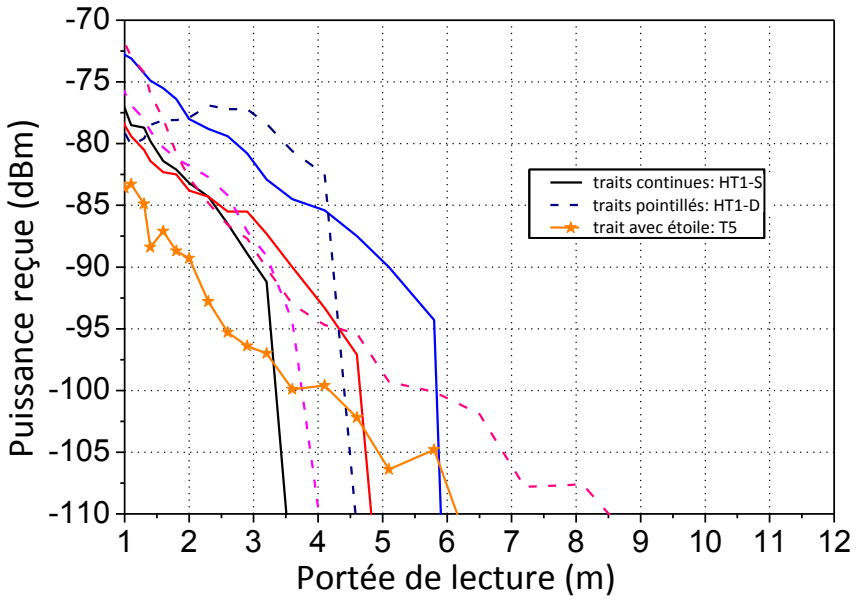

Figure 14: Distances de lecture obtenues pour tags HT1 à la $3^{ème}$ harmonique en fonction de la sensibilité du récepteur.

4.2 Source additionnelle de puissance pour les puces RFID UHF passives

Il a été démontré qu'un tag du commerce renvoie une information non seulement, sur la fréquence fondamentale mais aussi ses harmoniques. Ces harmoniques redondantes sont pris en compte dans cette nouvelle approche, cette fois en tant que "porteuses" de puissance. L'objectif est d'utiliser l'énergie perdue (et donc gaspillée) naturellement lors de la procédure de redressement comme énergie supplémentaire pour réaliser la télé-alimentation du tag passif. L'idée générale est donc de tirer parti de la nature non-linéaire des éléments de redressement afin de maximiser l'efficacité de conversion RF-continu. Il s'agit donc d'une nouvelle approche de

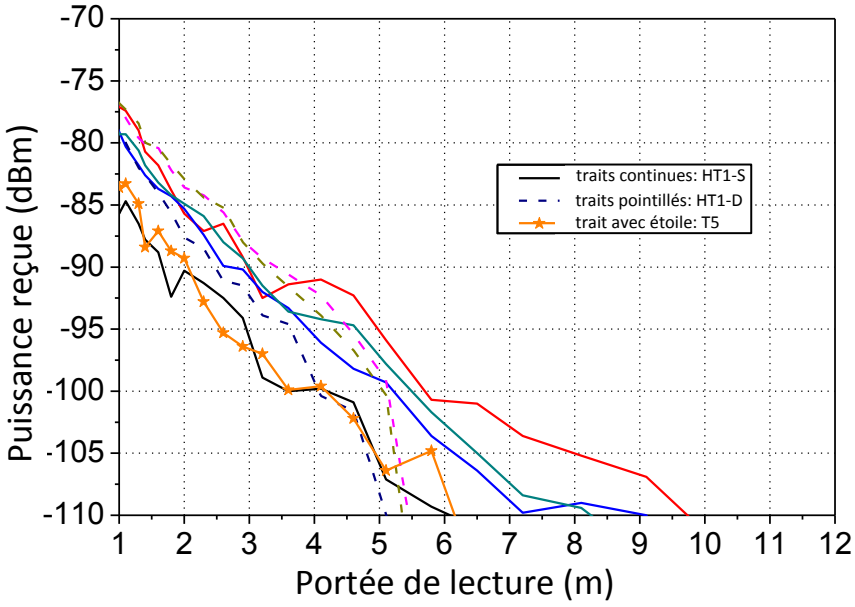

Figure 15: Distances de lecture obtenues pour tags HT2 à la $3^{ème}$ harmonique en fonction de la sensibilité du récepteur.

récupération d'énergie électromagnétique (EEH, Electromagnetic Energy Harvesting) exploitant la l'énergie provenant des harmoniques générées. Le dispositif ainsi réalisé est nommé RFID-TR (pour RFID Tag Rectenna). Une seconde approche développée consiste à réaliser un système EEH récupérant une source d'énergie RF externe au système RFID. En résumé, deux nouvelles approches sont développées :

- Système RFID-TR qui exploite une énergie RF environnante externe, dans le cas présent celle de la bande UMTS (Universal Mobile Telecommunications System) à $2,17$ GHz.
- Système RFID-TR qui réalise une auto-récupération d'énergie exploitant l'énergie produite par la puce RFID elle-même lors de son fonctionnement normal.

Pour des raisons pratiques, une puce RFID avec une entrée supplémentaire de tension continue, est utilisée car cela permet d'opérer en mode de batterie assistée (BAP).

4.2.1 Conception de dispositifs de récupération d'énergie au sein d'un tag

L'architecture complète fonctionnelle du système RFID-TR est représentée par la figure 16. Trois parties fondamentales la composent : la section de récupération d'énergie à $2,17$ GHz, la section de communication RFID et l'antenne qui est commune aux deux sections. Les deux dispositifs RFID-TR réalisés sont présentés par les figures 17 et 18. Le tag à récupération d'énergie externe illustré par la figure 17 est composé d'une antenne dual bande ainsi que d'une section EEH et d'une puce RFID reliées. Le tag à auto-récupération d'énergie illustré

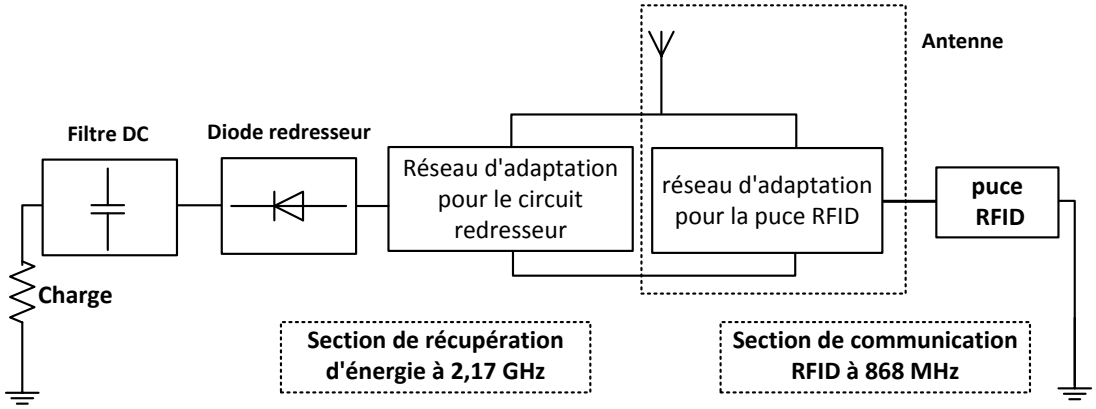

Figure 16: Schéma fonctionnel du RFID-TR proposé.

par la figure 18 est constitué d'une façon analogue mais l'antenne est mono-bande et la section EEH adaptée. Le substrat utilisé est de type Rogers RO4003 de permittivité $3,55$ et d'épaisseur $0,8$ mm. La puce RFID et les composants localisés sont soudés sur une structure spécialement conçue.

4.2.2 Tests et évaluation de performances des tags RFID-TR

Le mode BAP est activé par l'opération de rebouclage afin de réduire la sensibilité de la puce RFID. Deux configurations sont considérées pour évaluer de façon complète le fonctionnement des prototypes RFID-TR en terme de distance de lecture (table 3). Dans chaque cas, les mesures sont effectuées avec et sans rebouclage.

Table 3: Cas de configuration pour l'évaluation du RFID-TR.

Cas	Configuration de tranmission
(a)	Lecteur UHF RFID émettant à 868 MHz avec balayage en puissance
(b)	Source RF émettant à $2,17$ GHz et balayage en puissance et lecteur UHF RFID émettant à 868 MHz à puissance constante 30 dBm

Dispositif RFID-TR à récupération d'énergie environnante externe

La table 4 présente la distance de lecture maximale du dispositif RFID-TR récupérant l'énergie RF externe à $2,17$ GHz pour les cas (a) et (b); et ceci en comparant les cas où la section EEH est rebouclée ou non. Pour ces mêmes cas, la figure 19 montre les variations de distance de lecture lorsque la puissance PIRE (Puissance Isotrope Rayonnée Equivalent, en anglais EIRP, Equivalent Isotropically Radiated Power) du lecteur (notée R_{EIRP}) évolue. Ces résultats mettent

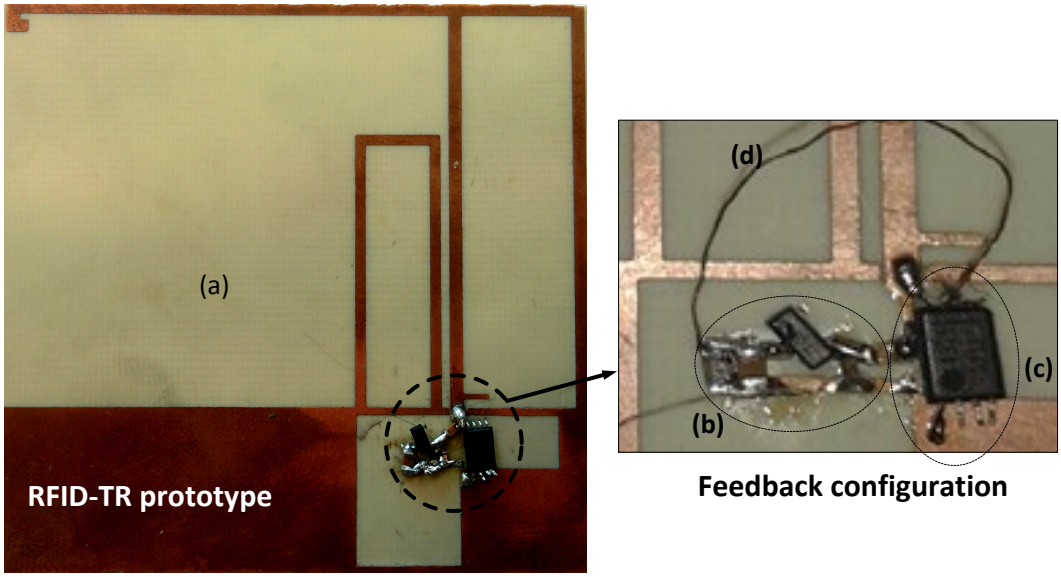

Figure 17: Prototype *RFID-TR récupérant de l'énergie RF environnante*. (a) antenne dual bande, (b) section EEH, (c) puce RFID, (d) fil de rebouclage.

clairement en évidence l'apport de la récupération d'énergie de source RF externe mis en place : portées de lecture qui augmentent et lectures du tag possibles à puissance moindre.

Table 4: Portée maximale de lecture avec et sans rebouclage de l'énergie récupérée.

Cas	Sans rebouclage (m)	Avec rebouclage (m)
(a)	3.9	5.4
(b)	3.9	6.9

Il est intéressant de noter que même sans présence de la source à $2,17$ GHz les performances sont améliorées. En fait, la section EEH bien qu'adaptée à la fréquence $2,17$ GHz permet de récupérer de l'énergie générée par les non-linéarités. Les résultats obtenus dans le cas de la configuration *(b)* sont donc aussi liées à l'effet combiné des deux sources RF (source à $2,17$ GHz et source liée aux non-linéarités).

Dispositif RFID-TR avec système d'auto-récupération d'énergie RF

Le dispositif RFID-TR à auto-récupération d'énergie est évaluée selon la configuration *(a)*. La distance de lecture maximale pour une puissance R_{EIRP} de 35 dBm est égale à 6 m. Comme dans le cas précédent, la figure 20 illustre la distance de lecture obtenue lorsque la puissance R_{EIRP}

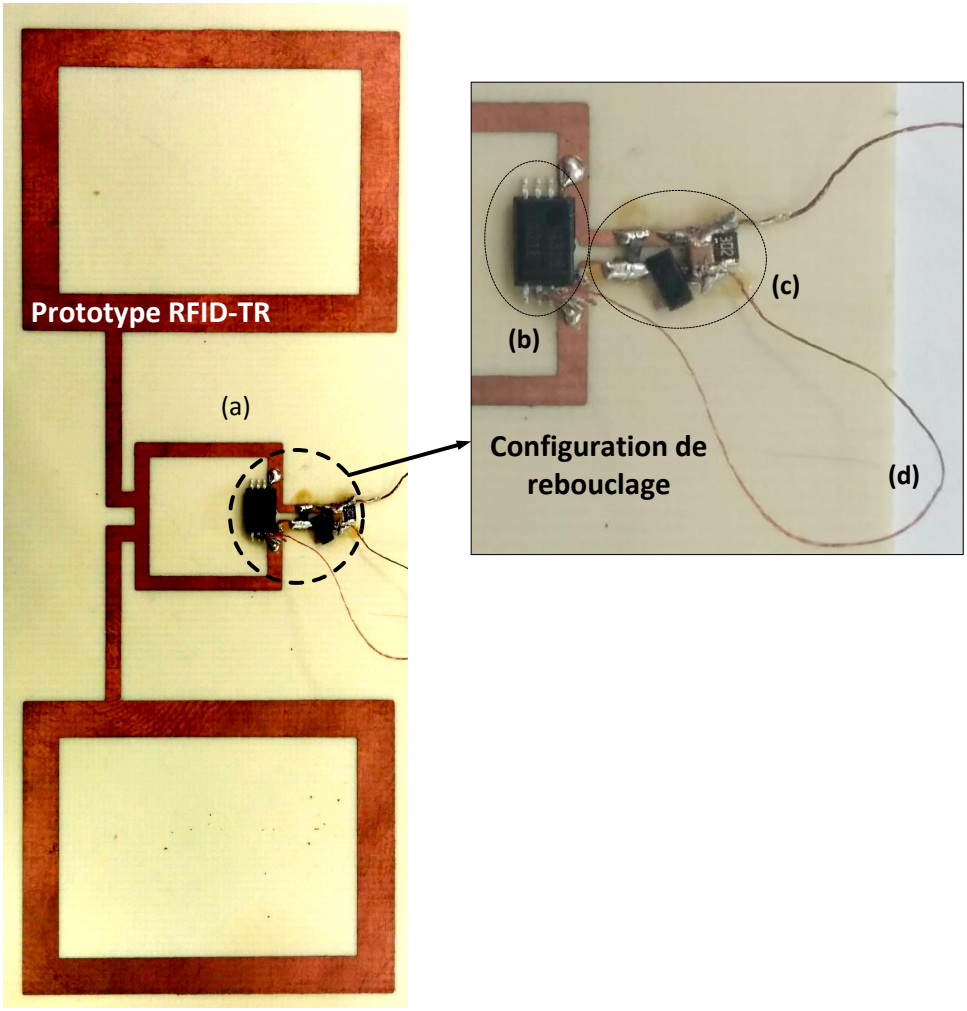

Figure 18: Prototype *RFID-TR qui auto-récupère l'énergie RF*. (a) antenne à bande unique, (b) puce RFID, (c) section EEH, (d) fil de rebouclage.

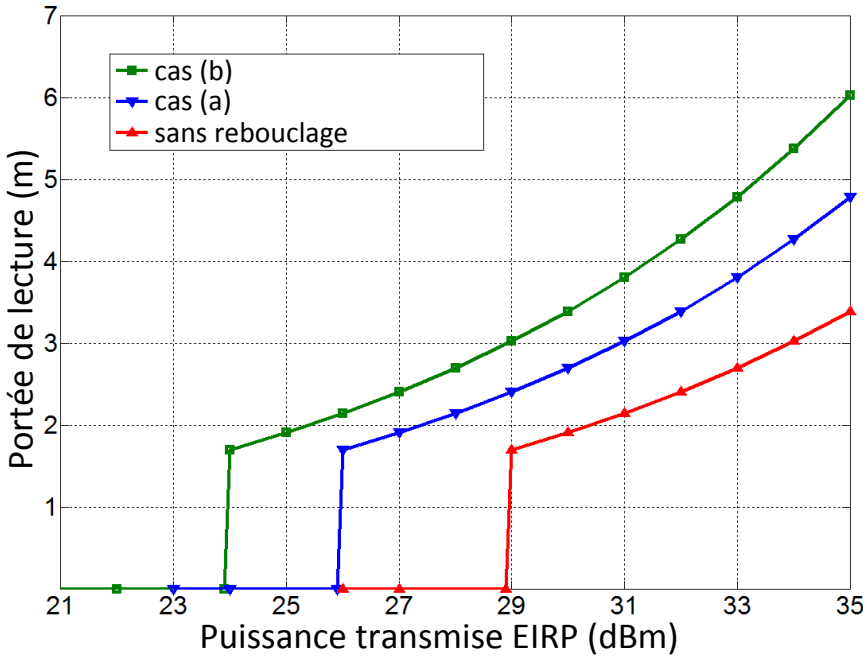

Figure 19: Portée de lecture du RFID-TR qui récupère l'énergie RF externe à $2,17$ GHz.

varie. Les résultats soulignent encore l'intérêt du rebouclage en termes de distance de lecture et de puissance minimale de réveil du tag.

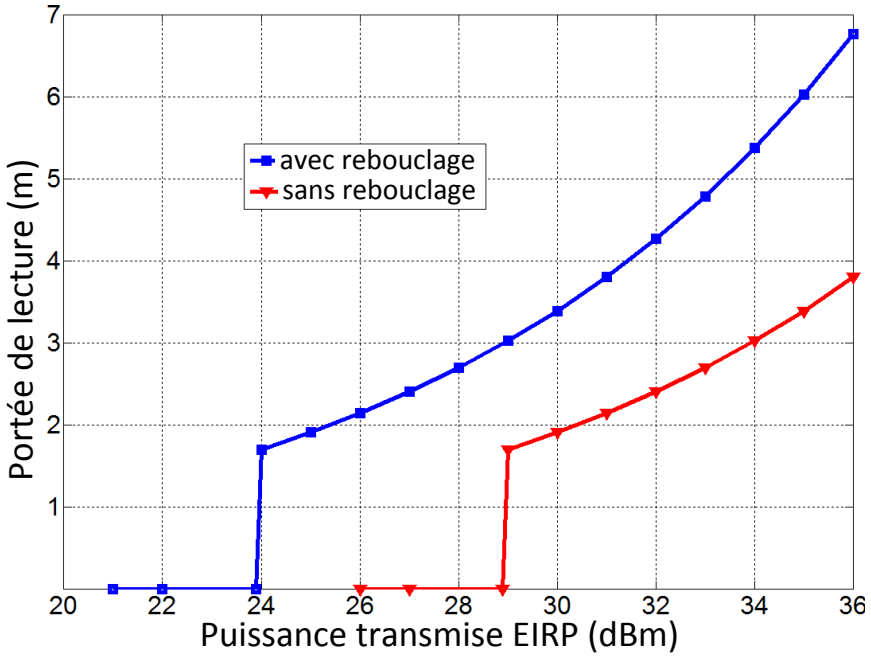

Figure 20: Portée de lecture du RFID-TR qui auto-récupère énergie RF.

5. Conclusions

Les travaux menés à travers cette thèse ont conduit à : 1) développer de nouvelles plateformes expérimentales et de nouvelles méthodes pour évaluer et caractériser les non-linéarités des tags et des puces RFID ; 2) proposer un nouveau modèle circuit-RF du tag mettant en évidence la génération des harmoniques et offrant de nouvelles perspectives pour leur exploitation (partie non présentée dans le résumé en français) ; 3) proposer deux nouvelles applications des tags RFID : canal de communication redondant (figure 21) et nouvelles approches de dispositifs de récupération d'énergie (figure 22).

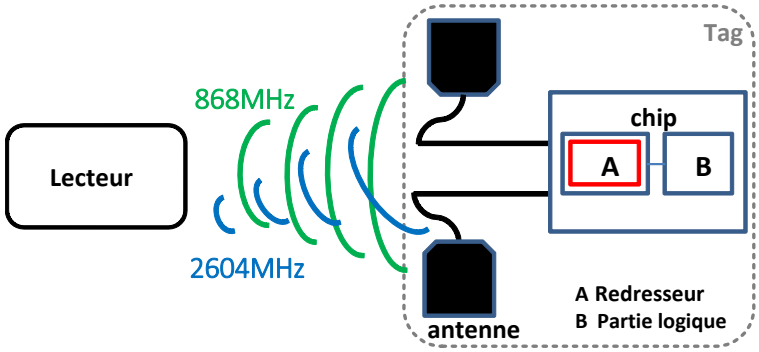

Figure 21: Nouveau canal de communication tag-lecteur sur la $3^{ème}$ harmonique en RFID passive.

Pour la première fois à notre connaissance, l'exploitation des non-linéarités des puces RFID a été démontrée et illustrée par plusieurs exemples. Les études présentées ouvrent la voie à de nouveaux champs de recherche sur des aspects à la fois fondamentaux et applicatifs. En perspectives, les deux nouvelles approches proposées permettent d'envisager de nombreux prolongements.

L'introduction d'un nouveau canal de communication sur la $3^{ème}$ harmonique présente plusieurs suites possibles exploitant ce concept et les spécificités associées : nouveaux tags capteurs, nouvelles approches dans le domaine de la localisation, nouvelles techniques pour contrer les effets des trajets multiples.

La démonstration qu'il est possible d'exploiter des sources d'énergie déjà présentes qui soient externes (dans l'environnement du système RFID) mais aussi internes offre des perspectives très intéressantes à la fois pour améliorer les performances des systèmes RFID et également dans un contexte où énergie et rayonnement RF doivent être utilisés à bon escient vers des systèmes type "green radio".

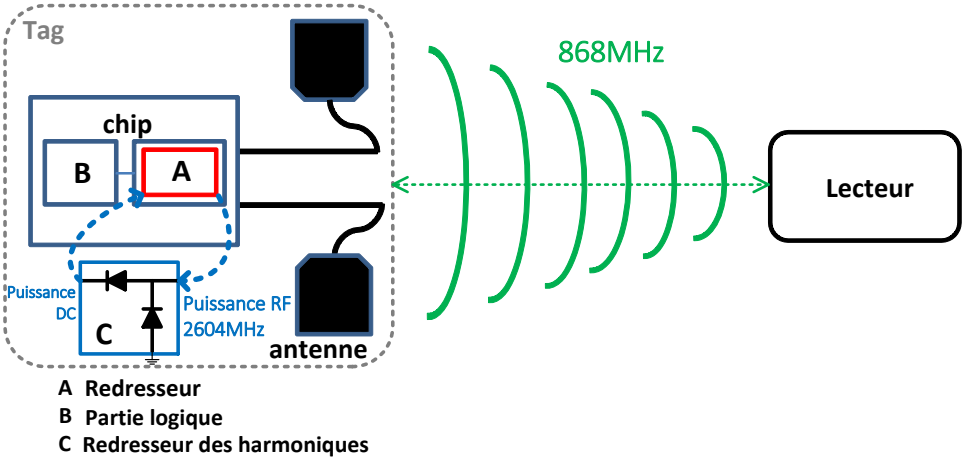

Figure 22: Principe de la récupération d'énergie basée sur les non-linéarités des puces.

PhD. Thesis

1. Introduction

1.1 Background

SPINNAKER is a RFID focused research project financed by OSEO (a public service delegation for research fundings in France [1]) led by the company TAGSYS [2], in collaboration with eight research labs headed by INP Grenoble LCIS [3], and four industrial entities. SPINNAKER [4] aims to transform the current state-of-art in RFID-based systems and enable a more widespread adoption of the technology, particularly in retail and healthcare sectors. The program addresses challenges and opportunities to improve the performance and real time interconnectivity of wireless-sensing systems throughout the supply chain, from manufacturing, distribution, and retail through to the end customer experience. The subject of the thesis here presented falls within one of the tasks identified in this project.

In the Internet of Things (IoT) era, the electronic labelling of things with wireless low-cost and self-powered tags, otherwise, the use of the passive RFID technology declares a constant evolution in this field. A review of this practice lets identify several areas in need of attention: (1) development of self-powered highly sensitive RFID chips, (2) efforts in physical layer around the tag antenna miniaturization, matching techniques and study of materials with sensing capabilities, and (3) the development of new software and processing treatments at the application layer with the objective to manage the data to produce some new information. Actually, RFID researchers have paid attention in one these three areas always in a horizontal manner (contributions in one of the areas at the time).

Looking to enhance the performance of actual applications and add new functionalities to the identification meaning in RFID, this thesis proposes a transversal contribution capable to exploit the three areas above identified. The idea is to propose the exploitation of the non-linear behavior of passive RFID chips proposing two main approaches: (1) a redundant information source (by meaning of declaring a new communication channel from tag-to-reader) and (2) an additional power source to benefit the passive RFID technology (by meaning of performing non-linear electromagnetic energy harvesting). Fields per example like location, energy harvesting, sensing or security among others can be impacted when non-linear phenomena introduce other assessable variables.

The main goal of this thesis is then the study and exploitation of non-linearities involved during a communication in the passive RFID system. The study unfolded in this thesis covers analytical aspects regarding the signal theory, as well as simulations and practical aspects regarding the characterization and design of RFID related prototypes.

The approach is original, because in most of cases, traditional theory on radio-frequency engineering does not consider the non-linearities as a useful phenomena in terms of power and information sources, but as spurious or interfering effects that should be avoided. In particular,

the exploitation of the n^{th} harmonic generated by RFID chips proposes a birth of applications providing to the RFID system an inroad for new functionalities so far difficult or impossible. The concept paves the way for a major field of investigation with great impact on both, the fundamental research as well as the application or exploitation fields. It is worth noting that these approaches must maintain, as much as possible, a low complexity for RFID tags. The exploitation of the non-linearity from RFID tags is generalized for all kind of rectifying devices such as diodes. The studies trigger on the developing of specialized characterization platforms and methods to evaluate the non-linearities of RFID tags, RFID chips, and rectifying diodes, through thorough parametric studies. Finally the design and evaluation of new RFID tags and multi-non-linear devices is performed.

1.2 Outline of the thesis

The issues related in this thesis are organized as follows [1]:

- Chapter 2 introduces the core technology in this research, that is the RFID technology. This chapter presents also a description of the state-of-art in the area where this thesis unfolds, it is the exploitation of non-linearities from RFID tags. Either characterization or related application works are presented to establish basic guidelines of the work pursued in next chapters.

- Chapter 3 presents a specialized characterization platform to perform a detailed study on the non-linear phenomena presented on UHF RFID signals between tag and reader, when the communication is established. The main objective in this chapter is to analyze the harmonics radiated by commercial UHF RFID EPC Class1 Gen2 tags. Great care is paid in the measurement setup and RFID air interface configuration. The analysis evaluates the non-linearity characteristic of tags without constraints on the kind of chip.

- Chapter 4 has as a central topic the RFID chip assessment. This chapter exposes a complete RFID test platform to characterize, in full operation mode and with automated methods, the non-linear phenomena in passive UHF RFID chips. The characterization method, platform composition, and operation are explained through real measurements on UHF Class-1 Generation-2 chips.

- Chapter 5 contrasts the experimental results with a theoretical model. In this chapter, the basics of the harmonic generation from passive RFID chips are explained. An electrical model is presented and its results are compared, in terms of harmonics strength, with real conducted measurements of different EPC Class-1 Gen2 RFID chips.

- Chapter 6 focuses on the exploitation of the evidenced non-linear harmonic responses. This chapter unfolds a new communication concept regarding the use of harmonics signals generated by the non-linear behavior of traditional passive UHF RFID chips. In

[1] The content of this thesis contains portions, sometimes verbatim, of the publications of the author product of the research in this domain

compliance of standard regulations, new and different RFID tags are designed with the aim to increase the power level of the harmonic response. The performance of the solution is illustrated from simulations and measurements. The chapter ends with a thorough parametric study of all prototypes.

- Chapter 7 presents alternative approaches for the exploitation of non-linear phenomena RF devices in benefit of the RFID technology. These approaches concern to the integration of the passive RFID technology to the theories of Wireless Power Transfer (WPT) and Electromagnetic Energy Harvesting (EEH). The solution takes advantage of the non-linear nature of rectifying elements in order to maximize the RF-to-dc conversion efficiency of EEH devices and increase the read range of passive RFID tags. The solution triggers on the design of a RF multi-device system. The design procedure and tests consider three non-linear phenomena: (1) the impedance power dependency, (2) the harmonic production, and (3) the dependence on the RF waveform.

- Chapter 8 presents final conclusions and future works of this thesis.

2. State-of-art

This chapter introduces the core technology and heart of the matter for the rest of chapters, that is the RFID technology. A general multi-layer vision of the RFID technology is presented and particular care is paid on the description of the passive UHF RFID system. Moreover, general theory of the response of non-linear RF networks in general is exposed. Additionally this chapter presents a description of the state-of-art in the exploitation of non-linearities from RFID tags. Either characterization or related application works are presented in order to introduce the basic guidelines of the pursued research.

2.1 RFID: A general multi-layer vision

Radio Frequency Identification (RFID) is a wireless data-collection technology very popular in many applications and services such as logistics, manufacturing and security [5]. Nowadays, the scope of the passive RFID technology is not limited to the identification, but has a vast applications in the sensing of environmental and human body parameters [6; 7], tag-to-tag communication [8], etc. Moreover, RFID is leading the new paradigm of Internet of Things (IoT) [9].

In order to positioning the work of this thesis, a modular and standard multi-layer model of the RFID systems is presented. Fig. 2.1 shows the proposed multi-layer model for the RFID system using the Open System Interconnection terms (OSI) which is compatible with the ISO standard 18000-1 [10]. The model provides parameter definitions for globally accepted frequencies in RFID [11] and also is valid for positioning new emerging RFID technologies, e.g. chipless RFID [12–14] which so far, neither standardization protocol nor regulation exists.

Three layers compose the presented model: the application layer, the communication layer and the physical layer [15].

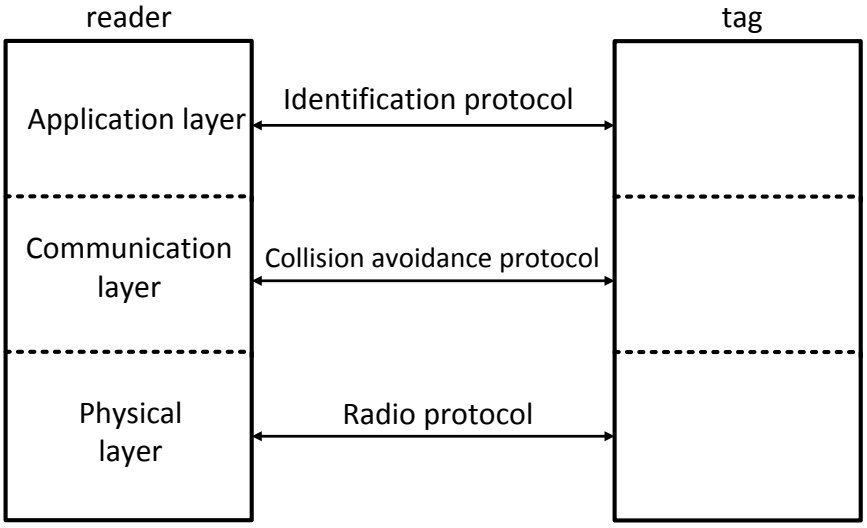

Figure 2.1: Air Interface protocol stack [15].

- **The application layer** represents the handled information defined by the user. This could be an identifier allowing the reader to extract the corresponding information from the tagged object to read or write data into a data base (e.g. the title of a book). In this layer, the protocols and rules for end-user software tools are positioned. In the case of the chipless RFID system, even if the standards are not yet defined, in this layer, the rules for chipless RFID reader softwares will be defined.
- **The communication layer** represents the way in which the readers and tags can communicate. Collision avoidance protocols are found in this layer as well as an identifier

that makes it possible to single out a specific tag for communication with a reader. Since there is not any intelligent element on the chipless tag, the basic definitions of collision avoidance should be split between its physical and application layers.

- **The physical layer** represents the air interface (that is to say, frequency, operating channels, modulation, data encoding, timings, bit rate), circuit connections, powering, signal strengths, chip architectures (reader and tag), structural connection (antenna-chip), structural shapes (responsible of the signature in chipless RFID), resonances and polarization. The features of these layers define if the tag works in LF, HF, UHF or microwave band and its consequent protocols in upper layers. Regardless of the frequency band, most of the RFID systems utilize only a few kHz to MHz of bandwidth and are thus classical narrow band systems

Following the multi-layer RFID model above presented, the research presented in this thesis is positioned in the physical layer. Most precisely, in the first layer of the passive RFID system which works under the EPC Class-1 Gen2 UHF RFID standard and where the RFID chip is the great protagonist.

The heart of the matter deals with the effects intrinsically produced as consequence of the non-linear behavior of RFID chips. The next two sections in this chapter crumble the theory and definitions of **passive UHF RFID** and **non-linear RF networks**; useful to unfold the scenery where this research works on.

2.2 Passive UHF RFID

2.2.1 Working principle

In passive UHF RFID tags EPCglobal Class-1 Gen-2 (adopted as ISO 18000-6C, [10]), the tag does not have an autonomous energy source like a battery, but is supplied via electromagnetic fields by the reader. The general working principle of passive UHF RFID is illustrated in Fig. 2.2. The reader generates a carrier wave that is transmitted by the reader antenna. Reader antennas are typically directive, i.e., they illuminate only a certain volume, the so-called read zone. If a tag is inside this read zone, the power transmitted by the reader activates this tag and it is ready to receive commands. Since the EPCglobal Class-1 Gen-2 is a *reader talks-first* protocol, i.e., the tags wait until they are addressed. Upon receipt of a command, which is transmitted via modulation of the Carrier Wave (CW), the tag sends its identification code or parts of its memory. The tag does not actively transmit this data, but reflects part of the incident reader carrier wave by deliberately de-tuning its own antenna generating two different Radar Cross Sections (RCS) as depicted in Fig. 2.2. This principle is known as backscatter modulation [16].

2.2.2 Reader

The reader or interrogator, which depending upon the design and the used technology, may be a read or write/read device. A practical example is shown in Fig. 2.3. A reader typically contains a radio frequency module (transmitter and receiver), a control unit and a coupling element to the

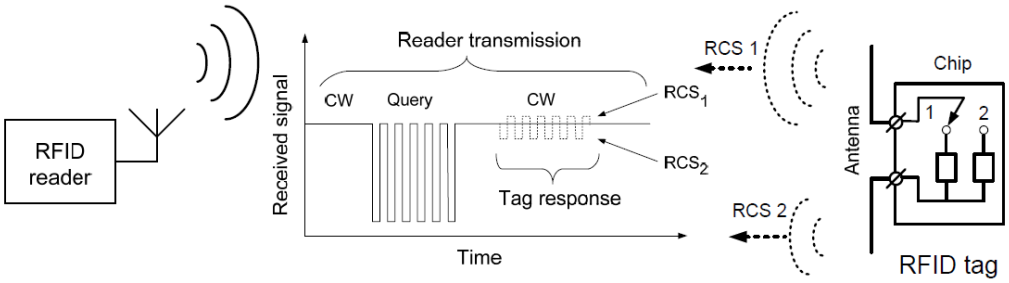

Figure 2.2: Working principle of passive UHF RFID [17]. Each impedance change produced by the deliberately de-tuning between antenna and chip, produces a RCS level

tag (reader antenna). In addition, many readers are fitted with an additional interface (Ethernet, RS 232, etc.) to enable them to forward the data received to another system (PC, robot control system, etc.)

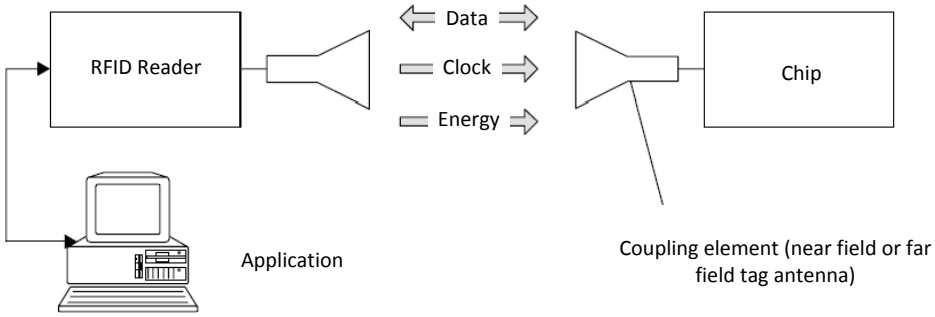

Figure 2.3: Reader and tag in a passive UHF RFID system [5].

2.2.3 RFID tag

Tag antenna

Tag antennas used for most applications in UHF RFID systems consist of a printed or etched metallization on top of a thin and flexible sheet of plastic or paper. Often tags are equipped with an adhesive film and can be attached to flat surfaces. Many fancy shapes of such antennas are found but technically most of them are dipole antennas having meandered conductors and a widened metallization at the dipole ends functioning as an end capacitance [18]. This techniques allows to size down the antenna compared to the half-wavelength dipole. To match the impedance of such electrically-small dipole antennas with the input impedance of the chip, several techniques are proposed. The most common technique is the inductively coupled loop or

slit implemented in the center of the dipole [18; 19]. The length of such antennas ranges between 5 cm and 15 cm. For even smaller tags a metallization in the form of a loop is used. Both antenna structures and thus most tags antennas radiate linear polarization and are omnidirectional in one plane.

From the application point of view, tag antennas can be considered the strategic point in the radio transmission chain of an RFID system. They are favored to be small which inevitably comes at the cost of low bandwidth and poor radiation efficiency. Furthermore, they are attached to objects that might contain fluids, metal, dielectric materials, or materials with high dielectric losses. Such objects often require specialized antenna designs or might even need boxing to generate some space around the tag. The reason for this is that electrically-small antennas are very prone to proximity effects. Materials in the proximity of the tag antenna cause a shift in center frequency and input impedance often referred as de-tuning [20]. This effect impairs the matching between the tag antenna and the chip which consequently reduces the power available to operate the digital circuits of the chip. Lossy materials in the proximity of the antenna will moreover absorb power. Fig. 2.4 shows the parametric study on the RFID tag reflection coefficient when its distance to a metal plate is varied. Drastic changes in the antenna electrical behavior occur when the tag get closer to the metal plate. Effects on the tag performance due to its proximity to the labeled object should be considered on the antenna design process for each application case.

Dual band tag antennas

Multiband operation is traditionally achieved in antennas by using several resonant elements. In RFID, different techniques as PIFA structures [21], slot antennas [22; 23], multilayer configuration [24], spiral coils [25–28] , asymmetric folding dipole [29] are used in the reader and tag side. The dual band operation has as objective, so far; the multi-standard operation, it means HF RFID jointly with UHF RFID [25; 26], or UHF-Europe (860MHz) joint with UHF-USA (902-928MHz) [27] or even UHF RFID and microwave region (2.45GHz and 5.2GHz) [22; 28; 29]. Fig. 2.5 shows some designs of these dual band antennas.

It should be noted that all dual band tag antennas for HF-UHF bands or UHF-microwave are proposed in a claimed scenery of a multi-standard RFID operation that does not exist yet. In this sceneries, it is expected one chip to be able to support more than one protocol of communication. One patent already protected this idea [30]. So far there is no works on exploiting the same RFID chip for more different and widely separated bands.

Passive RFID chip

As was described in Section 2.2.1, passive RFID tags do not have an internal battery and therefore must draw the power required for their operation from the electromagnetic field transmitted by the reader. The RF energy radiated by the reader is used both to supply the digital section of the tag and to allow data transmission from tag-to-reader through modulation of the backscattered radiation [31]. Next lines explain in detail the internal architecture of a RFID chip (Fig. 2.6) in order to understand the power supplying mechanism of the tag.

The architecture of a passive UHF RFID tag shown in Fig. 2.7 [31] is below detailed.

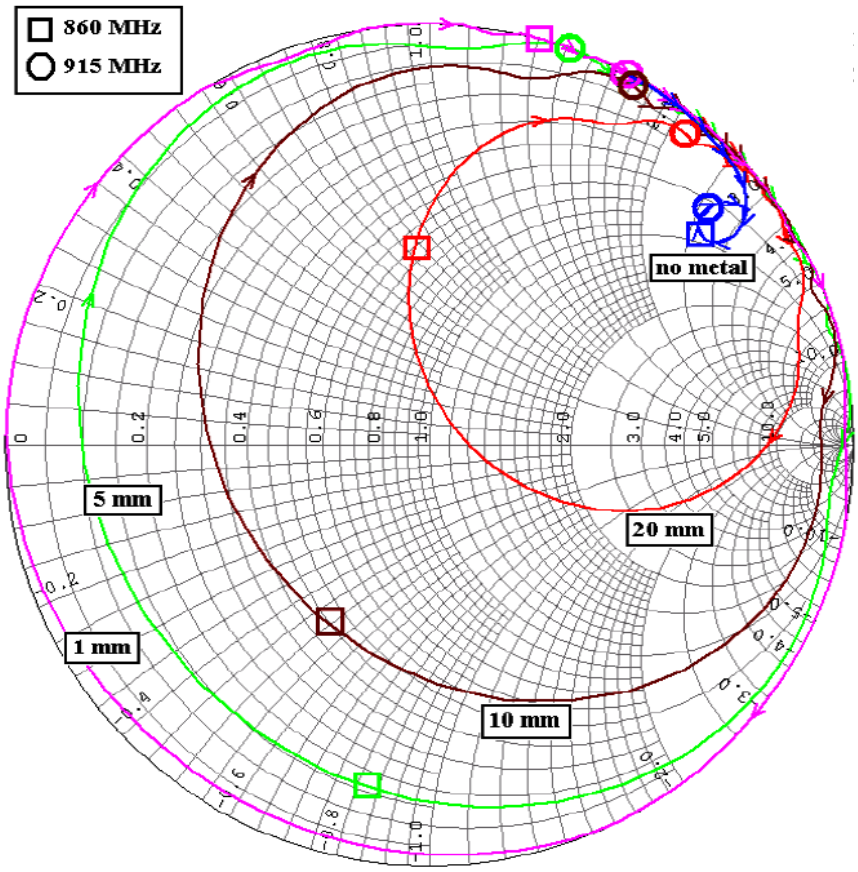

Figure 2.4: Simulated RFID tag reflection coefficient, when varying its distance to a infinitely extended metal plate. The detuning effect is harm at shorter distances [20].

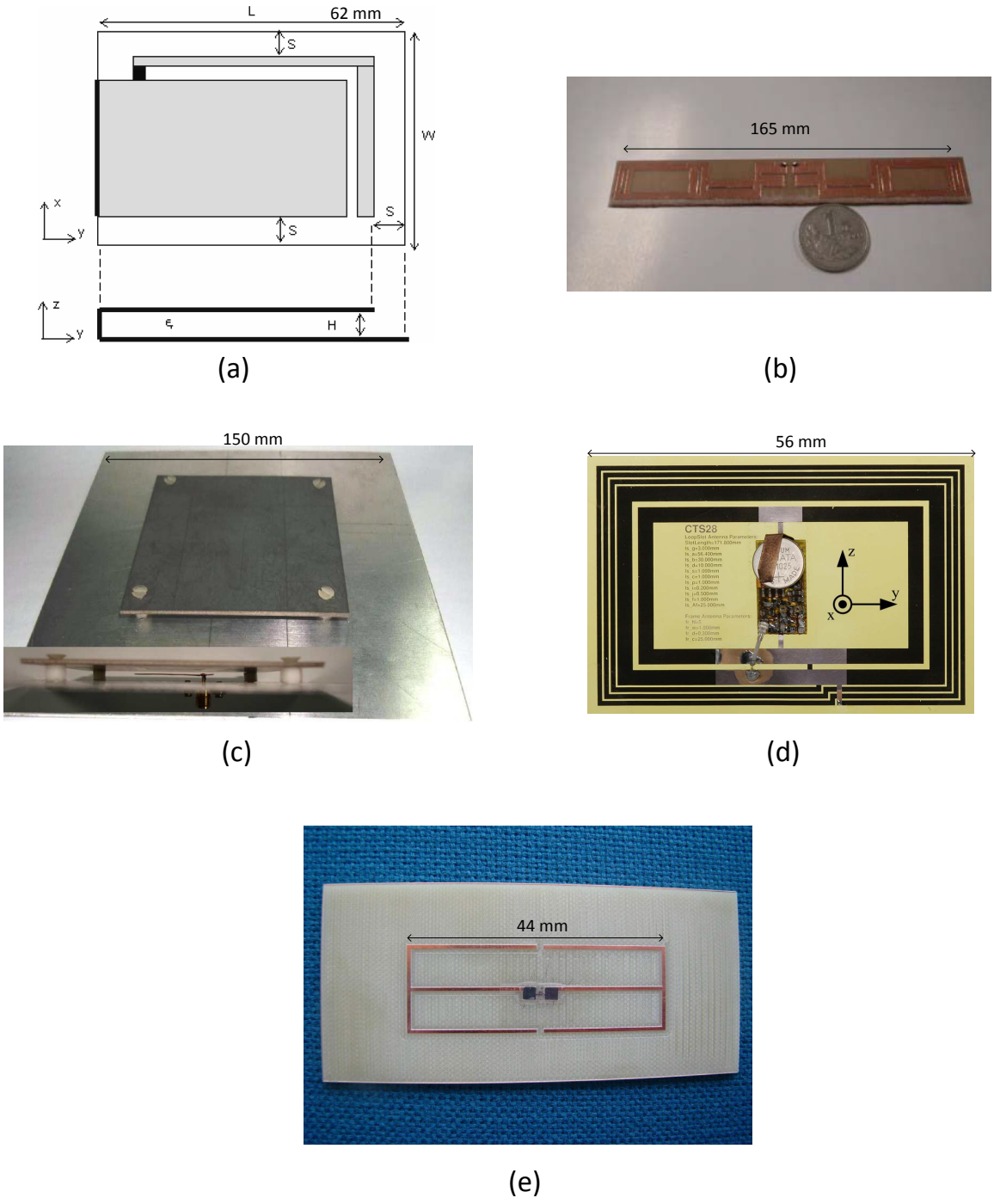

Figure 2.5: Dual band RFID antennas. (a) Dual-band PIFA design for RFID tag [21]. (b) Dual-band dipole slot antenna for RFID Tag [23]. (c) Multilayer high-gain dual-Band antenna for RFID reader [24]. (d) Spiral coils Dual-band RFID tag antenna for multi-standard operation [26]. (e) Dual-band RFID tag antennas by means of asymmetric dipoles [29].

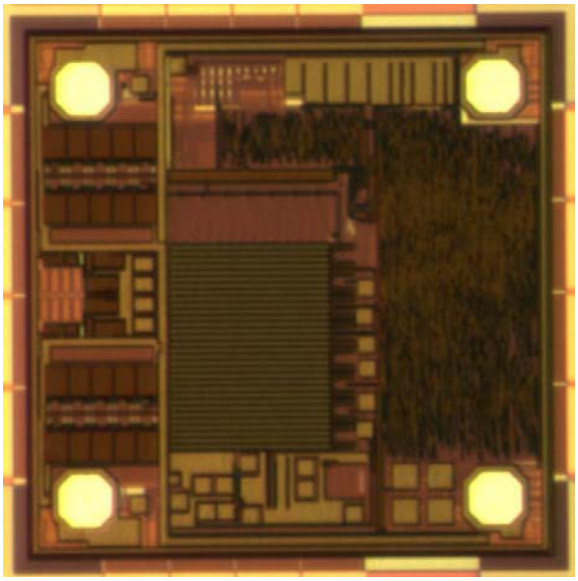

Figure 2.6: (a) Layout of the die of a passive Impinj Monza-4 RFID chip of 0.6 square millimeters [32]. (b) Conceptual model of dual independent ports.

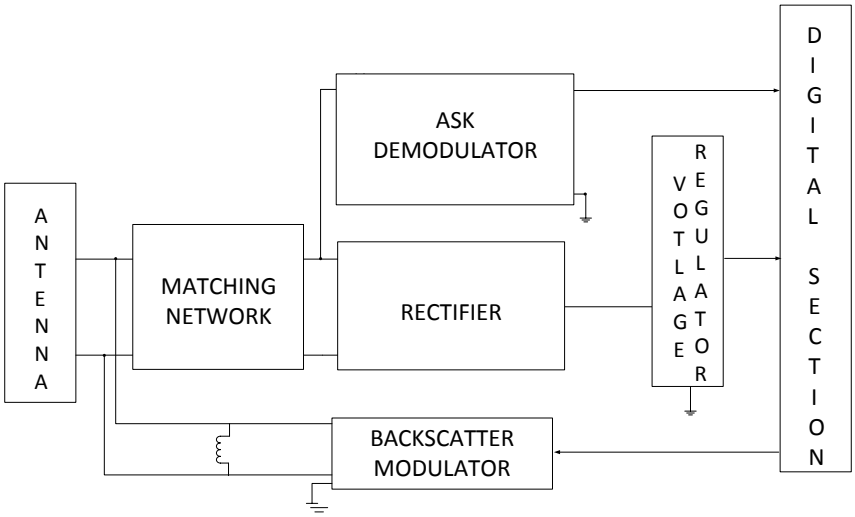

Figure 2.7: Architecture of the chip in passive UHF RFID [31].

- The coupling element is an antenna, which typically is a dipole (Details exposed in Section 2.2.3)
- An impedance matching network between the antenna (typically a dipole) and the RFID chip, ensures the maximum power transfer between these both elements in one of the impedance states of the chip.
- A rectifier circuit converts the input alternating voltage into a dc voltage, which is used by a series voltage regulator to provide the regulated voltage required for the correct operation of the tag. The architecture of the rectifier is based on a Cockcroft-Walton circuit with two or more diode-based voltage doubler stages. These diodes determine the non-linear behavior of the chip [31; 33; 34].
- An ASK demodulator composed basically by a peak detector circuit.
- A backscatter modulator is used to modulate the impedance seen by the antenna, when transmitting.
- The RF section is connected to a digital section, which typically is a finite-state machine able to manage the communication protocol.

The theoretical and practical aspects treated in this thesis, consider mainly the RF section of the passive RFID tag, i.e. antenna, matching network and rectifier sections.

2.3 Non-linear RF networks and harmonic generation

In this section, the response of non-linear RF devices in general is described. All realistic RF devices have at least small transmission losses. The ideal linear component does not exist in practice because all realistic devices are non-linear at very low signal levels due to noise effects. In addition, practical components may also become non-linear at high signal levels. In the case of active devices, such as diodes and transistors, this may be due to effects such as gain compression or the generation of spurious frequency components due to device non-linearities, but all devices ultimately fail at very high power levels. In either case, these effects set a minimum and maximum realistic power range, or dynamic range, over which a given component or network will operate as desired [34].

It is this non-linearity that is of great utility for desirable functions such as amplification, detection, and frequency conversion [35]. However non-linear device characteristics, can also lead to undesirable effects such as gain compression and the generation of spurious frequency components. These effects may lead to increased losses, signal distortion, and possible interference with other radio channels or services. Some of the many possible effects of non-linearity in RF and microwave circuits are listed below [36]:

- Harmonic generation (multiples of a fundamental signal);
- Saturation (gain reduction in an amplifier);

- Intermodulation distortion (products of a two-tone input signal);
- Cross-modulation (modulation transfer from one signal to another);
- Amplitude and phase conversion (amplitude variation causes phase shift);
- Spectral regrowth (intermodulation with many closely spaced signals).

Fig. 2.8 shows a general non-linear network, having an input voltage v_i and an output voltage v_0. In the most general sense, the output response of a non-linear circuit can be modeled as a Taylor series in terms of the input signal voltage:

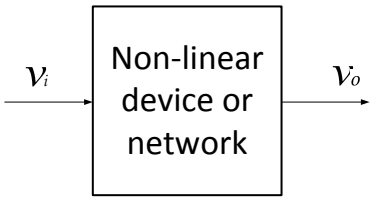

Figure 2.8: Non-linear Network [34].

$$v_0 = a_0 + a_1 v_i + a_2 v_i^2 + a_3 v_i^3 + ... \tag{2.1}$$

where the Taylor coefficients are defined as

$$a_0 = v_0(0)\ (dc\ output) \tag{2.2}$$

$$a_1 = \left.\frac{dv_0}{dv_i}\right|_{v_i=0} (linear\ output) \tag{2.3}$$

$$a_2 = \left.\frac{d^2v_0}{dv_i^2}\right|_{v_i=0} (squared\ output) \tag{2.4}$$

and higher order terms. Different functions can be obtained from the non-linear network depending on the dominance of particular terms in the expansion. The constant term, with coefficient a_0, in (2.1) leads to rectification, converting an AC input signal to dc and it is the base of the powering technique in passive RFID tags. The linear term, with coefficient a_1, models a linear attenuator when $a_1 < 1$ or an amplifier when $a_1 > 1$. The second-order term, with coefficient a_2, can be used for mixing and other frequency conversion functions.

Practical non-linear devices usually have a series expansion containing many nonzero terms, and a combination of several of the above effects will occur. For the interest of this thesis, the next section will paid special attention on the harmonic generation phenomena.

The traditional way of showing how new frequencies are generated in a generic non-linear network (Fig. 2.8) is to describe the behavior of the network considering the case where a single-frequency sinusoid is applied to its input

$$v_i = v_0 \cos \omega_0 t \tag{2.5}$$

In this case, Equation (2.1) gives the output voltage as

$$v_0 = a_0 + a_1 v_0 \cos \omega_0 t + a_2 (v_0 \cos \omega_0 t)^2 + a_3 (v_0 \cos \omega_0 t)^3 + ... \quad (2.6)$$

$$= \left(a_0 + \frac{1}{2} a_2 V_0^2 \right) + \left(a_1 V_0 + \frac{3}{4} a_3 V_0^3 \right) \cos \omega_0 t + \frac{1}{2} a_2 V_0^2 \cos 2\omega_0 t + \frac{1}{4} a_3 V_0^3 \cos 3\omega_0 t + \ ... \quad (2.7)$$

From (2.7) it can be observed that a portion of the input signal at frequency ω_0 is converted to other frequency components. For example, the first term of (2.7) represents a dc voltage, which would be a useful response in a rectifier application. The voltage components at frequencies $2\omega_0$ or $3\omega_0$ can be useful for frequency multiplier circuits. In specific devices (such amplifiers), the presence of other frequency components will lead to signal distortion if those components are in the passband. For a single input frequency, or tone, ω_0, the output will in general consist of harmonics of the input frequency of the form $n\omega_0$, for $n = 0, 1, 2, ...$ If these harmonics lie outside the passband of the device, then there will not be interfere with the desired signal at frequency ω_0. However, the situation is different, when the input signal consists of two closely spaced frequencies. The combination of the two input frequencies applied to the non-linear network produces the intermodulation products and it is the origin of the intermodulation distortion [36].

Regarding the composition of different frequencies of the output signal of a non-liner network, extended studies in antennas [37; 38] and circuits can be found in the literature [39]. Some related works in the RFID field as well as in battery-less non-linear devices will be detailed in the next section.

2.4 Related works

This section presents the state-of-art in non-linear studies and applications reported in the RFID field. Four main categories are highlighted in the state-of-art: (1) measurement of backscattered harmonics , (2) wireless sensors tags, (3) frequency diversity in RFID, (4) Electromagnetic Energy Harvesting (EEH) and non-linearities of RF devices.

2.4.1 Measurement of backscattered harmonics

An experimental characterization of harmonic scattering from passive UHF RFID tags were published in 2009 by P. V. Nikitin et al. [40]. With some limitations on equipment (regarding the activation and measuring of the RFID tag at the same time) the authors analyzed the first three harmonics of three commercial tags: AD-222, AD-223 and AD-224 [41].

The measurement setup used the compact broadband GTEM cell TESCOM TC5060 shown in Fig. 2.9. Such cells are often used for radiation and susceptibility testing and allow to create a controlled uniform field at desired location, excluding from consideration frequency dependent responses of transmitting antenna and anechoic chamber material. Fig. 2.9 shows the measurement setup.

The test consists on injecting a RF signal at 880 MHz and 10 dBm at the port one, this generates an electric field inside the cell. An RFID tag was placed inside the cell. The

backscattered field from the tag was detected with the sensing probe antenna connected to port two as shown in Fig. 2.9. The antenna was a simple half-wavelength dipole printed on FR4 substrate and located 10 *cm* away from the tag.

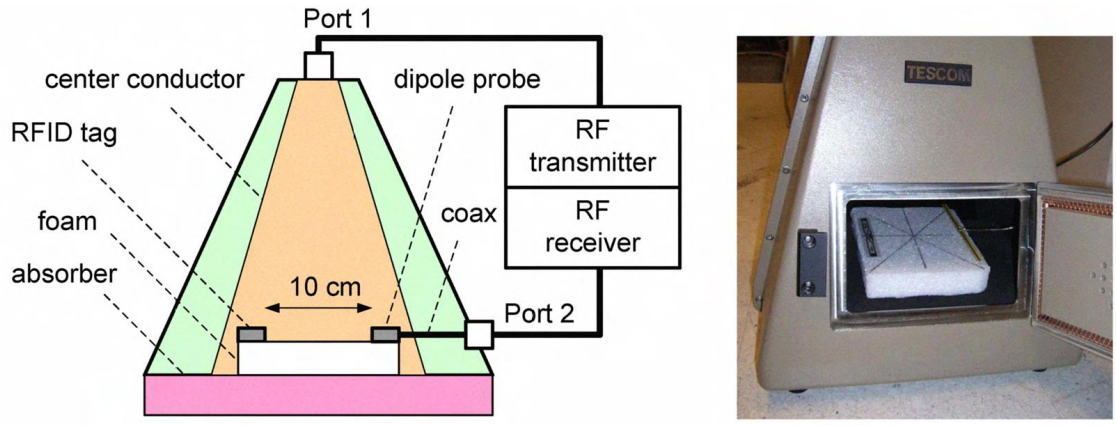

Figure 2.9: Fractal tag for harmonic radar application [42].

Table 2.1: Measured power of harmonics at 10 *dBm* input signal

Harmonic Power	No tag	AD-222	AD-223	AD-224
Freq. Fundamental	-4	-6	-6	-6
Second Harmonic	-72	-72	-72	-72
Third Harmonic	-86	-63	-64	-68

Results of the reported measurement are shown in Table 2.1. Experimental results seem to show the capability of passive UHF RFID tags to generate and backscatter harmonics whose powers depends on specific tag design. Results evidenced a 3^{rd} harmonic with around 5 *dB* higher level than 2^{nd} harmonics for the tags under test. Even if these results are interesting, the measurement does not consider an activated tag, so no real tag response is measured, but harmonic multiples of the carrier wave sent by the RF transmitter and multiplied by the tag circuitry. These studies evidenced certain interest on the field but no additional research efforts were followed, probably because the evidenced low power level and limitations on the characterization method. At this point it is declared that further efforts on the domain will require the used of specific characterization platforms to properly evaluate the backscattered harmonics.

2.4.2 Wireless sensors tags

Looking to applications in the state-of-art, two non-linear effects are so far used in RFID or battery-less devices based in rectifying diodes:

- **Harmonic generation** with applications better known as *frequency doubler tags*;
- **Intermodulation distortion**, with applications in location.

Frequency doubler tags

The harmonic generation is used in frequency doubler tags. This concept is illustrated in Fig. 2.10. Frequency doubler tags, also known as a one bit RFID tags [42], are so far used to check and monitor the possible presence of a tag in the interrogation zone of a reader by means of simple physical effects. The generation of harmonics is reliably adopted in the microwave frequency range, leading to the harmonic radar concept [43–45]. In this technique, an antenna

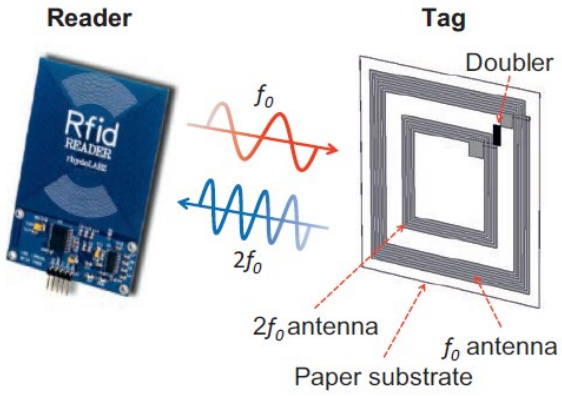

Figure 2.10: Frequency doubler tag [46].

(e.g. fractal loop [43] or crossed dipole [42]) is connected to a small and light low barrier diode Schottcky. The antenna is excited by the impinging radar wave, a current is induced through the diode and due to its non-linearity creates a harmonic which is backscattered by the antenna properly tuned for both frequencies. Such a signal can be detected by means of a microwave receiver without being masked by reflections from the surrounding scenario. The authors considered that the detection can be possible even if any modulation is applied to the carrier. The envisaged applications on this topic are the harmonic radar for insect tracking [43], traffic applications [47] and avalanche rescue in the snow [42].

Some recently works were presented with the same concept but now in near field operation (working at 7.5 MHz) and using multiplier diodes made in organic material (pentacene PEN diodes are organic devices that exploit pentacene as semiconductor, they are used in the harmonic tags to provide the non-linearity required to generate the harmonic) [46]. A parameter called *conversion loss*, defined as the difference (in dB) between the input power of the fundamental frequency and the detected harmonic power has been reported. The best *conversion loss* for

this harmonic tag of one bit is 52.5 *dB*, detected at a distance of 12.5 *cm* with 10 *dBm* of input power. The major drawback of this auto-proclaimed *eco-friendly chip-less tag* is the big size of the antenna (14 *cm* x 14 *cm*). It should be noted here that since only one diode is used, the most significant harmonic generated is the second one. Fig. 2.11, Fig. 2.12 and Fig. 2.13 show some structure examples of these harmonic tags used for harmonic radar applications.

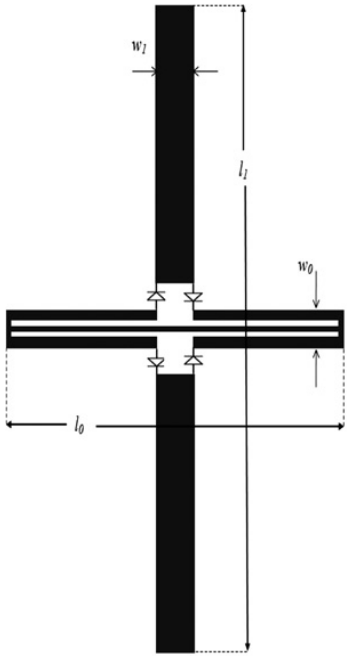

Figure 2.11: Crossed dipole tag for harmonic radar application [43].

Other application that exploits the harmonic generation of non-linear devices also in near field operation was presented in [48]. This involves the detection of counterfeit RFID cards based on the electromagnetic characteristics of these cards rather than the digital information that they transmit. On this technique, one of the stages considers the electromagnetic signature that RFID cards produce by radiating the harmonic frequencies of the communication carrier between reader and card at 13.56 MHz. Reported results show that different RFID card manufacturers can be distinguished automatically with the broadband analysis.

In the cited references for wireless sensor applications, no work have been reported regarding the characterization of the non-linear device (i.e. diode), neither in impedance nor in harmonics production. Details about the experimental characterization and modeling of generated harmonics from non-linear devices (i.e. RFID chips) will be discussed later in Chapters 3, 4 and 5.

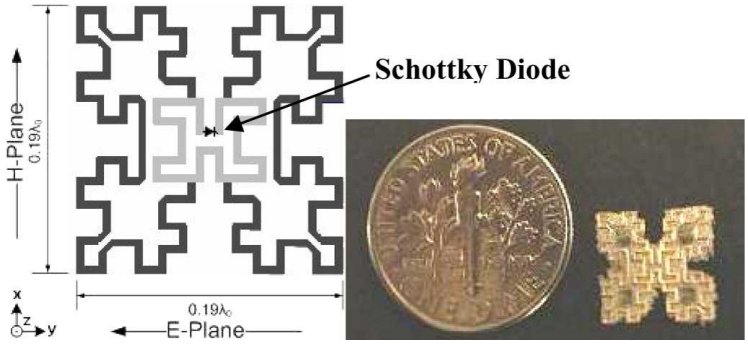

Figure 2.12: Fractal tag for harmonic radar application [42].

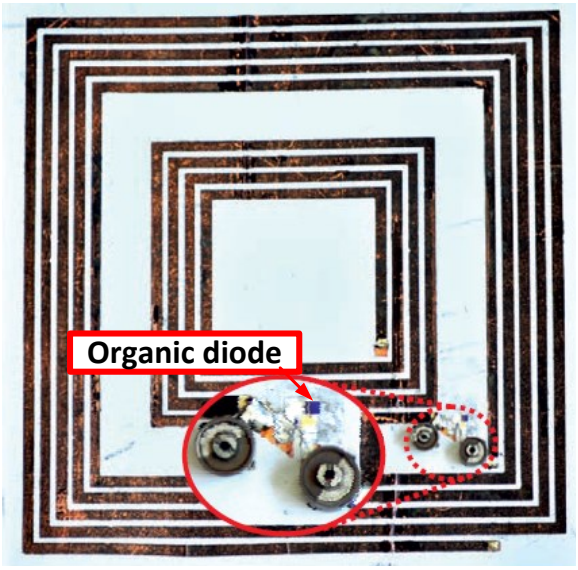

Figure 2.13: Organic tag zooming on the connected diode [46].

Intermodulation distortion

Looking at the literature, no specific application on totally battery-less devices were so far found. Next lines describe a semi-passive tag based on intermodulation distortion for location purposes.

Hugo Gomes et al. [49] proposes in 2009 the use of a tag in location scenarios with the operational principle shown in Fig. 2.14:

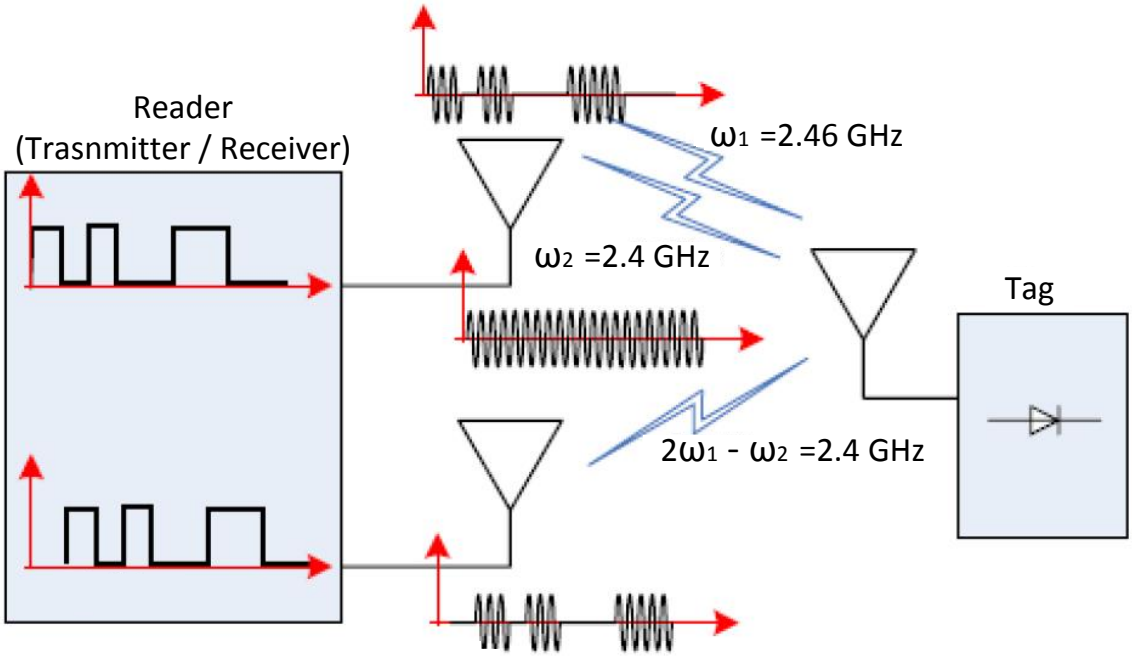

Figure 2.14: Location system exploiting the intermodulation phenomena [49].

- The reader sends a RF signal, at frequency ω_2, modulated by a pseudo-random sequence and in an un-modulated carrier RF signal at a different frequency ω_1.
- When the signal arrives to the tag, this is demodulated and re-modulated in a different carried product of the intermodulation and re-emitted to the air interface at the frequency $2\omega_1 - \omega_2$. The modulation allows to identify a specific tag in the analyzed environment.
- The reader has a receiver tuned to the frequency $2\omega_1 - \omega_2$, which allows it to receive a replica of the transmitted signal.
- The two pseudo random signals (transmitted and received) could be compared in time and the calculation of time of travel can be computed.
- The time delay indicates the distance between reader and tag. For a correct location of the tag, three readers are proposed to apply a triangulation computation.

Reported conclusions in [49] draw that the use of intermodulation distortion is a viable solution for location proposes. Some weak point that have been not described on this work, is the accuracy on location, since the modulation and demodulation needs accurate equipment in order to compute the time of arrival even in a triangulation scenery [50].

2.4.3 Frequency diversity in RFID

In order to increase the read range and overcome the power insufficient problem in passive RFID tags, authors of [51–56] proposed a multi-carrier UHF passive RFID system composed by a reader transceiver, a Carrier Wave Emitter (CWE) and a passive UHF RFID tag. The sketch of a traditional RFID system in Fig. 2.15 (a) is compared to the proposed system shown in Fig. 2.15 (b). The proposed system offers additional energy to Class 1 Generation 2 tags, and also generates frequency diversity on its modulated response by meaning of multiple carrier operation. The reader can be benefited from the frequency diversity gain and the multi-path fading problem can be mitigated.

The proposed approach profits from the narrow frequency range operation of passive RFID tags, using different carrier frequencies each one closer to the other. The operation is as follows. (1) The CWE located close to the tag, as a radio source, emits a carrier wave to illuminate the tags and provide them additional wireless power. The CWE frequency is around 10 MHz distanced from the standard carrier wave of the reader transceiver. (2) Additionally a transceiver carrying the logic of a RFID reader transmits and interprets the communication protocol with the tag at the standard frequency. (3) Special treatment of signals send from reader to tag are performed in order to mitigate the effect of additional carriers and in this manner let the tag to understand the commands.

Reported results show the tag responding with a modulated backscattering signal for each one of the carrier wave sources (CWE and transceiver). Snapshots of the tag response in each case are shown in Fig. 2.16 and Fig 2.17. This phenomenon is declared by the authors as frequency diversity and further work is envisaged in combining the modulated backscattered response around each carrier. Even if reported results showed an improvement in the read range of 4 times longer compared to ordinary Class 1 Generation 2 tags, some inconveniences are introduced in the tag side, which trigger in reader-to-tag command demodulation errors. Additionally the treatment changes the standard communication protocol for UHF passive RFID defined in [57], then being unviable for traditional/commercial applications. Further works from the same authors treat the problem proposing new architectures for passive RFID chips, but only simulated results were discussed [51].

2.4.4 EEH and non-linearities of RF devices

Harvesting harmonic power

A large number of investigations are being focused on wireless power or remote-powering technologies. Therefore, Wireless Power Transmission (WPT) has become a refreshed and refocused technique for powering electronic devices over distances. A rectenna circuit including antenna and rectifier is the most vital component of a microwave power transmission system

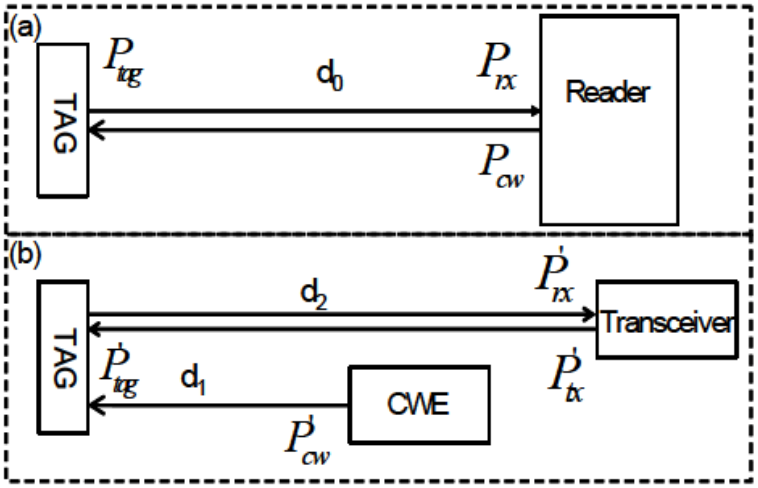

Figure 2.15: (a) An ordinary UHF passive RFID system. (b) A frequency diverse UHF passive RFID system with isolated CWE. [51].

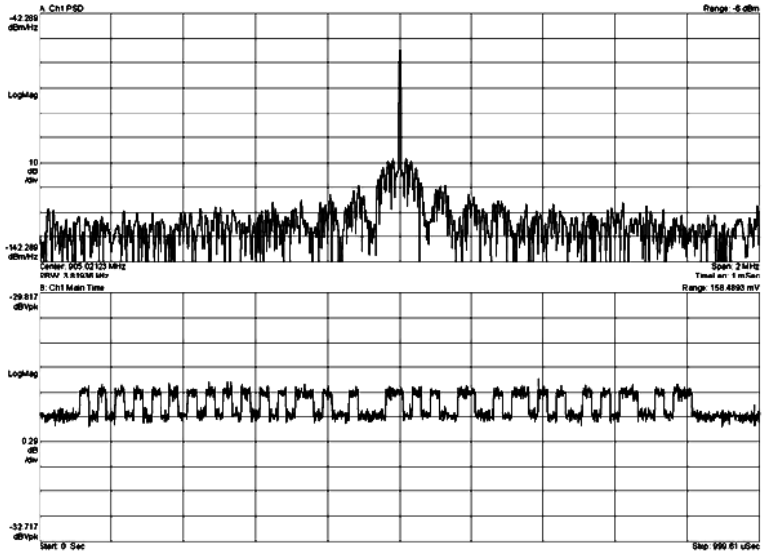

Figure 2.16: Snapshot of tag response around 905 MHz [53].

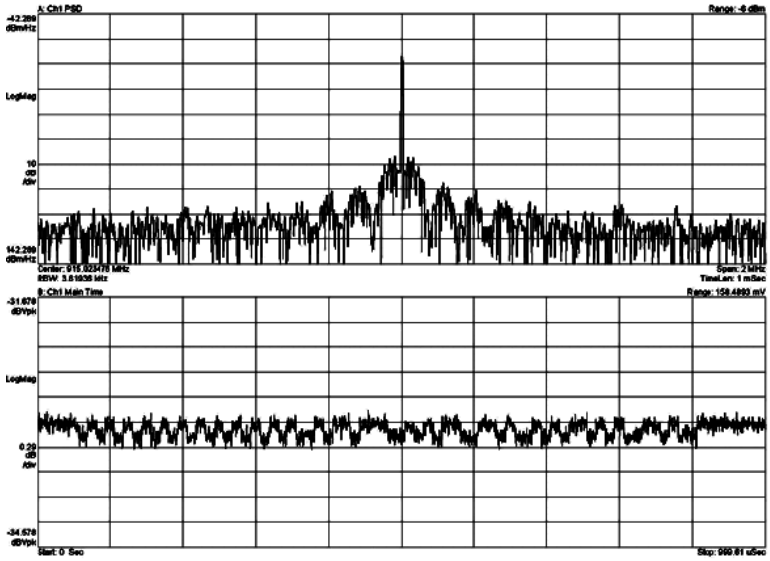

Figure 2.17: Snapshot of tag response around 915 MHz [53].

that wirelessly receives microwave power and converts it into dc. Rectenna efficiency is mainly determined by its rectifier circuit. Hence, designing a high-performance rectifier is a point of interest since it is directly related to the quality of a WPT system.

Till now, little work have been suggested the utilization of harmonic signals with energy harvesting intentions. The work reported in [58] proposes a millimeter-wave rectenna with high-efficient rectifier operation for medium and low level of RF input power. In this study, a special configuration of a voltage doubler rectifier that can successfully harvest harmonics signal generated by the non-linear effect of rectification at 35 GHz is explained. The harmonic harvesting operation increases the RF-to-dc conversion efficiency. Additionally the authors of [58], valorize their works in terms of compact size (with intentions to integrate the solution into any kind of antenna, as a rectenna for millimeter-wave power transmission systems.)

The referenced work exploits the 2^{nd} harmonic generated by conventional rectifiers operating at medium range of input RF power. A modified voltage doubler rectifier that is able to harvest the energy from harmonics is proposed. The dc output of the harmonic harvester and the fundamental harvester are added up at the end in a common dc load. Fig 2.18 shows the schematic diagram of the whole circuit as well as the realized prototype. Some of the details that authors of [58], did not explain is the strength of higher harmonics. Indeed, given the topology of the fundamental voltage doubler rectifier, it is expected to have a weak 2^{nd} harmonic, but a considerable higher 3^{rd} harmonic, so consequently a higher dc level can be still obtained. The predominance of harmonics of certain order (odd or even) in rectifying circuits is a topic that will be detailed discussed on Chapter 5.

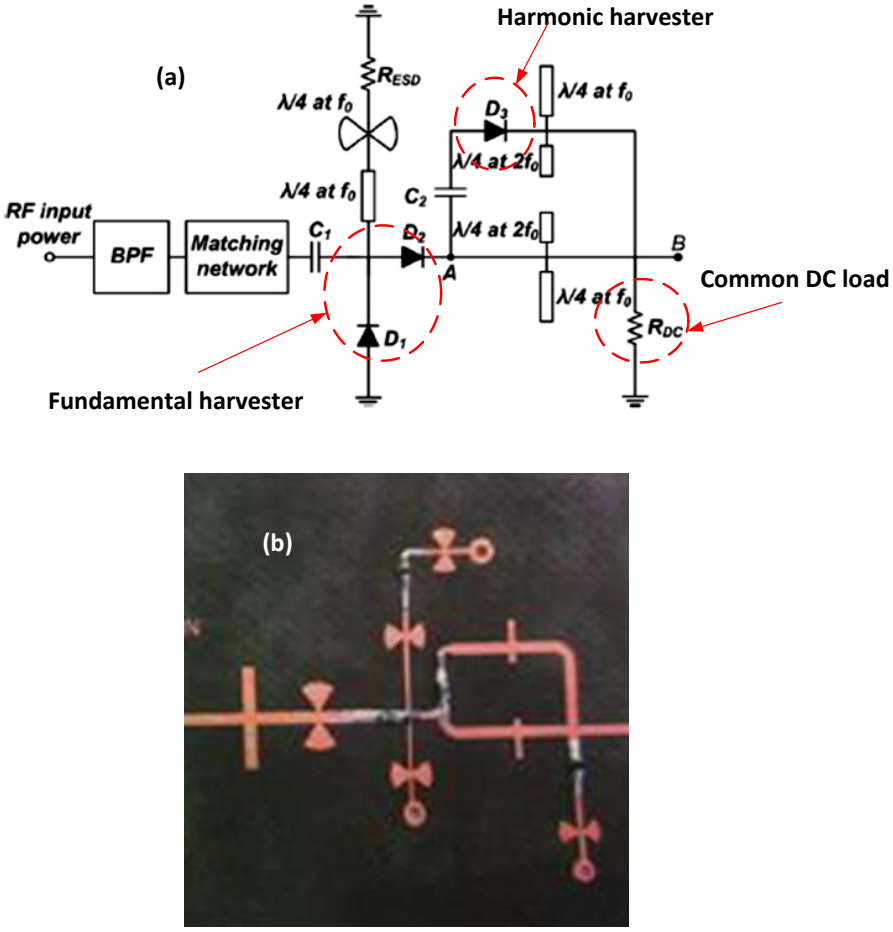

Figure 2.18: Harmonic harverter rectifier. (a) Schematic view. (b) Realized prototype [58].

Signal design for WPT

Several works have proposed the use of specific signal in a WPT in order to increase the RF-to-dc conversion efficiency of EEH circuits [59; 60; 60–63]. The basis behind these phenomena is the non-linear behavior of rectifying diodes under different input signals. Indeed, by using special designed signal waveforms at the transmitting terminal (that somehow excite the diode non-linear behavior in a more efficient way), the RF-to-dc conversion efficiency of the diode is increased.

The phenomena can be generalized by the use of *time varying envelope signals* as an efficient WPT technique, since they are capable to activate the rectifying devices for lower average input power levels, compared to signals of constant envelope and the same average power (see Fig. 2.20). Therefore, signals with large peak-to-average power ratios (PAPRs) provide higher RF-to-dc conversion efficiency than single carrier signals, meaning that for the same targeted distance, one needs to transmit less power.

The PAPR (dB) of a waveform can be defined as

$$PAPR = 10log_{10}\frac{max[x(t)^2]}{\langle x(t)^2\rangle} \tag{2.8}$$

where $x(t)$ is the time domain waveform of the signal of interest and $\langle\rangle$ refers to the time average operator.

In [63] an interesting study regarding the PAPR of three different signals compared with a single tone signal was presented, the signals are shown in Fig 2.20 and its corresponding PAPR values are depicted in Table 2.2.

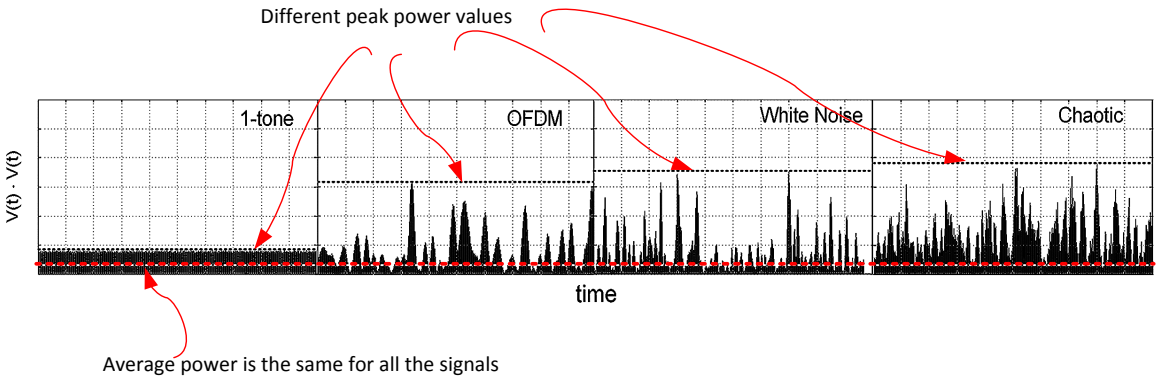

Figure 2.19: Instantaneous power of the different types of test signals [63].

Each one of these signals was used as input signal for a rectifier circuit centered at 433 MHz and results show the mentioned phenomenon: when higher the PAPR is in the received signal, higher is the rectifier RF-to-dc conversion efficiency.

The signal design for efficient WPT shows that even though high PAPR signals are not desired in communication systems due to the distortion that these signals suffer when amplified

Table 2.2: PAPR for three different *time varying envelope signals*.

Signal	PAPR (dB)
OFDM	12.0
White noise	13.7
Chaotic	14.8

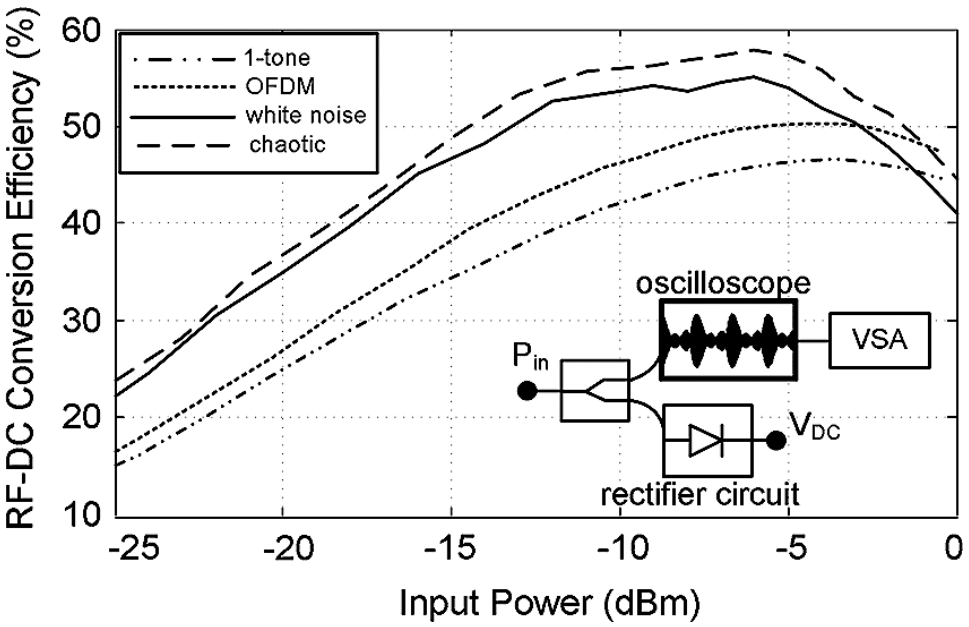

Figure 2.20: RF-to-dc conversion efficiency of the rectifier circuit versus total input power for different test signals [63].

in the transmitter, in EEH systems high PAPR signals are desired towards the improving of RF-to-dc conversion efficiency of rectifiers.

2.5 Conclusion

Harmonic generation and intermodulation distortion from non-linear devices are not new, but previous efforts have focused generally within the context of one bit system where the presence of harmonics or intermodulation components serve only to detect the presence of the tag. No special attention was paid, for sure without breaches to standard regulations, in the new features that a redundant signal that carries information can offers. By other side, and certainly in tags of the family Class 1 Generation 2 [57], the non-linear effects were always considered as undesirable as in most RF systems. The main treatment to control these phenomena is so far focused on ensuring the impedance matching between antenna and RFID chip at the fundamental frequency and at the threshold power of the chip. No great efforts were made at the harmonic frequencies, no constructive neither destructive approaches in terms of signal radiation from the tag side were reported so far.

By other hand, the works integrating EEH with non-linearites of RF devices, i.e. rectifying diodes, opened an interesting field of research in WPT considering both the transmitting and receiving ends. The challenges in the transmitting side are mainly in the selection of the optimum transmitted signal waveform. The final goal of most of these challenges is to take advantage of the non-linear nature of the rectifying elements in order to maximize the RF-to-dc conversion efficiency in the receiving end of WPT systems. Certainly, the integration of these new concepts into the passive RFID technology will write a transversal contribution also in the EEH theory, and in the WPT techniques for the deployment of the IoT.

On the next chapters, the passive UHF RFID tags and chips will be characterized in terms of its non-linear behavior under standard compliance. Details about the signal contents, the information carried on other frequencies, the specific characterization methods and experimental results will be widely discussed.

3. Non-linear characterization in passive UHF RFID tags

In this chapter, a detailed study on the non-linear phenomena presented in the UHF RFID signals when the communication between reader and tag is established, is proposed. The goal is to analyze the harmonics radiated by the tag antenna due the rectifying operation of the passive RFID chip. From experimentation, the characteristics of the non-linearities contained in the RFID signal are highlighted and linked to traditional theory of backscattering in the RFID context. Parametric experiences taking into account standard regulations were performed. Moreover, several commercial tags are considered in order to compare the parametric observations. Special care is paid on the configuration setup of the characterization platform. Details about the used equipment and the protocols are presented. In particular, the generation of periodic and reproducible sequence of bits is introduced and its advantages in the power spectral analysis are emphasized.

The results and discussions presented in this chapter consider the analysis of a whole tag (antenna + RFID chip), which means they include the antenna-chip impedance matching effects, without specific assessment of the chip harmonic production. Specific studies on the non-linear behavior of the chip itself will be treated in Chapter 4.

3.1 Introduction

The operation principle of the passive RFID system was presented in 2.2.1. It can be mainly resumed in two functional aspects:

- Wirelessly powering of tag, where the reader transfers energy to the tag in a wireless mode by sending RF power that the tag must collect and transform into dc power to operate and respond using the backscattering modulation technique.

- Wirelessly data collection, described by a constant interaction between reader and tag, where the reader acts as base station in order to read or write information from the tag.

The RF-to-dc power conversion task performed by the RFID chip, is the well known process of rectification, in which the chip obtains energy to complete its operation to be able to interact with the reader. The rectifier operation is possible thanks to the use of two or more diode-based voltage doubler stages (details on the rectifier architecture and operation will be discussed in Chapter 5). These diodes determine the non-linear behavior of the RFID chip [31; 33].

The objective is to observe the characteristics of the modulated backscatter signal and evaluate the information carried by harmonics due to the non-linearities. The study is done when the communication reader-tag is fully established. Additionally, some analysis regarding the reader harmonic production on the forward link are performed. An important contribution to facilitate the Power Spectral Density (PSD) analysis to easily evaluate the backscattered harmonics is done. The contribution uses a pre-configured RFID air interface in order to produce a periodic sequence of bits on the tag response.

The quantified harmonic level is evaluated and its relation with the performance at the fundamental frequency is analyzed. An experimental parametric study is performed considering the harmonic dependency on reader power, bits sequence structure, and channel in frequency hopping operation. The experimental study is based on calculating the PSD of RFID signals at the harmonic frequencies in forward and return link in compliance of the EPC Class1 Gen2 UHF RFID standard [57].

Section 3.2 explains the basis for the harmonic generation phenomena in passive UHF RFID tags. Section 3.3 proposes settings on the measurement procedure with special attention on the RFID air interface treatment. Section 3.4 describes the scatter capabilities of the measured tags. Section 3.5 presents the properties of the PSD on the analysis of backscattered harmonics. Section 3.6 shows the dependency analysis of the backscattered harmonics . Finally, in Section 3.7 some conclusions are drawn.

3.2 Harmonic backscattering

The reason why the harmonics currents are re-radiated by the tag antenna can be explained looking to similar technologies at low power rectification. The rectennas, devices conformed by one antenna loaded by one rectifier circuit commonly used for Electromagnetic Energy Harvesting (EEH) [64] have a similar rectifier architecture than passive RFID tags. Although rectennas used for EEH and passive RFID tags have a similar RF section, however there is a

small but crucial difference on the non-linear treatment. Because of the non-linearity behavior of the diodes used in the rectifier, appropriate techniques of simulation and optimization are used in those circuit designs. The Harmonic Balance (HB) is a simulation method that considers the effect of the harmonic currents produced by non-linear devices [65]. In the rectenna case, the harmonic currents flow to the dc section and to antenna terminals. If they are well filtered in the dc section side, a pure dc signal can be achieved at the output, then an enhanced the RF-to-dc conversion efficiency is achieved [65–67]. The phenomena can be simulated with the HB method, being possible to predict and to control the behavior of the complete rectenna, both in the dc section as in the antenna side. In passive UHF RFID chips, the harmonics reflected through the dc section, are surely treated during the chip design process, and then an optimal dc signal feeds the digital section of the chip. However, the harmonics are reflected through the antenna since no harmonic treatment is performed on the RFID antenna design. The antenna design in passive RFID tags begins directly from the knowledge of one impedance value. The known impedance is that one of the chip at the fundamental frequency provided in data sheets e.g. [68]. Resuming, the design process aims to ensure the matching at the frequency of operation, but the matching behavior antenna-chip around the harmonic frequencies is unknown. As long as the antenna and the chip are independently designed [16], and depending on the antenna structure, it can radiate some of the harmonic currents generated by the rectifier, which finally triggers in harmonic backscattering [40; 69].

3.3 Measurement procedure

The measurement procedure of backscattered harmonics is based on the observation of RFID signals in time domain and the calculation of its PSD by applying the Fast Fourier Transform (FFT). Fig. 3.1 shows the conceptual procedure. The FFT calculation is made over a Carrier Wave (CW) portion after the *Query* command as it is shown in Fig. 3.2. The measurement procedure directly exploits the possibilities that the RFID air interface offers on its physical layer to facilitate the spectral analysis. The challenge is done by parameterizing the tag response to produce a cyclic and reproducible signal that facilitates the PSD analysis. Details on the measurement procedure are below explained.

3.3.1 RFID air interface

The RFID air interface standard provides parameter definitions for communication protocols within a common framework for globally accepted frequencies in RFID [11]. The RFID air interface describes the way in which a tag communicates with a reader by wireless signals and it is positioned in the physical layer of the multi-layer definition of the RFID system presented in Chapter 2.1.

One of the contributions presented in this chapter is to highlight the characteristics of the backscattering modulation to clearly interpret the time domain signals and its PSD calculation. Characteristics as Backscattering Link Frequency (BLF), data encoding and preamble are pre-configured on the treatment of the physical layer in the UHF RFID system.

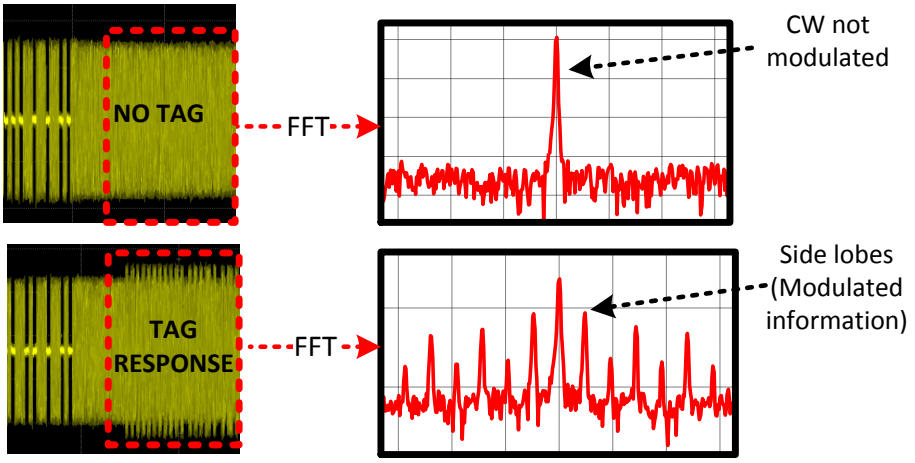

Figure 3.1: Measurement procedure focused on the PSD analysis of UHF RFID signals.

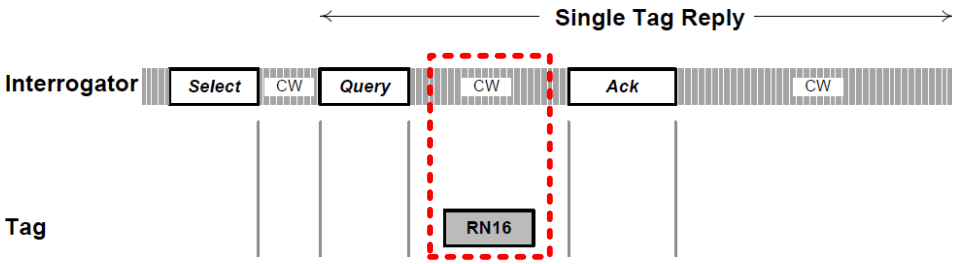

Figure 3.2: Frames timing in forward and return link [57].

3.3.2 Configuration of the physical layer in the UHF RFID system

The configuration of the UHF RFID physical layer is based on the manipulation of the Query command frame sent by the reader. The pre-set Query command achieves one tag responses which its PSD thus allowing to clearly identify its spectral content. It is intended that the BLF would be sufficiently higher to be distant from the carrier and further, make the tag responds with a periodic sequence of bits whose duration is sufficient to perform the FFT.

The tag response to the Query command contains 16-bits pseudo random called RN16. The RN16 response has a preamble with a well-known structure depending on how the Query is composed. Fig. 3.3 shows the Query structure.

	Command	DR	M	TRext	Sel	Session	Target	Q	CRC-5
# of bits	4	1	2	1	2	2	1	4	5
description	1000	0: DR=8 1: DR=64/3	00: M=1 01: M=2 10: M=4 11: M=8	0: No pilot tone 1: Use pilot tone	00: All 01: All 10: ~**SL** 11: **SL**	00: S0 01: S1 10: S2 11: S3	0: *A* 1: *B*	0–15	

Figure 3.3: Query command structure [57].

The experiences presented in this chapter use the Query 10001011000000000001101. The process to configure favorable values of BLF, the data encoding and the preamble is below detailed.

The first four bits allow identifying the command as Query command and last five bits corresponds to the Cyclic Redundancy Check (CRC5) for error detecting and depends of the information content. The information content is the sequence of bits between the Query command identifier and the CRC5. Inside the information sequence, there are three parameters for configuring a favorable tag response.

The bit in the fifth position called Divide Ratio (DR) determines where the BLF is defined. The value that the fifth bit can take " 0 " or " 1 " is traduced in $DR = 64/3$ or $DR = 8$ respectively. In the analysis of the PSD, the BLF which is the spectral distance between the CW component and the tag response will be higher when DR is higher. The calculation of the BLF is determined by the ratio $DR/Rtcal$ where $Rtcal = 5.5 \times Tari$ and $Tari$ is the reference time interval for reader to tag signaling and is equal to the duration of data " 0 " [57]. The couple of bits in sixth and seventh position is called M and sets the tag-to-reader data rate and encoding to which the tag responds. The couple of bits is set to " 01 " which traduces into $M = 2$, which instructs the tag to respond using Miller coding with two cycles per bit as the Fig. 3.4 shows. Finally the eighth bit position called TRext achieves the periodic sequence of bits on the tag response. When $M = 2$ and $TRext =$" 0 ", the tag prefixes a short duration preamble to its RN16 response, instead when $M = 2$ and $TRext =$ " 1 " the RN16 response prefixes an extended preamble of 16 bits of data " 0 " with two cycles per bit defined by $M = 2$. Fig. 3.5 shows the extended preamble scheme. The periodic sequence has approximately 65 μs duration (depending on $Tari$) enough to make the PSD calculation. Other parameters on the Query command were not configured since these are used for inventory purposes when the Select command is previously sent which is not the case. Anyway the values of these remaining parameters do not alter the results.

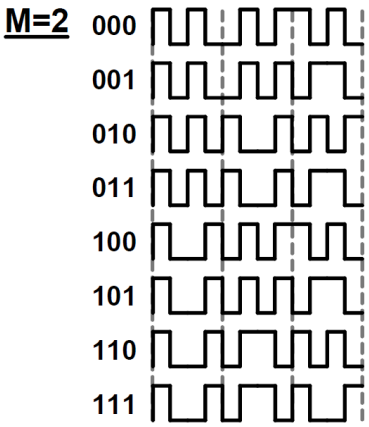

Figure 3.4: Miller sequences for $M = 2$ [57].

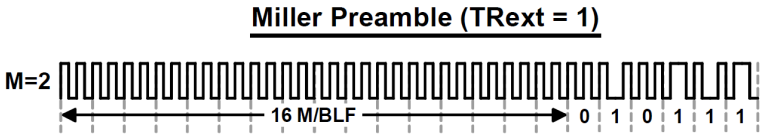

Figure 3.5: Tag $\rightarrow$ Reader preamble with Miller $M = 2$ [57].

3.3.3 Considered tags

In order to validate the measurement procedure, nine different commercially tags (inlays) were chosen. Tags are shown in Fig. 3.7 and details are listed on Table 3.2.

From the two possible options shown in Fig. 3.1, in case of absence of tag only the carrier component is expected on the PSD analysis. Contrary when there is an activated tag, the power of the first side lobe around the CW in the PSD analysis is considered as the power of the modulated tag response. The calculation of the PSD is repeated over the harmonics of the CW until the fifth harmonic order on each tag. The implemented modulation for all the studied tags is the Amplitude-Shift Keying ASK [57].

3.3.4 Measurement system

The measurement system includes a signal generator *Agilent N5182A* for synthesized RFID signal or an Alien Reader ALR-9780 for real RFID signals, a RF amplifier *Empower BBS314AAj* with 41 dB gain, a 12 GHz Digital Storage Oscilloscope *DSO Agilent 91204A* (40 Gsamples/s) and a PC for control and data processing. The set of signal generator and PC is called RFID tester, this configuration allows to manage the Query command. Fig. 3.6 shows the measurement setup in the anechoic chamber with a partition wall that offers 48 dB isolation between horn antennas to minimize the mutual coupling.

- The Element Under Test (EUT) tag is located at a distance of 1m from each horn antenna and oriented for maximum reception and re-radiation.
- The forward link signal is generated by only one of two ways: in synthesized signals, the baseband command generated by Matlab is transferred to the signal generator where it is modulated, amplified and sent to the tag via the transmitting antenna; in signals coming from a RFID reader, an ALR-9780 reader is set to replace the signal generator.
- The return link signal is always collected by the receiving antenna, observed and analyzed in RF band on the DSO.
- In compliance with the EPC Class1 Gen2 standard, the synthesized signal carries the Query command. In the case of signals coming from a RFID reader, the RFID air interface cannot be parameterized and standard handshake is made between reader and tag [57].

The amplifier was used only in power dependency tests, presented in Section 3.6.3.

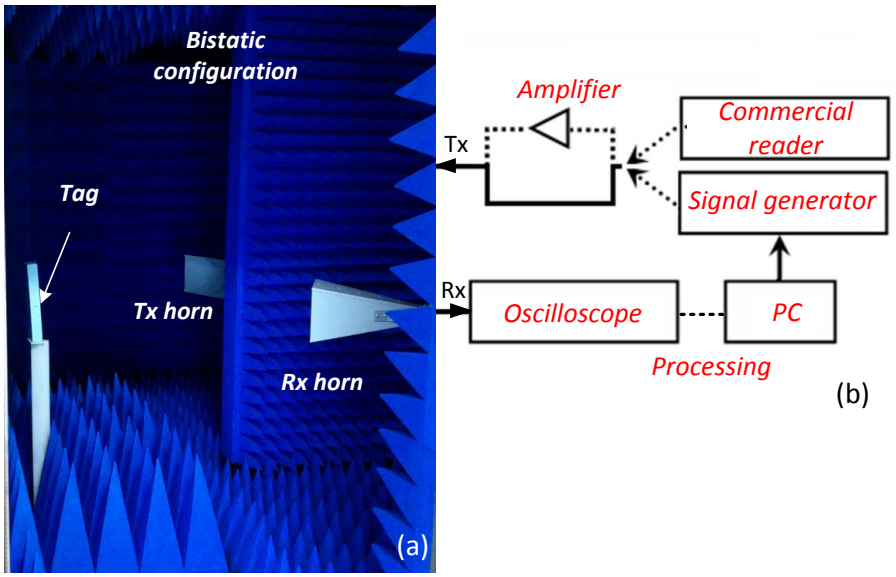

Figure 3.6: (a) Bistatic configuration in the anechoic chamber. (b) Equipment setup

3.3.5 Power budget

The power budget in the band 868 MHz - 922 MHz considering the measurement setup of Fig. 3.6 is described below. Antennas gain A_G varies increasingly between 5.69 dBi and 6.69 dBi on 868 MHz - 922 MHz respectively.

- In transmission: losses in cables 1, 2 and 3 including connectors are -0.73 dB, -0.73 dB and -1.45 dB respectively, the amplifier when is used, inserts a gain of 41 dB.

- In reception: losses in cable 4 and 5 are -0.73 dB and -1.46 dB respectively.
- The noise level inside the anechoic chamber is around -110 dBm.

The power P_{out} delivered by the RFID tester or the reader is varied according to the each tag activation needs. Considering the power budget in transmission and reception and the free space path loss (3.1) at distance R of 1m and the wavelength λ at each frequency in Table 3.1, then it is possible to calculate each tag sensitivity.

$$L = 20\log_{10}(\frac{\lambda}{4\pi R}) \tag{3.1}$$

Table 3.1: Free space path loss.

Frequency	**Loss (dB) European band** ***Fc=868 MHz***	**Loss (dB) US band** ***Fc=915 MHz***
Fundamental	-31.21	-31.67
2^{nd} **Harmonic**	-37.23	-37.69
3^{rd} **Harmonic**	-40.75	-41.21
4^{th} **Harmonic**	-43.25	-43.71
5^{th} **Harmonic**	-45.19	-45.65

3.3.6 Power tag sensitivity

The power tag sensitivity is defined as the minimum power received by the tag necessary to activate its chip and wait for a understandable response on the reader side. Table 3.2 presents each tag sensitivity at fundamental frequency calculated as P_{out} minus 28.12 dB in case of European tags and P_{out} minus 28.58 dB in case of US tags. These subtraction factors correspond to the described power budget.

3.4 Radar cross section and physical area of a RFID tag

3.4.1 Radar cross section and tag dimensions

The Radar Cross Section (RCS) of the tag or echo area is defined as the area intercepting that amount of power which, when scattered isotropically, produces at the receiver a density which is equal to that scattered by the actual object. The RCS σ for dipole antennas of half a wavelength or less, which is the case of common RFID tags is defined as follows [77]

$$\sigma = \frac{\lambda^2}{4\pi} G_t^2 \left| \frac{2R_A}{Z_L + Z_A} \right|^2 = \frac{\lambda^2}{4\pi} G_t^2 K \tag{3.2}$$

Table 3.2: Details of evaluated UHF RFID tags.

Label	Inlay / Manufacturer	Sensitivity) (dBm)	Performance band
T1	Dogbone / UPM [70]	-16.89	US
T2	Sec.Frog / UPM [71]	-12.93	EU
T3	Web / UPM [71]	-11.73	EU
T4	P9-2 / LCIS [72]	-11.29	US
T5	MemoryStick / UPM [73]	-12.29	US
T6	P10-1 / LCIS [72]	-13.63	EU
T7	RapidTrack / Tagsys [74]	-13.43	EU
T8	Tac.Frog / UPM [75]	-13.15	US
T9	AD222 / Avery Dennison [76]	-11.79	US

where Z_L is the impedance of the antenna load, i.e. the chip impedance, Z_A is the impedance of the tag antenna, G_t is the gain of the tag antenna and R_A is the real part of Z_A. The factor K defines the influence of the chip impedance mismatch on the amount of RCS. A matching polarization between reader and tag antennas is considered in (3.2).

It is possible to re-write (3.2) in terms of the power density of an electromagnetic wave incident on the tag antenna in free space, S and the power backscattered by the tag in direction of the reader P_{back} as (3.3)

$$\sigma = \frac{P_{back}}{S} = \frac{KP_cG_t}{S} \tag{3.3}$$

where the collected power by the tag antenna P_c is by definition the maximum power that can be delivered to its chip with a complex conjugate impedance. It can be expressed in terms of the effective area of the antenna A_e as (3.4) [77]

$$P_c = SA_e \tag{3.4}$$

The effective area of the antenna A_e is given by (3.5)

$$A_e = \frac{\lambda^2}{4\pi}G_t \tag{3.5}$$

Then (3.3) can be written as

$$\sigma = KA_eG_t \tag{3.6}$$

The two states of impedance of the RFID chip, which regulate the backscattering modulation technique between scavenging and reflecting condition, yield in two values of K or consequently in two values of RCS. Then from (3.6) it is possible to define the differential RCS or ΔRCS as

$$\Delta RCS = |\sigma_{scavenging} - \sigma_{reflecting}| = |\Delta K|A_eG_t \tag{3.7}$$

where $|\Delta K|$ means $|K_{scavenging} - K_{reflecting}|$. The ΔRCS evaluates the functional characteristics of the tag as read range or sensitivity because it is related to the efficiency of the backscattering modulation technique [16; 33]. Then finally the physical area A_p of the antenna can be linked with its effective area by the aperture efficiency ε_{ap} shown in (3.8)

$$\varepsilon_{ap} = \frac{A_e}{A_p} \tag{3.8}$$

3.4.2 Experimental validation

From (3.6) and (3.8), by considering the physical area of the tag antenna for a given tag, greater resonance surface means greater effective area then higher RCS. Fig. 3.7 shows 20 μs of tag response for the nine tags where the modulated backscatter is clearly distinguishable. Tag T1, which exhibits greater resonance surface, has a great scatter capability then higher RCS. In an ideal condition when $K = 1$ in scavenging state, an antenna loaded with a complex-conjugate impedance load scatters the same amount of power as the load absorbs thus causing a maximum ΔRCS. Although all tags are illuminated with the same power $P_{out} = 16.75$ dBm, It is highlighted in Fig. 3.7 that the amplitudes, directly related with the ΔRCS, vary up to 42%. $P_{out} = 16.75$ dBm represents the power to activate the tag with less sensitivity T4.

Consequently there are two factors involved on the $|\Delta RCS|$ variations (3.7):

- The matching degree between antenna and RFID chip in scavenging state;
- The physical area of the antenna.

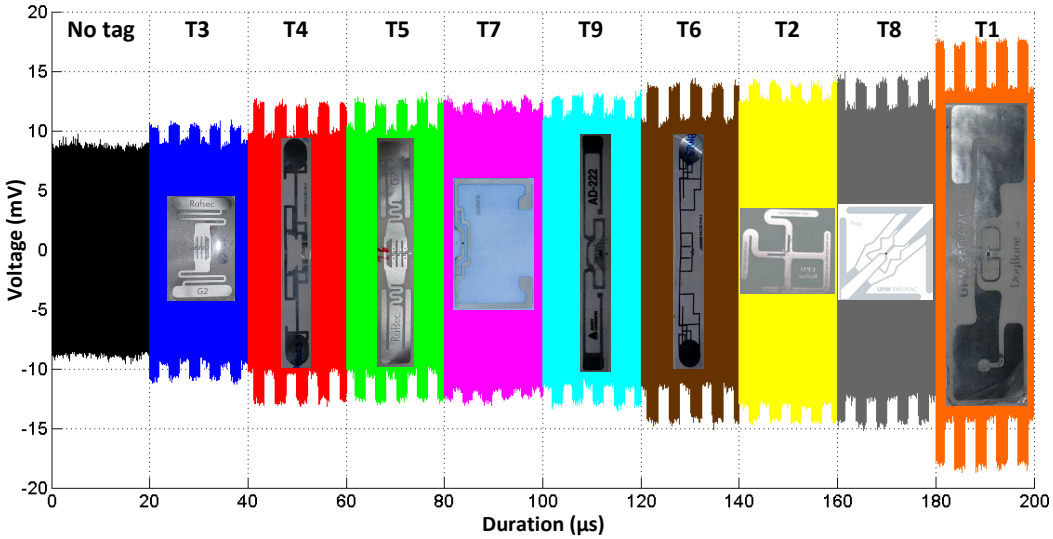

Figure 3.7: Time domain response from nine UHF RFID tags.

3.5 Power spectral density analysis in the RFID system

3.5.1 PSD properties

The interpretation of the PSD is enhanced due to the contribution of the RFID physical layer setting achieving a periodic sequence of bits on the tag response. This implies that the characteristics of the modulated signal coming from the tag are enhanced on the observed window. In effect, in this case the amplitudes of the spectrum are maximal and the BLF is distinguishably positioned at 230 kHz from the CW. It should be noted that for the following analysis, the power of the tag response will be quantified as the amplitude of first side lobe. Fig. 3.8, Fig. 3.9 and Fig. 3.10 show examples of the PSD calculation while the communication reader-tag is established. The PSD at CW fundamental and its harmonic frequencies are compared with the PSD when no tag is present. In this last case, the observed CW is essentially due to the coupling between horns.

Two operational modes of the passive UHF RFID tag are defined in both states of modulation:

- The structural mode M_S produced when the tag antenna is in matching condition. The scattered power contribution is always constant. In this mode $K = 1$ in (3.2),
- The antenna mode M_A is produced by the re-radiated power reflected by the chip load into the tag antenna. The antenna mode depends from the two values that the chip impedance can take. In ideal matching conditions on the scavenging state, the structural mode is equal to the antenna mode.

The scavenging state can be quantified in the PSD level at CW frequency. In reflecting state only the antenna mode changes. The PSD level of tag response in reflecting state is observed at the BLF. On the harmonic analysis, these PSD properties are also valid to analyze the scavenging and reflecting states.

Fig. 3.8 shows the PSD at 915 MHz. Fig. 3.9 and Fig. 3.10 show the PSD at 2^{nd} harmonic 1830 MHz and 3^{rd} harmonic 2745 MHz for tag T5. The tag T5 was chosen because it has the higher PSD level at 3^{rd} backscattered harmonic. In Fig. 3.8 and Fig. 3.10 the tag response with modulated information on the side lobes like a typical spectrum of the square waves is clearly seen. In the case of 2^{nd} harmonic in Fig. 3.9 no response was noted at the activation power.

3.5.2 Matching in scavenging state

In Fig. 3.8, when there is a tag, the PSD level of CW at the fundamental frequency in presence of tag is 6.9 dB higher compared when there is no tag. The 6.9 dB are taken as the total contribution of $M_S + M_A$. The difference at 3^{rd} harmonic is 3.27 dB in Fig. 3.10. On the PSD analysis, the matching in scavenging state can be quantified by the difference of levels at the CW frequency when there is a tag and when there is not tag. The difference has to be minimal representing only the RCS in structural mode. Large differences indicate mismatching reflections. The difference assesses indirectly the RCS characteristics from each tag at fundamental and harmonic frequencies.

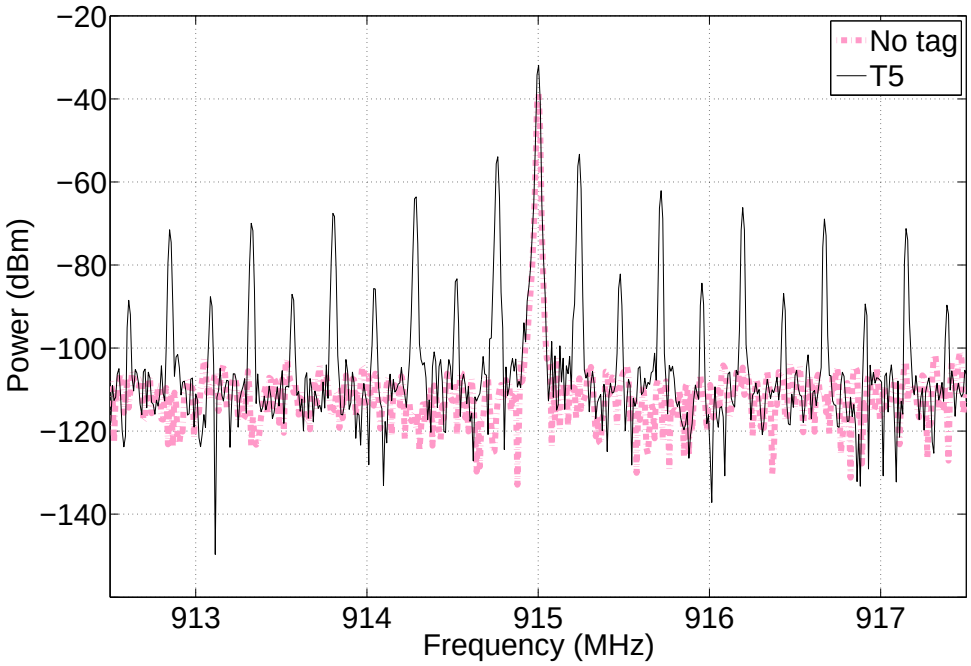

Figure 3.8: PSD at fundamental frequency for tag T5 when $P_{out} = 15.6$ dBm.

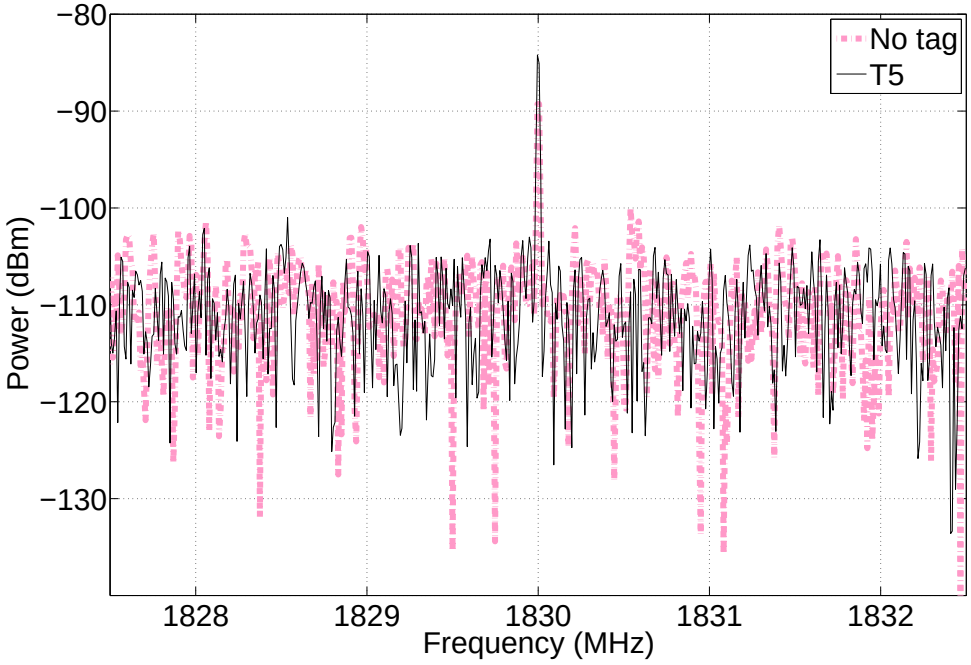

Figure 3.9: PSD at 2^{nd} harmonic frequency for tag T5 when $P_{out} = 15.6$ dBm.

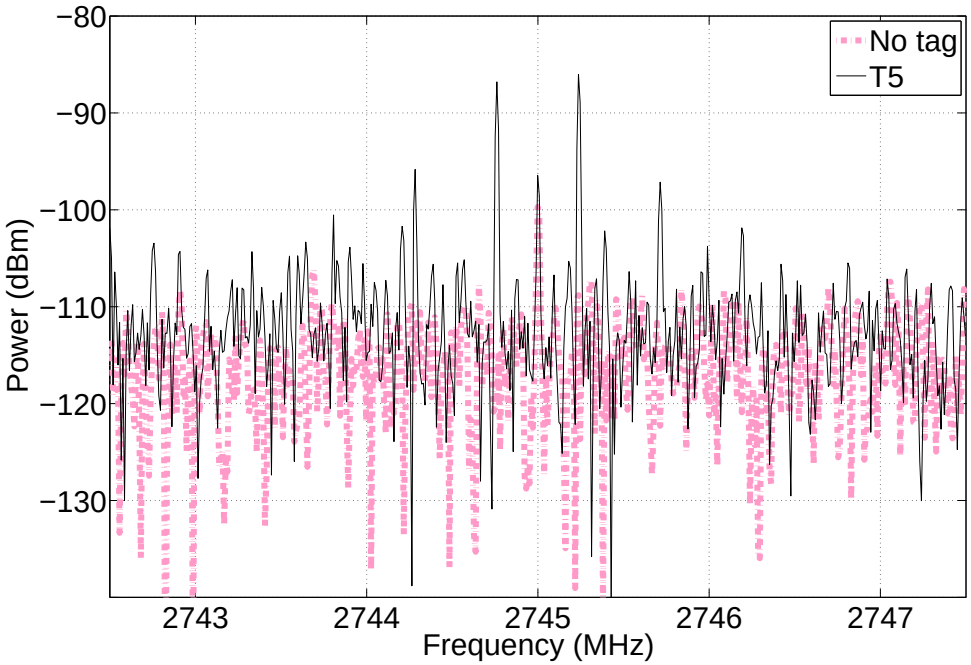

Figure 3.10: PSD at 3^{rd} harmonic frequency for tag T5 when $P_{out} = 15.6$ dBm.

Fig. 3.11 shows the PSD value on the CW fundamental frequency and CW harmonics for five representative tags until the $5th$ harmonic considering each tag sensibility. The mesh represents the measured CW power when no tag is present also until $5th$ harmonic. A decreasing behavior is observed while the harmonic order increases. Only tag T1 is the exception having a 2^{nd} backscattered harmonic weaker than 3^{rd} with revels scavenging properties at 2^{nd} harmonic. Tag T5 has the best scavenging performance, i.e., the better matching at 3^{rd} harmonic according to the criterion of minimal difference of PSD levels at the CW frequency.

In the performed setup, the PSD calculation at the CW frequency represents the coupling between the horn antennas which reveals CW harmonics coming from the RFID tester. Scatter capabilities of each tag varies the level of the observed CW, that depends on each tag RCS.

3.5.3 Backscattered harmonics

The level at the BLF in the PSD analysis at each CW harmonic represents the backscattered harmonics in reflecting state. It is important to explain the basis of harmonic radiation of the tag antenna usually designed as optimization process of a half wave dipole at fundamental frequency. Fig. 3.12 shows the harmonic current distributions on a half wave dipole working at fundamental frequency, which shows that for even harmonics the current at the antenna input is zero. Although if even harmonics were produced by the RFID chip, they would not be efficiently re-radiated since the half wave dipole would require infinite impedance at even harmonics, in fact practically impossible [78]. Fig. 3.13 shows the level contributed by five representative

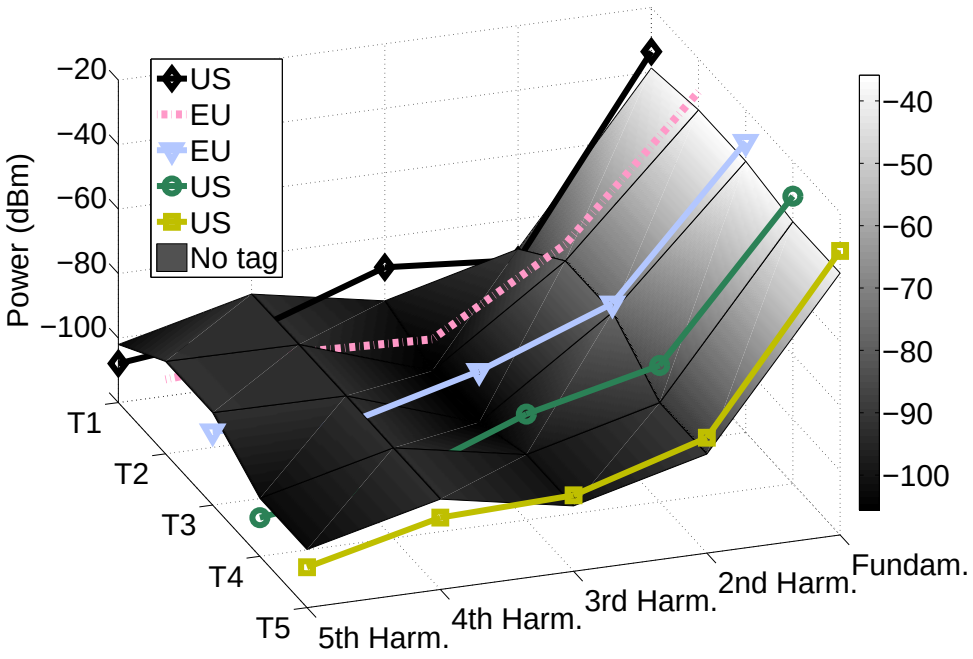

Figure 3.11: Measured PSD at CW harmonic frequencies with P_{out} considering each tag sensibility.

tags on its modulated response at each harmonic frequency. In all cases, the fundamental and 3^{rd} harmonic response is predominant. Even though 5^{th} is an odd harmonic, it has a hardly distinguishable level. Then the affirmation of a perceptible 3^{rd} backscattered harmonic carrying information is valid.

The higher power of the 1^{st} side lobe on 3^{rd} backscattered harmonic is for tag T5 with -86.03 dBm. Considering this value there were not significant 2^{nd} harmonics. Table 4.2 summarizes the results for the 2^{nd} and 3^{rd} harmonics for all tags regarding each tag sensitivity.

3.6 Dependency analysis of harmonic scattering

3.6.1 Dependency on operation at the fundamental frequency

Analyzing the harmonic performance respect to the results at the fundamental frequency, section 6.2 presents tag T1 with the best performance at fundamental frequency. However the analysis, made in section 3.5.3, presents tag T5 with the higher 3^{rd} backscattered harmonic. The performance of the tag depends basically on the antenna-chip matching and its physical characteristics (3.7) at the frequency of interest. Since the tag antenna has different designs, some of them can be close to a matching situation on some odd harmonics profiting the current distribution over the dipole shown in Fig. 3.12, specially the 3^{rd} one due its level. Certain degree of matching at the harmonic frequency may cause that the antenna re-radiates the harmonics produced by the RFID chip. But there is not directly dependency between performance at

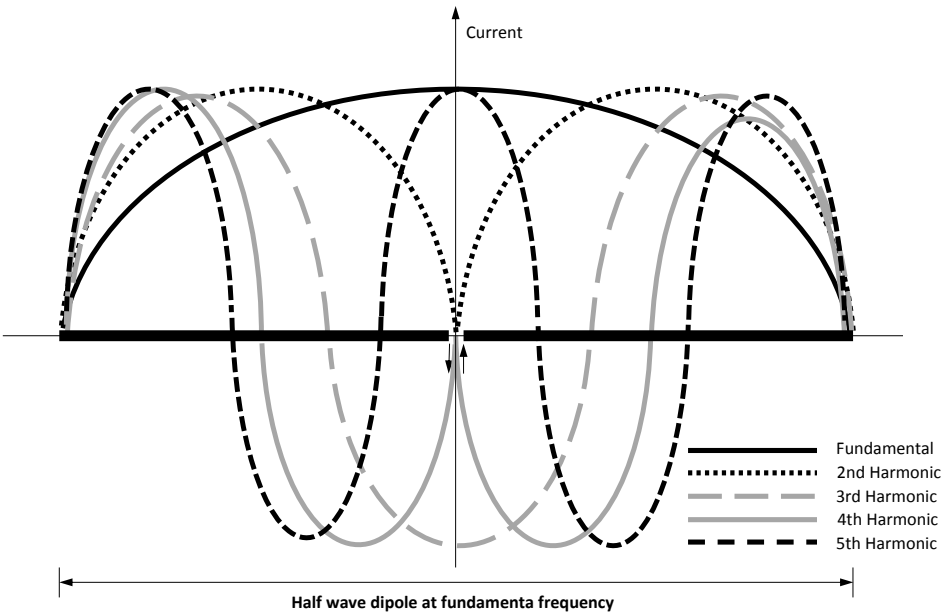

Figure 3.12: Current distribution until $5th$ harmonic along the length of a half wave dipole designed for fundamental frequency. The half wave dipole requires zero admittance at even harmonics to be able to radiate.

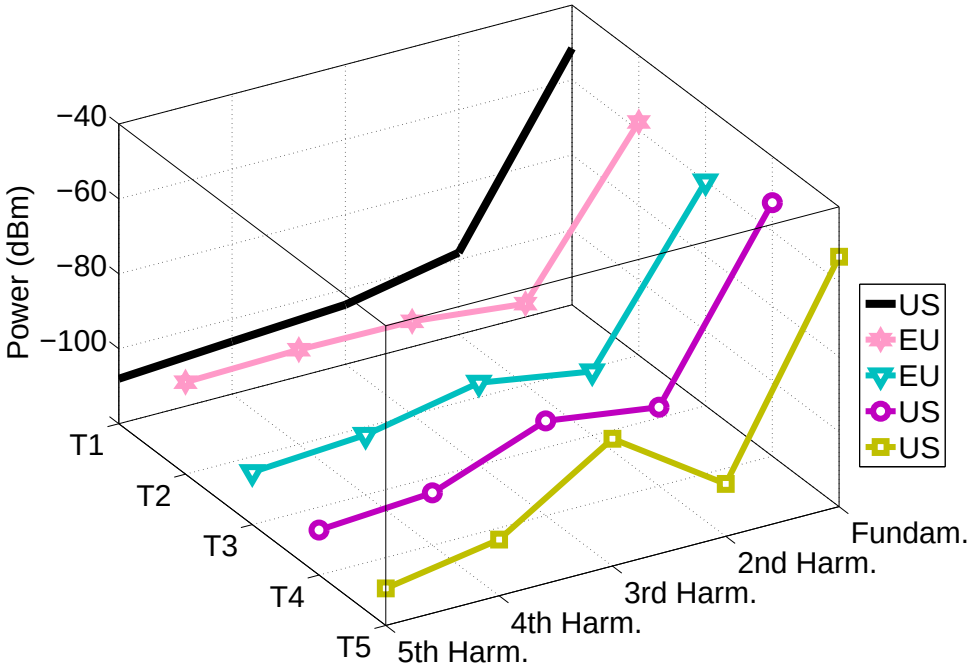

Figure 3.13: PSD of the tag response at the BLF. P_{out} considers each tag sensibility.

Table 3.3: Backscattered harmonics from tag response.

Tag	2^{nd} **harmonic Power (dBm)**	3^{rd} **harmonic Power (dBm)**
T1	-98.11	-104.1
T2	-98.29	-95.08
T3	-102.9	-98
T4	-99	-94.72
T5	-106	-86.03
T6	-100	-92.08
T7	-104.7	-104.5
T8	-102.4	-98.24
T9	-98.39	-93.34

fundamental and backscattered harmonics .

3.6.2 Dependency on bits sequence

Achieving the manipulation of the RFID air interface to reproduce tag responses with different bit structures, enables the development of a bit sequence dependency analysis. The dependency on the sequence of bits on the backscattered harmonic is studied by calculating the PSD over a random bits sequence, by randomly choosing a portion of the RN16 response instead of the preamble. Therefore the comparison of PSD was made on two different sequences when $P_{out} = 16.75$ dBm. Fig. 3.14 shows the PSD comparison at fundamental frequency for tag T4. As expected, the side lobes in the periodic sequences are thin and powerful compared to those in the random sequences. The same behavior is observed for the 3^{rd} harmonic in Fig. 3.15. In order to compare the power levels of the modulated tag response until 5^{th} harmonic from periodic and random sequences, Fig. 3.16 shows the data for tag T5. The PSD level of periodic signals is higher until 4^{th} harmonic. In the 5^{th} harmonic, the relation is inverse, but close to the noise level. Then the sequence of bits transmitted by the tag influences directly on the backscattered harmonics . The merit of the air interface configuration is that it can reproduce a tag response carrying a periodic sequence of bits over all EPC Class 1 Gen2 tags facilitating the PSD analysis. Looking into applications, the use of periodic sequences can be an advantage to achieve a distinguishable power to distinguish signals from different sources or positions.

3.6.3 Dependency on reader power

The reader power dependency is studied by varying P_{out} from the minimum level to activate the tag with less sensibility until reach the equipment limit or saturate the tag in certain cases. No low pass filter was used at the reader output in order to reproduce a normal scenery in compliance

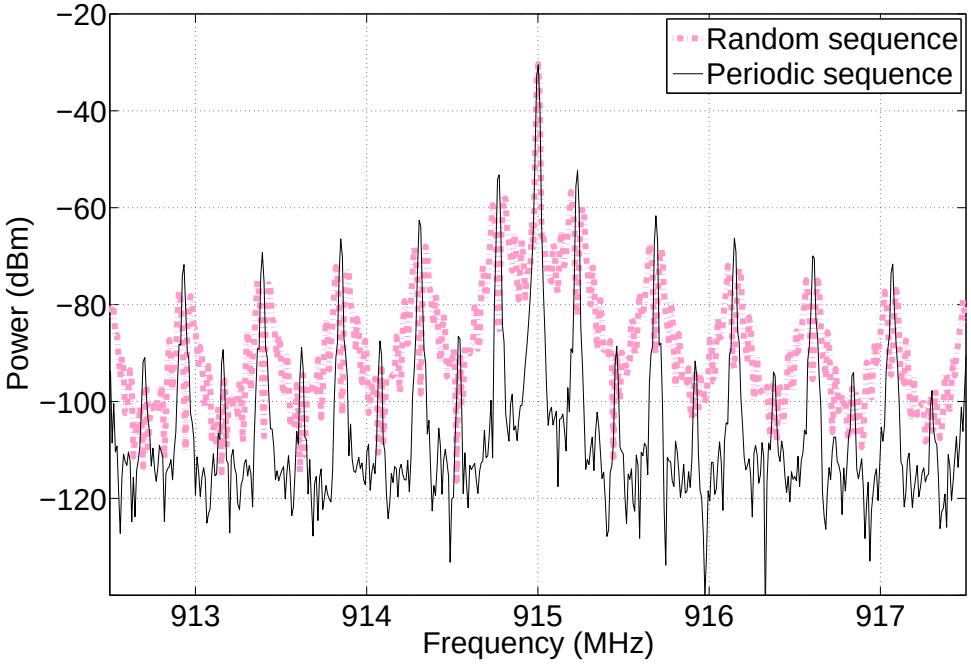

Figure 3.14: PSD of periodic and random sequence of bits in the response of tag T4 at fundamental frequency.

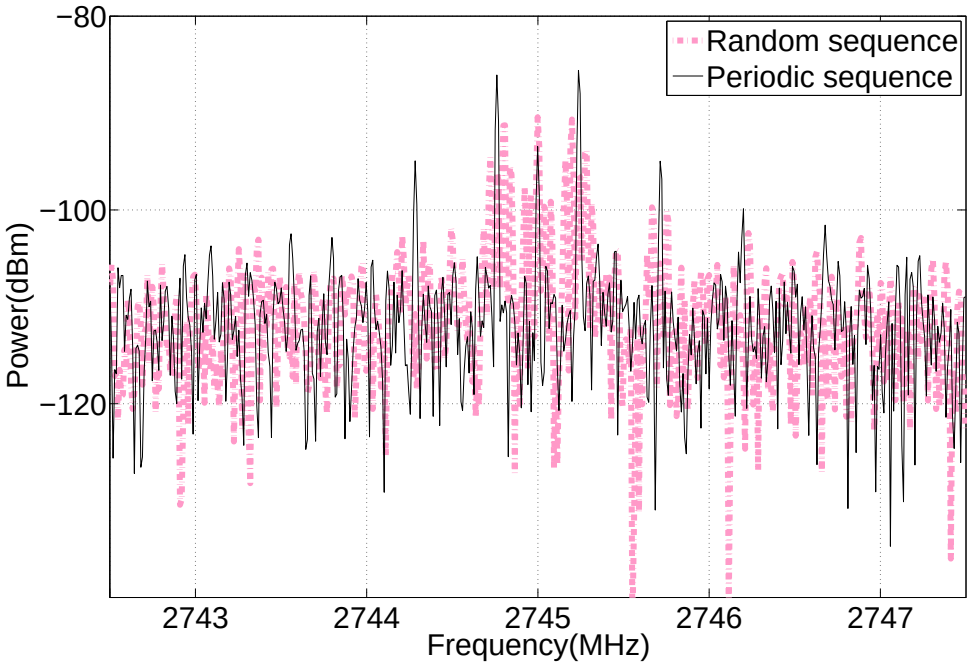

Figure 3.15: PSD of periodic and random sequence of bits in the response of tag T5 at 3^{rd} harmonic.

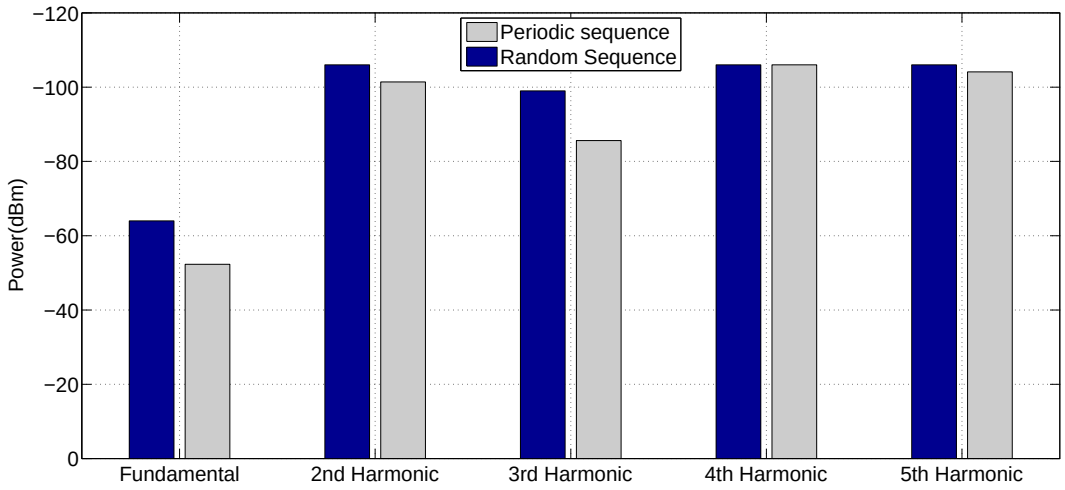

Figure 3.16: Comparison of PSD level from periodic and random sequence response for tag T5.

of the EPC Class 1 Gen2 standard regarding the transmitted power level at fundamental and spurious bands. For this experience two sources were considered: (1) RFID tester and (2) $ALR-9780$ reader. Fig. 3.17 shows the comparison of both sources. The 2^{nd} CW harmonic and 3^{rd} CW harmonic from the reader are even 14 dB and 2 dB greater than the RFID tester respectively, for 4^{th} and 5^{th}, the reader A second set of tests was performed this time introducing the amplifier after the signal generator, which allows evaluations on wide ranges of power. The amplifier introduces 41 dB of gain. P_{out} is first set to $P_{out} = -24.2$ dBm, which represents an average power of operation enough to work with all available tags. An increment of 19.2 dB which means $P_{out} = -5dBm$ does not affect the strength of tag response at fundamental frequency as can be seen in Fig. 3.18 but only affects the level at CW frequency. Contrary Fig. 3.19 and Fig. 3.20 shows that this effect is clearly constructively for the 2^{nd} and 3^{rd} harmonic of the tag response. Then the backscattered harmonics depends directly on the power level that the reader transmits. Two reasons can explain this effect both based on the increment of harmonic level from the reader:

- By increasing the reader power, the input impedance of the chip changes because its non-linear behavior and this make change the matching with the antenna. Depending on this, the shunt transistor, which regulates the internal supply voltage of the logic part, receives power to activate it and works increasing until its upper power limit [79].

- The tag could respond at the harmonic Query. The effect in which the tag responds at various frequencies is called *backscattering frequency diversity* and was reported in [51; 52].

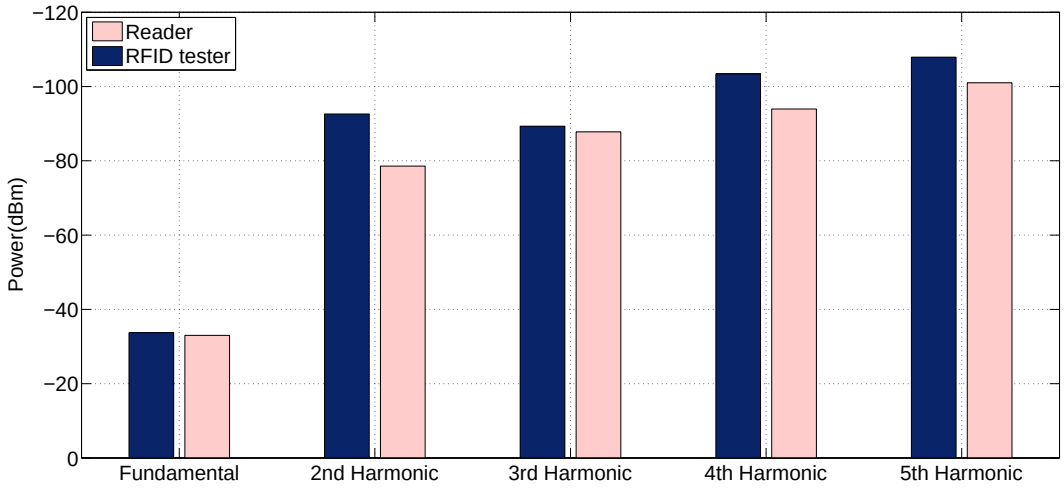

Figure 3.17: Comparison of harmonic levels generated from the RFID tester and one commercial reader.

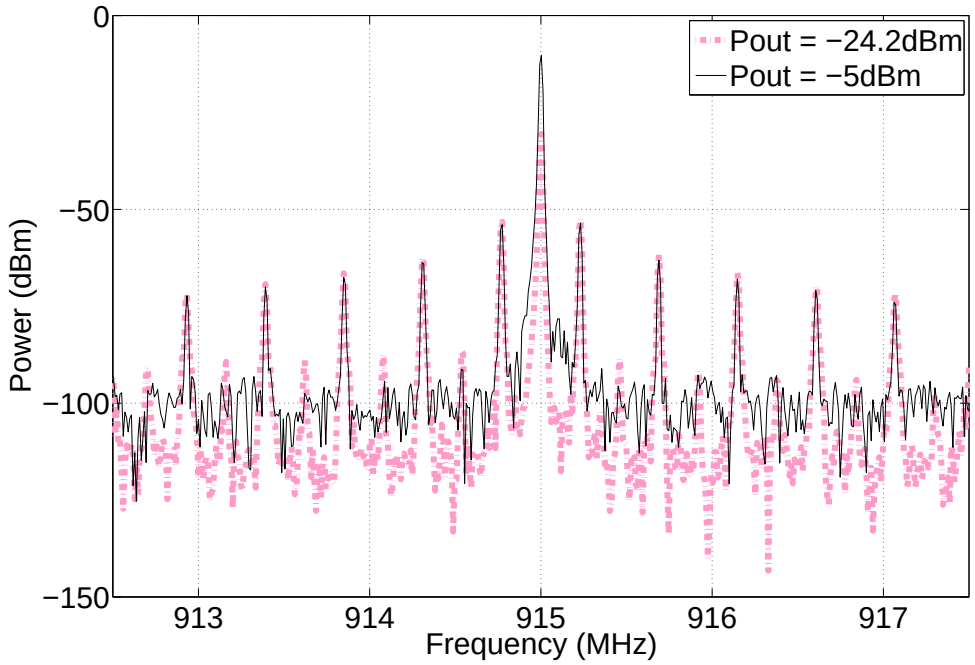

Figure 3.18: Effect of the transmitted power on the backscattered response at fundamental frequency.

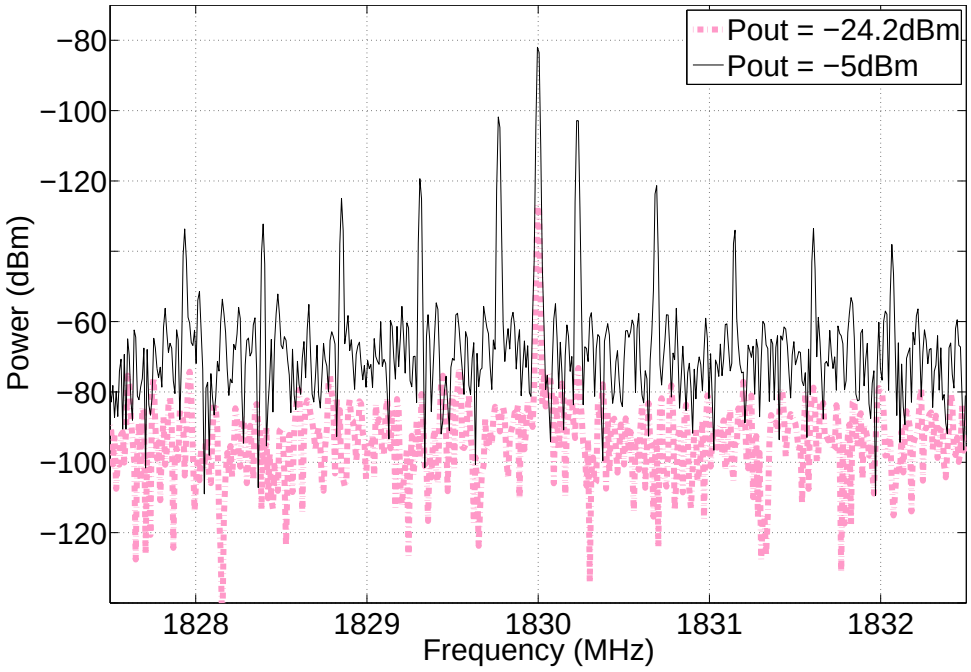

Figure 3.19: Effect of the transmitted power on the 2^{nd} backscattered harmonic.

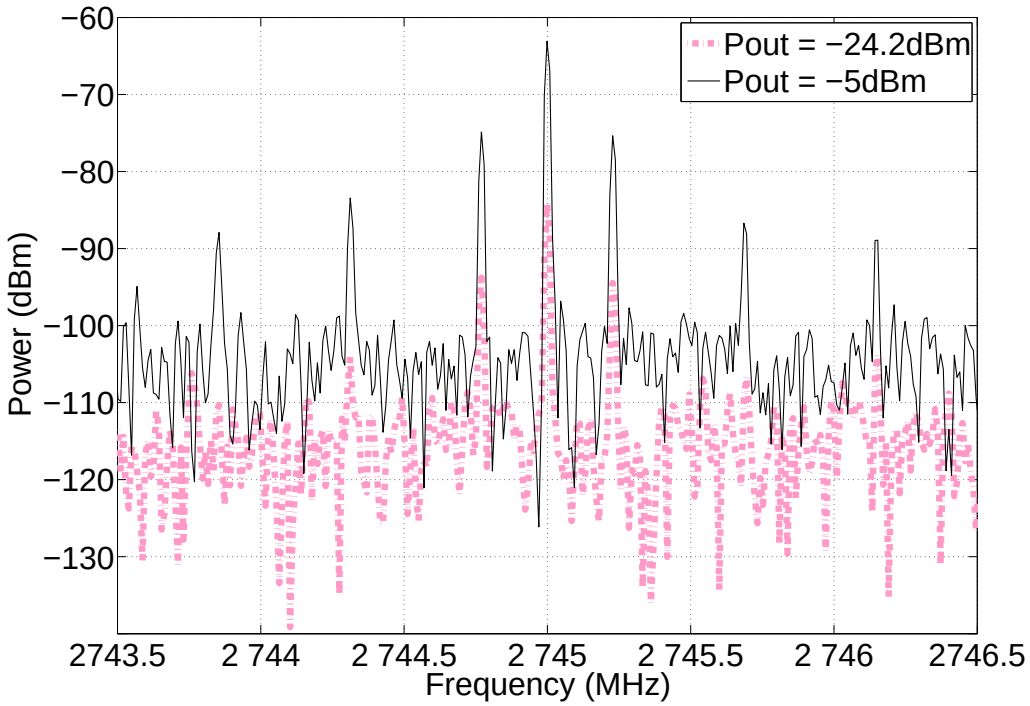

Figure 3.20: Effect of the transmitted power on the 3^{rd} backscattered harmonic.

3.6.4 Dependency on frequency hopping

The Frequency Hopping Spread Spectrum (FHSS) technique is based on the automatic hopping of the CW frequency at brief time intervals. The frequency is chosen in a pseudo random way from a set of frequencies covering much wider band than the bandwidth required to transmit the signal containing the useful data. In the US, according to the current Federal Communications Commission (FCC) regulation, the FHSS can be used to sweep the frequency band from 902 MHz to 928 MHz with 500 kHz width per channel [57]. Fig. 3.21 shows the PSD level at fundamental CW frequencies over the entire US band for tags T1, T4 and T5. The top curves represent the PSD at the CW frequency and bottom curves represent the PSD level at the BLF. The CW level varies 3dB over the entire band. The bottom curves however are almost constant. As was described before, the impedance of the RFID chip varies according to the received power. Then this variation is capable to help or harm the chip performance at fundamental harmonic depending on the tag antenna impedance bandwidth. In this case, the 3 dB variations on the CW level are not affecting the tag response on the US band. Fig. 3.22 shows the PSD level at 3^{rd} CW harmonics for the same tags T1, T4 and T5. The PSD level at BLF on the 3^{rd} harmonic varies until 10dB while the PSD level at the BLF varies 5dB. The non-constant level of the tag response at 3^{rd} harmonic is consistent since the tag impedance bandwidth is not tuned over this band. The variations of PSD level at BLF on the 3^{rd} harmonic band shows indirectly relation with the FHSS channel. The indirectly relation states that there is a major cause: it is in fact the matching degree at 3^{rd} harmonic. The PSD level at the BLF also depends on the channel conditions which are different in each band due to fading phenomenon [80]. Then there is not directly dependency on the FHSS technique.

3.7 Conclusion

A practical experimentation of the non-linearities in the RFID UHF system was performed in this chapter. The measurement procedure is based on the PSD analysis performing a temporal acquisition directly in RF band while the communication tag-to-reader is fully established. By setting the Query parameters it is possible to manipulate the RFID physical layer in order to facilitate the PSD interpretation. The PSD calculation reveals harmonics on the return signal consequence of the not treated non-linearity effects of the RFID chip. It was also noted harmonics generated by the reader in the forward signal. The uncontrolled non-linearity in the current UHF RFID technology allows the tag to generate harmonics signals carrying information without constraints to the EPCGlobal Class 1 Gen 2 standard. The backscattered harmonics are independent of the performance at the fundamental harmonic and of the FHSS transmission technique but depend on the power sent by the reader and the sequence of bits that the tag transmits.

The analysis made on this chapter considers the entire tag (antenna and RFID chip) as element under test. The analysis evaluates the non-linearity characteristic of a UHF RFID EPC Class1 Gen2 tag without specific consideration on the kind of chip used. In order to assess the harmonic generation from the chip itself, the characterization of the RFID chip alone will be the heart of the matter in the next chapter.

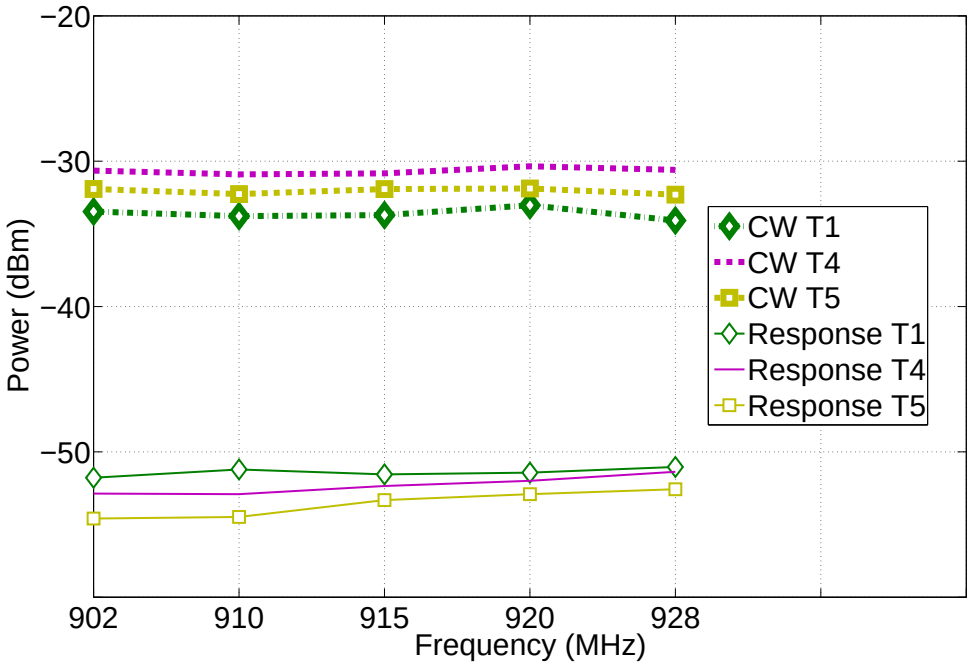

Figure 3.21: Power on frequency hopping channels at fundamental frequency.

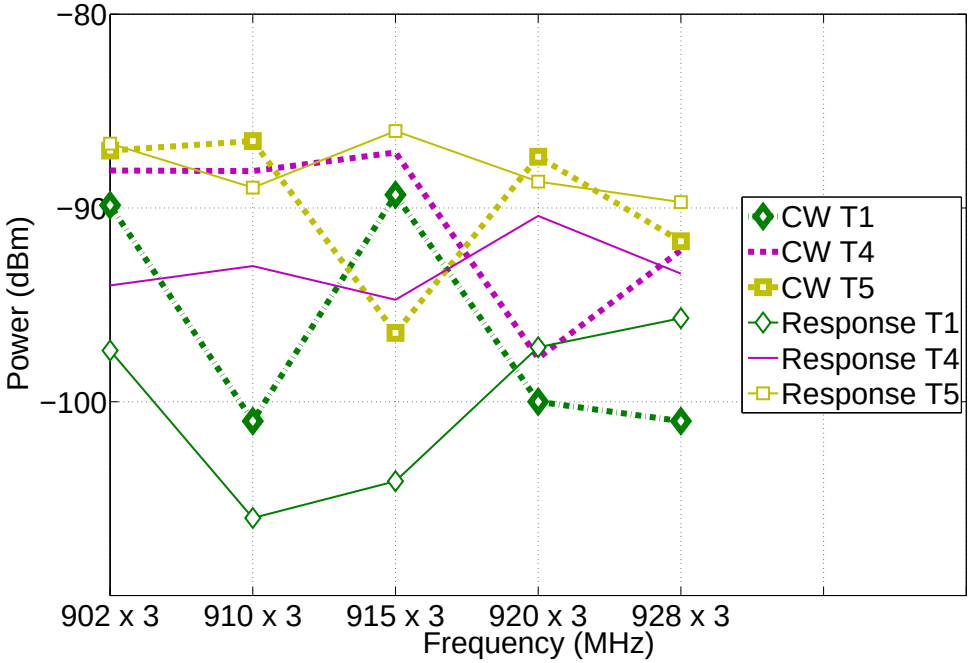

Figure 3.22: Power on frequency hopping channels at the 3^{rd} harmonic.

4. Non-linear characterization in passive RFID Chips

This chapter presents a complete RFID test platform to characterize the non-linear effects produced by passive UHF RFID chips. In full operation mode, automated measurements of activation power, harmonic response level, and impedances are performed in a wide frequency range up to the 4^{th} harmonic. The characterization method, platform composition, and operation are explained through real measurements on UHF Class-1 Generation-2 chips. A harmonic treatment is presented thanks to the joint use of an RFID tester and impedance tuners. The effect of the antenna-chip impedance matching on the harmonic responses is compared before and after treatment. So far, no similar platform has been presented in the literature.

4.1 Introduction

In passive UHF RFID systems, the challenge is always to develop reduced size and cheap tags. For this purpose, new test platforms, characterization methods, and prototype techniques are definitely required to accurately characterize the tag performance and propose design improvements. The existing test platforms, such as in [81–87] are based on the measurement of, at that time, traditional features of the tag, e.g. the chip-antenna integration [81], impedance matching condition [82; 85–87] or differential radar cross section (ΔRCS) and sensitivity [83–86]. In addition, most of the methods to characterize the RFID chip are performed without activating the chip during measurements [81; 82; 86; 87] and always at the fundamental frequency. These existing test platforms and methods are not well suited to evaluate the new functionalities of RFID tags, especially those caused by their non-linear behavior.

Chapter 3 showed the existence of modulated backscattering signals backscattered by the tag at harmonic frequencies of the CW. So far, it is known that the diode-based rectifier operation performed by the RFID chip determines the non-linear behavior of the chip resulting in harmonic signal production [31; 33] where the impedance modulation is still carried producing a redundant backscattering modulation. This concept is illustrated in Fig. 8.1, showing an RFID tag backscattering information not only on the fundamental frequency (e.g. 868 MHz) but also, for example, at the 3^{rd} harmonic (i.e. 2604 MHz). Further details about the rectifier architecture and operation will be discussed in Chapter 5.

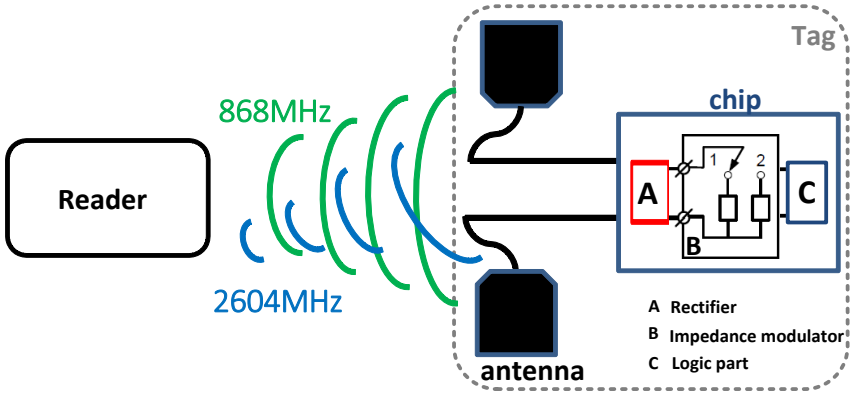

Figure 4.1: Illustration of the presence of multiple channels in the tag-to-reader communication link. The impedance modulation is still contained in the harmonic signal.

As was experimentally demonstrated in Chapter 3 by means of radiating measurements, commercial tags radiate some of the reflected harmonic currents generated by the rectifier, due to independent design of antenna and RFID chip [88]. In order to delimit and characterize the source of non-linearities in RFID tags, the definition of a specific test platform, enabling accurate measurements during RFID chip operation in a wide frequency range (including harmonics), is needed. With such a motivation, this chapter aims to meet two main objectives:

- to define a new RFID Non-linear Test Platform (RFID-NTP) to perform a thorough

characterization and a study of the non-linear phenomena (particularly harmonic signals carrying information during an RFID communication);

- to carry out an experimental study to show the effect of the non-linear treatment from the tag antenna side (basically based on antenna-chip matching experiences at different bands).

This chapter is organized as follows. Section 4.2 describes in detail the proposed RFID-NTP and explains the measurement procedure of harmonics in passive UHF RFID chips. Section 4.3 presents a measurement example. Sensitivity, harmonic response level, temporal analysis, and impedance are measured at the fundamental and harmonic frequencies. Additionally, some drawbacks on the conducted measurements are discussed by comparing the performance of this method with on-chip measurements. Section 4.4 presents harmonic treatment studies by emulating antenna-chip matching conditions. The assessment of the non-linear effects on the tag performance is presented and the possibility to exploit them by implementing frequency diversity with the same chip is also discussed. Finally, conclusions are drawn in Section 4.5.

4.2 Non-linear characterization platform

Regarding the feature functionalities of the above reported characterization platforms, three groups of contributions are below highlighted in order to guide the developing of the envisaged RFID-TP.

- So far, all contributions have reported measurement techniques and methods only at the fundamental frequency;

- Most of contributions do not allow the activate the RFID chip while characterizing it [81; 82; 86; 87], with the only exception of the platform reported in [79], which uses a special fixture to hold the RFID chip;

- The work reported in [86] and [87] proposes a simple fixture, by means of using standard 50 Ω SMA connectors to hold the RFID chip without special matching.

The measurement procedure presented in this chapter combines two techniques: [86] for the simple chip fixing and [79] for measurement in temporal and frequency domain while the chip is activated. Additionally, the measurement is performed in a wide frequency range allowing to characterize until the 4^{th} harmonic of 868 MHz. The waking up of the chip, according to the EPC Class-1 Generation-2 UHF RFID standard [57], was done as in the measurement setup described in Chapter 3. The analysis method is based on the measurement of the Power Spectral Density (PSD). Unlike the radiated measurements presented in Chapter 3, the RFID-NTP includes a vectorial characterization of the RFID chip. One of the contributions of the RFID-NTP is the possibility to measure both impedance modulation states (scavenging and reflecting) in a wide range of frequencies.

4.2.1 System description

The block diagram of the RFID-NTP is shown in Fig. 4.2. Two main parts are highlighted: the first one consists of specialized equipments for microwave measurements and named RFID tester; the second one is based on two impedance tuners connected in series and providing the complex conjugate of the chip impedance of the scavenging state which, in fact, is the optimum antenna impedance. This last part is named antenna impedance emulator. With the described configuration, a complete characterization can be performed under full communication between RFID tester and chip. The setup of the RFID-NTP depicted in Fig. 4.3 is described below:

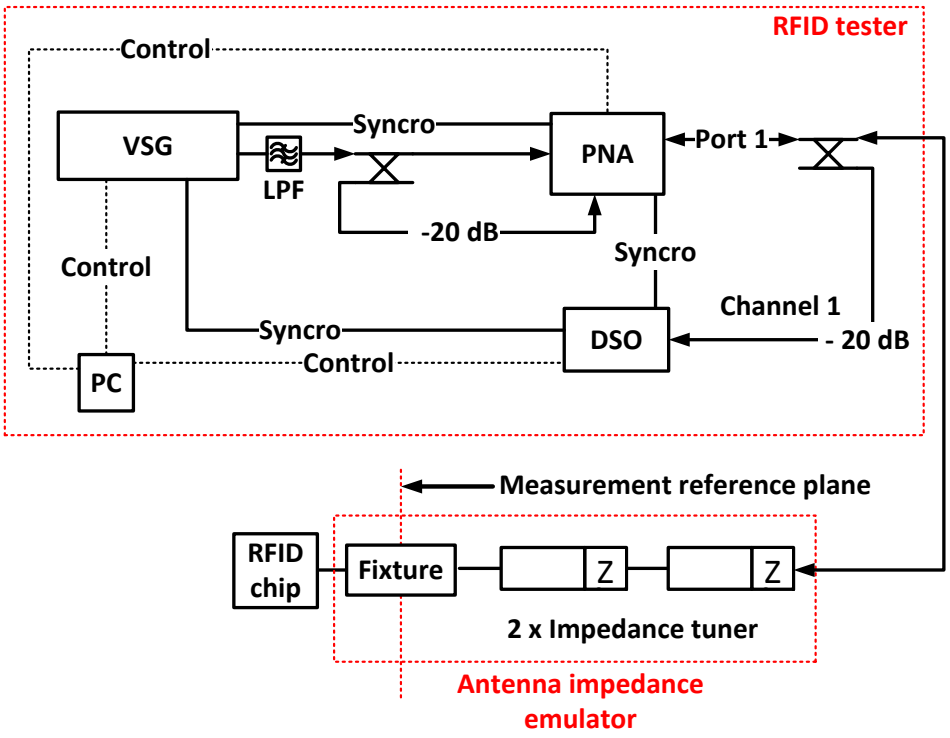

Figure 4.2: Structure of the RFID-NTP used to characterize the backscattered harmonics by RFID chips.

RFID chip fixture

The RFID chips were fixed over 50 Ω SMA connectors [86]. Soldered connections and gluing by conductive ink connections are possible. The chip fixtures and calibration kit are shown in Fig. 4.4 (a).

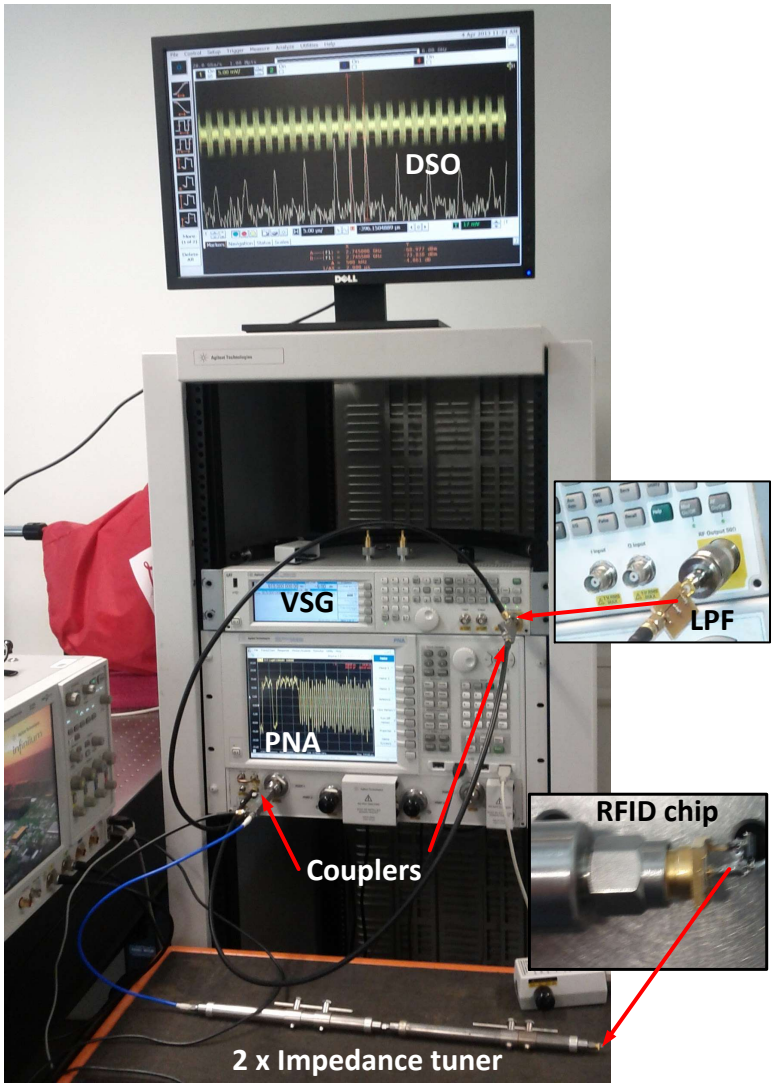

Figure 4.3: RFID-NTP with the RFID chip connected.

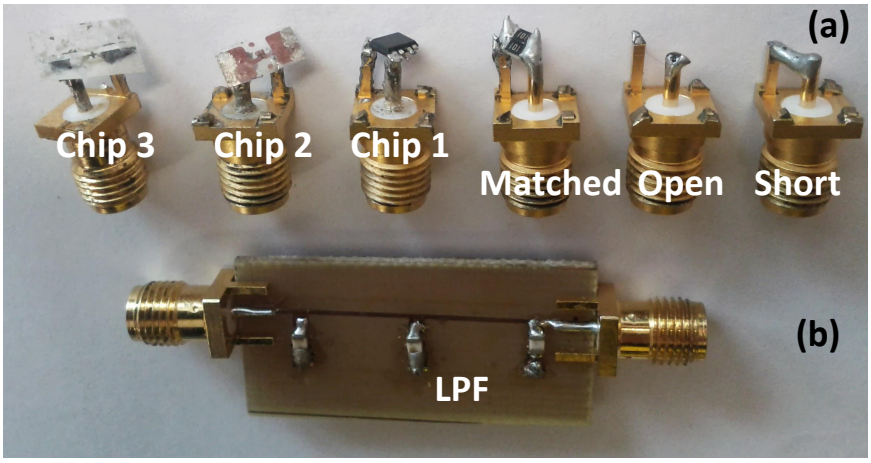

Figure 4.4: (a) RFID chips and calibration kit. (b) Low pass filter used to reject harmonics from the RFID tester.

Antenna impedance emulator

Two impedance tuners Microlab SF-30F are connected in series to provide matching between the 50 Ω RFID tester and the RFID chip. When the matching is achieved, the chip is in scavenging state and, once activated, it switches between the two modulation states. Details are shown in [79].

RFID tester

- an Agilent N5182A Vector Signal Generator (VSG) is used to generate and to send the Query command (1000)[57] at 868 MHz;
- a 20 dB Low Pass Filter (LPF) is connected at the RF output of the VSG in order to filter its harmonics and ensure the chip harmonic response is self-generated. Fig. 4.4 (b) shows the adopted LPF;
- an Agilent N5224A Programmable Network analyzer (PNA) used as external source the VSG. After the Query command is sent, the PNA determines the impedance of the chip during scavenging and reflecting states over a temporal sweep at the frequencies of interest. The use of the PNA allows to perform a vectorial characterization of the RFID chip;
- a first C123E-20 ATM 20 dB directional coupler is used to inject the signal coming from the VSG (input port of the coupler) to the PNA (transmitted and coupled ports of the coupler). This setup allows to properly configure the external source for the PNA [89];
- a second C123E-20 ATM 20 dB directional coupler allows to visualize the chip response from the coupled port, on the oscilloscope, and to separated it from the CW. The

visualization allows to set the optimal position of the impedance tuners by minimizing the CW level. The direct port goes to the PNA;

- a 12 GHz 40 Gsamples/s Agilent 91204A Digital Storage Oscilloscope (DSO) connected to the coupled port of the second coupler allows to clearly see the chip response. Additionally, a PSD analysis is performed over the time window to assess the level response of the chip;

- output power, timing, synchronization, triggering and data acquisition are controlled by a Matlab program running on the host PC.

4.2.2 Calibration

The flow diagram shown in Fig. 4.5 describes the calibration and measurement procedure used for each chip. The minimum activation power for a given chip was found by an iterative up-and-down process until the PSD detected a tag response. In the calibration step, a first traditional calibration at the measurement reference plane shown in Fig. 4.2 was done using the PNA E-cal module [90]. After this, the de-embedding of the SMA connector was performed by means of a second calibration at the same plane, now using the pre-defined Short Open Load (SOL) kit shown in Fig. 4.4 (a). In the power budget calibration, the losses of the directional couplers, cable and connector must be considered. Finally, the characterization of harmonic responses consists in applying the same procedure, but now by setting the temporal sweep of the PNA and the PSD analysis in the DSO, to the frequency of the harmonic. Note that the VSG transmits only at the fundamental frequency 868 MHz and the chip activation is always observed at this frequency.

This process was repeated for each chip under test. The data acquisition was automated by a Matlab script which uses the Agilent Command Expert tool [91] to easy program the interconnection between equipments, scope options, and sweep parameters.

4.3 Measurement example

The RFID-NTP described in this chapter was used to measure and characterize several RFID chips. As an example, this section presents the measurement results for three commercial RFID chips: (1) G2XM NXP SOT505-1 [92], (2) G2XM NXP SOT1040-AA1 [92] with strap, and (3) Impinj Monza 5 [68] extracted from the commercial inlay AKtag [2]. Example results of the PSD analysis in the DSO, in a frame where the chip respond are shown in Fig. 4.6.

4.3.1 Sensitivity and impedance

A power sweep was performed to determine the activation power of the chip remaining the impedance tuners fixed after the calibration. For each power step, the response level and chip input impedance for the fundamental and its harmonics until the 4^{th} were measured. Fig. 4.7 shows the response level at the fundamental frequency for the three chips. The waking up point for each chip determines its minimum operating power, also known as chip sensitivity. For

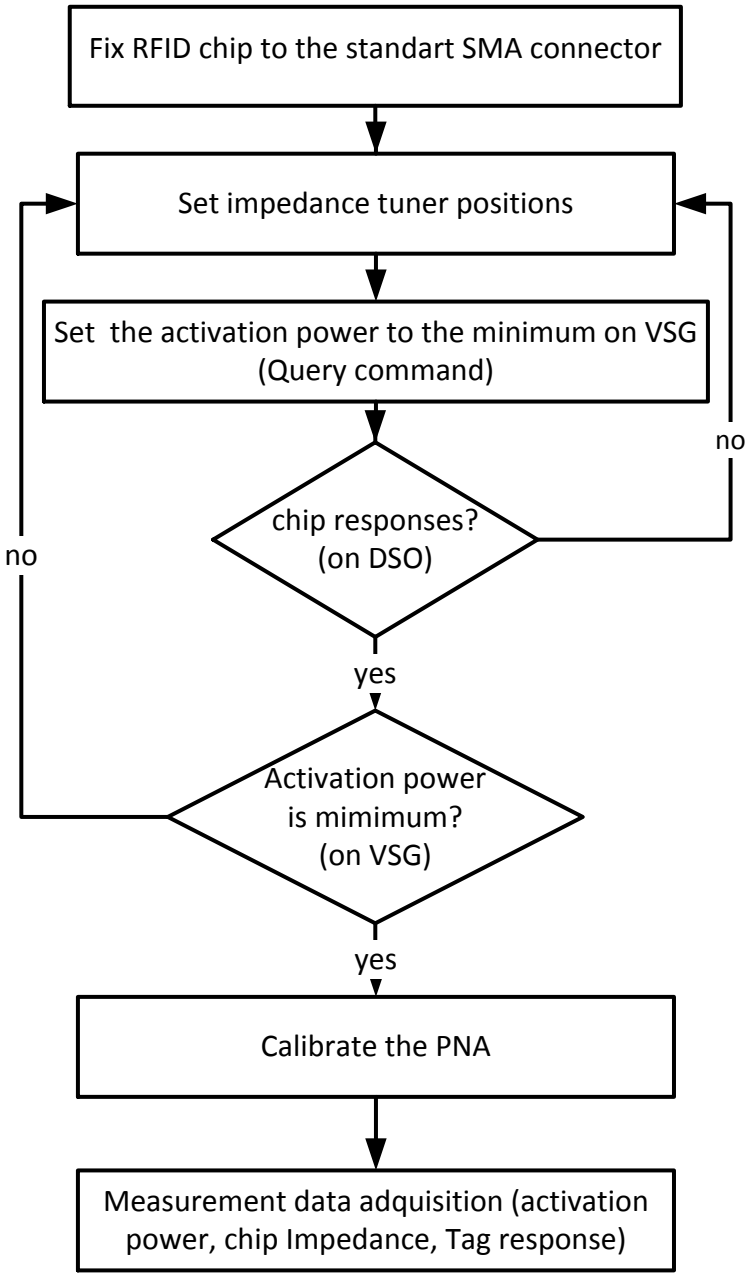

Figure 4.5: Flow diagram of the measurement procedure in the RFID-NTP.

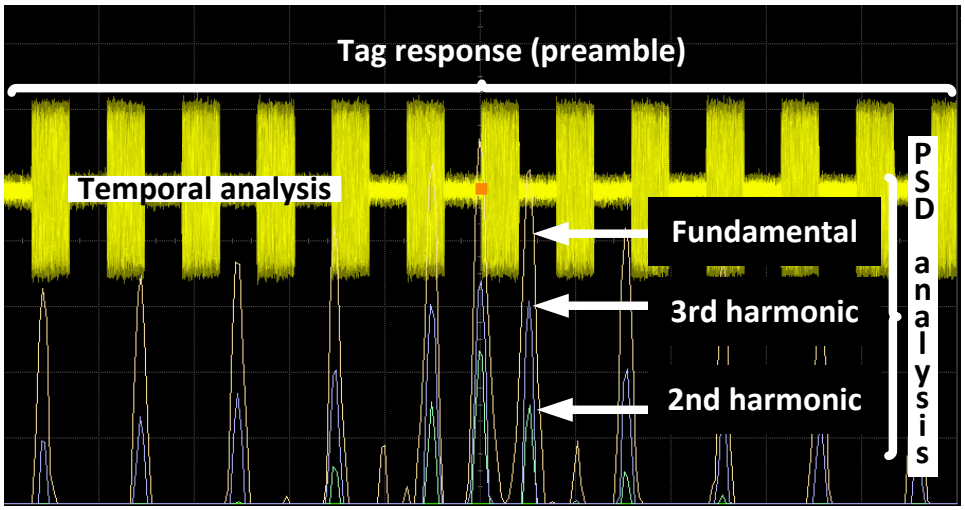

Figure 4.6: Harmonic characterization method on the DSO. The visualization allows to set the optimal position of the impedance tuners by minimizing the CW level.

these three chips, the sensitivity varies between -13.2 dBm and -11.5 dBm. A chip sensitivity of -15 dBm, measured at the chip pads, is reported in datasheets [92]. The difference from the results presented here, is due to the losses on the test fixture, considering that on-chip measurements have slightly higher accuracy compared to this method. In the case of chip 3, a saturation point at higher power levels is observed. This is due to the shunt control that regulates the internal supply voltage for the logic part of the chip. The saturation is above 8.8 dBm for this chip.

Fig. 4.8 shows the measured impedances during the scavenging state for chips 1 and 3 at the fundamental frequency. Impedance results are in good agreement with values reported in the datasheets (see Table 4.1) at the activation power. Although chip 1 and chip 2 have the same IC component, they have different packages, which explains why the difference on its impedance values. The optimum antenna impedance is the complex conjugate of the chip impedance at the sensitivity point shown in Fig. 4.7. Quite significant changes on the impedance can be observed while increasing the input power. This changes show the non-linear behavior of the chip, more precisely due to the rectifier characteristics [31; 93]. A relatively constant impedance can be observed at low input power levels, once the chip is activated. This is explained by the fact that, as electromagnetic energy harvesters, the RFID chips are also optimized to start operating at low input power. The non-linear effect depends on the number of rectifier stages that each RFID chip uses [59].

4.3.2 Harmonic responses

The harmonic response level was measured for the three chips until the 4^{th} harmonic, by performing the PSD analysis over the same chip response frame. Results are shown in Fig. 4.9. As already discussed in Chapter 3, the 3^{rd} harmonic is predominant for all the chips under

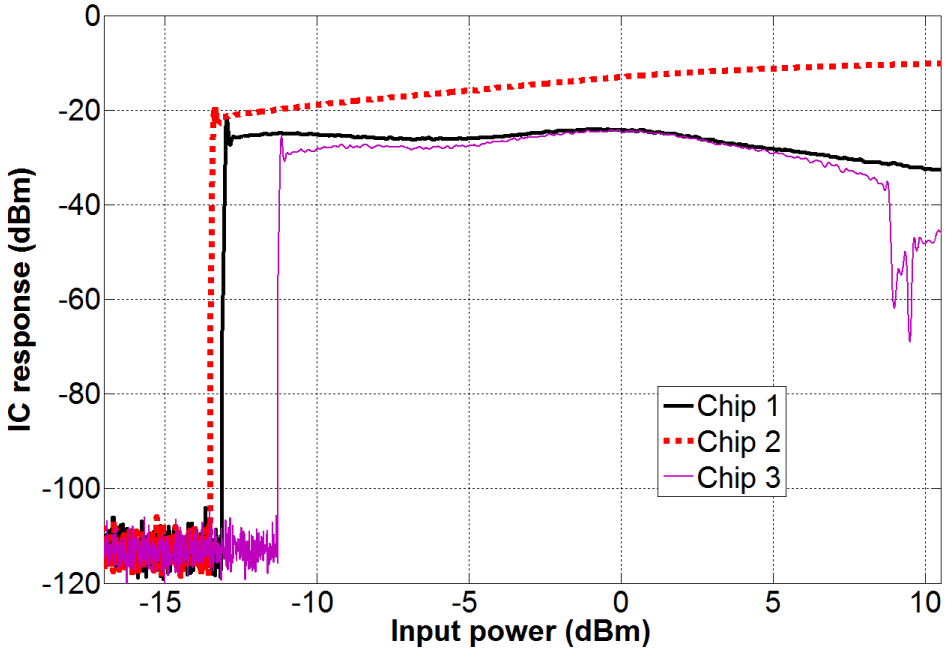

Figure 4.7: Measured power sensitivity of RFID chips.

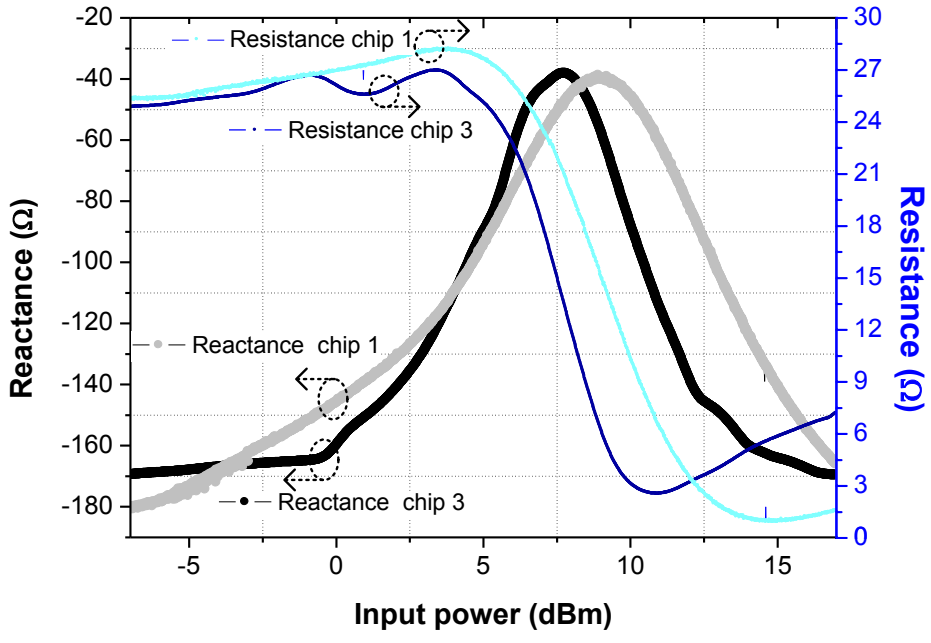

Figure 4.8: Impedance for chip 1 and chip 3 in scavenging state for a sweep of power.

Table 4.1: Impedance results at the fundamental frequency.

Chip	Measured (Ω)	Datasheets [68; 92] (Ω)
chip 1	22 - j182	22 - j195
chip 2	19 - j178	22 - j195
chip 3	20 - j170	16 - j171

test. It is worth noting that, even until the 4^{th} harmonic, a modulated response is detected. This becomes more clear for an input power above 3 dBm in the case of chip 1 and chip 3. Details at the activation power are shown in Table 4.2.

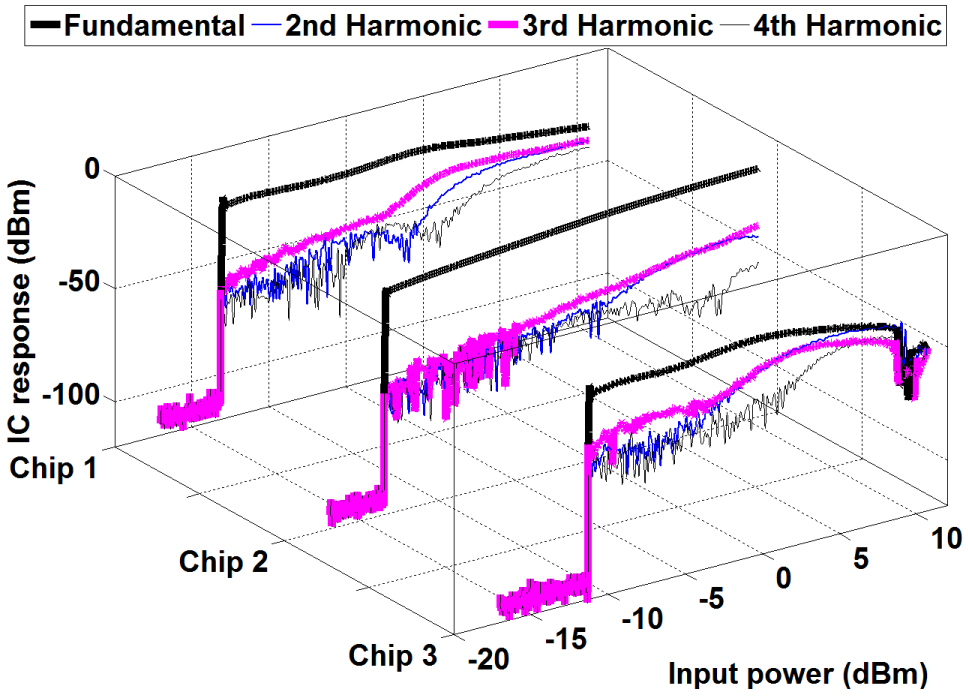

Figure 4.9: Harmonic responses measured for the three chips for a sweep of power. A characterization until the 4^{th} harmonic is presented.

4.4 Harmonic treatment tests

In this section, a treatment of the non-linearities is proposed by using the impedance tuners named as antenna impedance emulator in Fig. 4.2, and hereafter called *antenna part*. In

Table 4.2: Harmonic responses from RFID chips.

Chip	fund. (dBm)	2^{nd} harm. (dBm)	3^{rd} harm. (dBm)	4^{th} harm. (dBm)
chip 1	-21.9	-66.7	-61.3	-76.2
chip 2	-19.9	-66.5	-61.6	-79.4
chip 3	-25.4	-60.8	-49.3	-68.5

the design process of RFID tags, only the impedance value at the fundamental frequency is considered [94]. Theoretically, this is enough to ensure the operation at the desired frequency. But no special attention is paid on the harmonics produced by the chip. RF criteria says that the harmonics should be filtered, for example in order to increase the purity of the RF to dc conversion performed by the rectifier part and, thus providing a greater read range since a clean dc signal provides more power to the chip. The aim of this section is to evaluate the effects produced on the fundamental frequency by the non-linear behavior of the chip, by changing the matching condition between *antenna part* and chip in a wide range of frequencies.

The experience is based on observing the chip response and its harmonics, by activating the PSD analysis in real time on the DSO (see Fig. 4.6) and by setting the impedance tuners to a position that produces a change in the level of the fundamental frequency and/or in its harmonics. This process can be considered as a practical experimentation of the Harmonic Balance (HB) method used in circuit simulators to analyze non-linear components [95].

4.4.1 Treatment tests

The performance of the chip after an impedance tuning of the supposed *antenna part* is evaluated here. Fig. 4.10 shows the harmonic responses of chip 1 until the 4^{th} one, in a scenario were the harmonics are increased by tuning the impedance of the *antenna part*. This is achieved at the expense of a 1.5 dB reduction on the chip sensitivity and 7 dB reduction on the chip response at the fundamental frequency. Table 4.3 compares the results before and after the harmonic treatment.

Table 4.3: Harmonics treatment.

Chip 1	Sensit. (dBm)	Fund. (dBm)	2^{nd} h. (dBm)	3^{rd} h. (dBm)	4^{th} h. (dBm)
No harmonic treatment	-12.9	-21.9	-66.7	-61.3	-76.2
Harmonic treatment	-11.4	-28.9	-61.3	-50.2	-87.6

Fig. 4.11 and Fig. 4.12 show the input impedance of the chip 1 in both modulation states

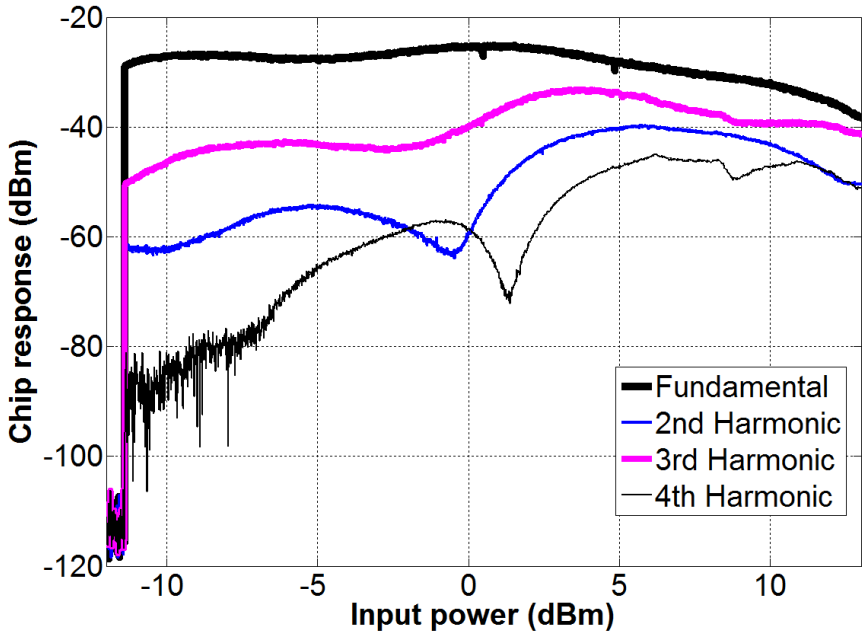

Figure 4.10: Harmonic characterization for chip 1 after the harmonic treatment.

after the harmonic treatment for the fundamental and its 3^{rd} harmonic respectively. These measurements were performed at the new activation power. At the 3^{rd} harmonic, the resistive part decreases, and the reactance becomes more capacitive compared to the impedance at the fundamental frequency. Moreover, the difference between the modulation states is lower which means that, in a radiating scenario, the ΔRCS [96] will be smaller than that one at the fundamental frequency.

Results from Table 4.3 clearly show that an increase in the 2^{nd} and 3^{rd} harmonics results in slightly diminished performance at the fundamental frequency.

4.4.2 Results exploitation

After the chip is completely characterized, it is possible to export the scattering parameters measured with the RFID-NTP for a wide frequency range. Therefore antenna designers can use the scattering parameters in order to optimize the antenna design in a CAD software, and ensure for example the complete filtering of backscattered harmonics. Indeed, the complex reflection coefficient of the RFID tag $\tilde{\rho}$ defined in (4.1), can be calculated for each impedance state [33; 97].

$$\tilde{\rho} = \frac{Z_c - Z_a^*}{Z_c + Z_a} \tag{4.1}$$

where $Z_a = R_a + jX_a$ is the complex antenna impedance, and Z_c is the complex RFID chip impedance in one state (scavenging or reflecting).

Thereby, a trade-off or independent optimization of the read range (Load Factor LF defined

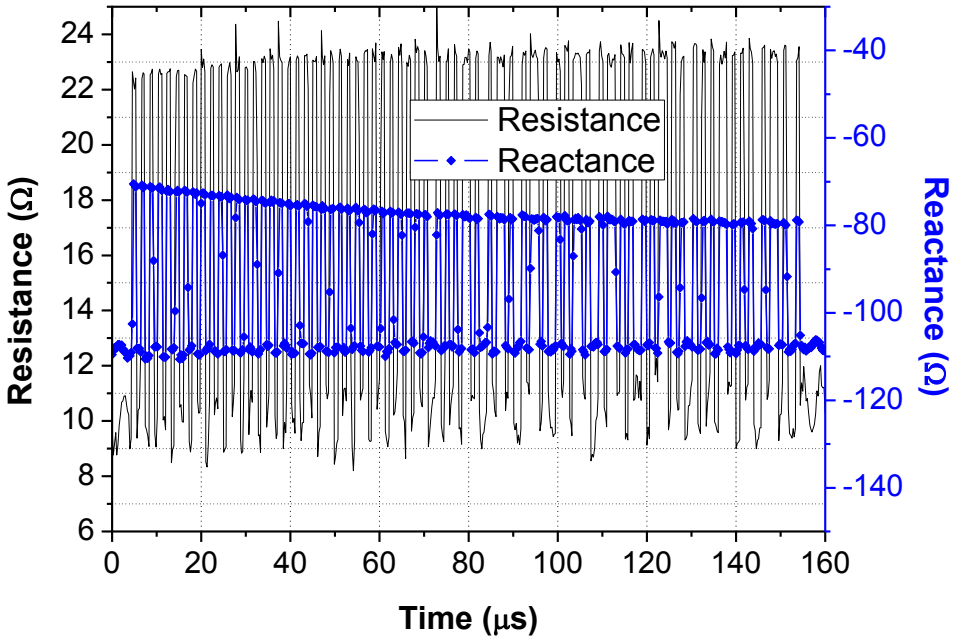

Figure 4.11: Measured chip input impedance for the fundamental frequency in a temporal sweep. Scavenging and reflecting states can be seen.

in (4.2)) and/or the ΔRCS (Modulation Efficiency ME defined in (4.3)) of the RFID tag can be performed at the design stage [33].

$$LF = 1 - |\tilde{\rho}_{sca}|^2 \tag{4.2}$$

$$ME = \left|\tilde{\rho}_{ref} - \tilde{\rho}_{sca}\right|^2 \tag{4.3}$$

with $\tilde{\rho}_{sca}$ and $\tilde{\rho}_{ref}$, the complex reflection coefficient of the tag in scavenging and reflecting states respectively.

On the other hand, it is interesting to note that both states of modulation are visible even at the 3^{rd} harmonic. This observation validates the hypothesis of a redundant information originated on the same chip. Therefore the design of a tag antenna radiating the fundamental signal and the 3^{rd} harmonic can be envisaged using the same LF and ME design parameters approach. It is worth noting that the two main drawbacks to take into account in the harmonic exploitation: (1) the low power of the 3^{rd} harmonic response and (2) the small ΔRCS.

4.5 Conclusion

A complete characterization of the harmonics produced by the non-linearities of passive UHF RFID chips has been presented in this chapter. The measurement procedure introduces vectorial information allowing an evaluation of the RFID chip in full operation mode in a wide frequency range.

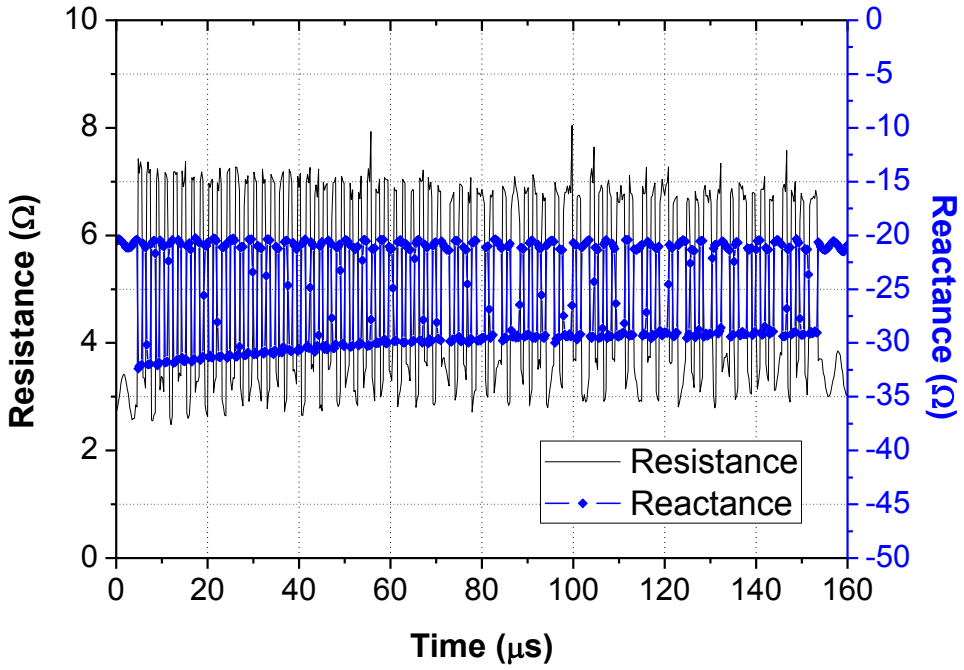

Figure 4.12: Measured chip input impedance for the 3^{rd} harmonic frequency in a temporal sweep. Both states of modulation can be distinguished.

The RFID chip performance and the real effect of the harmonics are evaluated by a practical experimentation of harmonic compensation, similar to the HB method. The proposed analysis can be extended for any kind of Class-1 Generation-2 RFID chip, and it can be taken into account for the tag antenna design.

Harmonic treatment tests have shown that by setting certain impedance matching condition between antenna and RFID chip, the harmonic levels can increase at the expense of a 1.5 dB reduction on the chip sensitivity and 7 dB reduction on the chip response at fundamental frequency. Subsequent lines of research can be undertaken by properly filtering the harmonics in order to improve the read range and/or the differential radar cross section in benefit of the performance of the whole RFID tag in existing applications.

By other side, and contrary to traditional approaches, additional efforts on exploiting the 3^{rd} harmonic response by specialized tag antenna design, promises new applications and improvements on the existing ones declaring a redundant communication from tag-to-reader. Nevertheless, the ability of the reader to collect and process harmonics should be enhanced to make this exploitation a reality. These topics together with experimental and parametric analysis will made the core of the next chapter.

5. Modeling: Harmonics in passive RFID chips

In this chapter, the main objective is to perform a depth study of the non-linear behavior of passive RFID chips and to show that the produced non-linearities can be exploited to benefit the operation techniques of passive UHF RFID systems. A theoretical analysis about the harmonic production from passive RFID chips and the effect of the matching network and tag antenna on the backscattering harmonic is performed. A new harmonic tag model which offers a maximum profit from the signals generated by the chip at fundamental and third harmonic frequencies is proposed. The theoretical analysis is confronted to radiated and conducted measurements

5.1 Introduction

As long as antenna and chip are independently designed [88], and due to the non-linear behavior of the RFID chip [31; 33; 40], the tag antenna will radiate some of the harmonic currents of the CW that feed the chip. These harmonics are also carrying the impedance modulation effect, producing then a redundant backscattering modulation. Some theoretical basics behind these phenomena were explained and experimentally demonstrated in Chapter 3 and Chapter 4 by means of radiating measurements considering the whole tag, and by conducted measurements in where a test bench is directly connected to the RFID chip.

The exploitation of harmonic signals as information carriers establishes frequency diversity from tag to reader, without breaches in standard regulations. The concept establishes a foundation for new potential applications that the chip self-generated harmonic signal with redundant information can offers. With such a motivation, this chapter aims to meet one main objective:

- To perform a theoretical analysis of harmonic signals produced by the RF section of passive RFID tags. The analysis pinpoints in the operation of a traditional tag working at the fundamental frequency of the system (f_0), but also in the operation of a new tag able to enhance the backscattered signal strength at its 3^{rd} harmonic ($3f_0$), hereinafter so-called Harmonic Tag (HT)

The chapter explains the harmonic production of passive RFID chips, and the effects of the matching network and tag antenna on the harmonic backscattering phenomena. The theoretical analysis is done in three stages: (1) The calculation of a general expression for the current in the rectifier part of RFID chips. The expression comprises fundamental and harmonic components. (2) The study of the matching network used in traditional RFID tags in order to evaluate the harmonic backscattering strength. (3) The study of a new matching network architecture that enhances the backscattering strength at $3f_0$ maintaining the operation at f_0, therefore constituting the HT operation theory. The analysis presented in this section uses lumped components to abstract the operation of a distribute impedance matching network integrated in antennas used in passive RFID.

5.2 Analysis of harmonic currents in the rectifier

5.2.1 Review of Dickson analysis

The most extended architecture used to study the rectification process in UHF RFID is the Dickson charge pump and its derived equations [98–101]. Although the rectifier architecture used in this chapter is very similar to the Dickson charge pump, it has some significative differences [102]. Since UHF tags operate with significantly lower signal levels and higher frequency than the original Dickson analysis, some modifications must be made to RF-to-dc equation proposed by Dickson. The original Dickson analysis assumes constant forward voltage drop of the rectification device, so called Şthreshold voltageŤ, though this forward voltage drop is actually a function of the load current of the rectifier. This variation is not significant for

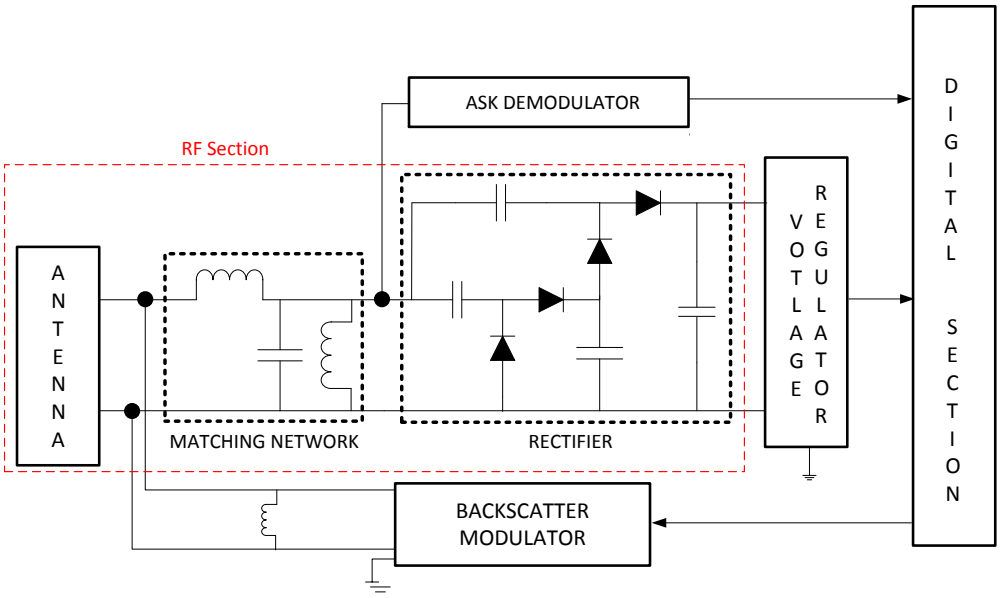

Figure 5.1: Passive tag architecture.

large voltage swings across the diode as is the case for the charge pump application. However in passive UHF RFID, the RF input voltage is very small, on the same order of the forward voltage drop. As a result, the non-linear forward voltage drop has significant impact on the RF-to-dc equation. A parametric non-linear analysis theory has been developed to incorporate the effect of the non-linear forward voltage drop. It was first applied to predict the RF-to-dc conversion for single-diode rectifiers in [103] and was later expanded to multi-stage rectifiers in [31].

The multi-stage voltage multiplier model and the analysis method used in this chapter is supported by several works that use similar architectures to predict the RF-to-dc conversion for rectifiers in UHF RFID applications being aware of the low RF input voltage present in this technology [31; 104–106]. Fig. 5.1 shows the RF section of a passive RFID tag, having a 2-stage voltage multiplier, hereinafter referenced as rectifier. The rectifier circuitry is composed by a cascade of N-stage voltage multiplier.

Because of the non-linear effects of the rectifier part of the RFID chip, the current in the antenna I_{ant} presents components at frequencies that are integer multiples of the operation frequency. Indeed in scavenging state, the input voltage induced in the tag antenna, and then, conducted to the rectifier at f_0, generates an input current I_{in} dominantly constituted by the odd harmonic components of f_0. Fig. 5.2 shows the Schottky diode model and its different configurations for the analysis.

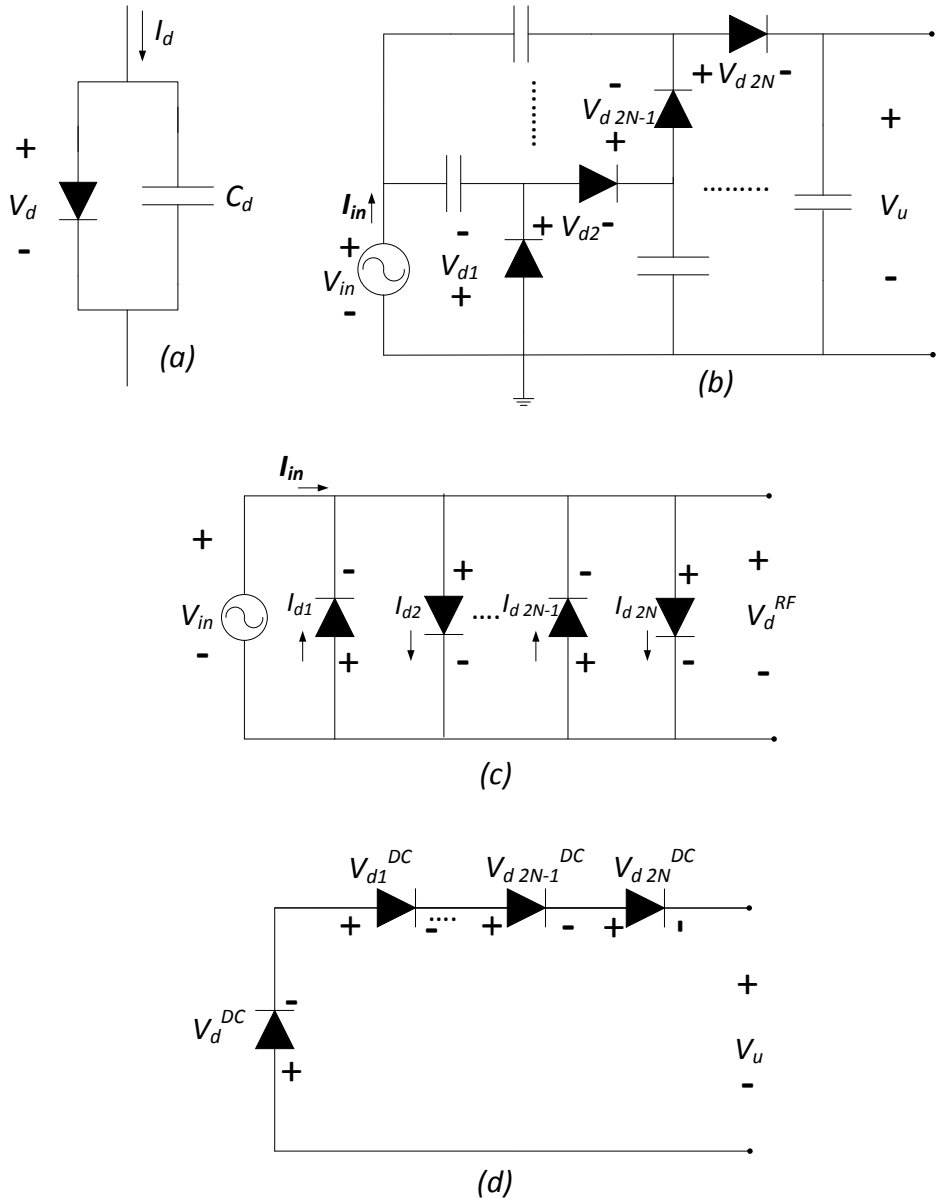

Figure 5.2: Equivalent circuit of the Schottky diode for the analysis in dc and RF. (a) Equivalent circuit of the Schottky diode. (b) Equivalent rectifier circuit under steady state. (c) RF equivalent circuit, the capacitors become short circuits and the 2N diodes are in parallel. (d) dc equivalent circuit, the capacitors do not let the current go through, and the diodes are in series.

$$I_{in} = NI_s \left[e^{-\frac{V_u}{2NV_T}} \left(e^{\frac{V_0 cos(\omega_0 t)}{V_T}} - e^{-\frac{V_0 cos(\omega_0 t)}{V_T}} \right) \right] - 2NC_d V_0 \omega_0 sin(\omega_0 t) \tag{5.4}$$

5.2.2 Calculation of the harmonic currents

In order to determine the general expression of the input current to the rectifier, I_{in} in Fig. 5.2 (b), it is necessary to introduce the Current-Voltage expression of the diode:

$$I_d = I_s(e^{\frac{V_d}{V_T}} - 1) + C_d \frac{dV_d}{dt} \tag{5.1}$$

where I_s is the saturation current of the diode, V_d is the voltage at the diode terminals, and V_T is the thermal voltage around 25.8 mV and at 300 K. $V_T = kT/e$ where k is Boltzmann constant, e the electron charge and T the temperature. C_d is the junction capacitance of the diode. It should be noted that this model does not consider the parasitic effects of the package.

Being V_{in} a sinusoidal voltage with a frequency f_0 and an amplitude V_0 at the input of the rectifier if the capacitors in the rectifier are well dimensioned, it is reasonable to consider that the rectifier presents the following equivalent circuits for RF signals and dc signals:

- RF analysis: the capacitors are short circuited, the RF voltage at each diode is $V_d^{RF} = \pm V_0 cos(\omega_0 t)$ and all the diodes are in parallel (ω_0 stands for the angular frequency $\omega_0 = 2\pi f_0$). The sign of V_d^{RF} depends on the orientation of the diode.
- dc analysis: the capacitors are open circuited, all the diodes are in series. The dc voltage is equally divided in each diode $V_d^{dc} = -\frac{V_u}{2N}$, where V_u is the output voltage.

Then the voltage V_d in each diode is:

$$V_d = V_d^{RF} + V_d^{dc} = \pm V_0 cos(\omega_0 t) - \frac{V_u}{2N}, \tag{5.2}$$

and replacing (5.2) in (5.1), yields in

$$I_d = I_s(e^{\frac{V_0 cos(\omega_0 t)}{V_T} - \frac{V_u}{2NV_T}} - 1) \pm C_d \frac{d(V_0 cos(\omega_0 t))}{dt} \tag{5.3}$$

In order to calculate I_{in} for a N-stage rectifier, it is necessary to calculate the current in a single stage node and then multiply it by N, yielding in (5.4) at the top of next page.

The exponential of a cosine function in (5.4) can be expanded using the Fourier series,

$$e^{\pm X cos(\omega t)} = B_0 (\pm X) + 2 \sum_{n=1}^{\infty} B_n(\pm X) cos(n\omega t) \tag{5.5}$$

where $B_n(X)$ is the modified Bessel function of the first kind, of order n and argument X. The input current, generated by a sinusoidal input voltage at the operation frequency, can be written using (5.5) in (5.4), yielding in (5.6) in the next page, the current-voltage expression of a 2N-stage rectifier circuit.

$$I_{in} = 4NI_s e^{-\frac{V_u}{2NV_T}} \sum_{n=1}^{\infty} B_{2n-1} \left(\frac{V_0}{V_T}\right) cos\left[(2n-1)\omega_0 t\right] - 2NC_d V_0 \omega_0 sin(\omega_0 t) \tag{5.6}$$

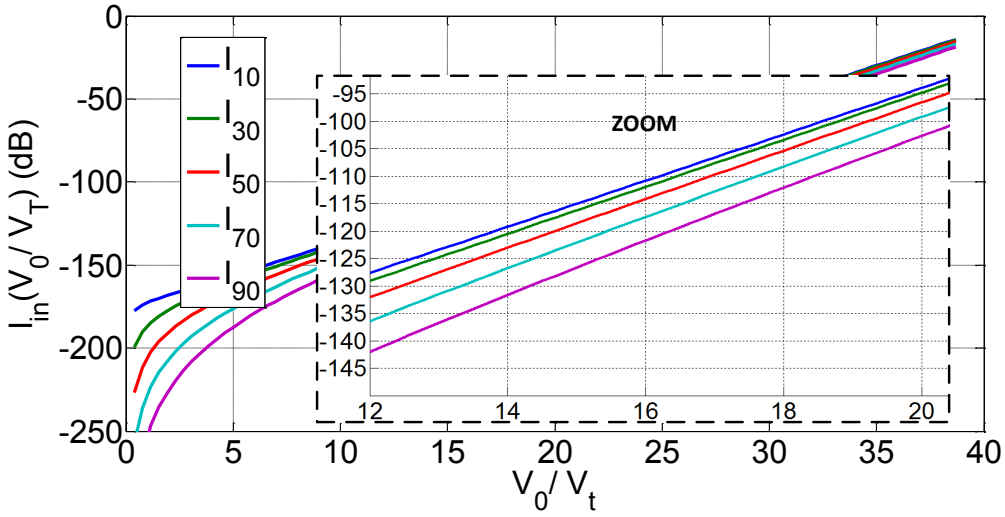

Figure 5.3: Current-voltage curve for a rectifier of N voltage-multiplier stages, modeled using the modified series of Bessel. The total current is composed only by the odd harmonic components. A similarity between the current amplitude at f_0 and current amplitude at $3f_0$ can be noted.

From (5.6), it is observed how the even RF components of ω_0 are eliminated due to the opposite sense of currents in each diode at each voltage doubler stage (RF analysis in Fig. 5.2 (c)). This phenomenon explains the odd harmonic predominance in voltage doublers in general. Additionally, in a N-stage rectifier, the total capacitance hereinafter called C_{eq} is equal to $2NC_d$ and if the matching network (Fig. 5.1) is well dimensioned, the current contribution through internal capacitors C_d in (5.6) is eliminated since C_{eq} is compensated by the shunt inductance of the matching network. Details about the operation and design of the matching network are exposed in the next section.

The first components of the input current of the rectifier described in (5.6) are shown in Fig. 5.3 in logarithmic scale when using representative values $N = 6$, $V_T = 0.025\ V$, $V_u = 1\ V$ and $I_s = 10^{-17}\ A$ [107]. It can be seen that the amplitude current component at f_0 (i.e. I_{10}), and the amplitude current component at $3f_0$ (i.e. I_{30}) are close to each other. Focusing the analysis on the components at f_0 and at $3f_0$, Fig. 5.4 represents the ratio I_{30}/I_{10} in logarithmic scale. The ratio is an intrinsic consequence of the non-linear nature of diode-based devices. From (5.6), the rectifier produces harmonic currents which the ratio does not depends on the parameters N, V_T, V_u, I_s but only on V_0. From Fig. 5.4, it can be seen for instance when $V_0/V_t \geq 6$ ($V_0 \geq 0.15\ V$), the amplitude of I_{30} is half of the amplitude of I_{10} and they become closer as V_0 increases. For values of $V_0 \geq 0.44\ V$, the difference between I_{30} and I_{10} is shorter than 1 dB. The non-linear effect in rectifier devices is higher when V_0 increases, which leads to a current amplitude at $3f_0$

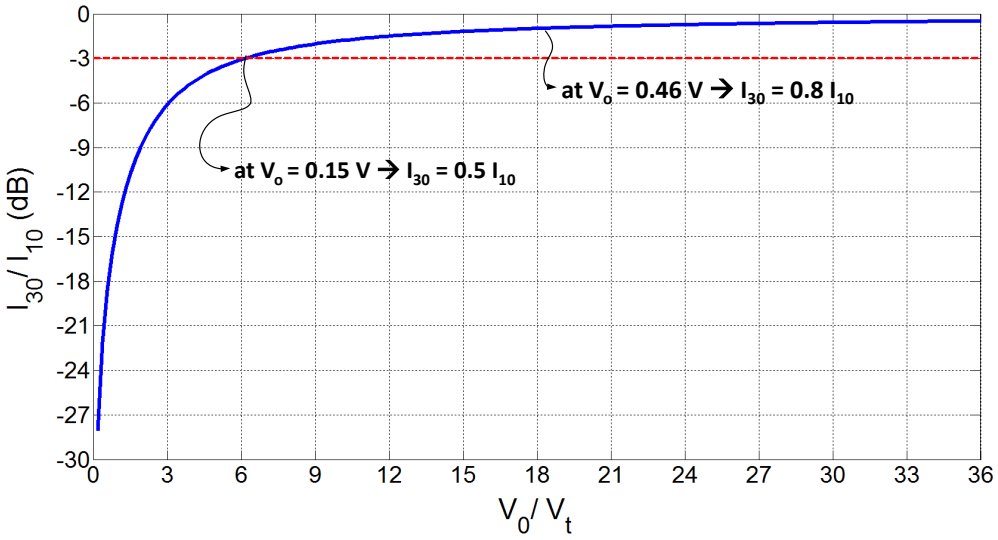

Figure 5.4: Comparison of I_{30}, the amplitude of the current in the rectifier at $3f_0$, respect to I_{10}, the amplitude of the current in the rectifier at f_0. At $V_0/V_t = 6$ ($V_0 = 0.15$ V), I_{30} is the half of I_{10} and it becomes closer as V_0 increases.

closer to the current amplitude at f_0.

5.3 Third harmonic in traditional tags

5.3.1 Impedance matching network for f_0

Given the capacitive nature of RFID chips at f_0 due to the diode-based rectifier circuit [31; 33; 106], an impedance matching network is always introduced between the RFID chip and a pure resistive antenna (dipole of around 73 Ω). Fig. 5.5 shows the typical matching network for a passive RFID tag. The RFID chip impedance is represented by the parallel configuration of a capacitance C_{eq} and a resistance R_{eq}. The first element of the matching network is the shunt inductance $L^{'}$ that compensates C_{eq} and represents the traditional inductive loop used in RFID antenna design [18] (C_{eq} describes the capacitive nature of the RFID chip). Once the chip reactance is canceled, the remaining high shunt resistance R_{eq} (around 1.8 $k\Omega$ [68]) needs to be transformed to the comparatively low series resistance of a dipole antenna hereinafter R_A [108]. The LC network is often employed to perform the transformation as follows: (1) C transforms the shunt resistance of the RFID chip R_{eq} to a smaller series value matching it to R_A, being $C = Q/(\omega_0 R_{eq})$; (2) L cancels C, being $L = QR_A/\omega_0$. The parameter Q defines the quality factor of the LC network and it is bounded to the resistance transformation ratio between chip and antenna. In other words, Q defines the performance of the LC network in function of the power

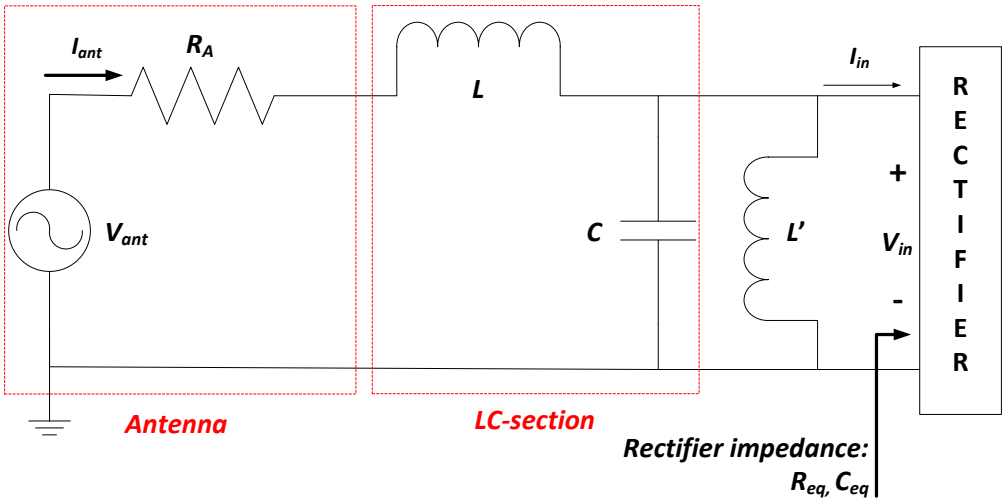

Figure 5.5: Equivalent circuit of the RF section of a passive RFID tag.

transferred between antenna and chip and viceversa at f_0, and is given by

$$Q = \sqrt{\frac{R_{eq}}{R_A} - 1} \tag{5.7}$$

Fig. 5.6 shows the transmission coefficient of the LC network for different values of Q, keeping fix R_{eq}. A higher Q ensures a better power matching at 868 MHz, therefore higher isolation at frequencies different than f_0.

It is worth no note that the assumption of a capacitive impedance for the chip (R_{eq} and C_{eq}) and a pure resistive impedance for the antenna (R_A) is realistic. Indeed, passive RFID chips and rectifier diode-based circuits have in general capacitive impedance, typically on the order of $20 - j150$ around 868 MHz [18; 68; 92]. Regarding the antenna, the analysis considers a resonant dipole with a dimension closely to a half-wave length (i.e. zero imaginary component at the resonant frequency).

5.3.2 Influence of Q in the backscattered signal at $3f_0$

The effect of Q on the signal radiated by traditional tag antennas at $3f_0$ is modeled using the architecture depicted in Fig. 5.5. Being V_{ant} the open circuit voltage of the tag antenna and V_{in} the input voltage of the rectifier, both at f_0, and assuming a lossless matching network, then the delivered input power, equal to V_{ant}^2/R_A, must be equal to its output power, V_{in}^2/R_{eq}. The input power to the matching network is $P_{ant} = V_{ant}I_{ant}$, and the output power of the matching network is $P_{eq} = V_{in}I_{in}$, where I_{ant} is the current at the tag antenna at f_0, and I_{in} is defined in (5.6). Therefore it is also valid to say

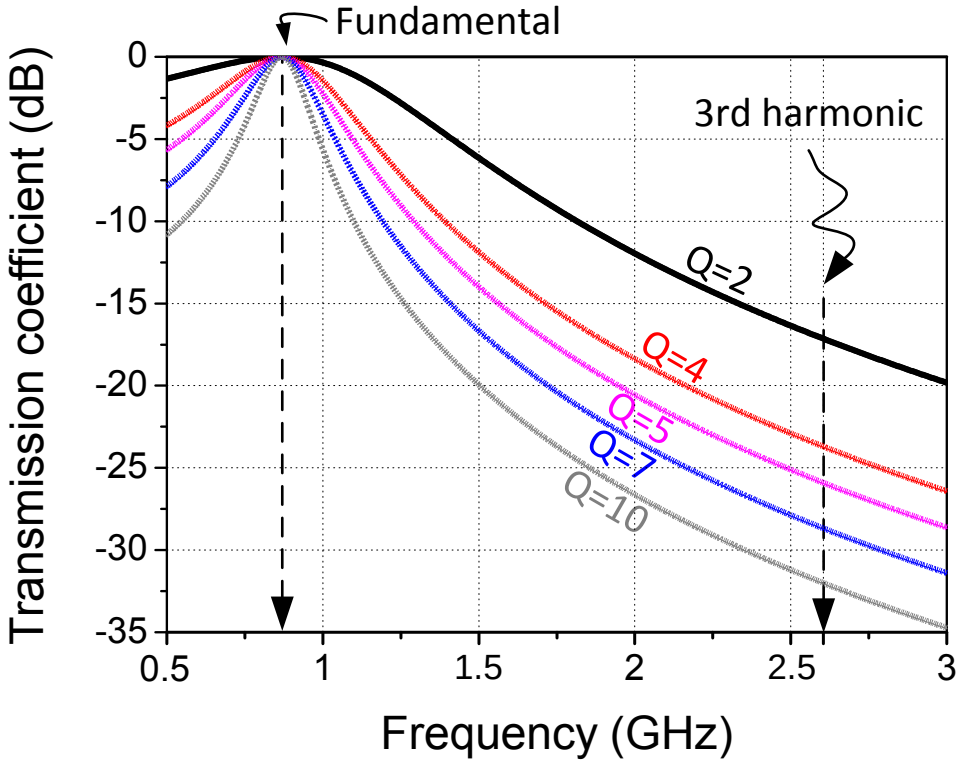

Figure 5.6: Transmission coefficient of the LC network with different Q values.

$$\frac{I_{in}}{I_{ant}} = \sqrt{\frac{R_A}{R_{eq}}}. \tag{5.8}$$

From (5.8) and (5.7), the amplitude of the current in the antenna I_{1ant} at f_0 is given by

$$|I_{1ant}| = I_{10}\sqrt{Q^2+1} \tag{5.9}$$

where I_{10} is the amplitude of the rectifier input current I_{in} at f_0 given by (5.6). In order to find a similar relation between I_{3in}, the component of the rectifier input current at $3f_0$, and I_{3ant}, the reflected current in the antenna terminals at $3f_0$, an equivalent model of the tag backscattering the harmonic is presented in Fig. 5.7. Let V_3 the shunt voltage when the current I_{3in} at $3f_0$ is generated by the rectifier in Fig. 5.7, therefore $V_3 = I_{3in}Z_{3in}$. Z_{3in}, the input impedance seen by the rectifier, is given by

$$Z_{3in} = \frac{-\omega^2 LL^{'} + j\omega^2 L^{'} R_A}{R_A(1-\omega^2 L^{'}C) + j\omega(L^{'} - \omega^2 LL^{'}C + L)} \tag{5.10}$$

V_3 must be equal to the voltage $I_{3ant}(R_A + j\omega L)$, which triggers in $I_{3in}Z_{3in} = I_{3ant}(R_A + j\omega L)$. Replacing the relations between C, L, R_A, R_{eq} and Q above exposed, and $\omega = 3\omega_0$, it is possible to

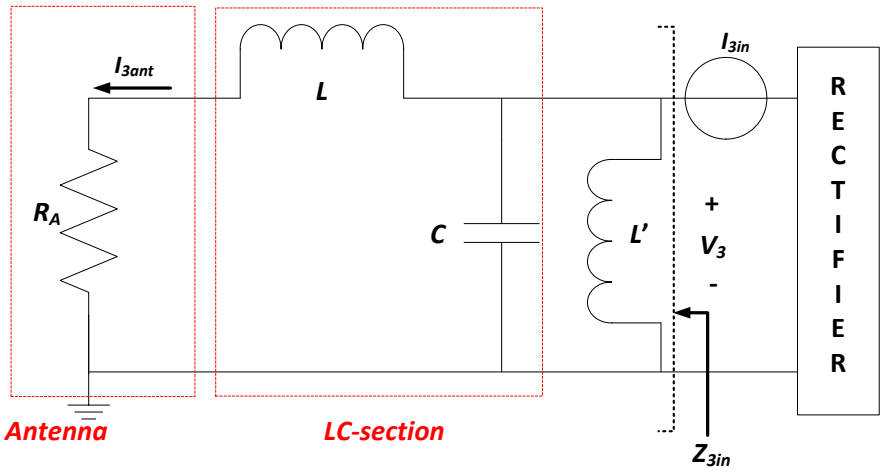

Figure 5.7: Equivalent circuit of the tag when the current at $3f_0$ is being reflected in the antenna.

calculate the amplitude of the current in the antenna I_{3ant} at $3f_0$ due to the current I_{3in} generated by the rectifier at $3f_0$, as

$$|I_{3ant}| = \frac{3I_{30}L^{'}\omega_0(Q^2+1)}{\sqrt{(R_{eq}-9\omega_0 L'Q)^2+9\left(QR_{eq}+(1-8Q^2)\,\omega_0 L'\right)^2}} \tag{5.11}$$

where I_{30} is the amplitude of I_{3in}, the component of the rectifier input current I_{in} at $3f_0$ in (5.6). From the capacitive nature of the RFID chip, the resistance conversion of the matching network from a high shunt resistance R_{eq} (around 1.8 $k\Omega$), to a comparatively lower series resistance R_A (around 73 Ω), imposes that $C \gg C_{eq}$. Since $L^{'}$ resonates with C_{eq} at the f_0, then $L^{'} = \frac{1}{C_{eq}\omega_0^2}$. The following statement, consequent with [31] is then derived:

$$Q\omega_0 L^{'} \gg R_{eq} \tag{5.12}$$

Using (5.12) it is possible to rewrite (5.11) as follows:

$$|I_{3ant}| = \frac{I_{30}\left(Q^2+1\right)}{\sqrt{64Q^4-7Q^2+1}} \tag{5.13}$$

The power delivered to the tag antenna terminals at f_0 and at harmonic frequencies is differently affected by the matching network and can be expressed in terms of Q. From (5.9) and (5.13), it is possible to calculate the power delivered to the tag antenna terminals at f_0 and at $3f_0$, P_1 and P_3 respectively as follows:

$$P_1 = \frac{1}{2}|I_{1ant}|^2 R_A = \frac{I_{10}^2(Q^2+1)R_A}{2} \tag{5.14}$$

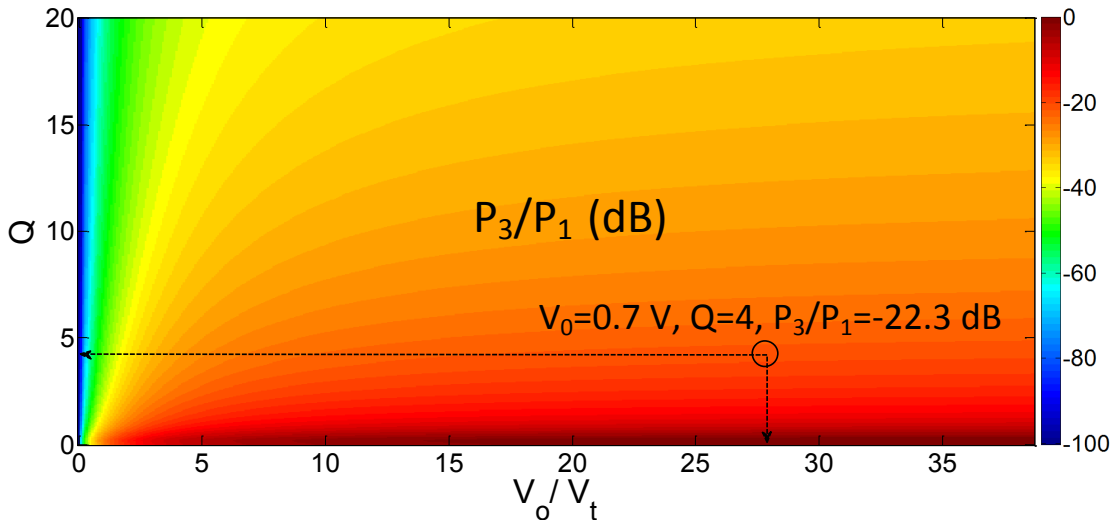

Figure 5.8: Law decay of the power at $3f_0$ respect to the power at f_0 in function of Q and V_0/V_t for traditional tags.

$$P_3 = \frac{1}{2}|I_{3ant}|^2 R_A = \frac{I_{30}^2(Q^2+1)^2 R_A}{2(64Q^4-7Q^2+1)} \tag{5.15}$$

Fig. 5.8 represents the law decay of the power P_3 at $3f_0$ respect to the power P_1 at f_0, in function of Q and the ratio V_0/V_t. Two major patterns can be distinguished:

- the power level at $3f_0$ approaches the power level at f_0 as the input voltage to the rectifier V_0 increases;
- the power level at $3f_0$ approaches the power level at f_0 as Q decreases.

It is expected that with higher Q, the rectifier input voltage at f_0 is also higher, leading to a greater non-linear effect therefore causing the rectifier to produce a higher component at $3f_0$. However a higher Q also ensure a higher attenuation at frequencies different than f_0. Summarizing, when higher is Q higher is the suppression of the power transmitted from the chip to its antenna at $3f_0$.

The harmonic power can be potentially radiated if the antenna structure allows it, i.e. profiting from the current distribution of harmonics in a specific antenna structure [69]. According to the exposed model, a traditional RFID tag having a dipole antenna structure which has a current distribution at $3f_0$ different than zero at the input and an distributed matching network with $Q = 4$, radiate a signal at $3f_0$ being 22.3 dB lower than the signal at f_0. This model explains why certain commercial tags backscatter a signal at $3f_0$ with stronger level than others, certainly depending on the tag antenna structure as evidenced in Chapter 3 for the tag Rafsec MemoryStick [109].

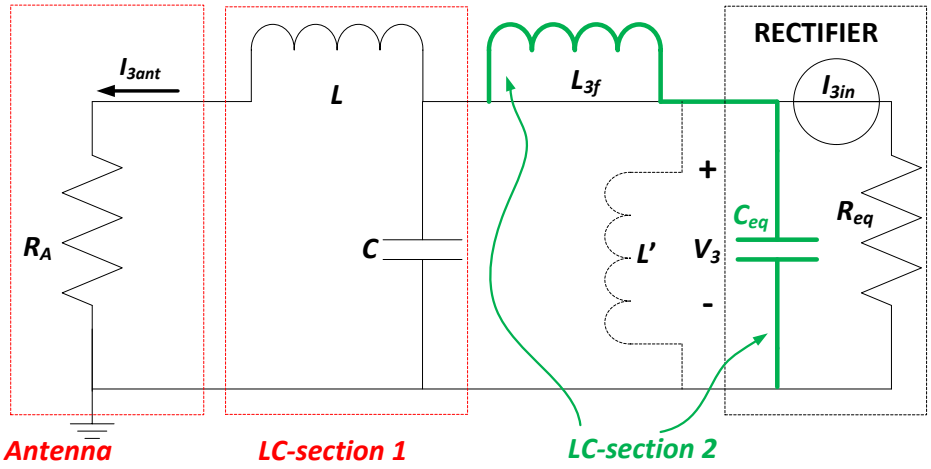

Figure 5.9: Proposed matching network to exploit the signal generated by the RFID chip at $3f_0$. The cascade LC matching network allows the chip to transmit a maximum power towards the antenna at $3f_0$. $L^{'}$ being always considered in the analysis.

5.4 Third harmonic enhancement in new harmonic tag antennas

5.4.1 Dual band impedance matching network

The analysis presented in this section develops the operation theory of the HT extending the equivalent model presented in Fig. 5.7. A new matching network that could enhance the backscattering strength of HTs at $3f_0$ is presented in Fig. 5.9. The new matching network composed by the cascading of two LC networks [110] is characterized by a new quality factor Q^* calculated as

$$Q^* = \sqrt{\left(\frac{R_{eq}}{R_A}\right)^{1/2} - 1} \tag{5.16}$$

The new element introduced is the series inductance L_{3f} that resonates with both, the original LC network and C_{eq} at $3f_0$. The new matching network should be dimensioned choosing a L_{3f} which does not affect the traditional operation at f_0, i.e. L_{3f} should act as a short circuit at f_0. In the same way, the dimensioning criteria has to consider that the shunt inductance $L^{'}$ should not intervene in the operation at $3f_0$, i.e. $L^{'}$ should act as an open circuit at $3f_0$. The first step to choose the L_{3f} value is to calculate the inductance necessary to compensate the chip capacitance at $3f_0$ (inductive matching), and depending on the values of the original LC network, $L^{'}$ should be tuned to resonate at $3f_0$. Realistic values for the proposed model are $C_{eq} = 1.2\ pF$, $R_{eq} = 1.8\ K\Omega$, $L^{'} = 27.8\ nH$, $L_{3f} = 10.6\ nH$, $C = 0.6\ pF$, $L = 52.8\ nH$, and $R_A = 73\ \Omega$.

Fig. 5.10 shows the transmission coefficient of the proposed matching network for the HT, compared to the matching network of a traditional tag.

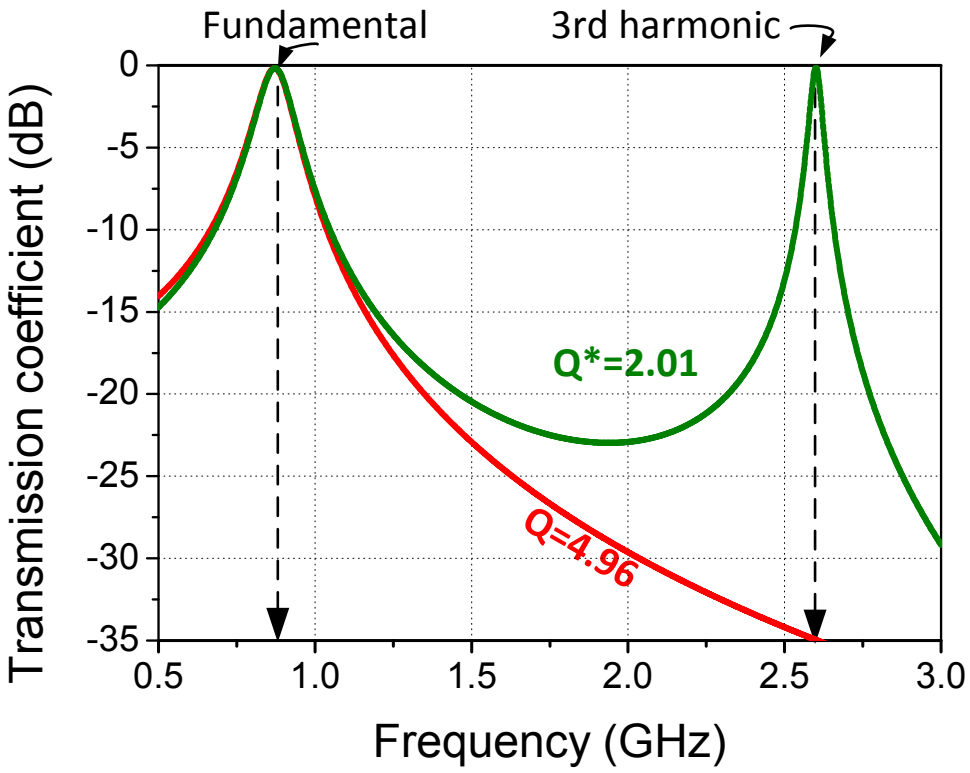

Figure 5.10: Transmission coefficient of the cascade LC network of the HT antenna ($Q^* = 2.01$) compared to an original LC network in traditional tags ($Q = 4.96$).

5.4.2 Backscattered signal at $3f_0$ by the HT

From (5.8) and (5.16), the amplitude of the current at $3f_0$ at the HT input I_{3ant} can be write as

$$I_{3ant} = I_{30}(Q^{*2} + 1) \tag{5.17}$$

and from (5.7) and (5.16), the relation between Q^* and Q is

$$Q^* = \sqrt{\sqrt{Q^2 + 1} - 1} \tag{5.18}$$

Replacing (5.18) in (5.17), the current in the antenna at $3f_0$ is

$$|I_{3ant}| = I_{30}\sqrt{Q^2 + 1} \tag{5.19}$$

From (5.9) and (5.19), it can be observed how the new matching network treats in a similar manner the current of the chip at f_0 and at $3f_0$.

Using (5.9) and (5.19) in (5.14) and (5.15) respectively, the power radiated by the HT at f_0 and $3f_0$ harmonic can be expressed as:

$$P_{1HT} = \frac{I_{10}^2(Q^2 + 1)R_A}{2} \tag{5.20}$$

$$P_{3HT} = \frac{I_{30}^2 (Q^2+1) R_A}{2} \tag{5.21}$$

Fig. 5.11(a) represents the law decay of the power P_{3HT} at $3f_0$ respect to the power P_{1HT} at f_0, in function of Q^*, Q and the ratio V_0/V_t. If the matching network is well designed, which means an antenna having a distributed matching network that cancels the RFID chip reactance at f_0 and $3f_0$, the difference between the backscattered power by the HT at $3f_0$ and at f_0 depends only on the intrinsic non-linear behavior of the chip (Fig. 5.4) and is represented in Fig. 5.11(b) at certain level of input voltage V_0.

Experimental tests reported in Chapter 4 have shown the feasible enhancement of the signal generated by the chip at $3f_0$ using an antenna impedance emulator. The tests so-called harmonic treatments are based on emulating proper matching networks that could enhance the response at $3f_0$ compared to the case of an optimum emulated antenna at f_0 having the same chip. An enhancement of 11 dB on the response at $3f_0$ is reported performing conducted measurements.

5.5 Conclusion

A complete theoretical analysis of the harmonics produced by the non-linear behavior of passive UHF RFID chips had been presented in this chapter. The analysis based on a modified version of the Dickson rectifier, considers different input tensions and it is valid to analyze the chip behavior when low input signals as the used ones in passive RFID are present.

It is explained the particular predominance of even or odd harmonics depending on the architecture of the rectifier circuit, which determines the canceling or not of currents in the electrical analysis. Indeed, a single diode will produce all the harmonics with predominance of those ones of low order, i.e. the 2^{nd} harmonic. However if the rectifier is composed by voltage doublers stages (number of diodes multiple of two), an odd harmonic predominance is presented.

The antenna-chip impedance matching is treated with a lumped model that abstracts the operation of antenna structures that includes a distributed matching network. The theoretical analysis is confronted to the operation of traditional tags reported in Chapter 3. A new harmonic tag antenna model that comprises a matching network that fully exploits the fundamental and third harmonic signals generated by EPC Class-1 Gen2 RFID chips is proposed. The analysis of this new harmonic tag is also confronted to experimental harmonic treatment tests reported in Chapter 4 and confirms the feasible exploitation of the 3^{rd} harmonic signal of passive RFID chips.

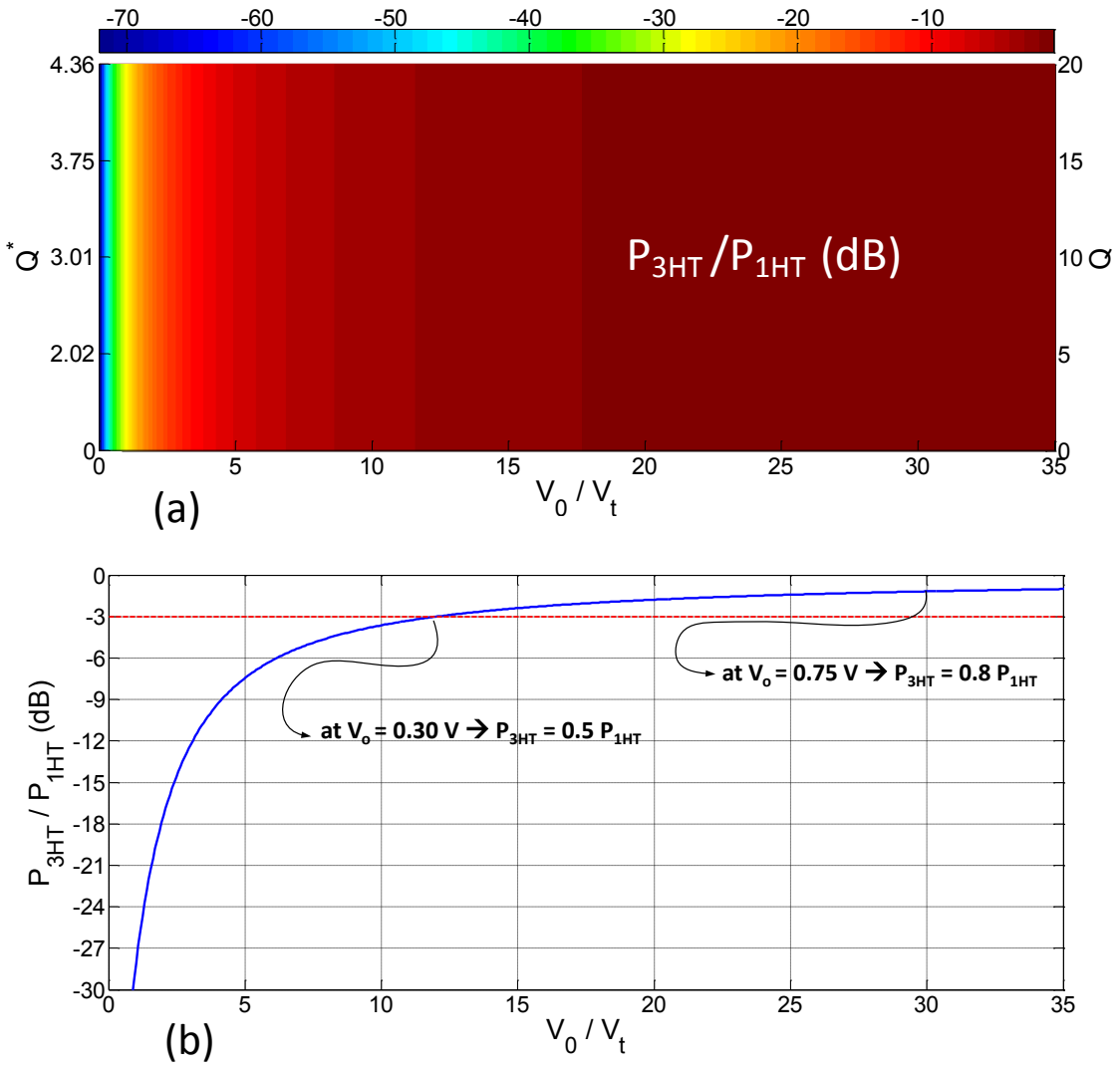

Figure 5.11: Law decay of the power at $3f_0$ respect to the power at f_0 for the harmonic tag. (a) Law decay in function of Q^*, Q and V_0 for the harmonic tag. (b) Law decay in function of V_0. If the matching network is well dimensioned, the ratio depends only on the non-linearity of the chip.

6. Harmonic communication in passive UHF RFID

This chapter unfolds a new concept about the exploitation of non-linear phenomena in passive RFID, i.e the use of harmonics signals generated by the non-linear behavior of traditional passive UHF RFID chips. Specifications and methodology are explained in a harmonic communication scenario. The regulations, harmonic RFID reader, harmonic tag guidelines design and metrics for its evaluation are discussed. In compliance of standard regulations for EPC Class-1 Gen2 RFID, the design of four kinds of harmonic tags that increase the power level of the harmonic response, while operating also at the fundamental frequency is presented. The performance of the solution is illustrated from simulation and measurements. Additionally, a thorough parametric study is carried out for all the prototypes, with special care in the antenna structure, kind of chip used, received power, and read range. Finally, the proposed optimal solution presents a read range greater than 5 m for fundamental frequency and its 3^{rd} harmonic simultaneously.

6.1 Introduction

The study and exploitation of the non-linearity in diode-based devices are not new. Approaches based on one bit system in where the harmonic or intermodulation components serve to indicate tag presence without a specific communication are known as harmonic radar. Used as a tracking solution, the invention has been patented in 1975 [111] leaving the path for several derived applications e.g., in insect tracking [44]. With the boom of RFID systems, the harmonic radar concept has been recently re-purposed. In [112; 113] a tag response is achieved by exploiting the intermodulation phenomenon of a diode. In [114], a specific non-linear RF circuit is developed with the aim to enhance the harmonic strength compared to multiplier diodes used at 10 GHz. The circuit integrated to an antenna conforms a harmonic transponder of one bit and later on the transponder was used for accurate indoor ranging [115]. Authors of [116; 117] have studied and generalized the design techniques for harmonic transponders based on a single detector or varactor diode. The concept was adopted for low-cost solutions using paper substrates and inkjet printing technology [118; 119] or even an eco-friendly solution using an organic diode [120]. Another exploitation idea [48] proposes the detection of counterfeit RFID cards based on its electromagnetic characteristics rather than the digital information that they transmit. In this approach, one of the stages considers the electromagnetic signature that harmonic signals produce. An emerging field in where the non-linearity of diode-based devices is also being exploited is the electromagnetic energy harvesting. Authors of [59; 61; 63; 121] have proposed power-optimized waveforms to improve the range and reliability of RFID systems. By using special designed signal waveforms at the transmitting terminal that somehow excite the diode non-linear behavior of rectifying diodes in a more efficient manner, the RF-to-dc conversion efficiency of the diode is increased. In the same field, the work reported in [122] proposes a millimeter-wave rectenna at 35 GHz that also harvests the harmonic signals generated by its rectifier. The proposed solution enhances the RF-to-dc conversion efficiency.

In the specific field of passive UHF RFID, the experimentation on backscattered harmonics have been first introduced in [40] in 2009, but no additional research efforts were followed, probably because the evidenced low power level and limitations on the characterization method.

Contrary to the conventional paradigm in RF communication circuits where non-linearities are undesired and their level is highly reduced [31; 33], this chapter develops the concept of a new communication function by exploiting non-linearities of passive EPC Class-1 Gen2 RFID chips. The exploitation of harmonic signals as information carriers establishes frequency diversity from tag to reader, without breaches in standard regulations. The benefit of the frequency diversity is the possibility to use a spectrum which has much reduced self and multi-path interference, therefore countering multi-path and leakage effects at reception, but not a read range enhancement. The developed concept establishes a foundation for new potential applications that the chip self-generated harmonic signal with redundant information can offers. With such a motivation, this chapter aims to meet two specific objectives:

- To define exploitation policies when the harmonic communication between Harmonic Tag (HT) and reader is envisaged. The policies treat regulation definitions, considerations on the reader side, metrics to evaluate the HT performance and design guidelines for the HT.

- To explain the HT design and operation with a real HT design examples and a depth parametric study at different powers, at different frequencies and the read range performance.

6.2 RFID harmonic communication: specifications and methodology

The theoretical analysis has shown the possibility to increase the backscattering strength at $3f_0$ by exploiting the harmonic generation of passive RFID chips. This section aims to present considerations on the use of HTs in a tag-to-reader harmonic communication regard. Indeed it is intended to declare the diversity in frequency where signals from tag-to-reader at f_0 and at $3f_0$ carry the same information. Aspects as deployment regulations, harmonic reader operation considerations, HT evaluation metrics and HT design guidelines are unfolded.

6.2.1 Compliance with regulations

Regulations at f_0

In order to not create obstacles or delays in the use of the HT, e.g. regarding the compatibility with other systems, the parent design policy is to respect current standard and local regulations on passive UHF RFID [57; 123]. In that regard, since dual band operation is desired (at f_0 from the passive UHF RFID system i.e. in Europe 868 MHz, and at $3f_0$ i.e. 2604 MHz), reader and tag spectrum mask regulations must be accomplished.

Any particular change is envisaged on the transmitter side of the RFID reader, in other words HTs should operate with RFID readers that meet the spectrum mask regulations [57]. In the same manner, the tag spectrum mask defined in [123] should be respected. The first side lobe of the tag response signal shall not exceed -20 dBm of Effective Radiated Power (ERP) at f_0. All other spurious signals like its harmonics should neither exceed these limits.

Regulations at $3f_0$

In Europe, the spectrum regulations allocate the frequency band of 2500-2690 MHz to broadband mobile services (e.g. LTE and WIMAX with transmitters of tens of watts and operation distances up to 4 Km) [124]. In other regions (e.g. where $3f_0 = 2745$ MHz), the band of 2700-2900 MHz is worldwide allocated to meteorological and air traffic radar systems with high power (the equivalent isotropically radiated power could be on the order of 10^9 watts) [124; 125]. Studies, based on worst case assumptions (i.e. line-of-sight conditions), have shown that there is potential interference from mobile service to radar and vice versa which will depend on the deployment scenario with factors such as frequency separation, relative antenna orientation, and distance (in the order of kilometers) but nevertheless the systems are still compatible [124].

Given the backscattering modulation nature of passive UHF RFID systems, even if the tag response at $3f_0$ is enhanced for the harmonic communication approach, it remains weak (the equivalent isotropically radiated power on the order of 10^{-11} watts at few meters) [126], and does not represent an incompatibility issue compared to the possible radar effects over the mobile

service. If reader and tag masks regulations are respected, the operation at $3f_0$ ensures the regulations compliance.

6.2.2 Harmonic reader considerations

In a communication scenario reader-HTs, some considerations should be taken into account for the dimensioning of the harmonic branch receiver of an envisaged RFID harmonic reader. Specific details in the baseband treatment and the analog-to-digital conversion are out of the scope of this work, and can be taken as future line of research. However, some directives on the harmonic RFID reader design can be stated. A critical issue in the design of traditional RFID readers (i.e. working at f_0) is the suppression of the carrier wave signal that unintentionally leaks into the received path due to the use of common isolation techniques as circulator or couplers. The reader has to transmit a strong carrier wave signal to supply passive tags with sufficient operating power. The response of the tag on the other hand is generated by passive backscattering, which is achieved by a modulation of the RFID chip input impedance. Since only a small fraction of the power incident upon the tag is reradiated, the signal received by the interrogator antenna is very weak compared to the transmitted carrier wave signal [127]. Therefore the reduction of the transmitted leak is crucial and leads traditional reader architectures that aims to increase the reception sensitivity of RFID readers [127–129].

From measurement results in passive UHF RFID [69], the carrier wave in reception at $3f_0$ is around 60 dB below the carrier wave at f_0. By using harmonic backscattering, in case of a receiver at $3f_0$, the limitations imposed by the carrier wave leakage does not represent a great inconvenience. Indeed the conditions are favorable to design a receiver with higher sensitivity than the traditional receivers at f_0. Some noise may result from $3f_0$ leakage due to the synchronization circuitry at reception but it is much smaller than the circulator or coupler leakage at f_0 [115]. As in traditional passive RFID, the overall system performance in the harmonic communication scenario is limited by the tag. Thus exploiting the harmonic signal produced by RFID chips at $3f_0$ with the proper antenna design offers a gain in the tag-to-reader power link budget at $3f_0$.

6.2.3 Harmonic tag antenna basics

In the intention to integrate the antenna-chip impedance matching network directly in the antenna design, RFID antenna design is widely documented (impedance-matching, size-reduction techniques, etc.) [18; 88]. In the case of the HT, the main difference respect to traditional tag antennas is the dual band operation. As exposed in Section 5.4, the HT should include a distributed matching network that cancels the RFID chip reactance at f_0 and $3f_0$. Depending on the envisaged application, some antenna parameters can be optimized with respect to others (size, directivity, materials, etc.).

The HT design process is illustrated in a flow chart shown in Fig. 6.1. As in traditional RFID [88], the design requirements are linked to the envisaged application (size, directivity, read range, operation conditions, materials of the tagged object, etc).

Having fixed the material, the design of an HT antenna begins by importing the scattering parameters of the chips in scavenging state into a 3D electromagnetic simulator [130]. The

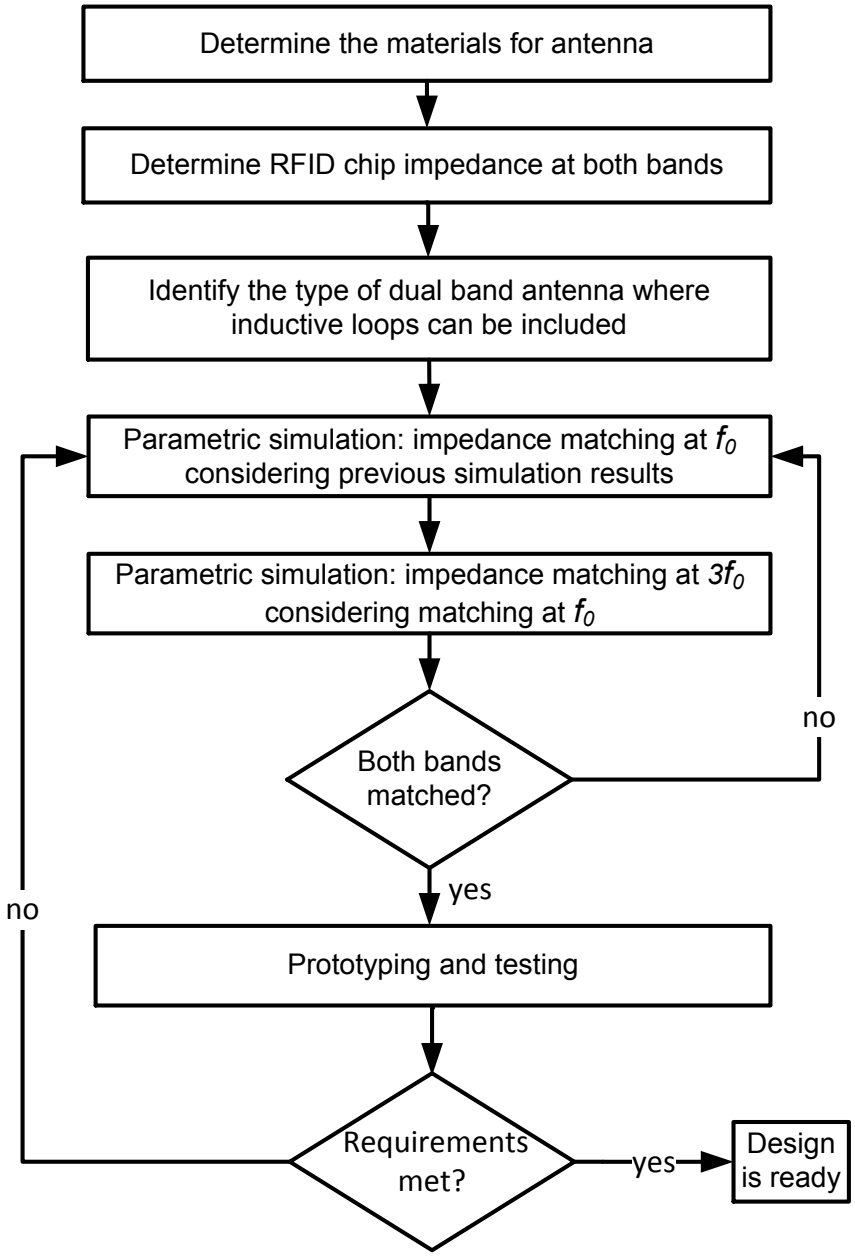

Figure 6.1: RFID HT antenna design process.

impedance of the RFID chip at $3f_0$ is still capacitive [130], therefore similar techniques to the inductively loop matching used at f_0 can be used.

Regarding the antenna structures, useful designs and techniques used for rectennas and harmonic radar can be applied in the design of the HT antennas [116; 117; 131; 132] because of the common idea of inductive compensation of capacitive diode-based circuits. Under

this criterium the chosen antenna structure should include two inductive loops, each one to cancel the capacitive effects of the chip at f_0 and $3f_0$. The simulation is usually led by structure optimization based on the design requirements (impedance matching, antenna gain, read range, de-tuning effects). Starting with the impedance matching at f_0 and after at $3f_0$, certain changes on the dimensions of the resonant structures at f_0 could be necessary, nevertheless the optimization by simulation facilitates the procedure once the structure operation is mastered. Finally some prototypes should be fabricated and tested in order to validate the design requirements.

6.2.4 Setup and metrics to evaluate harmonic RFID tags

The evaluation of the HT performance is based on radiated measurements performed in confined environment. Similar testing environments to those ones used for traditional passive RFID can be used [133] but some considerations should be made on the methods used, i.e. using power spectral density analysis (PSD) to quantize the HT response. Specific details about the measurement methodology and RFID air interface setting used to evaluate harmonic signals can be found in Chapter 3. A calibrated power budget should allow to perform accurate measurements of the HT response at f_0 and at $3f_0$.

The tests reported in this chapter use the measurement setup shown in Fig. 6.2. An anechoic chamber with bi-static configuration (1 m distance between horn antennas and tag) is connected to the RFID Test-Platform (RFID-TP). The RFID-TP performs a PSD analysis in real time at f_0 and at $3f_0$. The results reported in this chapter consider the following directives regarding the power budget and measurements:

- **HT sensitivity at different frequencies.** The necessary ERP power sent by the RFID-TP to activate the HT is considered (i.e. transmitted power before the antenna). The ERP power is calculated using the power approach defined in [134]. Since the measurement setup is completely calibrated and controlled, the ERP is known. This consideration allows to evaluate the HT performance independently of the kind of reader antenna used.

- **HT response at different RFID-TP power.** The HT response is evaluated in terms of the isotropic received power (values calibrated to a receiving antenna of 0 dBi gain) in function of the EIRP transmitted by the RFID-TP. Furthermore, in the measure of the HT response, the PSD analysis considers the addition of power from both first side lobes of the modulated response, contrary to calculations explained in Chapter 3 where only one side lobe is considered. It is worth to note that the harmonic response exists conditioned to the existence of the response at f_0.

- **HT read range performance.** The read range is calculated using the law of decay $20log(d)$, where d is the distance between tag and reader beyond 1 m, being known the tag response at 1 m, and considering a radiated level of 35 dBm EIRP for the RFID-TP [135]. Therefore, the calculation of the HT response at f_0 and at $3f_0$ beyond 1 m is possible and it is compatible with the methods used in the literature [88]. For the read range evaluation, a 6 dBi antenna gain is considered for the EIRP of the RFID-TP. This analysis allows to represent the read range for a given sensitivity of the reader receptor at f_0 and at $3f_0$.

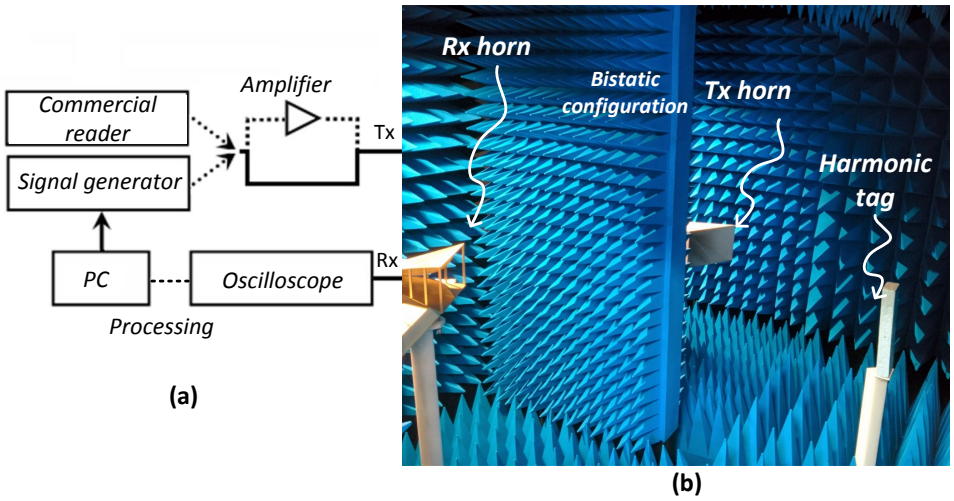

Figure 6.2: (a) Equipment setup for bi-static. (b) Anechoic chamber configuration.

6.3 Harmonic tag design example

The requirements for the HT in this example are: (1) a maximum read range at $f_0 = 868\ MHz$ and $3f_0 = 2604\ MHz$, (2) an antenna size comparable to the dimensions of existing RFID antennas and (3), the use of low-cost materials and prototype techniques. The materials chosen are PET with 3.2 permittivity and 0.05 mm thickness for the substrate as in traditional RFID tag inlays and aluminum as trace conductor. Regarding the impedance at both bands, the design example uses two kinds of chips: (1) G2XM NXP SOT1040-AA1 [92] with measured impedances $19 - j178\ \Omega$ at f_0 and $9.2 - j54.2\ \Omega$ at $3f_0$ and chip (2) Monza with measured impedances $20 - j170\ \Omega$ at f_0 and $3.4 - j29.4\ \Omega$ at $3f_0$ (conducted measured details in Chapter 4). The next step is to choose an antenna structure as reference in where the double inductive loop matching technique can be applied. The next paragraphs pinpoint on the design procedure for two kind of antennas.

6.3.1 Antenna design

Yagi-Uda structures

A modified Yagi-Uda antenna following similar structural approaches reported in [132] was designed. Fig. 6.7 shows the Yagi-Uda HT prototype composed of three main parts:

- **Fundamental resonator:** the resonant structure at f_0 is a curved dipole conforming a loop [Fig. 6.7 (a)], that at the same time, serves as inductive loop for the impedance matching at f_0 [18];
- **Harmonic resonator:** the resonant structure at the 3^{rd} harmonic is a dipole joint to an inductive loop [Fig. 6.7 (b)], for the conjugate chip impedance matching at the 3^{rd} harmonic;

- **Reflector:** a reflector at the rear of the antenna [Fig. 6.7 (c)] serves to increase the directivity at the harmonic frequency; and at the same time, its position and dimensions allow to tune the resistance of the antenna.

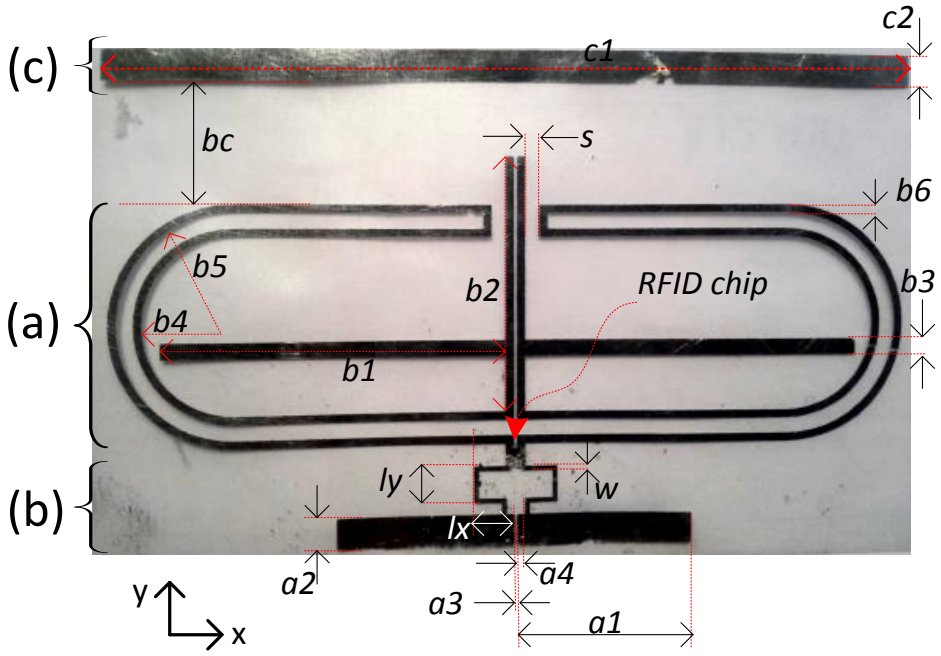

Figure 6.3: Harmonic tag prototype. (a) Fundamental resonator, (b) harmonic resonator, and (c) reflector.

The harmonic resonator and the fundamental resonator are joined by two parallel lines, where in each line, one port of the chip is connected. The antenna can be tuned by trimming the dipoles and reflector, the distance between the parallel lines *a3*, and the size of the inductive loops. Table 6.2 summarizes all the optimum design parameters.

The simulated reflection coefficient Γ of the harmonic antenna normalized to the chip impedance is depicted in Fig. 6.4. The conjugate impedance chip matching was achieved at two frequencies, with $\Gamma = -14.5$ dB at 868 MHz, and $\Gamma = -10.1$ dB at 2604 MHz. This dual band matching represents the main difficulty during the HT design process, and triggers in small bandwidths. The simulated realized gain at 868 MHz and at 2604 MHz is of 2.5 dBi and of 2.9 dBi respectively. It is worth noting that different dual band antenna structures can be used [136; 137].

The simulated directivity in the plane E (xy), and plane H (zy), is depicted in Fig. 6.5 and Fig. 6.6 respectively. The pattern at f_0 is comparatively featured more close to a omni-direction. By contrast, at the 3^{rd} harmonic, the pattern is slightly directive due to the antenna structure, which improves the harmonic performance in one direction.

In order to enhance the performance of the HT and profiting from the options that Yagi-Uda structures offer, a new version of the antenna above presented, and with the same materials,

Table 6.1: Yagi-Uda antenna type without director: design parameters.

Parameter	Value (mm)	Parameter	Value (mm)
a1	18.6	**b6**	0.8
a2	3.3	**c1**	85
a3	0.4	**c2**	3.3
a4	0.8	**lx**	2.2
b1	35.5	**ly**	3.3
b2	27.2	**w**	0.4
b3	1.2	**bc**	12.8
b4	9.3	**s**	1.5
b5	11.9	-	-

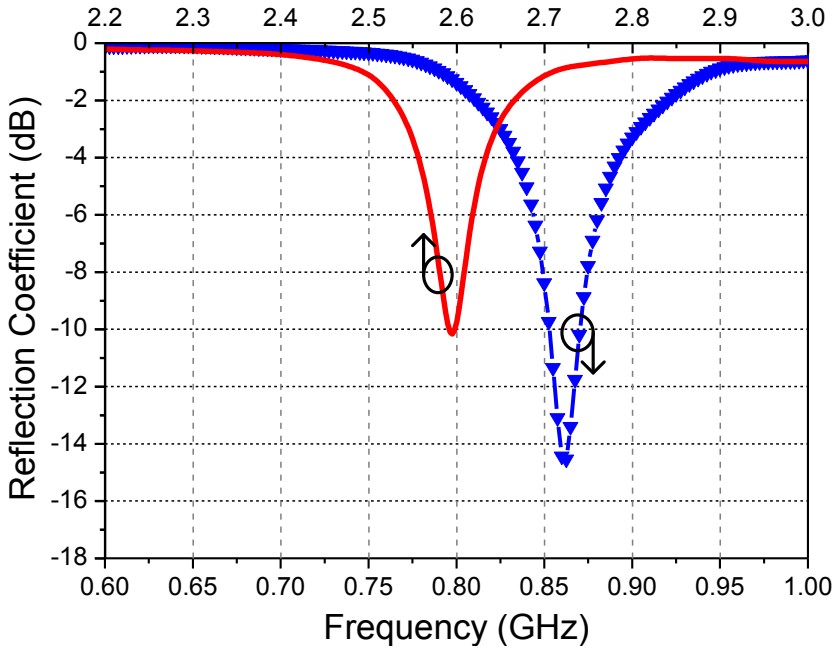

Figure 6.4: Simulated reflection coefficient of the HT normalized to the chip impedance.

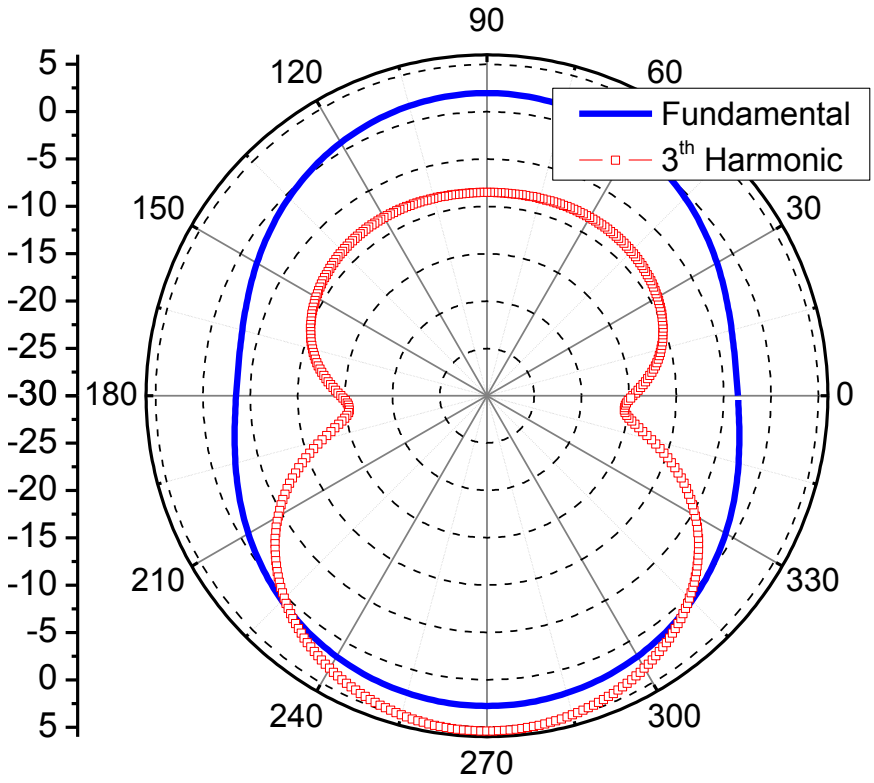

Figure 6.5: Simulated directivity in the plane E for the HT.

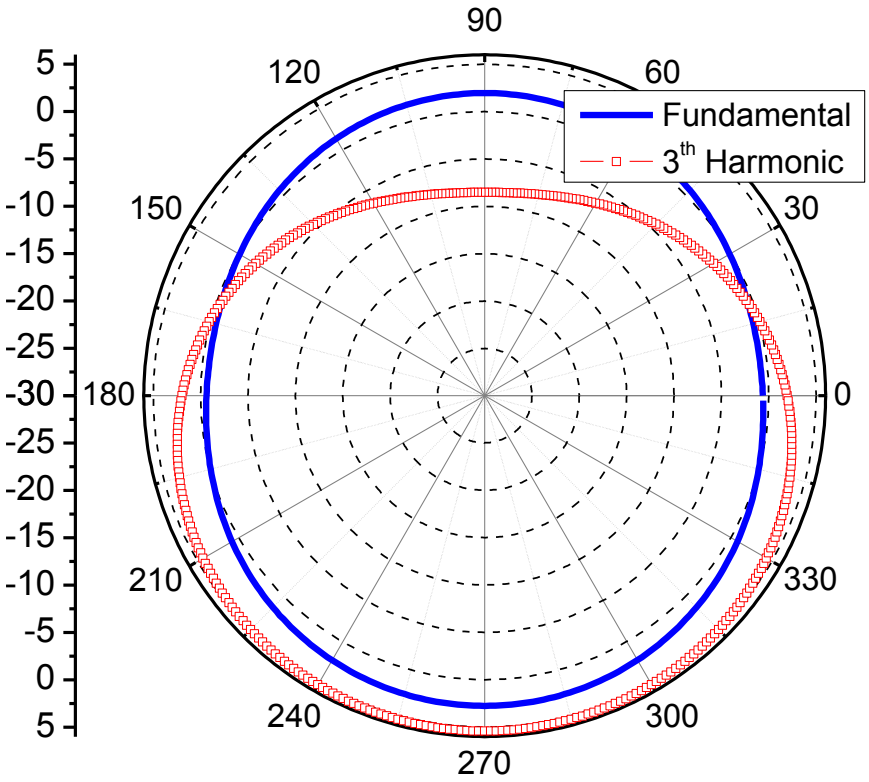

Figure 6.6: Simulated directivity in the plane H for the HT.

is also developed. This new version incorporates a director element aiming to increase the directivity of the antenna. Fig. 6.7 shows the structure for the Yagi-Uda HT with director, which is now composed by four main parts:

- **Fundamental resonator:** shown in Fig. 6.7 (b), with the same operation functions described in the HT version without director.
- **Harmonic resonator:** shown in Fig. 6.7 (a), with the same functions described in the first version.
- **Reflector:** shown in Fig. 6.7 (c), with the same serving functions as the previous version.
- **Director:** located at the front of the antenna as Fig. 6.7 (d) shows, it serves to increase the directivity at the harmonic frequency.

The position and dimension of the director are optimized by simulation, following for the other structure elements, the same tuning policies of the HT version without director above exposed. Table 6.2 summarizes all the optimum design parameters for the new HT antenna.

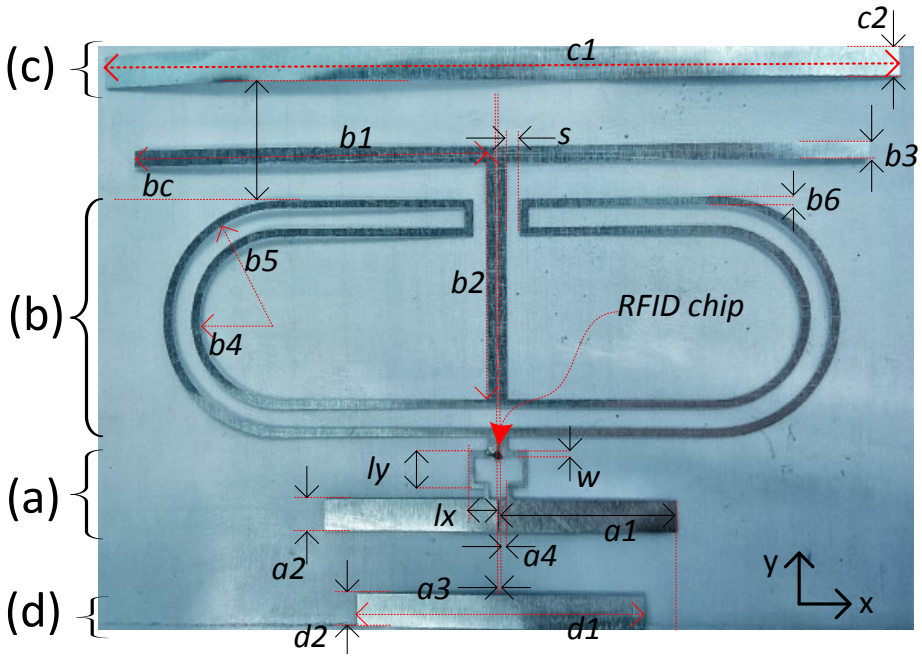

Figure 6.7: New version of the harmonic tag prototype with director element. (a) Harmonic resonator , (b) fundamental resonator, (c) reflector, and (d) director.

With this structure arrangement, a hybrid directivity of the HT with director is conformed by:

- a quasi-omnidirectional pattern at f_0: i.e. the directivity at 868 MHz is now 2.18 dBi, slightly higher than the 1.8 dBi reported in the HT without director.

Table 6.2: Yagi-Uda antenna type with director: design parameters.

Parameter	Value (mm)	Parameter	Value (mm)
a1	18.6	**c1**	85.0
a2	3.3	**c2**	3.3
a3	0.4	**lx**	2.9
a4	0.9	**ly**	3.8
b1	38.1	**w**	0.4
b2	25.5	**bc**	12.8
b3	1.7	**s**	1.5
b4	8.8	**d1**	30.6
b5	11.9	**d2**	3.4
b6	0.9	-	-

- a directive pattern at $3f_0$: i.e. the directivity at 2604 MHz is 6.31 dBi, being also slightly higher than the 6 dBi reported in the HT without director.

Readings at f_0 and/or the 3^{rd} harmonic frequency for the HT with hybrid directivity, introduce an information data unit, because it considers the spacial arrangement of the HT respect to the reader. Fig. 6.8 and Fig.6.9 show the directivity of the HT with director and without director in plane E (xy) and plane H (zy), respectively.

LF-Inverted structures

A modified L-F inverted antenna is designed [136] in polyester substrate PET with permittivity of 3.2 and 0.05 mm thickness. Each part of the planar inverted-F structure is designed and optimized to be able to resonate at UHF band centered in 868 MHz. The inverted-L part of [136] becomes here a complete loop going back to the ground, each part of which, along with the distance between the inverted-F are optimized to have a resonance at 2604 MHz. The capacitive impedances seen by the antenna at f_0 and at $3f_0$ are reduced by creating inductive loops in the ground. Fig. 6.10 presents the structure of the antenna hereafter called HT2. In Table 6.3, all the optimum design parameters for this structure are summarized.

Results for directivity in plane E (xy) and plane H (xz) are depicted in Fig. 6.11 and Fig. 6.12 respectively. With this structure arrangement, the HT is conformed by also a quasi-omnidirectional pattern at f_0 and a directive pattern at $3f_0$, having 1.44 dBi and 6.01 dBi directivity respectively.

Theoretical analysis of HT sample

The HT with Yagi-Uda structure is chosen for this analyisis. In order to estimate the Q factor of the distributed matching network included in the HT example, from (5.7) it is necessary to know R_{eq} and R_A for each HT. R_{eq} for each chip is obtained by converting the series RC impedance measured to a shunt RC equivalent model. Thus, an $R_{eq} = 1.7$ kΩ and an $C_{eq} = 1.03$ pF is

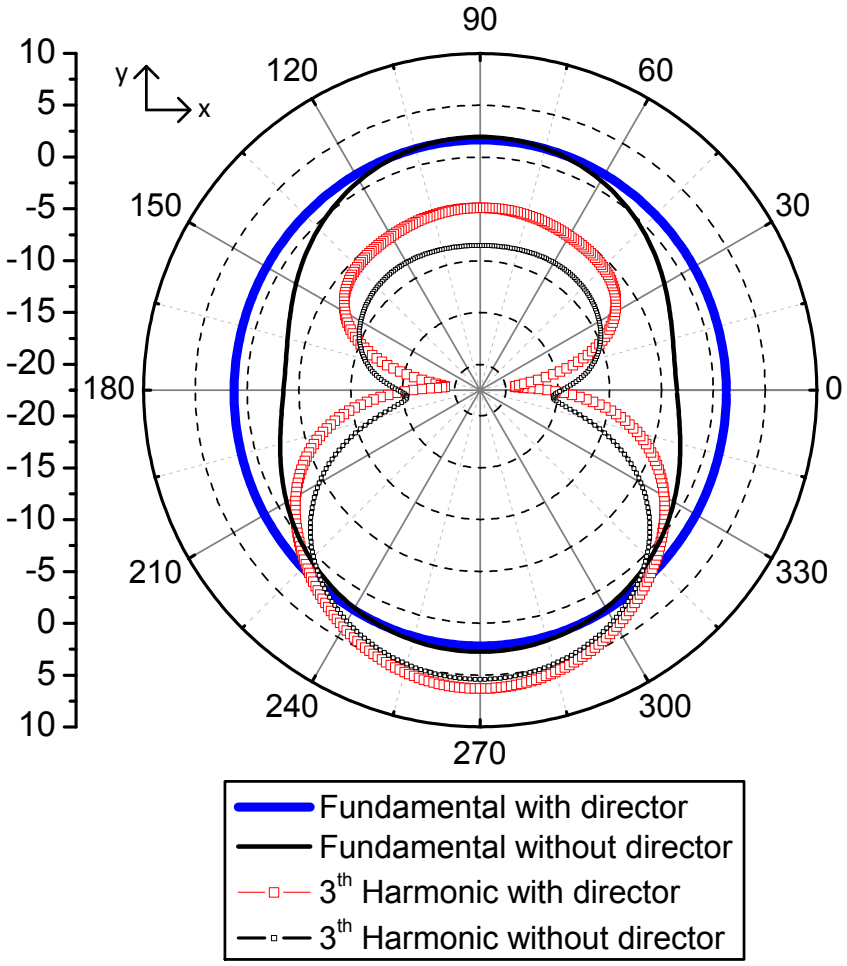

Figure 6.8: Simulated directivity in the plane E for the Yagi-Uda HT with and without director.

Table 6.3: LF-inverted antenna parameters.

Parameter	Value (mm)	Parameter	Value (mm)
g1	62.0	**a5**	2.3
g2	17.0	**b1**	7.0
g3	15.6	**b2**	28.0
g4	11.0	**b3**	2.7
g5	5.6	**x1**	0.2
g6	10.0	**x2**	0.2
a1	60.4	**x3**	0.2
a2	11.9	**x4**	1.0
a3	47.5	**x5**	1.0
a4	3.3		

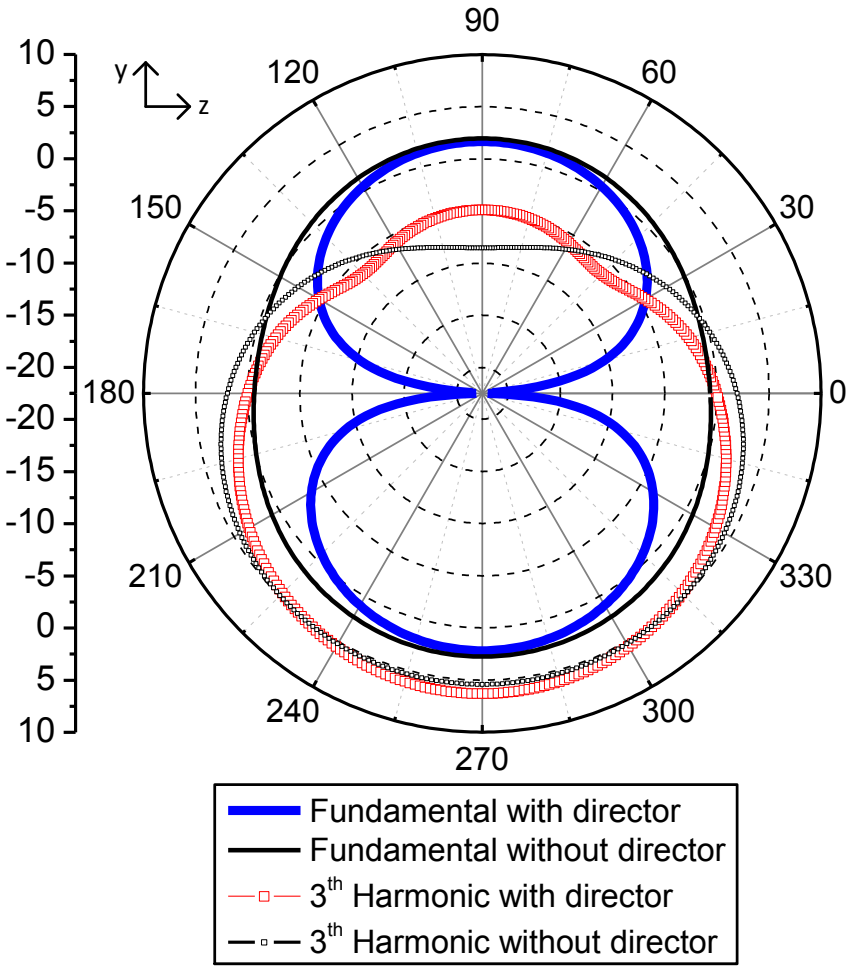

Figure 6.9: Simulated directivity in the plane H for the Yagi-Uda HT with and without director.

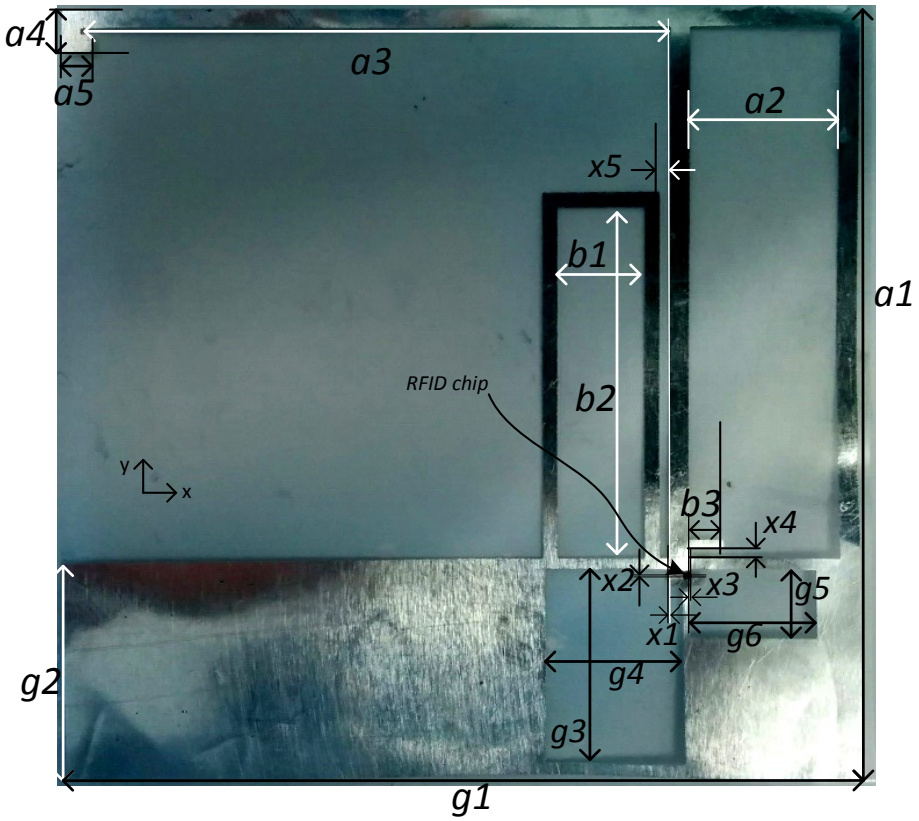

Figure 6.10: Harmonic tag prototype in LF-Inverted structure.

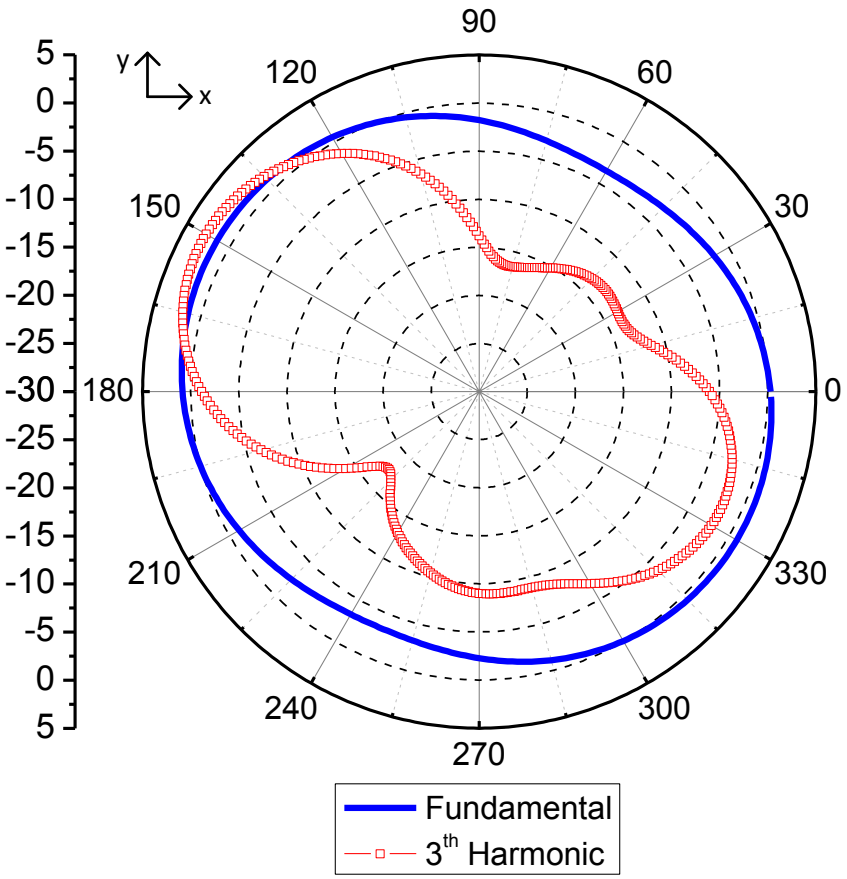

Figure 6.11: Simulated directivity in the plane E for the LF inverted HT.

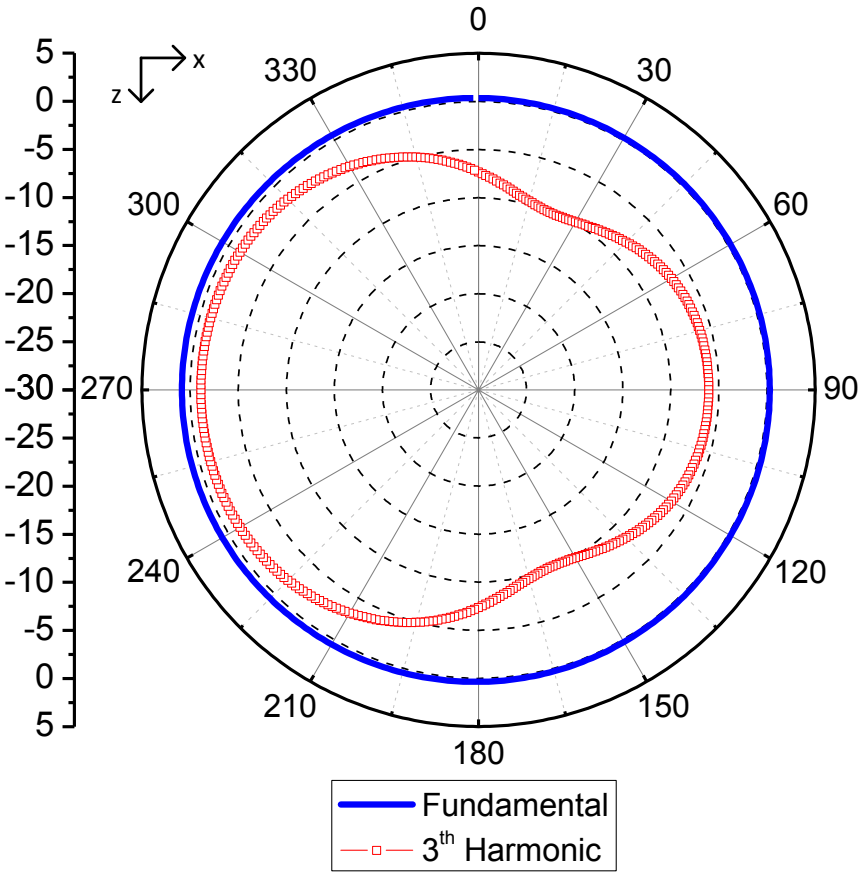

Figure 6.12: Simulated directivity in the plane H for the LF inverted HT.

obtained. The calculation of R_A is not straightforward, given that antenna structures already consider an integrated matching network, its input impedance in a resistive design is unknown. Nevertheless, simulations were carried out in order to approximate the values of R_A. In the case of the HT example the simulation mainly considers: (1) a fulfilled conductor for the fundamental resonator of Fig. 6.7 (b) avoiding the internal inductive gap effect; (2) a feeding port at the middle of the fundamental resonator. An $R_A = 61.7\ \Omega$ is obtained for the chosen antenna, allowing to calculate a quality factor $Q = 5.2$ and a $Q^* = 2.1$ for the HT prototype. In accord to the analysis presented in Section 5.4, the HT example offers a similar treatment to the signals produced by the chip at f_0 and at $3f_0$.

6.4 Experimental results

In this section, results from parametric analysis on the HT prototypes are presented. Details about the methods and setup are below exposed.

Table 6.4: Different configurations of the HTs under test.

Antenna structure	HT Configuration label	RFID chip	Figure legend	Structure
HT1 Yagi-Uda (without director)	HT1-S	NXP UCODE [92]	straight line	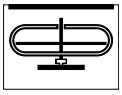
HT1 Yagi-Uda (with director)	HT1-D	NXP-UCODE [92]	dash line	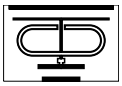
HT2 L-F inverted	HT2-N	NXP-UCODE [92]	straight line	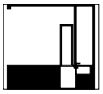
HT2 L-F inverted	HT2-M	Monza 5 [68]	dash line	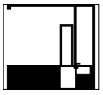
Dipole (commercial tag [109])	T5	-	symbol line	

- **HT under test**: four different configurations of HT using the two kinds of antenna

structure described in Section 6.3 are studied. Henceforth, the notation HT1 refers to tags with Yagi-Uda structure, and HT2 refers to tags with LF-inverted structure. Additionally, from the study performed in Chapter 3, and as comparative reference, the commercial tag so-called T5 with the best performance at the harmonic band was chosen for the study. Details about the four HT configurations under test are shown in Table 6.4.

- **HT prototyping**: all the HT were fabricated on PET substrate with 3.2 permittivity and 0.05 mm thickness. The common trace conductor is aluminum, and the chip mounting technique is flip-chip [138]. For each HT configuration shown in Table 6.4, five samples were fabricated with the same procedure and conditions in order to realize a fabrication sensitivity study. For meaningful and easy understanding reasons, the most representative results will be reported.

- **Measurement setup**: the performance of the prototypes was evaluated in an anechoic chamber with the same RFID Test Platform (RFID-TP) and configuration used in Chapter 3 (1 m distance between RFID-TP and tag). It is worth noting that the RFID-TP considers the communication protocol between reader and tag while tests are performed [57].

- The HTs under test were evaluated under a parametric analysis performed on three main parameters: (1) performance of the HTs at the UHF RFID band. Results are shown in 6.4.1, (2) performance of the HTs at different power sent by the RFID-TP,at f_0 and at $3f_0$. Results are shown in Section 6.4.2, and (3) performance of the HTs at different reading distances, at f_0 and at $3f_0$. Results are shown in Section 6.4.3.

- Results for each one of the studied parameters are organized considering four main features: (1) fabrication sensitivity, (2) bandwidth, power or read range, in each parameter case, (3) kind of chip used, and finally (4) the performance of the HT compared to the commercial tag T5.

- All figures use the same legends to represent each HT configuration in a different type of line. In straight line, the results for tags of type HT1 (or HT2-M), in dash line the results for tags of type HT1-D (or HT2-N) and in symbol-line the results for the tag T5; different colors of the same type of line, correspond to a different sample of the same HT configuration.

6.4.1 Performance of the HTs in the UHF RFID band

Following the nomenclature presented in Table 6.4, Fig. 6.13 and Fig. 6.14 show the Effective Radiated Power (ERP) transmitted by the RFID-TP, in function of the frequency, respectively for the Yagi-Uda structure and LF-inverted structure. Each HT sensitivity is evaluated in terms of the ERP (transmitted power before the antenna). The ERP evaluation allows to perform a general analysis, independent of the kind of reader antenna used. The analysis results are presented in detail below.

- **Fabrication sensitivity**: design directives for all HTs, imposed a first resonance centered in 868 MHz. From Fig. 6.13 and Fig. 6.14, in both structure cases, a detuning effect is

observed, mainly due to the capacitive effect introduced by the flip-chip mounting process. Although the evidenced detuning, the performance of the HTs are always evaluated at 868 MHz and its 3^{rd} harmonic.

Comparing both kind of structures, HT1 tags are most sensible to manufacture process due to the small dimensions of its particular shapes. It can be seen in Fig. 6.13 that for a same structure (HT1 or HT1-D) and a same kind of chip, approximately a 15 MHz variation in the resonance is observed.

- **Bandwidth**: with 20 MHz, the narrower bandwidth is for HT1 tags, compared to the 65 MHz bandwidth for HT2 tags.
- **Kind of chip**: tags with Monza 5 chip (HT2-M) in Fig. 6.14, have better performance in terms of lowest activation power in the whole frequency band studied. These results are consequent with the different sensitivity reported in data-sheets for both kind of chips studied.
- **Comparison with commercial tag**: the commercial tag T5 reports a wider bandwidth. Regarding the activation sensitivity, HT2-M tags have a better performance than T5.

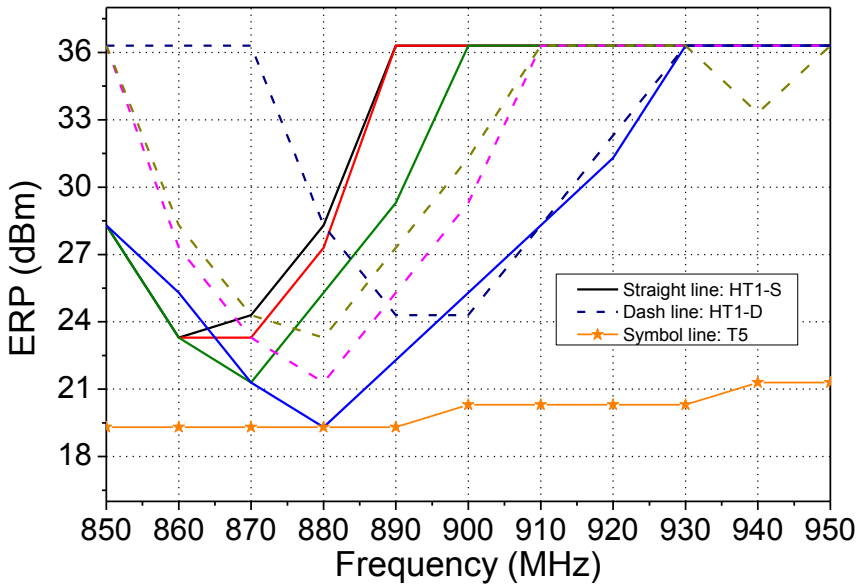

Figure 6.13: ERP transmitted by the RFID-TP in function of the frequency for tags of type HT1 compared with a commercial tag. The analysis is performed around f_0.

6.4.2 Performance of the HTs at different power sent by the RFID-TP

The HT response is evaluated in terms of the isotropic received power (values calibrated to a receiving antenna of 0 dBi gain) in function of the EIRP transmitted by the RFID-TP.

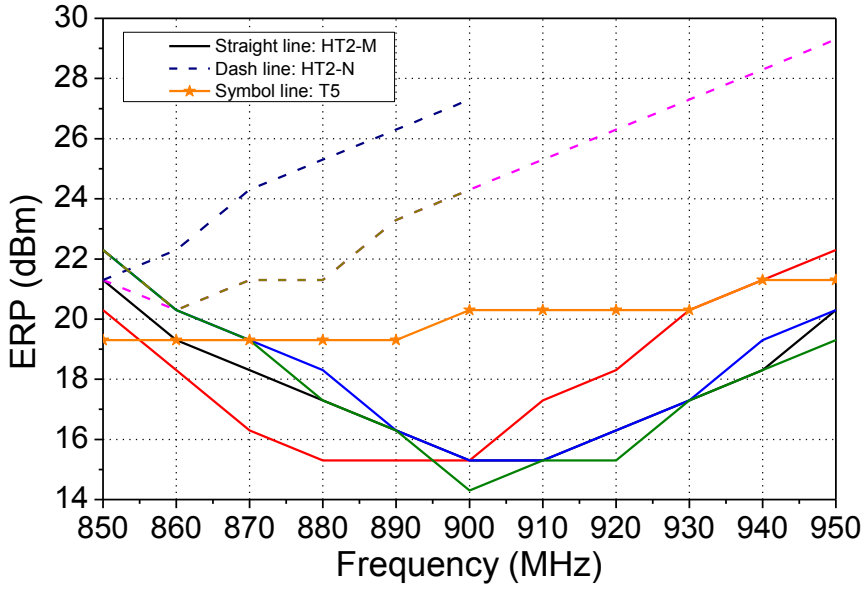

Figure 6.14: ERP transmitted by the RFID-TP in function of the frequency for tags of type HT2 compared with a commercial tag. The analysis is performed around f_0.

Furthermore, in the measure of the HT response, the power spectral density analysis considers the addition of power from both first side lobes of the modulated response, contrary to results reported in Section 3.5 and Section 4.3.2, where only one side lobe is considered.

Fig. 6.15 and Fig. 6.16 show results at f_0 for the tag configurations of type HT1 and tag configurations of type HT2, respectively. Fig. 6.17 and Fig. 6.18 presents same results at $3f_0$. It is important to note that the harmonic response exists conditioned to the existence of the response at f_0, as a non-linear phenomenon of the RFID chip. The analysis results are presented in detail below.

- **Fabrication sensitivity**: Considering the analysis frequency at 868 MHz and its 3^{rd} harmonic, the effects due to the manufacture process in the HTs performance is analyzed. A direct effect on the activation power which relies in the antenna-chip impedance matching is reported. From Fig. 6.15, tags of type HT1 (having all the same chip) are most sensible with a difference of 5 dB in the activation power (horizontal axis) than tags of type HT2 as can be seen in Fig. 6.16. Tags of type HT2 are in general less sensible to manufacture processes due to straight and relatively big structure details. Indeed, the distributed matching network dimensions in tags of type HT1 (Table 6.2: lx, ly, w, a3, a4, b4, b5 and b6) have shorter dimensions than that one of tags of type HT2 (Table 6.3: g1-g6). The same behavior is repeated at the 3^{rd} harmonic frequency in Fig. 6.17 and Fig. 6.18.

- **Tag response level**: once activated, tags of type HT1 in Fig. 6.15 (having all the same chip), present a 5 dB higher response level than those ones of type HT2 shown in Fig. 6.16.

The reason is the higher gain of Yagi-Uda designs. Among tags of type HT1, HT1-D tags have as expected a 2 dB higher response level than HT1-S tags, due to the director element. The behavior is repeated also at the harmonic frequency in Fig. 6.17 reaching in the best case a 3^{rd} harmonic response of -77 dBm for HT1-D. Lower harmonic responses are reported for tags of type HT2 in Fig. 6.18.

- **Kind of chip**: besides the lower activation power of Monza 5 chips, the kind of chip also influences in the hysteresis of the tag response. Indeed, for NXP-UCODE chips, the tag response remains quasi-constant upon activation even if the reader power increases as can be seen for HT1 and HT1-D in Fig. 6.15 and HT2-N in Fig. 6.16. Contrary, for Monza 5 chips, the tag response increases with the reader EIRP, reaching a constant or saturated level at higher powers. Similar behavior is also observed at the 3^{rd} harmonic frequency in Fig. 6.17 and Fig. 6.18. This behavior is intrinsically related to the internal (and proprietary) circuit architecture of each manufacturer, specifically about the voltage regulator design [31].

- **Comparison with commercial tag**: in all cases the proposed HTs have better performance (lower activation power and higher tag response) than the commercial tag T5, at f_0 and at $3f_0$;

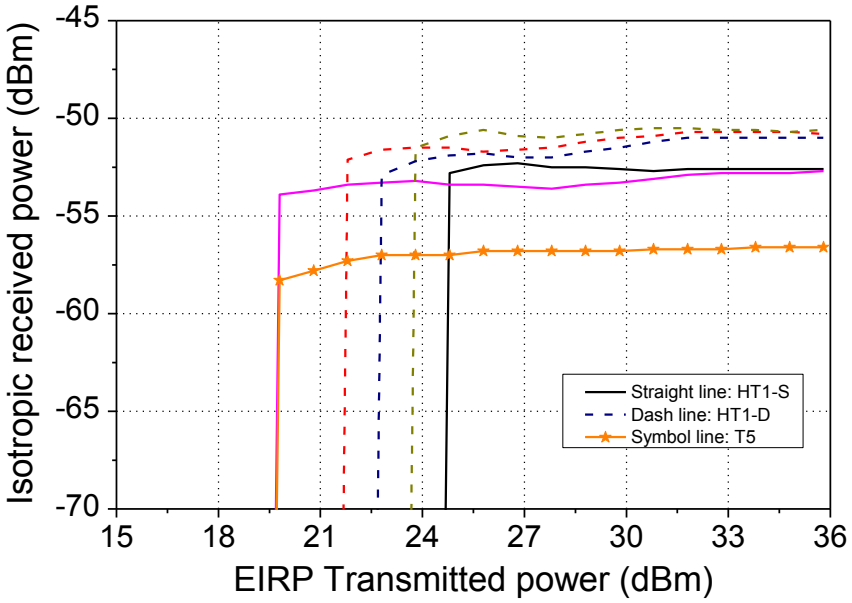

Figure 6.15: Power of the tag response from tags of type HT1 at f_0 in function of the EIRP transmitted by the RFID-TP. The measured power considers an isotropic antenna at reception.

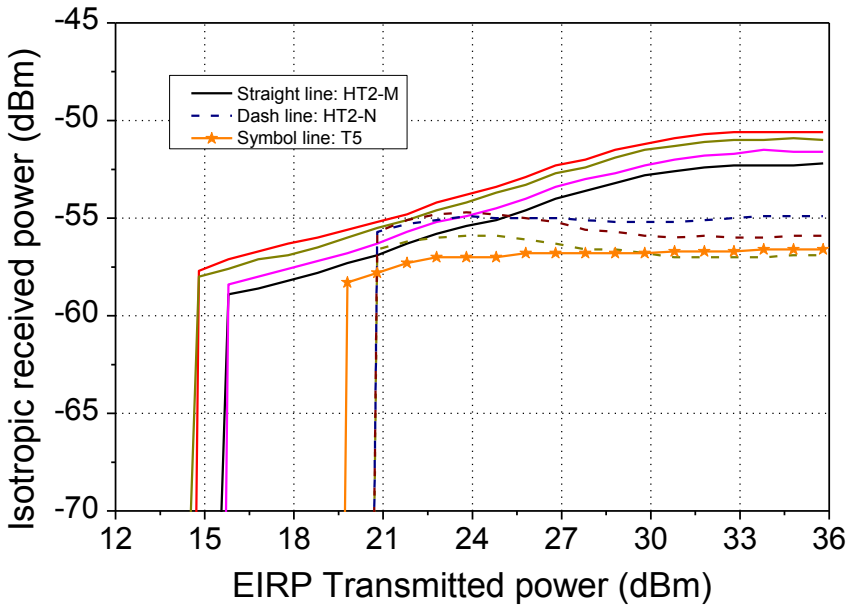

Figure 6.16: Power of the tag response from tags of type HT2 at f_0 in function of the EIRP transmitted by the RFID-TP. The measured power considers an isotropic antenna at reception.

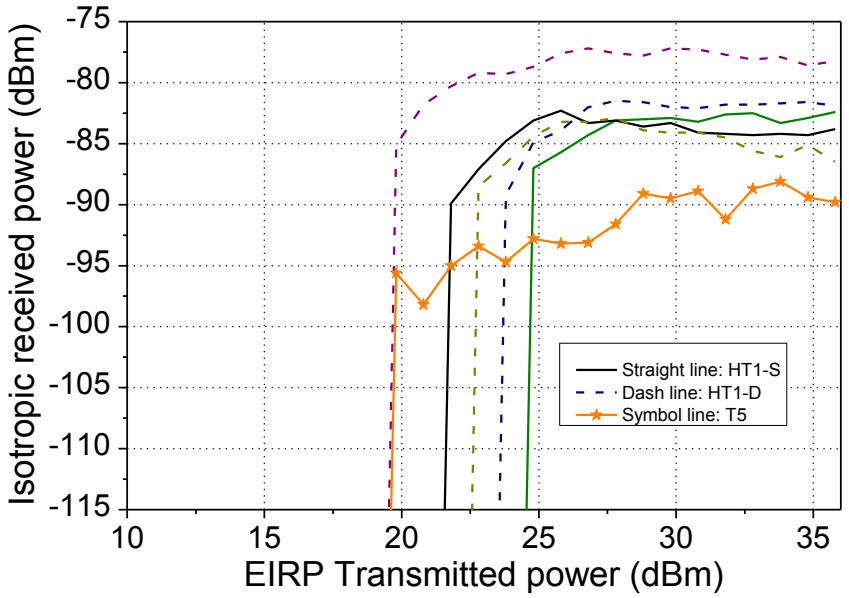

Figure 6.17: Power of the tag response from tags of type HT1 at $3f_0$ in function of the EIRP transmitted by the RFID-TP. The measured power considers an isotropic antenna at reception.

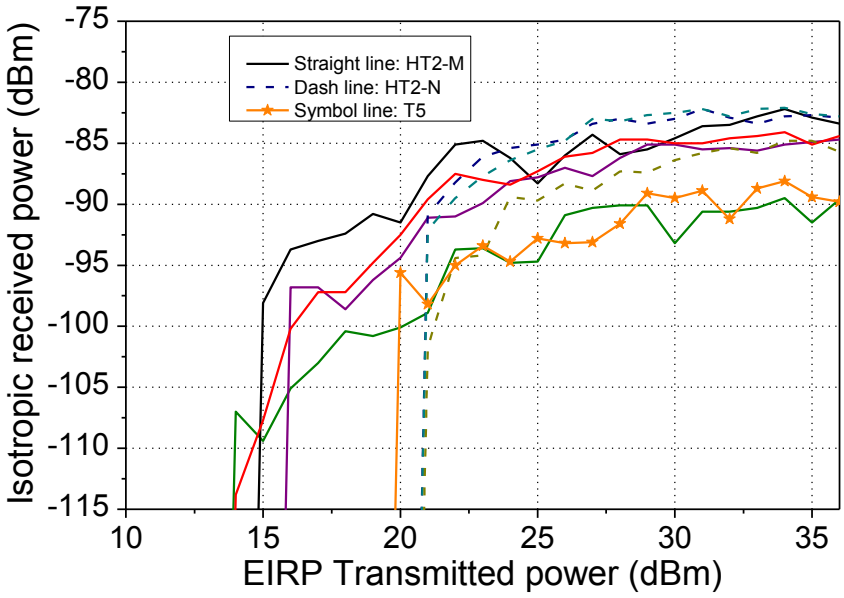

Figure 6.18: Power of the tag response from tags of type HT2 at $3f_0$ in function of the EIRP transmitted by the RFID-TP. The measured power considers an isotropic antenna at reception.

6.4.3 Parametric study on read range

Using the traditional definition of read range definition [88], and considering the measured sensitivity of each HT, the tag response level at the receptor side, at f_0 and at $3f_0$ is calculated, when the EIRP from the RFID-TP is 35 dBm [135]. This analysis allows to represent the read range for a given sensitivity of the receptor.

Fig. 6.19 and Fig. 6.20 show the results at f_0, for tags of type HT1 and tags of type HT2, respectively. Fig. 6.21 and Fig. 6.22 show same results for the 3^{rd} harmonic frequency. The results of the analysis are below presented.

- **Fabrication sensitivity**: the manufacture process introduces an effect on the read range, which is different on each kind of HT configuration. From Fig. 6.19, as expected, tags of type HT1 are the most sensible with a difference of 5.5 m read range (horizontal axis). Tags of type HT2 are in general less sensible to this parameter. Similar behavior is observed at the 3^{rd} harmonic frequency in Fig. 6.21 and Fig. 6.22.

- **Read range**: when simultaneous operation is aimed, the 3^{rd} harmonic response limits the read range of HTs at f_0. For the case of HT1 tags in Fig. 6.21, greater than 5 m read range at the harmonic frequency is achieved if a receiver sensitivity of -90 dBm is attained [139]. For the case of HT2 tags in Fig. 6.22, nearly 4 m read range at $3f_0$ is achieved with -90 dBm of receiver sensitivity.

- **Kind of chip**: the chip sensitivity favors the read range at f_0, reaching for the Monza 5 chip a maximum of 9 m (HT2-M in Fig. 6.20) if the receiver sensitivity were -70 dBm.

Contrary at the harmonic frequency, the hysteresis effect of NXP-UCODE chips triggers in higher harmonic response levels, which favors the feasibility of the receptor sensitivity.

- **Comparison with commercial tag**: higher read range at f_0 and its 3^{rd} harmonic were achieved by the proposed HTs compared to tag T5. From Fig. 6.21 or Fig. 6.22, if the receiver sensitivity were -90 dBm, barely two meters read range is calculated for the commercial tag T5.

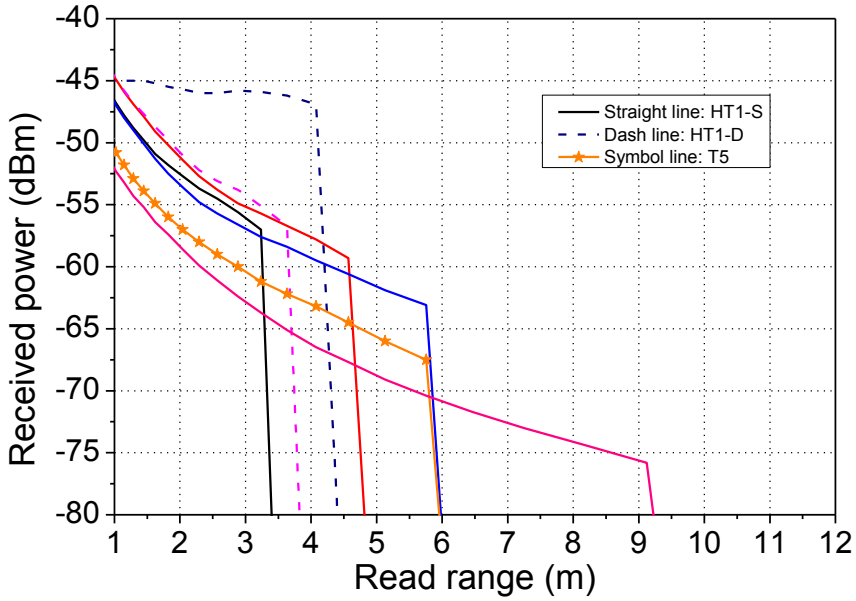

Figure 6.19: Read range for tags of type HT1 at the f_0 in function of 35 dBm EIRP transmitted by the RFID-TP. The measured power considers a 6 dBi antenna at reception.

6.5 Conclusion

Operation concepts for the harmonic communication considering current regulations, harmonic reader, design guidelines for harmonic tags and methods for its evaluations were discussed. The work on exploiting the response at the third harmonic by specialized tag antenna design was experimentally demonstrated with harmonic tag design examples. The evaluation of the prototypes reports a simultaneous read range operation at fundamental and third harmonic frequency greater than 5 m.

The parametric study on the prototypes shows that the HT performance can be enhanced with the antenna structure and also the kind of chip. The frequency analysis shows that the LF-inverted tags have a wider frequency bandwidth than Yagi-Uda tags. Regarding the harmonic response strength, tags having Yagi-Uda structure presents a 5 dB higher response than those ones having LF-inverted structure. The kind of chip used is clearly an advantage in

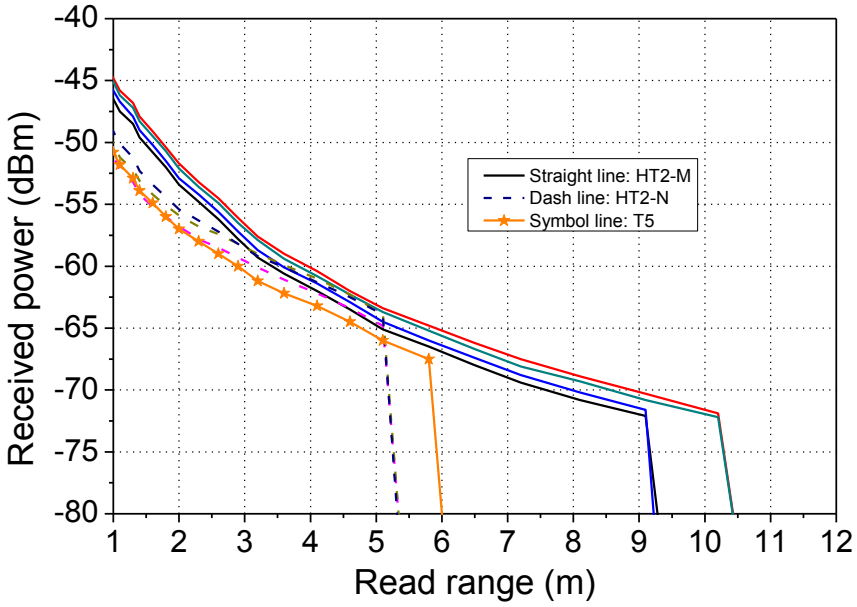

Figure 6.20: Read range for tags of type HT2 at the f_0 in function of 35 *dBm* EIRP transmitted by the RFID-TP. The measured power considers a 6 *dBi* antenna at reception.

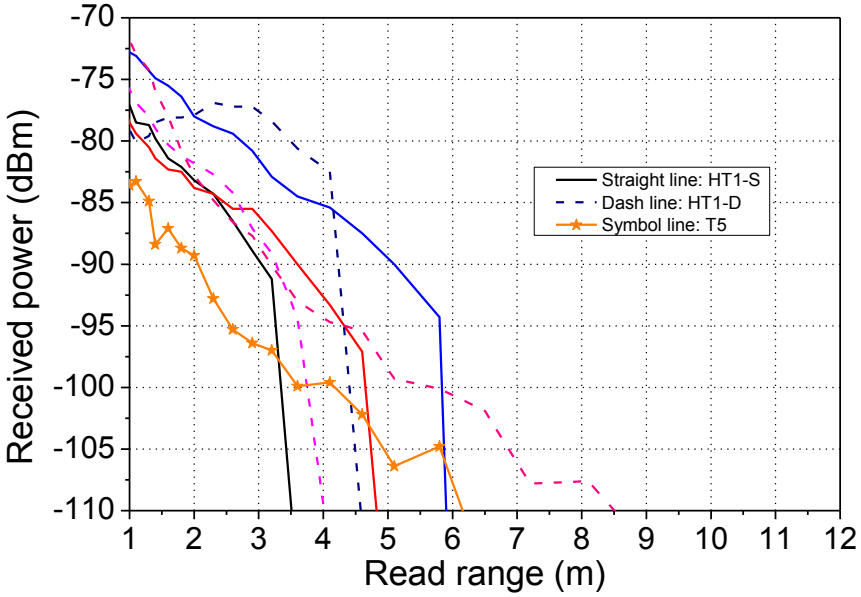

Figure 6.21: Read range for tags of type HT1 at the 3^{rd} harmonic frequency in function of 35 *dBm* EIRP transmitted by the RFID-TP. The measured power considers a 6 *dBi* antenna at reception.

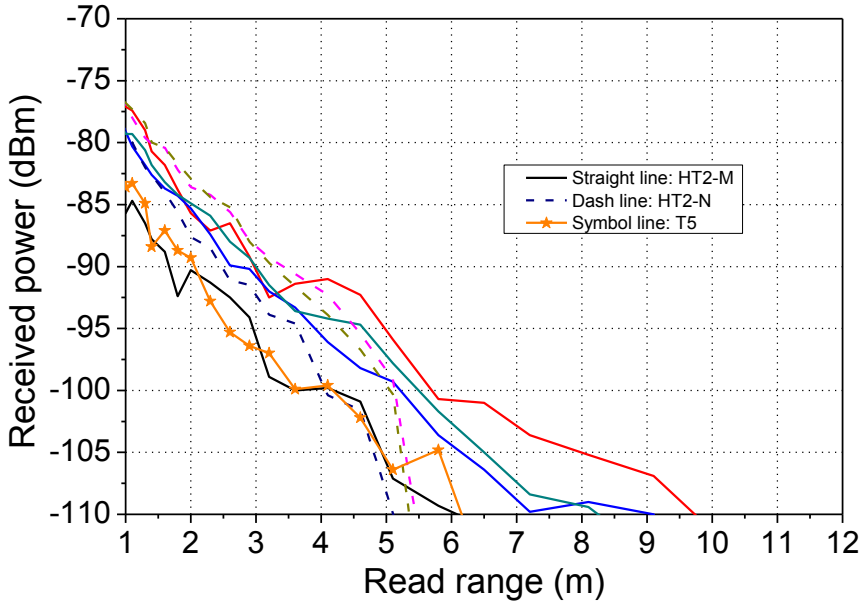

Figure 6.22: Read range for tags of type HT2 at the 3^{rd} harmonic frequency in function of 35 dBm EIRP transmitted by the RFID-TP. The measured power considers a 6 dBi antenna at reception.

the HT performance enhancement. The chip sensitivity favors the read range at the fundamental frequency, reaching in the favorable case 9 m for Monza 5 chips, with a reader sensitivity of -70 dBm. Contrary at the harmonic frequency, the hysteresis effect of NXP UCODE chips, favors the feasibility of the reader sensitivity in a 3^{rd} harmonic reception scenery, because the clear, higher and constant harmonic response produced by this kind of chip. The harmonic tags present higher sensitivity to the fabrication process due to the significant electrical dimensions that the structures take around the third harmonic. Therefore special care and mastery of the sources of losses are necessary in the fabrication stage in order to predict the performance by simulation.

Regarding the benefits of the contribution, they are based on the frequency diversity operation that uses the modulated third harmonic signal produced by the chip, and in where the spectrum has much reduced self and multi-path interference. The redundant signal offers to counter multi-path and leakage effects at reception. Contrary to the traditional efforts in passive RFID, the main contribution of this work is to have a second communication channel from tag-to-reader and not to increase the read range.

Chapter 7 will focus on a different approach for the exploitation of the deeply studied harmonics: electromagnetic harmonic-energy harvesting.

7. Non-linear harvesting and passive UHF RFID

In this chapter some theoretical aspects and experimental results are discussed by linking three attractive concepts: electromagnetic energy harvesting (EEH), Radio Frequency Identification (RFID) communication, and non-linear exploitation from RF devices. The approach takes advantage of the non-linear nature of rectifying elements in order to maximize the RF-to-dc conversion efficiency of EEH devices and to increase the read range of passive RFID tags. The solution triggers on the design of a RF multi-device system. The design procedure and tests exploit three non-linear phenomena: (1) the impedance power dependency, (2) the harmonic production, and (3) the dependency on the RF waveform. In this context, two new approaches for RFID-EEH are proposed by means of integrating an RFID chip working at 868 MHz and a EEH device working at a different frequency in the microwave region, both working in a common antenna:

- An *RFID tag-Rectenna with external harvesting* that exploits the mutual benefit that a joint operation of RFID chip and a rectifying diode offers.
- An *RFID tag-Rectenna with self-harvesting* that exploits the wasted energy naturally generated during the rectification process performed by passive RFID chips.

In both approaches, the re-injection of the harvested energy into the RFID chip produces a read range improvement on the RFID communication function.

7.1 Introduction

In the deployment of ubiquitous sensor networks, it has increased the requirement of additional functions from the smart tags spread on the environment constituting the Internet of Things (IoT) [9; 140–143]. This requirement has caused the need of additional sources of energy. Additionally, a major requirement is currently imposed for all electronic development, it concerns the use of ecofriendly solutions [7]. Then, the most attractive solution may be the energy harvesting of non-conventional sources such as solar [144], human body temperature [145] or Electromagnetic Energy Harvesting (EEH). Among these harvesting solutions, the technology that best suits the needs and where great research efforts are being subscribed due its Wireless Power Transmission (WPT) operation is the passive RFID technology [146; 147].

In the WPT context in sensor networks, the design of EEH devices among them passive RFID tags and rectennas, requires the developing of efficient transmission and reception power transfer techniques. These techniques have been addressed in the literature in a direct or indirect manner by considering the non-linear behavior of EEH devices. Actually, it is possible to classify the non-linear phenomena reported for EEH and WPT in three main categories: (1) impedance-power dependency [65; 93; 132], (2) harmonic generation [58; 126; 130], and (3) efficient waveform design [60–63].

This chapter presents an approach to efficiently exploit the three non-linear phenomena above enumerated into the passive RFID technology. The non-linear exploitation offers satisfying the great requirement of additional power in the deployment of the ubiquitous sensor network in the Internet of Things (IoT) era. If the power needs are satisfied, the read range limitations of the spread sensor devices can be overcome and even additional functions can be envisaged to be included in these sensors. With such a motivation, the main aim of this chapter is: to integrate a rectifier device and a passive RFID tag seeking for a mutual benefit that purposely considers each non-linear phenomena in the design procedure.

This chapter is organized as follows. In Section 7.2, two techniques to enhance the energy harvesting efficiency of EEH devices are proposed and their applications are directly addressed to the passive RFID technology. Section 7.3 details the design procedure of two different prototypes, each one to evaluate each technique of harvesting enhancement. Section 7.4 presents experimental results that validate the efficiency of the proposed techniques on both prototypes. Finally, Section 7.5 presents the final conclusions and perspectives.

7.2 Techniques for harvesting enhancement

This section explains the theory and the proposed techniques to enhance the performance of EEH devices addressing an application for the passive RFID technology. The system architecture used for this purpose is depicted in Fig. 7.1. The approach considers the integration of an EEH circuit with a passive RFID chip all with a single feed antenna, hereinafter so-called RFID Tag-Rectenna (RFID-TR). A distributed matching network as part of the antenna design is considered for the RFID section, while a lumped matching network is considered for the EEH section. The global performance enhancement is based in the simultaneous operation of the communication part, i.e. the RFID section and the EEH section, where the harvested

energy is re-injected into the system. Hereinafter the dc power re-injection is so-called feedback configuration. In passive RFID, the feedback configuration can be done so far using RFID chips which have additional Battery Assisted Power option (BAP). The technique to feedback the harvested energy into the RFID chip reduces the RFID chip sensitivity. Two techniques are proposed to enhance the global performance of the RFID-TR.

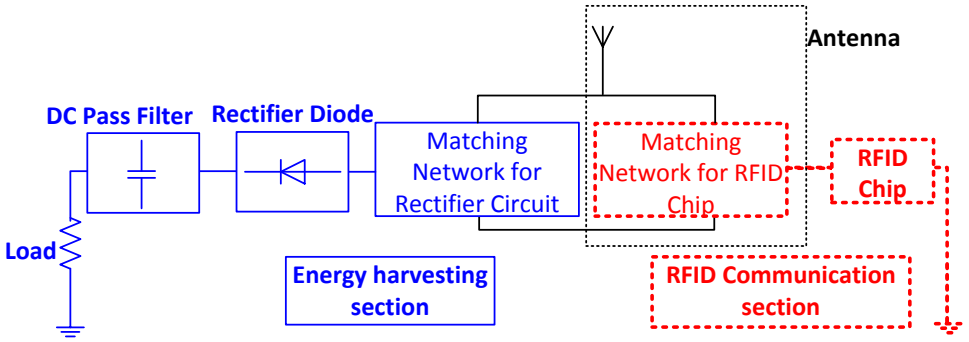

Figure 7.1: Architecture of the proposed RFID-TR system. The system consists of an EEH section (straight line), an RFID section (dash line) and a single feed antenna. A distributed matching network is considered for the RFID section. The EEH section considers lumped elements for the matching network.

7.2.1 Multi-device Waveform

The mutual benefit effect that RFID and EEH sections produce in simultaneous operation can be achieved thanks to the RF waveform produced by the multi-device coexistence. Indeed, the effect is defined in the literature as efficient techniques for WPT by using *time varying envelope signals* [60–63]. The signal waveforms are capable to activate the rectifying devices for lower average input power levels, compared to signals of constant envelope and the same average power. Therefore, when higher the Peak-to-Average Power Ratio (PAPR) is in the received signal, higher is the rectifier RF-to-dc conversion efficiency. In this context, the EEH section of the envisaged RFID-TR system, seeks for receiving a higher PAPR signal. The proposed approach aims to meet this requirement by using the modulated harmonics produced by the RFID chip. Indeed the harmonic signals from the RFID chip are intended to be reflected towards the EEH section in order to produce a *time varying envelope signal* with higher PAPR than a single tone. In order to produce a specific input signal to the EEH section, this method considers both RF sources radiating, i.e. RFID reader and external source and a dual band antenna for the RFID-TR is required.

7.2.2 Harvesting harmonic energy

A different method that improves the performance of the RFID-TR is based on a self-harvesting operation. In this method the harmonics produced by the RFID chip are considered to be harvested instead to contribute to the waveform design. Only the RFID reader source is

necessary avoiding the need of a dual band antenna for the RFID-TR. In [69; 130] it was evidenced that the stronger harmonic produced by the passive RFID chip is the 3^{rd} one. Therefore the EEH section of the RFID-TR should be tuned at the 3^{rd} harmonic frequency of the communication carrier. The concept can be generalized for all diode-based rectifier circuits given that at medium range of RF input power, the rectifier circuits waste a substantial portion of energy in harmonics generated due to the rectification process. The developing of harmonic rectification techniques which profit from the wasted energy declares a new source of energy for ultra low power applications, besides its eco-friendly nature.

7.3 Design Procedure

With the architecture shown in Fig. 7.1 and given the two enhancement methods above proposed, two different RFID-TR prototypes are envisaged, both operating as a passive RFID tag being illuminated by an RFID reader source at 868 MHz, but each one harvesting RF energy from different sources.

- ***RFID-TR with external harvesting.***
  The *external harvesting* feature stands for an EEH section designed to harvest RF energy emitted by an additional external RF source. The external RF source is intended to be the Universal Mobile Telecommunications System (UMTS) band, centered at 2.17 GHz. In order to produce a signal with higher PAPR, the harmonics produced by the RFID section and reflected towards the EEH section in addition to both RF sources are considered to contribute to the waveform signal design for a efficient EEH operation.

- ***RFID-TR with self-harvesting.***
  The *self-harvesting* feature stands for an EEH section designed to harvest RF energy carried on the harmonic with higher power level generated by the RFID chip itself during its normal operation, i.e. the 3^{rd} one.

It is important to note that the procedure is the same for the two prototypes and so for the two techniques for harvesting enhancement. In order to consider the non-linear behavior of RFID chip and rectifier diode in the design process, a sequential design is performed:

1. The impedances of the RFID chip and the rectifier diode, with respect to the incident RF power and frequency are characterized before the antenna design (Section 7.3.1).

2. An equivalent non-linear model with similar features is proposed in an electrical simulator, for each device (Section 7.3.2).

3. The procedure is followed by the antenna design considering complex impedance matching techniques (Section 7.3.3).

4. Finally, an electrical and electromagnetic co-simulation integrates each electrical model and the antenna for a global optimization of the RFID-TR (Section 7.3.4).

The design process is valid for all kinds of passive RFID chips, rectifier diode and antenna structure, regardless the frequency or application power chosen.

7.3.1 Characterization of non-linear devices

Using a test platform similar to that one presented in [130], the passive RFID chip EM4325 (TSSOP-8 package) with BAP option [148] and the HSMS 2860 Schottky diode (SOT23 package) [149] are characterized at the frequencies of interest (868 MHz, 2.17 GHz and 2.604 GHz).

Due to the non-linear dependency of impedance with the input power in non-linear circuits, the characterization of both devices is performed setting a fixed input power of -10 dBm at all frequencies. It is worth noting that the minimal directive during the devices characterization is to reach the activation threshold for the RFID chip. The measured RFID chip impedance in scavenging state at 868 MHz is $18 - j130\ \Omega$, and at 2.604 GHz it is $6 - j49\ \Omega$. Following the same principles, the impedance of the Schottky diode is also measured reporting $30 - j242\ \Omega$, at 2.17 GHz and $24 - j211\ \Omega$, at 2.604 GHz.

7.3.2 Electrical model of non-linear devices

Rectifying diode model

The electrical model of the EEH section is simulated using CST Studio Suite. The EEH section consists of a single rectifier Schottky diode (*Diode*) that converts the RF input into dc output whereas a capacitor filters its output to smooth the desired dc signal, which can be measured across a load resistor. The architecture of the circuit is shown in Fig. 7.2. The chosen diode HSMS 2860 presents the following electrical parameters: low series resistance $R_s = 6\ \Omega$, zero-bias junction capacitance $C_jo = 0.18$ pF, breakdown voltage $V_{br} = 7$ V and high detection sensitivity equal to 35 mV/uW [149]. The proposed electrical model ensures a rectifier circuit having a similar non-linear operation than a real sample (conversion efficiency, harmonics generation and power capacity [150])

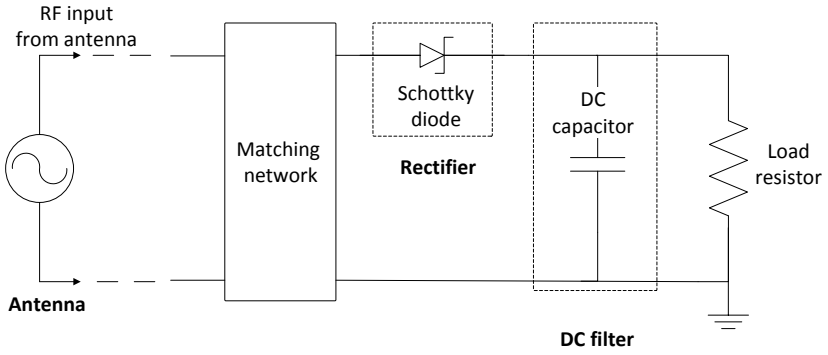

Figure 7.2: EH section of the RFID-TR.

RFID chip model

The internal architecture of the RFID chip consists on a rectifier circuit based on a Cockcroft-Walton topology with two or more diode-based voltage doubler stages [31]. The rectifier circuit, responsible of the harmonic production, mostly determines the input impedance of the chip. The rectifier impedance domination can be generalized for all EEH devices, with some considerations on the architecture, which will establish the predominance of odd or even harmonics [31]. A sketch of the RFID tag architecture with a highlighted rectenna part is shown in Fig. 7.3. In order to consider the non-linear behavior of the RFID chip in the

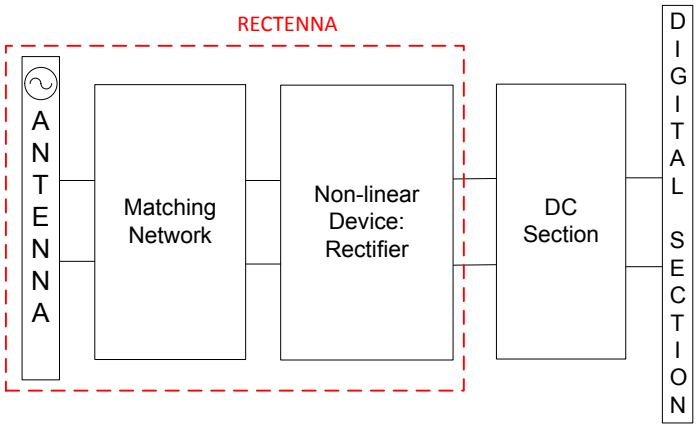

Figure 7.3: Internal architecture of a passive RFID tag.

design, an equivalent electrical model with similar impedance to the measured value is proposed. Using CST Studio Suite, the RFID chip model is simulated with the aim to produce similar impedance behavior to the characterized values at -10 dBm input power. The equivalent circuit is composed by three voltage multiplier stages using Schottky diodes, coupling capacitors (Cc) and ended in a dc load resistance ($Load$) as shown in Fig. 7.4. Additionally, a shunt resistor (Rin) and a shunt capacitance (Cin) at the input represent the resistance of the RFID chip and the capacitance of packaging, respectively. Design parameters for the equivalent circuit are given as: $Cc = 4.3$ mF; $Cin = 0.146$ pF; $Rin = 965\ \Omega$; $Load = 10\ k\Omega$; using the Spice model of the HSMS 2860 as $Diode$. This circuit has assured an input impedance value closer to the measured input impedance of the RFID chip ($18 - j130\ \Omega$) being closely equal to its datasheet value i.e. $23 - j145\ \Omega$, at 868 MHz. In the same way, at 2.604 GHz the simulated values for the RFID chip are closer to the measured ones.

Impedance characterization results of the RFID chip and the Schottky diode are in good agreement with their equivalent electrical model as it is shown in Fig. 7.5. With these non-linear models, a common antenna is designed in the next section.

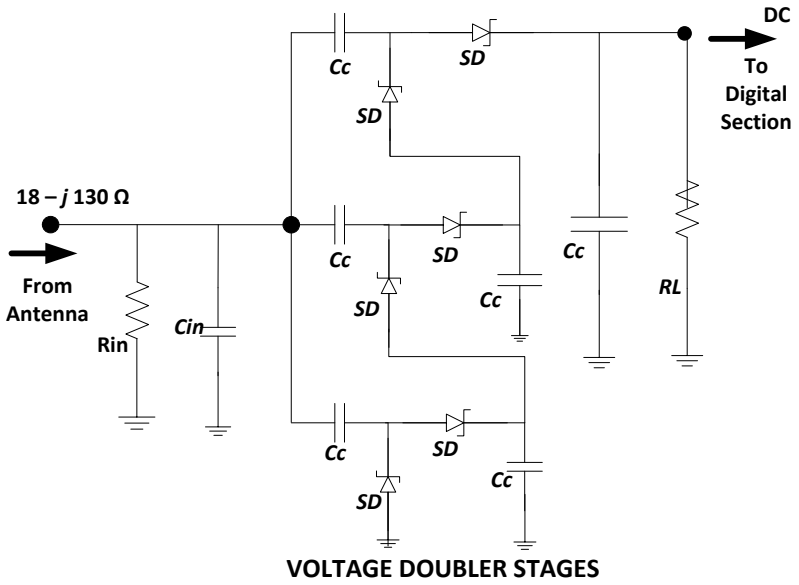

Figure 7.4: RFID chip equivalent circuit with three voltage doubler stages, based on Cockcroft-Walton topology.

7.3.3 Antenna design

By appealing to techniques of RFID antenna design such as inductive loops to cancel the capacitive impedance of RFID chips, and size reduction [18; 151], the design of two antennas is envisaged: (1) a single feed dual band antenna for the *RFID-TR with external harvesting*, and (2) a single band antenna for the *RFID-TR with self-harvesting*. Two different antennas are required since the frequency operation of the EEH section of each RFID-TR is different. In the first case the EEH is performed from an external source while in the second case, the EEH is performed from a locally generated harmonic.

Single feed dual band antenna

The first antenna resonance should be centered at 868 MHz to operate as UHF RFID tag antenna. The second antenna resonance should be centered at 2.17 GHz to serve to the harvesting section. These requirements allow to use a similar dual band antenna to that one presented in [136] based in a modified L-F inverted antenna. The antenna structure allows using a ground plane and radiator, all in a common face. Therefore the ground plane is used for the rectifier circuitry. Moreover, two loops in the ground plane allow to perform inductive impedance matching useful to reduce the capacitive effect of attached devices connected at the input of the antenna, i.e. the total capacitive impedance seen by the EEH circuit. Fig. 7.6 illustrates the single feed dual band antenna.

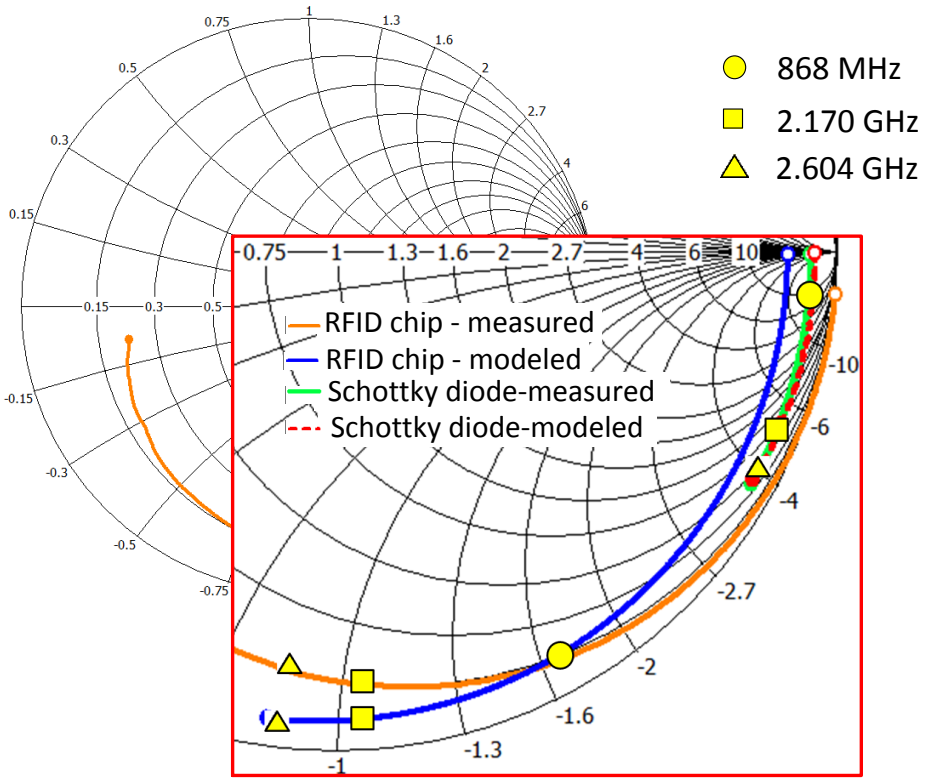

Figure 7.5: Measured and modeled impedances for the RFID chip and Schottky diode, both at −10 dBm. Values are normalized to 50 Ω

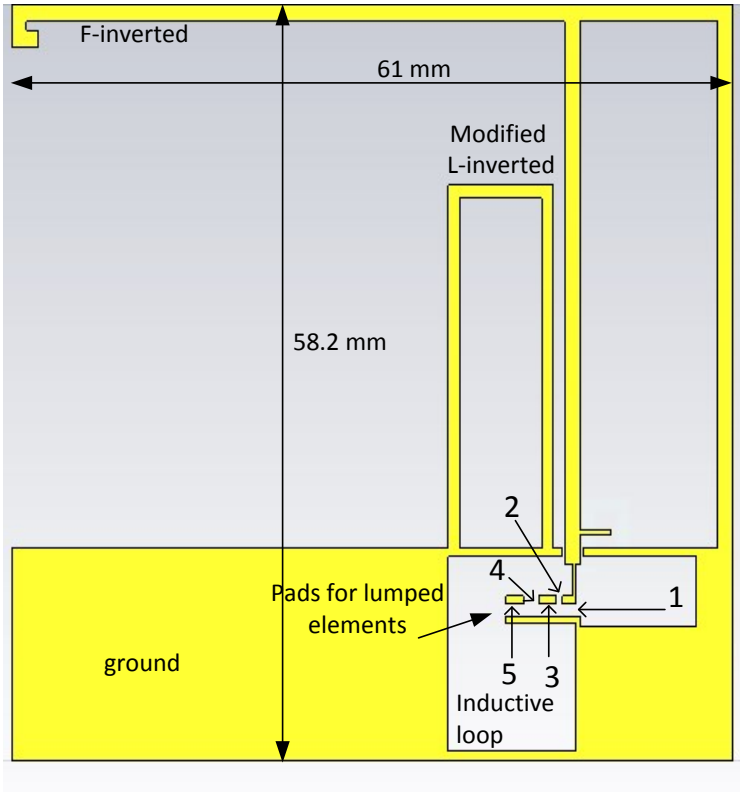

Figure 7.6: Structure of the single feed dual band antenna. The arrows indicate the pads (ports) where the lumped elements of the EEH section are connected. The pads are considered in the electromagnetic simulation.

Single band antenna

Since a traditional single band operation at 868 MHz is aimed for RFID communication, an antenna based on a dipole structure using an inductive loop to match the impedance of the RFID chip is designed [144]. Fig. 7.7 shows the proposed single band antenna structure.

In order to consider the harmonic generation of each device, the electromagnetic simulation for the antenna is performed from 0 to 10 GHz in order to cover the first fourth harmonics of the microwave frequency and also the first five harmonics of the UHF RFID carrier. The antenna structure is optimized with the goal of reaching a conjugate impedance matching with the RFID chip at 868 MHz. It is worth noting that the wide simulation frequency range is useful in the co-simulation process, when the EEH section is introduced in order to quantify the harmonic strength of the RFID chip in concordance with the antenna behavior.

7.3.4 Co-simulation method for the RFID-TR system

An electrical-electromagnetic co-simulation is carried using CST Studio Suite to integrate the electrical models above described with the antenna for each RFID-TR type. The co-simulation is performed in order to optimize the performance of the EEH section choosing proper lumped components and the antenna structure. It is worth noting that the antenna multiport S-parameters consider the pads used for the rectifier circuitry (five ports shown in Fig. 7.6). It is important to note that the optimized design ensures -10 dBm RF power at the input of the RFID chip. It is worth also noting that the impedance modulation of the RFID chip at 868 MHz produces small variations in the impedance at upper frequencies 2.17 GHz and 2.604 GHz. This impedance modulation will not produce considerable mismatching with the impedance seen by the EEH section.

The co-simulation triggers in two optimized lumped impedance matching networks for the EEH section, each one for each RFID-TR type as depicted in Fig. 7.1: (1) for the *RFID-TR with external harvesting tuned at* 2.17 *GHz, the matching networks is composed by a* 0.2 *pF capacitor in series with a* 6.8 *nH inductor in shunt. (2) for the* RFID-TR with self-harvesting *tuned at* 2.604 *GHz, it is composed by a* 0.05 *pF capacitor in series with a* 12 *nH inductor in shunt. Regarding the dc* section, a single 10 nF capacitor connected in shunt forms the Low Pass Filter (LPF) to bypass the RF components (fundamental frequency, harmonics of the rectifying diode, and reflected harmonics produced by the RFID chip) in both RFID-TR types. Finally an arbitrary 3 $k\Omega$ load is chosen to collect the dc power at the output. Fig. 7.8 presents the block diagram of the co-simulation method integrating all the sections of the proposed RFID-TR system. For simulation purposes, an ideal directional coupler is used to integrate the S-parameters of the antenna with the RFID chip model and an AC source.

7.4 Experimental results

The realized *RFID-TR with external harvesting* and *RFID-TR with self-harvesting* are pictured in Fig. 7.9 and Fig. 7.10 respectively. The substrate is Rogers RO4003 with 3.55 permittivity and 0.8 mm thickness. The RFID chip and lumped components are soldered in the pads.

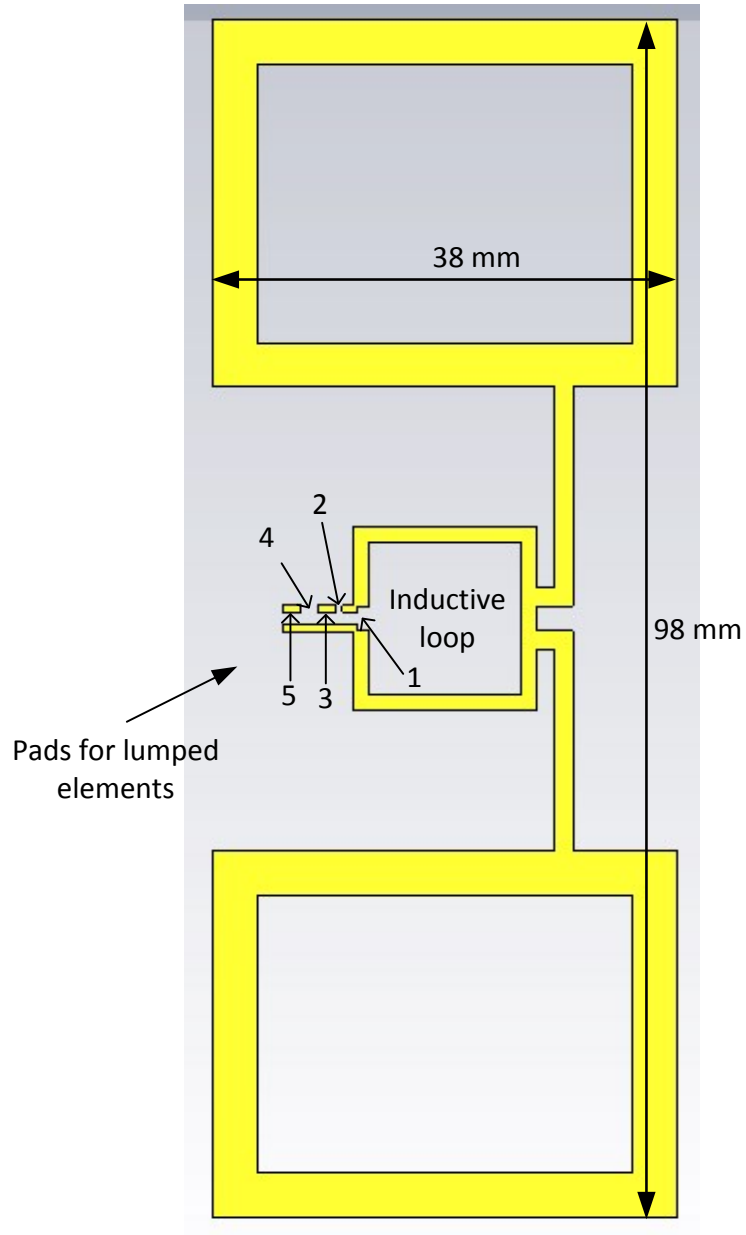

Figure 7.7: Structure of the single band antenna at 868 MHz. The arrows indicate the pads (ports) where the lumped elements of the harmonic EEH section are connected. The pads are considered in the electromagnetic simulation.

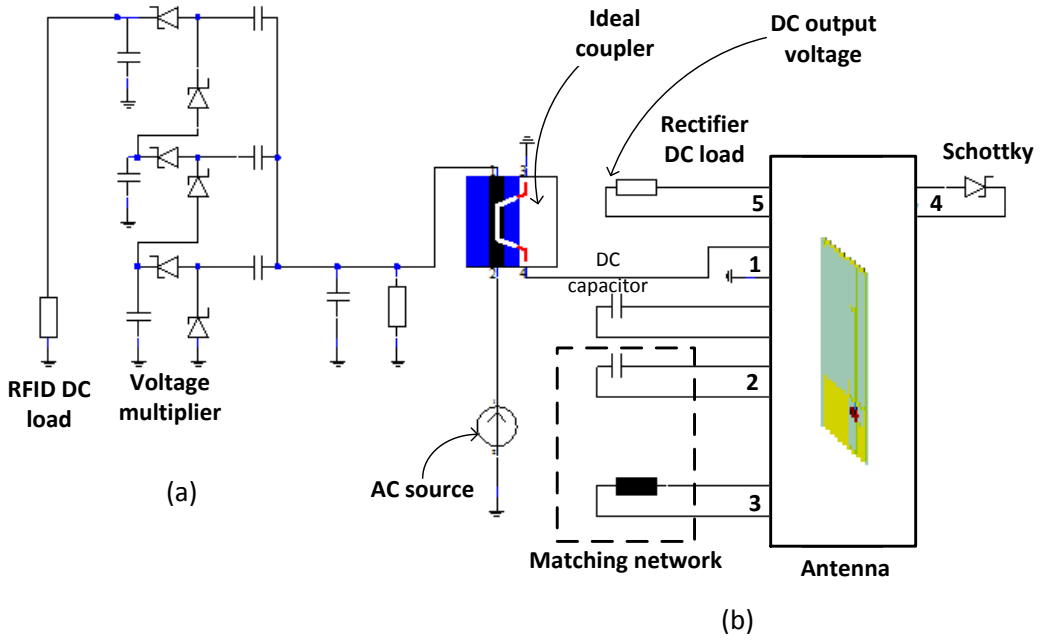

Figure 7.8: Electric-electromagnetic co-simulation of the proposed RFID-TR. (a) non-linear model of the RFID chip, (b) co-simulation integration of the RFID-TR.

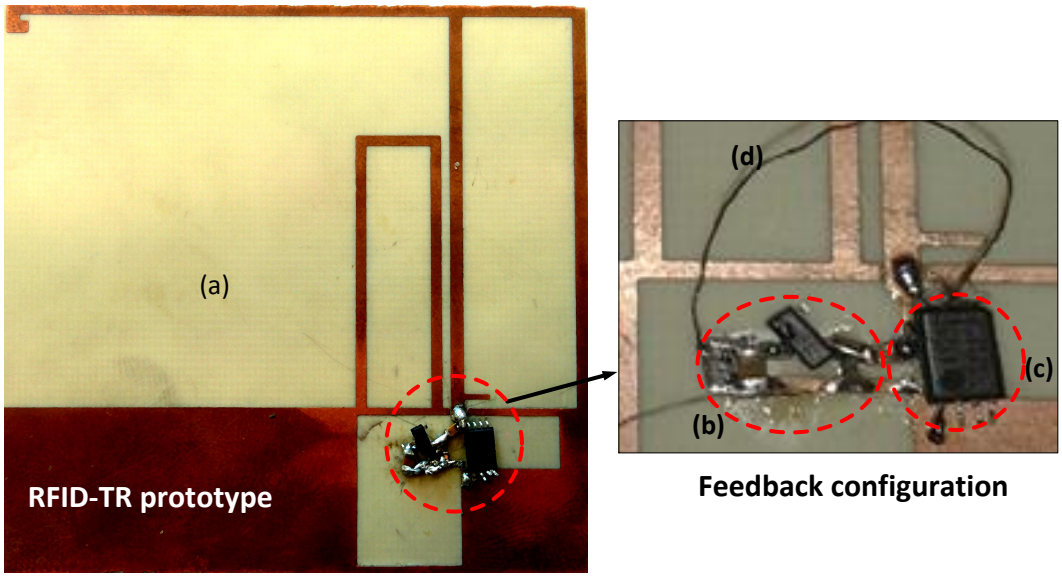

Figure 7.9: Prototype of the *RFID-TR with external harvesting*. (a) dual band antenna, (b) EEH section, (c) EM4325 RFID chip, (d) feedback wire.

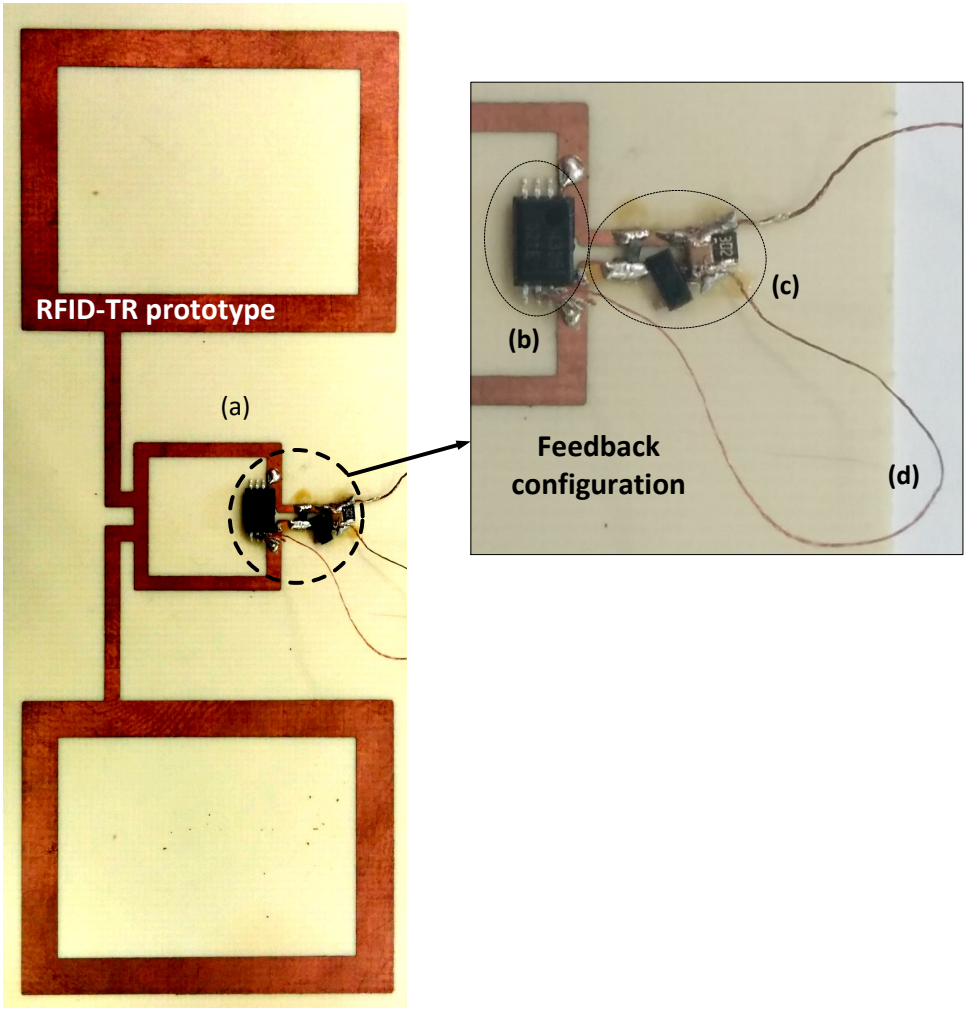

Figure 7.10: Prototype of the *RFID-TR with self-harvesting*. (a) single band antenna, (b) EM4325 RFID chip, (c) EEH section, (d) feedback wire.

7.4.1 Measurement setup

In order to evaluate the performance of each RFID-TR, measurements were performed in an anechoic chamber. The measurement procedure has two goals: (1) to measure the dc output across the load resistor in the EEH section, and (2) to measure the response of the passive RFID tag in terms of read range. The measurement setup illustrated in Fig. 7.11 is composed as follows:

- An external source centered in the UMTS band 2.17 GHz is emulated by an Agilent N5182A signal generator. A 10 dB gain horn antenna is used in transmission;
- For the RFID communication, an Impinj Speedway *R*420 Revolution RFID reader operating at 868 MHz, jointly with a circularly polarized 6 dB gain antenna;
- An dc voltmeter is connected to each RFID-TR in order to measure the harvested dc voltage;
- A computer controls the equipment for data acquisition and data processing.

In the setup calibration, the power budget considers antenna gains, free space propagation losses, and cable losses. Given the presence of two RF sources, three different transmission

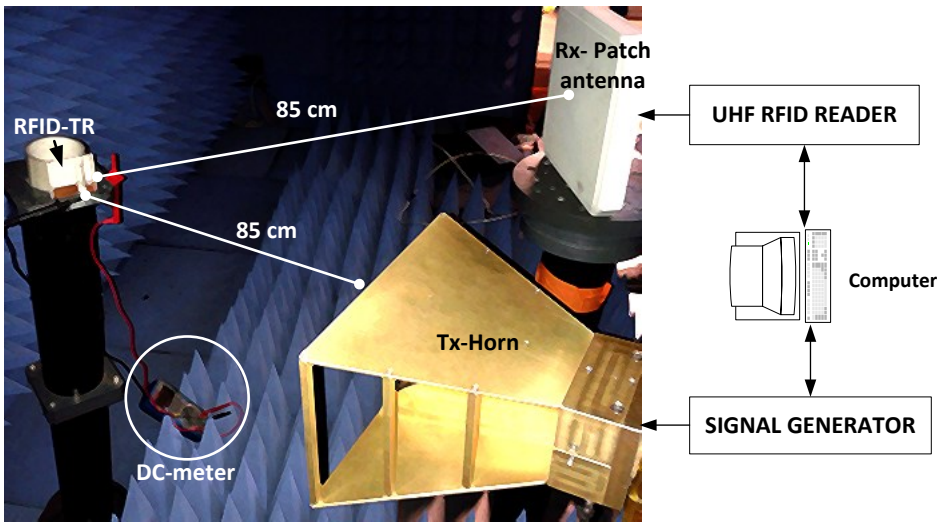

Figure 7.11: Measurement setup for the performance evaluation of the RFID-TR.

configurations are considered to better evaluate the operation of the RFID-TRs. In each case the measurements are performed with and without feedback. Table 7.1 shows the three considered cases.

Table 7.1: Transmission configurations for the RFID-TR evaluation.

Case	Tranmission configuration
(a)	UHF RFID reader transmitting at 868 MHz sweeping in power
(b)	RF source transmitting at 2.17 GHz sweeping in power
(c)	RF source transmitting at 2.17 GHz sweeping in power and UHF RFID reader transmitting at 868 MHz fixed in 30 dBm

7.4.2 EEH evaluation

RFID-TR with external harvesting

The dc output voltage measured at 0 dBm received input power is given in Table 7.2 for the three configurations previously presented in Table 7.1. A considerable shift between the dc voltage measured without feedback and the dc voltage measured with feedback is reported at 0 dBm received input power in all configuration cases. In case *(c)* a considerable shift from 48.4 mV to 111.9 mV is noted. This shift is due to the enlarged resistance where the dc power is consumed (load resistor of the EEH circuit is added in series with an internal load resistor of the dc input of the RFID chip).

On the other hand, having the feedback configuration set, the great difference from the measured dc with only one source transmitting (case *(a)* and case *(b)*) compared to the measured dc with two sources transmitting (case *(c)*) demonstrates a mutual enhanced performance of each section over the other.

Table 7.2: Measured dc output without and with EEH feedback.

Case	Without feedback (mV)	With feedback (mV)
(a)	1.8	7.1
(b)	26.4	107.4
(c)	48.4	111.9

The measured dc output versus the received input power at 2.17 GHz for the three cases of Table 7.1 is shown in Fig. 7.12. As can be seen, when the RFID reader transmits its maximum power in case *(a)*, the EEH section starts producing some weak dc level. Even if the EEH section is tuned at 2.17 GHz, the 2^{nd} and 3^{rd} harmonics of 868 MHz are being rectified. Furthermore, the curve in case *(b)* shows an rising trend in function of its received input power. Finally, the mutual benefit that a joint operation of RFID chip and a rectifying diode offers is represented by the curve for case *(c)*. The mutual cooperation effect, explained in Section 7.2.1, is based on the

effect that *time varying envelope signal* produces in rectifier diodes. The input RF waveform to the EEH in case *(c)*, is expected to have higher PAPR due to the reflected modulated harmonics of the RFID chip over the EEH section.

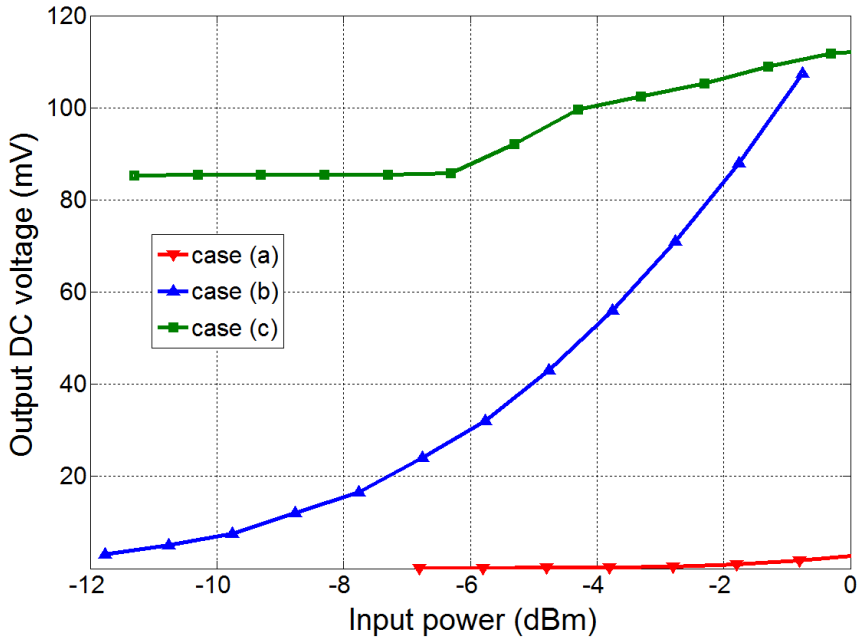

Figure 7.12: Rectified dc output voltage versus received input power for the RFID-TR with external harvesting.

In order to quantify the results comparing the RFID-TR performance when both sources transmit respect to the case when only the UMTS source transmits, it is defined a power gain figure (G_P). The factor G_P defines the power gain obtained in case *(c)* regarding to the power gain obtained in case *(b)* [60]. Since the dc load resistance is in both cases the same (in feedback configuration), the dc power can be defined as function of the dc voltages. G_P is defined in (7.1) and the results are shown in Fig. 7.13. A better cooperation is found for low input power between -11.3 dBm and -7 dBm, showing consequence with the optimization design stage focused at -10 dBm. The reported G_P at the lowest input power -11.3 dBm, is 33 dB.

$$G_P = 10\log_{10}\left(\frac{V_c^2}{V_b^2}\right) \tag{7.1}$$

RFID-TR with self-harvesting

The dc output for the self-harvester is measured only in case *(a)* because here the RFID reader is the only power provider. At the maximum transmitted power allowed by the reader, i.e. 30 dBm, the measured dc output for the self-harvester is 158 mV without feedback and 242 mV

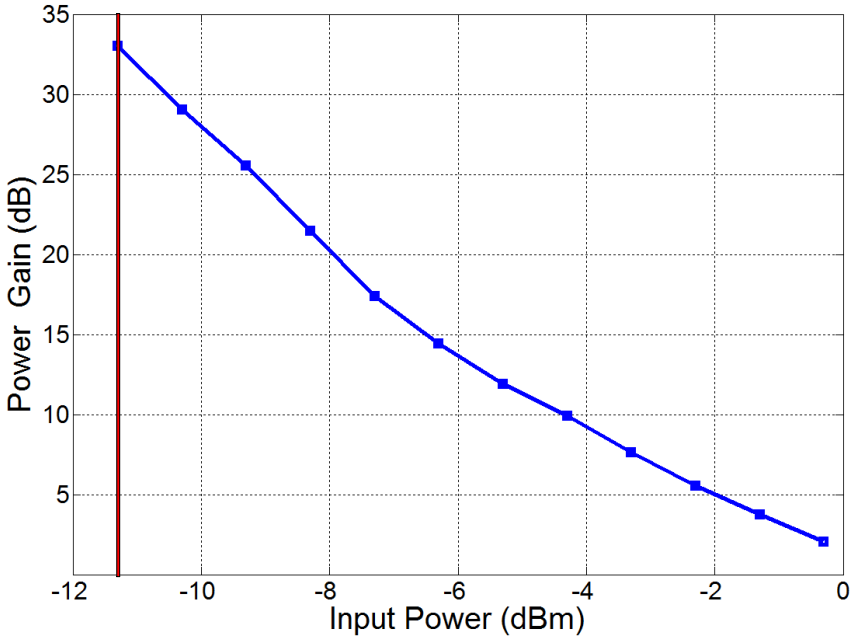

Figure 7.13: Power gain as function of input power (dBm) for the RFID-TR with external harvesting.

with feedback. The same shift effect on the dc values measured without and with feedback is found, due to the change of the total load where the dc power is consumed. The RF power at the fundamental frequency makes the chip to generate a 3^{rd} harmonic signal whose level needs to be calculated in order to quantify the RF-to-dc conversion efficiency of this prototype.

In order to calculate the RF input power to the EEH section at the 3^{rd} harmonic of 868 MHz, reported measures of harmonic production in passive RFID chips are used [130]. This input power is approximated as the RF power delivered to the RFID chip at the fundamental frequency (considering 1.64 dB simulated gain for the tag antenna and threshold activation for the RFID chip) minus 35 dB. This substraction corresponds to the difference between the RFID chip sensitivity of -10 dBm and a 3^{rd} harmonic response equal to -45 dBm, which is congruent with values reported in Table 4.2. Fig. 7.14 shows the measured dc output for the self-harvester, with feedback configuration, in function of the input power to the chip at the 3^{rd} harmonic.

With these considerations, the RF-to-dc conversion efficiency reports a maximum of 60% at -42 dBm of 3^{rd} harmonic input power as it is shown in Fig. 7.15.

7.4.3 Read range evaluation

RFID-TR with external harvesting

The performance of the *RFID-TR with external harvesting* working as RFID tag is evaluated by calculating its read range with similar methods to [88]. The read range is calculated for case *(a)*

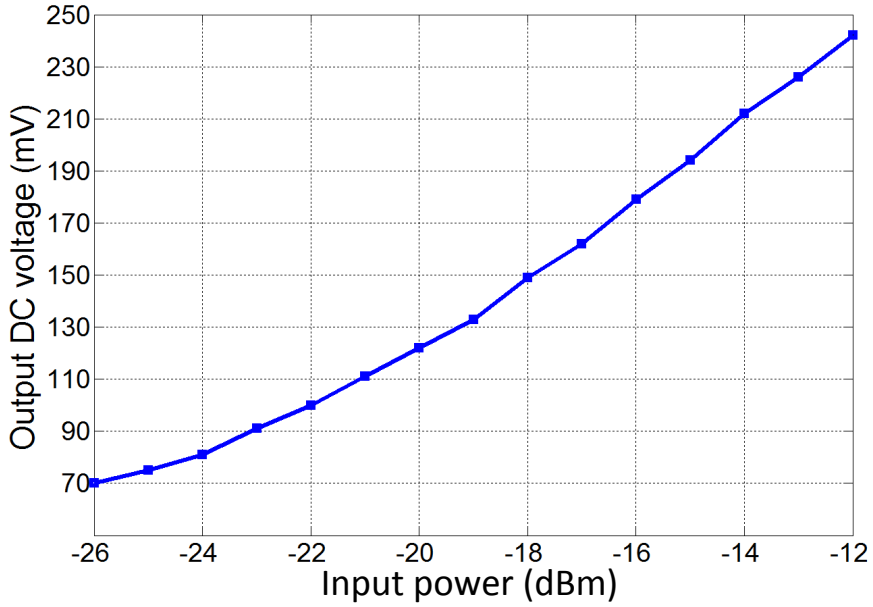

Figure 7.14: Rectified dc output voltage versus the received input power at the 3^{rd} harmonic for the RFID-TR with self-harvesting.

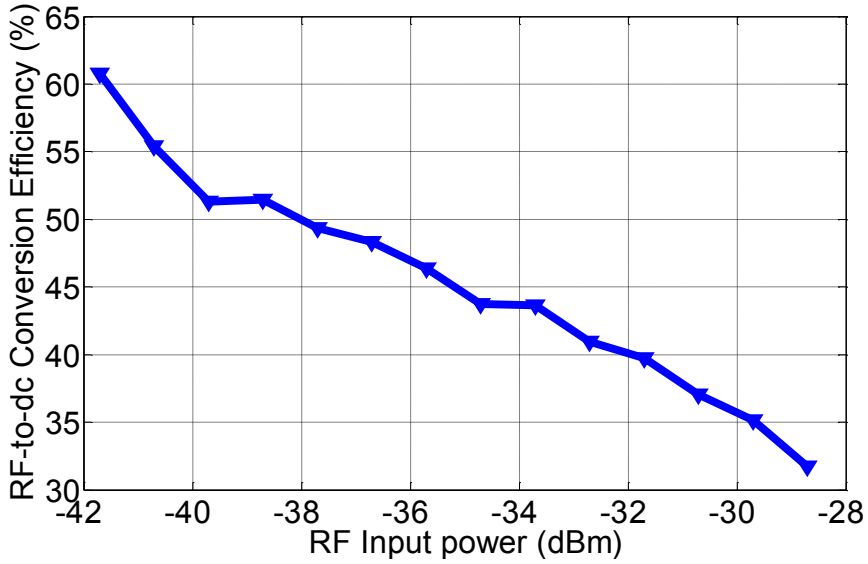

Figure 7.15: RF-to dc conversion efficiency versus the received input power at the 3^{rd} harmonic for the RFID-TR with self-harvesting.

and case *(c)* because these are the only cases where there is RFID communication. The variations of read range with respect to the Reader Equivalent Isotropically Radiated Power (R_{EIRP}) are shown in Fig. 7.16 and compared to the scenario without feedback. The R_{EIRP} includes the gain of the reader antenna. Read range results at 868 MHz are presented in Table 7.3.

Table 7.3: Maximum read range without and with EEH feedback.

Case	Without feedback (m)	With feedback (m)
(a)	3.3	4.8
(c)	3.3	6.1

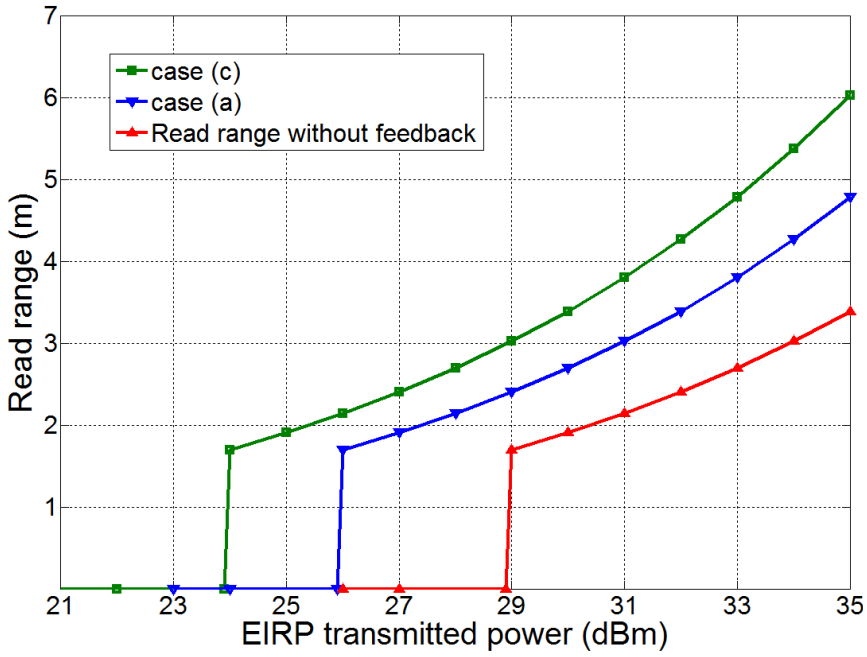

Figure 7.16: Read range for the RFID-TR with external harvesting.

The feedback operation in case *(c)* allows to read the RFID-TR at low R_{EIRP} (i.e. 24 dBm) and at approximately 2 m distance, while without harvested feedback the RFID-TR is not read. Furthermore, when the RFID-TR is read without feedback at 35 dBm R_{EIRP}, the fact of injecting the harvested power (feedback configuration) improves the read range in approximately 1.5 m in case *(a)* and in 2.8 m in case *(c)*.

The enhanced read range in case *(a)* is due to the harvesting of modulated harmonics produced by the RFID chip, even if the EEH section is tuned at 2.17 GHz, the 2^{nd} and the 3^{rd} harmonic affect the waveform of the rectified signal. At the other hand, the improvement of

read range in case *(c)* is mainly due to the harvesting operation at 2.17 GHz, but also due to the effective combined effect of both RF sources producing a signal with higher PAPR as presented in Section 7.2.

RFID-TR with self-harvesting

The performance of the *RFID-TR with self-harvesting* working as RFID tag is evaluated by measuring its read range only for case *(a)*. The maximum read range is 6 m at 35 dBm (R_{EIRP}). The variations of read range with and without feedback operation, both with respect to (R_{EIRP}) are shown in Fig. 7.17. A similar behavior to that one observed in the *RFID-TR with external*

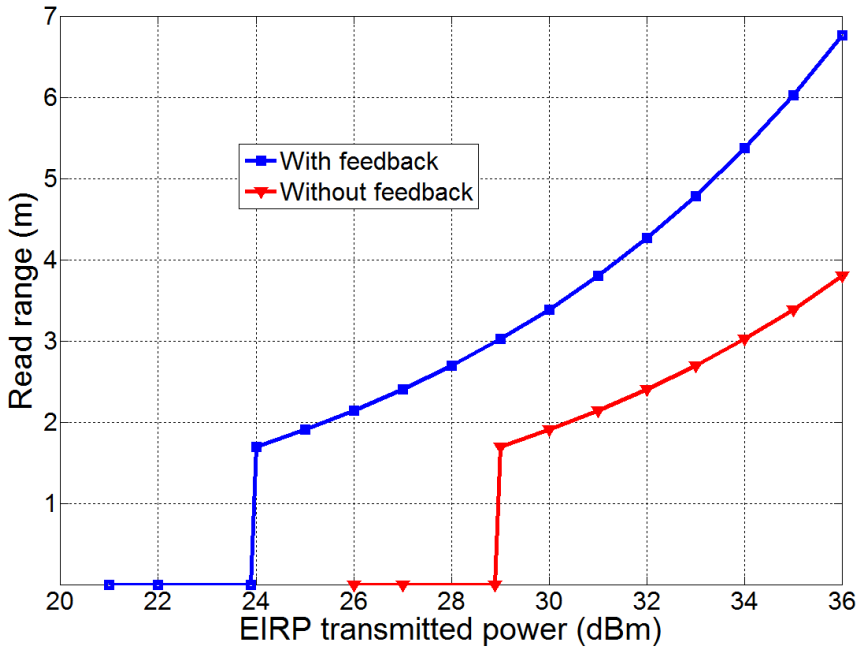

Figure 7.17: Read range for the RFID-TR with self-harvesting.

harvesting is reported. The harvesting feedback operation allows to read the *RFID-TR with self-harvesting* at 24 dBm R_{EIRP} at approximately 2 m distance, while without feedback the RFID-TR is not read. The feedback operation improves the read range in approximately 2.5 m, when an $R_{EIRP} = 35$ dBm is transmitted.

7.5 Conclusion

The work presented in this chapter proposes to enhance the harvesting efficiency of EEH devices by exploiting its non-linear nature. Two new techniques are proposed, (1) Multi-device Waveform and (2) Harvesting harmonic energy. Afterwards, the techniques are integrated with the passive RFID technology in order the enhance the read range performance of

the tag. For each technique a prototype was designed and fabricated. The prototypes consist of an RFID tag operating at 868 MHz, an electromagnetic energy harvester operating at a different frequency (2.17 GHz or 2.604 GHz), and a common antenna. The proposed solutions, so-called RFID Tag-Rectenna (RFID-TR), were tested reporting the following milestones:

- Multi-device Waveform. An RFID-TR is designed to perform *external harvesting* from a 2.17 GHz source and to exploit the benefit that a joint operation of RFID chip and a rectifying diode offers. The phenomenon is based on the effect that *time varying envelope signal* produces in the RF-to-dc conversion efficiency of non-linear rectifiers, since they are capable to activate the rectifying devices for lower average input power levels compared to signals of constant envelope and the same average power. Accordingly with this theory, when both RF sources (RFID reader and 2.17 GHz source) illuminate the RFID-TR, the re-injection of the harvested energy into the RFID chip produces a 2.8 m read range enhancement compared to the case without harvesting.

- Harvesting harmonic energy. An RFID-TR is designed to perform *self-harvesting* from a self-generated 3^{rd} harmonic of the passive RFID chip. The operation exploits the wasted energy naturally generated during the rectification process performed by passive RFID chips. The re-injection of the harvested energy into the chip produces in this case a 2.5 m read range enhancement compared to the case without harvesting.

Further research efforts should be dedicated to enhance the performance of proposed approaches, for example by integrating several rectifier sections working at different frequencies and benefiting each other from its fundamental and harmonic signals, in order to produce a higher dc level. An effective frequency arrangement of fundamental signals and its harmonics can produce efficient techniques for WPT.

8. Conclusions and future workS

8.1 Original contributions of the author

This thesis has devoted to the study of non-linearities from passive UHF RFID chips. Theoretical studies and experimental characterizations guide the work to propose an analytical model and to develop exploitation approaches of these non-linearities. The main contributions to knowledge presented by the author in this thesis include the following:

- The development of a measurement platform and method to characterize the non-linear behavior of UHF EPC Class-1 Gen2 RFID tags. The method highlights the configuration of the RFID air interface by generating a periodic and reproducible sequence of bits in the tag response, in order to facilitate the power spectral density analysis. The platform allows to perform measurements of the radiated tag response of commercial passive RFID tags, in full operation mode and including harmonic frequencies. Valued in [III,XV][1].

- The development of a RFID test platform to characterize the non-linear behavior of UHF EPC Class-1 Gen2 RFID chips. In this platform, the RFID chip is directly connected to test bench, allowing to perform conducted measurements in full operation mode. Automated measurements of the non-linear effects linked to the activation power, the harmonic response level, and the impedances up to the 4^{th} harmonic of the UHF carrier can be performed. Valued in [II].

- To perform a theoretical analysis of harmonic signals produced by the RF section of passive RFID chips and to demonstrate that the produced non-linearities could be exploited by antenna designing. The analysis pinpoints in the operation of a traditional tag working at the fundamental frequency of the system (f_0), but specially in the operation of a new tag able to enhance the backscattered signal strength at its 3^{rd} harmonic ($3f_0$), so-called Harmonic Tag (HT)

- The development of harmonic RFID tags working at UHF and microwave bands that exploit the non-linear behavior of RFID chips. The study and establishment of basics for the harmonic tag antenna design, operating at the fundamental frequency in UHF and its 3^{rd} harmonic are carried out with special care on the impedance matching procedures. Valued in [I,VIII,XIII].

- The development of a new communication concept between tag and reader. It relates to a harmonic communication system, where contrary to traditional RF approaches, the

[1] Roman numbering refers to the list of publications of the author located in the last pages of the document

3^{rd} harmonic generated by passive RFID chips is exploited as redundant signal in terms of power and information carrier. The performance of the solution is illustrated from simulation and measurements. Valued in [I,VIII,XIII,XIV,XVII].

The above-mentioned set of contributions ultimately constitute a patent application seeking for an international protection of the so-called invention *RFID communication system* [VIII]. Fig. 8.1 illustrates an overview of the invention. The invention relates to a RFID communication system comprising an RFID reader and a passive RFID HT. According to the invention, the reader is arranged to receive a second reply signal from the HT whose frequency is a multiple of the predetermined carrier wave at the fundamental frequency, versed otherwise, a harmonic signal generated by the non-linear behavior of the RFID chip. The harmonic signal is processed by the reader in order to complete or improve the functionality of the RFID system.

- Additional contributions focused on the development of alternative techniques to exploit the non-linear behavior of rectifying devices. It concerns to the integration of the passive RFID technology to the theories of WPT and EEH, taking advantage of the non-linear nature of rectifying elements in order to maximize the RF-to-dc conversion efficiency of EEH devices and increase the read range of passive RFID tags. The alternatives to the non-linear exploitation are based on three phenomena of EEH devices: (1) its impedance power dependency, (2) its harmonic production, and (3) its rectifying dependence on the RF waveform. Valued in [IX,XI,XII].

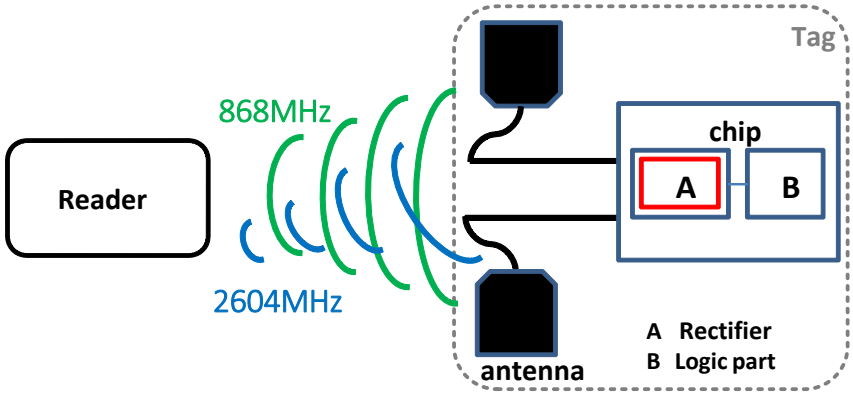

Figure 8.1: RFID harmonic communication system.

8.2 Final conclusions

The main conclusions of this thesis can be summarized as follows:

- ***Measurement of radiated responses from commercial passive UHF RFID tags***. A complete characterization of the communication signals involved in a passive RFID

system has been studied and developed. The measurement procedure is based on the PSD analysis performing a temporal acquisition directly in RF band while the communication tag-to-reader is fully established. By setting the Query parameters it is possible to manipulate the RFID physical layer in order to facilitate the PSD interpretation.

The PSD calculation reveals harmonics on the return signal consequence of the not treated non-linearity effects of the RFID chip. It were also noted harmonics generated by the reader in the forward signal. A parametric analysis reports that backscattered harmonics by commercial tags are independent of: (1) the performance at the fundamental harmonic, and (2) the FHSS transmission technique, but dependent on: (1) the power sent by the reader and, (2) the sequence of bits that the tag transmits.

- ***Characterization of non-linear behavior of commercial passive UHF RFID chips***. The developed RFID-TP allows to characterize passive RFID chips, with an easy and direct connection to the platform. The measurement introduces vectorial information allowing an evaluation of the RFID chip in full operation mode in a wide frequency range. The result of its use for harmonic treatment tests have shown that by setting a particular impedance matching condition between antenna and RFID chip, the harmonics can be increased at the expense of a 1.5 dB reduction on the chip sensitivity and 7 dB reduction on the chip response at fundamental frequency.

- ***Modeling the non-linear behavior of harmonic production in passive RFID chips***. A complete modeling and characterization of harmonics produced by the non-linear behavior of passive UHF RFID chips based on the analysis of the rectifier section has been presented. It is explained the particular predominance of even or odd harmonics depending on the architecture of the rectifier circuit, which determines the canceling or not of currents in the electrical analysis. For example a single diode will produce all the harmonics with predominance of those ones of low order (i.e. the 2^{nd} harmonic), however if the rectifier is composed by voltage doublers stages (number of diodes multiple of two), an odd harmonic predominance is present.

- ***Exploitation of the non-linear behavior of passive UHF RFID chips***. Two approaches for a practical non-linear exploitation have been studied:

  (1) ***Harmonic communication approach in passive UHF RFID.***
  The approach proposes design guidelines and operation concepts for new harmonic tags with consideration on current standard regulations. The work on exploiting the 3^{rd} harmonic response by specialized tag antennas design, was experimentally demonstrated by prototyping and measuring several HT samples.

  A parametric study shows that the HT performance can be enhanced with the antenna structure and also the kind of chip. An hysteresis effect is observed for NXP-UCODE chips, i.e. the tag response remains clear and quasi-constant upon activation even if the reader power increases. The hysteresis effect is observed at the fundamental frequency and its 3^{rd} harmonic. The hysteresis effect of specific kind of chips facilitates the reader reception at the harmonic frequency due to the clear, higher and constant harmonic response of this kind of chip.

The ability of the reader to collect and process harmonics should be enhanced to make this exploitation a reality. It is worth noting that the two main difficulties to take into account in the harmonic exploitation: a weak 3^{rd} harmonic response and a small ΔRCS.

(2) *Non-linear harvesting approach.*
The approach presents an alternative exploitation of the non-linear phenomena present in rectifier devices. The study, design and experimentation are performed to develop EEH techniques by exploiting three non-linear effects:

- *The impedance power dependency*. It was taken into account to design the integration of two non-linear devices (RFID chip and rectifier diode) working at different frequencies;
- *The harmonic production*. It was taken into account to enhance the performance of the harvester by performing harmonic harvesting;
- *The rectifying dependence on the signal waveform*. It was taken into account to enhance the performance of harvester section by producing efficient signals for WPT.

Two new approaches for energy harvesting were proposed by means of integrating an RFID tag working at 868 MHz and a EEH device working at a different frequency in the microwave region, both working in a common antenna:

- *RFID tag-Rectenna with external harvesting* from 2.17 GHz. It exploits the mutual benefit that a joint operation of RFID chip and a rectifying diode offers. The phenomena is based in the effect that *time varying envelope signal* produces in non-linear rectifiers;

- *RFID tag-Rectenna with self-harvesting*. It exploits the wasted energy naturally generated during the rectification process performed by passive RFID chips.

In both approaches, the re-injection of the harvested energy into the RFID chip produces an improvement on the read range of the RFID tag function compared to the case without re-injection. The reported research allows to develop promising techniques to enhance the performance of actual applications and add new functionalities to current state-of-art by means of the non-linear exploitation.

8.3 Future research lines

Several research paths can be declared as extension of the milestones presented as final conclusions, some ideas are given below.

- ***Future works based on new functionalities of the HT.*** These future works refer to efforts than can be conducted considering the use of both frequencies (fundamental and harmonic) and the new *RFID communication system*.

In sensing.
Efforts can be dedicated to the study and parametrization of impedance changes caused by the non-linear behavior of passive RFID chips (harmonic strength and impedance dependency on power) in both impedance modulation states at both frequencies (fundamental and harmonic). The study can profit from the easy control of the RFID air interface and wide scope analysis provided by the characterization platforms. Subsequent research studies on the mapping of physical phenomena to impedance changes can be done. Impedance expansion networks can be integrated in order to highlight small impedance chances [152]. Additionally studies on the modeling and design of HTs which integrate those impedance expansion network can be done. Applications in E-Healthcare like non-contact physiological radar monitoring systems based primarily on backscattering radars using the harmonic redundance of passive RFID chips can be envisaged. Future lines of research can be devoted for example on the to the study of physiological measuring such as measures of pulmonary, cardiac, or patient movement [153].

In location.
Given the diversity in frequency introduced by HTs, the performance of current location applications which use passive RFID as carrier technology, can be enhanced by means of using the redundant backscattered harmonic and HTs and reader antennas with hybrid directivity. Research efforts in the physical layer by specific HT design, as well as in the application layer to propose new signal processing techniques can be devoted by means of re-purposing existing backscattering processing techniques, such as *Angle of Arrival* (AoA), *Time of Arrival* (ToA), *Phase of Arrival* (PoA) or *Received Signal Strength Indicator* (RSSI), and proposing other new ones.

Countering fading and multi-path effects.
Given the frequency selective effect of multi-path and fading phenomena, additional efforts can be devoted to the study of counter these propagation phenomena exploiting the frequency diversity that HTs offer. Applications in harm sceneries where the reader CW leakage (only at fundamental frequency) can be significantly detrimental for the tag detection (e.g. inside metallic boxes) may be envisaged based on detection of the tag harmonic response. Additionally, the design of specific HTs can play an important role in this purpose (introducing diversity in polarization per example).

RFID anticollision algorithms.
In dense scenarios, one of the main problems which reduces the efficiency of the passive UHF RFID system is the collision between the tag responses. Current solutions are based on collision avoidance at the communication layer (i.e. MAC layer Protocols). These can be a time consuming process since they discard the signals of physical layer, requiring retransmission. Some works have been done on distinguishing multiple UHF RFID tag responses based on physical layer characteristics [154]. Research efforts can be

dedicated on the developing of new algorithms and signal processing techniques to solve the passive UHF RFID tags collision problem based in the advantages that the redundant backscattered harmonic offers at the physical layer.

- ***Future works based on current functionalities of RFID tags.*** Below lines present future research efforts to enhance the performance of the traditional RFID tags operating only at the fundamental frequency (UHF RFID band).

  Improving performance of passive RFID tags.
  New elements are given to quantified the harmonic strength on passive RFID chips. Subsequent lines of research can be undertaken on the improvement of current design techniques and manufacture techniques of RFID tags. It concerns to the treatment of the harmonic signals with filtering intentions, in all the integration procedures of antenna and RFID chip, looking for an improvement on the performance of RFID tags in terms of read range.

  Enhancement of RFID chip powering capabilities.
  Conventional rectifiers operating at medium range of input RF power waste a substantial portion of the rectified energy in generation of harmonics due to the rectification process. Efforts on developing harmonic rectification circuits can increase the efficiency of rectifiers. Therefore, in passive RFID chips, a modified rectifier architecture that is able to harvest the energy from its itself generated harmonics can enhance the powering capabilities of the chip, which will triggers in a greater read range. Additionally, multiband rectifier sections for RFID chip architectures can be designed in order to enhance the RFID chip powering operation. In this context, and using the proposed RFID characterization platforms, new RFID tags can be designed to exploit the multiband rectification operation.

References

[1] OSEO. **Investissements d'avenir.** 53

[2] TAGSYS RFID WEBSITE. **AK / RFID Tags / Our Products & Services / TAGSYS RFID - Radio Frequency Identification - Tagsys RFID.** 53, 109

[3] LCIS. **Laboratoire de Conception et dIntegration des Systemes.** 53

[4] SPINNAKER-PROJECT. **Item-level sensing, anywhere, anytime**. 53

[5] KLAUS FINKENZELLER. *RFID Handbook: Fundamentals and Applications in Contactless Smart Cards and Identification*. John Wiley & Sons, Inc., New York, NY, USA, 2 edition, 2003. 58, 60

[6] A.A. NAZARI SHIREHJINI, A. YASSINE, AND S. SHIRMOHAMMADI. **An RFID-Based Position and Orientation Measurement System for Mobile Objects in Intelligent Environments**. *Instrumentation and Measurement, IEEE Transactions on*, **61**(6):1664–1675, 2012. 58

[7] YVAN DUROC AND DARINE KADDOUR. **RFID Potential Impacts and Future Evolution for Green Projects**. *Energy Procedia*, **18**:91 – 98, Jun. 2012. 58, 164

[8] P.V. NIKITIN, S. RAMAMURTHY, R. MARTINEZ, AND K. V S RAO. **Passive tag-to-tag communication**. In *RFID (RFID), 2012 IEEE International Conference on*, pages 177–184, 2012. 58

[9] YVAN DUROC AND GIANFRANCO ANDIA VERA. **Towards Autonomous Wireless Sensors: RFID and Energy Harvesting Solutions**. In *Internet of Things*, pages 233–255. Springer, 2014. 58, 164

[10] ISO/IEC 18000-1. **Information technology AIDC techniques RFID for item management air interface, part 1 generic parameters for air interface communication for globally accepted frequencies.** 58, 59

[11] ISO/IEC 18000. **Automatic identification radio frequency identification for item management communications and interfaces.** 58, 83

[12] I. JALALY AND I.D. ROBERTSON. **Capacitively-tuned split microstrip resonators for RFID barcodes**. In *Microwave Conference, 2005 European*, **2**, pages 4 pp.–, Oct 2005. 58

[13] V. DEEPU, A. VENA, E. PERRET, AND S. TEDJINI. **New RF identification technology for secure applications**. In *RFID-Technology and Applications (RFID-TA), 2010 IEEE International Conference on*, pages 159–163, June 2010.

[14] S. PRERADOVIC, I. BALBIN, N.C. KARMAKAR, AND G. SWIEGERS. **Chipless Frequency Signature Based RFID Transponders**. In *Microwave Conference, 2008. EuMC 2008. 38th European*, pages 1723–1726, Oct 2008. 58

[15] GILDAS AVOINE AND PHILIPPE OECHSLIN. **RFID traceability: a multilayer problem**. In *Proceedings of the 9th international conference on Financial Cryptography and Data Security*, FC'05, pages 125 – 140, Berlin, Heidelberg, 2005. Springer-Verlag. 58

[16] DOMINIQUE PARET. *RFID at Ultra and Super High Frequencies: Theory and application*. Wiley Publishing, 2010. 59, 83, 90

[17] P.V. NIKITIN AND K.V.S. RAO. **Theory and measurement of backscattering from RFID tags**. *Antennas and Propagation Magazine, IEEE*, **48**(6):212 –2 18, dec. 2006. 60

[18] G. MARROCCO. **The art of UHF RFID antenna design: impedance-matching and size-reduction techniques**. *Antennas and Propagation Magazine, IEEE*, **50**(1):66 –79, feb. 2008. 60, 61, 125, 126, 138, 141, 169

[19] DAT SON NGUYEN, XUAN CHIEN LE, TIEN THONG PHAM, VIET HOA NGUYEN, MAU CHIEN DANG, AND SMAIL TEDJINI. **Novel Design of RFID UHF Passive Tag for Wideband Applications by Direct and Contactless Chip Connection**. In *IEEE 2012 International Conference on RFID -Technologies and Applications (RFID - TA) (IEEE RFID-TA 2012)*, pages 131–136, Nice, France, France, November 2012. 61

[20] D.M. DOBKIN AND S.M. WEIGAND. **Environmental effects on RFID tag antennas**. In *Microwave Symposium Digest, 2005 IEEE MTT-S International*, pages 4 pp.–, June 2005. 61, 62

[21] M. HIRVONEN, K. JAAKKOLA, P. PURSULA, AND J. SAILY. **Dual-Band Platform Tolerant Antennas for Radio-Frequency Identification**. *Antennas and Propagation, IEEE Transactions on*, **54**(9):2632–2637, Sept 2006. 61, 63

[22] S. JEON, Y. YU, AND J. CHOI. **Dual-band slot-coupled dipole antenna for 900MHz and 2.45 GHz RFID tag application**. *Electronics Letters*, **42**(22):1259–1260, Oct 2006. 61

[23] MINGZHI ZHANG AND SHU YAN. **A Novel Dual-Band Dipole Antenna for RFID Tag**. In *Logistics Engineering and Intelligent Transportation Systems (LEITS), 2010 International Conference on*, pages 1–4, Nov 2010. 61, 63

[24] A.T. MOBASHSHER, M.T. ISLAM, AND N. MISRAN. **A Novel High-Gain Dual-Band Antenna for RFID Reader Applications**. *Antennas and Wireless Propagation Letters, IEEE*, **9**:653–656, 2010. 61, 63

[25] ZI LONG MA, LI JUN JIANG, JINGTIAN XI, AND T.T. YE. **A Single-Layer Compact HF-UHF Dual-Band RFID Tag Antenna**. *Antennas and Wireless Propagation Letters, IEEE*, **11**:1257–1260, 2012. 61

[26] L.W. MAYER AND A.L. SCHOLTZ. **A Dual-Band HF / UHF Antenna for RFID Tags**. In *Vehicular Technology Conference, 2008. VTC 2008-Fall. IEEE 68th*, pages 1–5, Sept 2008. 61, 63

[27] F. PAREDES, G.Z. GONZALEZ, J. BONACHE, AND F. MARTIN. **Dual-Band Impedance-Matching Networks Based on Split-Ring Resonators for Applications in RF Identification (RFID)**. *Microwave Theory and Techniques, IEEE Transactions on*, **58**(5):1159–1166, May 2010. 61

[28] C. PHONGCHAROENPANICH AND R. SUWALAK. **Dual-band RFID-reader antenna using annular plate with curved and rectangular slots**. In *Electromagnetics in Advanced Applications (ICEAA), 2010 International Conference on*, pages 633–636, Sept 2010. 61

[29] G.N. MALHEIROS-SILVEIRA, A. MORETTI, H.E. HERNANDEZ-FIGUEROA, R.T. YOSHIOKA, J.E. BERTUZZO, AND L.L. BRAVO-ROGER. **Exploring dual-band RFID tag antennas by means of asymmetric dipoles**. In *Microwave Optoelectronics Conference (IMOC), 2011 SBMO/IEEE MTT-S International*, pages 244–248, Oct 2011. 61, 63

[30] L.W. MAYER. **Dual-band antenna**, May 8 2012. US Patent 8,174,454. 61

[31] G. DE VITA AND G. IANNACCONE. **Design criteria for the RF section of UHF and microwave passive RFID transponders**. *Microwave Theory and Techniques, IEEE Transactions on*, **53**(9):2978 – 2990, sept. 2005. 61, 64, 65, 82, 104, 111, 120, 121, 125, 128, 136, 157, 168

[32] IMPINJ. **Monza 4 Tag Chip Datasheet.** 64

[33] J.C. BOLOMEY, S. CAPDEVILA, L. JOFRE, AND J. ROMEU. **Electromagnetic Modeling of RFID-Modulated Scattering Mechanism. Application to Tag Performance Evaluation**. *Proceedings of the IEEE*, **98**(9):1555 – 1569, sept. 2010. 65, 82, 90, 104, 115, 116, 120, 125, 136

[34] DAVID M POZAR. *Microwave Engineering*, **Third**. Wiley, 2005. 65, 66

[35] M.E. HINES. **The Virtues of Nonlinearity–Detection, Frequency Conversion, Parametric Amplification and Harmonic Generation**. *Microwave Theory and Techniques, IEEE Transactions on*, **32**(9):1097–1104, Sep 1984. 65

[36] S.A. MAAS. *Nonlinear Microwave and RF Circuits*. Artech House microwave library. Artech House, 2003. 65, 67

[37] R. JANASWAMY AND SHUNG-WU LEE. **Scattering from dipoles loaded with diodes**. *Antennas and Propagation, IEEE Transactions on*, **36**(11):1649–1651, 1988. 67

[38] L. CABRIA, J.A. GARCIA, E. MALAVER, AND A. TAZON. **A PHEMT frequency doubling active antenna with BPSK modulation capability**. *Antennas and Wireless Propagation Letters, IEEE*, **3**(1):310–313, 2004. 67

[39] E. FONG AND R. ZEMAN. **Analysis of harmonic distortion in single-channel MOS integrated circuits**. *Solid-State Circuits, IEEE Journal of*, **17**(1):83–86, 1982. 67

[40] P.V. NIKITIN AND K.V.S. RAO. **Harmonic scattering from passive UHF RFID tags**. In *Antennas and Propagation Society International Symposium, 2009. APSURSI '09. IEEE*, pages 1 – 4, june 2009. 67, 83, 120, 136

[41] AVERY DENNISON RFID. **Avery Dennison UHF RFID Inlays.** 67

[42] G. ORECCHINI, F. ALIMENTI, V. PALAZZARI, A. RIDA, M.M. TENTZERIS, AND L. ROSELLI. **Design and fabrication of ultra-low cost radio frequency identification antennas and tags exploiting paper substrates and inkjet printing technology**. *IET Microwaves, Antennas & Propagation*, **5**(8):993, 2011. 68, 69, 71

[43] D. PSYCHOUDAKIS, W. MOULDER, CHI-CHIH CHEN, HEPING ZHU, AND J.L. VOLAKIS. **A Portable Low-Power Harmonic Radar System and Conformal Tag for Insect Tracking**. *Antennas and Wireless Propagation Letters, IEEE*, **7**:444–447, 2008. 69, 70

[44] B.G. COLPITTS AND G. BOITEAU. **Harmonic radar transceiver design: miniature tags for insect tracking**. *Antennas and Propagation, IEEE Transactions on*, **52**(11):2825–2832, 2004. 136

[45] L. ROSELLI, F. ALIMENTI, M. VIRILI, F. LOLLI, B. POPESCU, D. POPESCU, S. LOCCI, AND P. LUGLI. **Feasibility study of a fully organic frequency doubler for harmonic RFID applications**. In *Silicon Monolithic Integrated Circuits in RF Systems (SiRF), 2012 IEEE 12th Topical Meeting on*, pages 203–206, 2012. 69

[46] C. MARIOTTI G. ORECCHINI F. ALIMENTI P. COSSEDDU P. MEZZANOTTE A. BONFIGLIO L. ROSELLI M. VIRILI, G. CASULA. **7.5-15 MHz Organic Frequency Doubler Made with Pentacene-Based Diode and Paper Substrate**. In *Microwave Symposium Digest (MTT), 2014 IEEE MTT-S International*, pages 1–3, Jun. 2014. 69, 71

[47] HAROLD STARAS AND JOSHUA SHEFER. **Harmonic radar detecting and ranging system for automotive vehicles**, December 2 1973. US Patent 3,781,879. 69

[48] H.P. ROMERO, K.A. REMLEY, D.F. WILLIAMS, AND CHIH-MING WANG. **Electromagnetic Measurements for Counterfeit Detection of Radio Frequency Identification Cards**. *Microwave Theory and Techniques, IEEE Transactions on*, **57**(5):1383–1387, May 2009. 70, 136

[49] HUGO CRAVO GOMES AND NUNO BORGES CARVALHO. **RFID for Location Proposes based on the intermodulation distortion**. *Sensors and Transducers Journal*, **106**(7):85–96, 2009. 72, 73

[50] YVAN DUROC, G ANDIA VERA, AND JP GARCIA MARTIN. **Modified RSSI Technique for the Localization of Passive UHF RFID Tags in LOS Channels**. *International journal of microwave and wireless technologies*, **5**(05):645–651, 2013. 73

[51] MING-HSIEN LEE, CHIA-YU YAO, AND HSIN-CHIN LIU. **Passive Tag for Multi-carrier RFID Systems**. In *Parallel and Distributed Systems (ICPADS), 2011 IEEE 17th International Conference on*, pages 872 – 876, dec. 2011. 73, 74, 98

[52] HSIN-CHIN LIU, YI-FAN CHEN, AND YUNG-TING CHEN. **A Frequency Diverse Gen2 RFID System with Isolated Continuous Wave Emitters**. *Science*, **2**(5):54 – 60, 2007. 98

[53] HSIN-CHIN LIU, XIN-CAN GUO, AND WEN-SHIN TZENG. **A UHF Passive RFID System with Frequency Diversity**. In *2007 International Symposium on Antennas and Propagation (ISAP2007)*, pages 20–24. 74, 75

[54] HSIN-CHIN LIU, YUNG-TING CHEN, AND WEN-SHIN TZENG. **A multi-carrier UHF passive RFID system**. In *Applications and the Internet Workshops, 2007. SAINT Workshops 2007. International Symposium on*, pages 21–21. IEEE, 2007.

[55] HSIN-CHIN LIU AND JHEN-PENG CIOU. **Performance analysis of multi-carrier RFID systems**. In *Performance Evaluation of Computer & Telecommunication Systems, 2009. SPECTS 2009. International Symposium on*, **41**, pages 112–116. IEEE, 2009.

[56] HSIN-CHIN LIU, WANG-CHI LIN, MING-YUH LIN, AND MIN-HSIANG HSU. **Passive UHF RFID Tag With Backscatter Diversity**. *Antennas and Wireless Propagation Letters, IEEE*, **10**:415–418, 2011. 73

[57] EPCGLOBAL STANDARDS. **Global, EPC. UHF Standards EPCglobal Products&amp Solutions GS1 The global language of business.** 73, 79, 82, 84, 85, 86, 87, 101, 105, 108, 137, 154

[58] SHABNAM LADAN AND KE WU. **35 GHz Harmonic Harvesting Rectifier for Wireless Power Transmission**. In *Microwave Symposium Digest (MTT), 2014 IEEE MTT-S International*, pages 1–3, Jun. 2014. 75, 76, 164

[59] A. BOAVENTURA, A. COLLADO, N.B. CARVALHO, AND A. GEORGIADIS. **Optimum behavior: Wireless power transmission system design through behavioral models and efficient synthesis techniques**. *Microwave Magazine, IEEE*, **14**(2):26–35, 2013. 77, 111, 136

[60] A.S. BOAVENTURA AND N.B. CARVALHO. **Maximizing dc power in energy harvesting circuits using multisine excitation**. In *Microwave Symposium Digest (MTT), 2011 IEEE MTT-S International*, pages 1–4, June 2011. 77, 164, 165, 178

[61] M.S. TROTTER, J.D. GRIFFIN, AND G.D. DURGIN. **Power-optimized waveforms for improving the range and reliability of RFID systems**. In *RFID, 2009 IEEE International Conference on*, pages 80–87, April 2009. 136

[62] A. COLLADO AND A. GEORGIADIS. **Improving wireless power transmission efficiency using chaotic waveforms**. In *Microwave Symposium Digest (MTT), 2012 IEEE MTT-S International*, pages 1–3, June 2012.

[63] A. COLLADO AND A. GEORGIADIS. **Optimal Waveforms for Efficient Wireless Power Transmission**. *Microwave and Wireless Components Letters, IEEE*, **24**(5):354–356, May 2014. 77, 78, 136, 164, 165

[64] J.O. MCSPADDEN, T. YOO, AND K. CHANG. **Theoretical and experimental investigation of a rectenna element for microwave power transmission**. *Microwave Theory and Techniques, IEEE Transactions on*, **40**(12):2359 –2366, dec 1992. 82

[65] A. GEORGIADIS, G. ANDIA, AND A. COLLADO. **Rectenna Design and Optimization Using Reciprocity Theory and Harmonic Balance Analysis for Electromagnetic (EM) Energy Harvesting**. *Antennas and Wireless Propagation Letters, IEEE*, **9**:444 – 446, 2010. 83, 164

[66] JI-YONG PARK, SANG-MIN HAN, AND T. ITOH. **A rectenna design with harmonic-rejecting circular-sector antenna**. *Antennas and Wireless Propagation Letters, IEEE*, **3**(1):52 – 54, dec. 2004.

[67] EREZ FALKENSTEIN, MICHAEL ROBERG, AND Z. POPOVIC. **Low-Power Wireless Power Delivery**. *Microwave Theory and Techniques, IEEE Transactions on*, **60**(7):2277–2286, July 2012. 83

[68] IMPINJ. **Impinj UHF RFID Product downloads - Monza tag chips.** 83, 109, 113, 125, 126, 153

[69] G. ANDIA VERA, Y. DUROC, AND S. TEDJINI. **Analysis of Harmonics in UHF RFID Signals**. *Microwave Theory and Techniques, IEEE Transactions on*, **61**(6):2481–2490, 2013. 83, 129, 138, 166

[70] UPM RAFLATEC DOGBONE. **General purpose high-end product for global supply chain management and item-level use,UPM RAFLATAC, Dixon, IL, USA, 2013**. 89

[71] UPM RAFSEC FROG. **Dry inlay, global UHF C1G2 EPC, UPM, Dixon, IL, USA, 2013.** 89

[72] E. PERRET, S. TEDJINI, AND R.S. NAIR. **Design of Antennas for UHF RFID Tags**. *Proceedings of the IEEE*, **100**(7):2330–2340, July 2012. 89

[73] UPM RAFSEC MEMORYSTICK. **Wet inlay, Global UHF C1G2 EPC, UPM, Dixon, IL, USA, 2013**. 89

[74] RAPIDTRAK UHF TAG. **Close proximity, Omni-directional reading of hanging items at retail points-of-sale (POS) TAGSYS RFID, King of Prussia, PA, USA, 2013**. 89

[75] UPM RAFLATAC FROG. **Orientation insensitive product for global supply chain. Suited for corrugated materials and plastics UPM RAFLATAC, Dixon, IL, USA, 2013.** 89

[76] AD-222 RFID INLAYS. **Dry Inlay Specifications**. 89

[77] CONSTANTINE A. BALANIS. *Antenna Theory: Analysis and Design*. Wiley-Interscience, 2005. 88, 89

[78] K. CHAMBERLIN. **Quantitative analysis of intermodulation product interference**. *Electromagnetic Compatibility, IEEE Transactions on*, **31**(3):316 – 319, aug 1989. 93

[79] LUKAS W MAYER AND ARPAD L SCHOLTZ. **Sensitivity and Impedance Measurements on UHF RFID Transponder Chips**. *Int EURASIP Workshop on RFID Techn*, pages 1 – 10, 2007. 98, 105, 108

[80] J.S. COLBURN, M.A. JENSEN, AND Y. RAHMAT-SAMII. **Indoor ISM band multipath fading: frequency and antenna diversity**. In *Antennas and Propagation for Wireless Communications, 1998. 1998 IEEE-APS Conference on*, pages 9 – 12, nov 1998. 101

[81] SUNG-LIN CHEN AND KEN-HUANG LIN. **Characterization of RFID Strap Using Single-Ended Probe**. *Instrumentation and Measurement, IEEE Transactions on*, **58**(10):3619–3626, 2009. 104, 105

[82] SUNG-LIN CHEN, KEN-HUANG LIN, AND R. MITTRA. **A Measurement Technique for Verifying the Match Condition of Assembled RFID Tags**. *Instrumentation and Measurement, IEEE Transactions on*, **59**(8):2123–2133, 2010. 104, 105

[83] L. CATARINUCCI, D. DE DONNO, R. COLELLA, F. RICCIATO, AND L. TARRICONE. **A Cost-Effective SDR Platform for Performance Characterization of RFID Tags**. *Instrumentation and Measurement, IEEE Transactions on*, **61**(4):903–911, 2012. 104

[84] D. DE DONNO, F. RICCIATO, AND L. TARRICONE. **Listening to Tags: Uplink RFID Measurements With an Open-Source Software-Defined Radio Tool**. *Instrumentation and Measurement, IEEE Transactions on*, **62**(1):109–118, 2013.

[85] L. CATARINUCCI, D. DE DONNO, M. GUADALUPI, F. RICCIATO, AND L. TARRICONE. **Performance analysis of passive UHF RFID tags with GNU-radio**. In *Antennas and Propagation (APSURSI), 2011 IEEE International Symposium on*, pages 541–544, 2011. 104

[86] P.V. NIKITIN, K.V.S. RAO, R. MARTINEZ, AND S.F. LAM. **Sensitivity and Impedance Measurements of UHF RFID Chips**. *Microwave Theory and Techniques, IEEE Transactions on*, **57**(5):1297 – 1302, may 2009. 104, 105, 106

[87] P.V. NIKITIN AND K. RAO. **Effect of Gen2 protocol parameters on RFID tag performance**. In *RFID, 2009 IEEE International Conference on*, pages 117 – 122, april 2009. 104, 105

[88] K.V.S. RAO, P.V. NIKITIN, AND S.F. LAM. **Antenna design for UHF RFID tags: a review and a practical application**. *Antennas and Propagation, IEEE Transactions on*, **53**(12):3870 – 3876, dec. 2005. 104, 120, 138, 140, 159, 179

[89] AGILENT TECHNOLOGIES. **Triggering PNA Microwave Network Analyzers for Antenna Measurements, White Paper**. 108

[90] AGILENT TECH. **Agilent Electronic Calibration (ECal) Modules for Vector Network Analyzers**. 109

[91] A. TECHNOLOGIES. **Agilent Command Expert**. 109

[92] NXP. **UCODE G2XM and G2XL Product data sheet COMPANY PUBLIC.** 109, 111, 113, 126, 141, 153

[93] M. ROBERG, T. REVEYRAND, I. RAMOS, E.A. FALKENSTEIN, AND Z. POPOVIC. **High-Efficiency Harmonically Terminated Diode and Transistor Rectifiers**. *Microwave Theory and Techniques, IEEE Transactions on*, **60**(12):4043–4052, 2012. 111, 164

[94] G. ANDIA VERA, Y. DUROC, AND S. TEDJINI. **Redundant Backscattering Modulation of Passive UHF RFID Tags**. In *Microwave Symposium Digest (MTT), 2013 IEEE MTT-S International*, pages 1–3, Jun. 2013. 114

[95] AGILENT TECHNOLOGIES. **Harmonic Balance Simulation**. 114

[96] S. SKALI, C. CHANTEPY, AND S. TEDJINI. **On the measurement of the delta Radar Cross Section (ΔRCS) for UHF tags**. In *RFID, 2009 IEEE International Conference on*, pages 346 – 351, april 2009. 115

[97] P.V. NIKITIN, K. V S RAO, AND R.D. MARTINEZ. **Differential RCS of RFID tag**. *Electronics Letters*, **43**(8):431–432, 2007. 115

[98] J.F. DICKSON. **On-chip high-voltage generation in MNOS integrated circuits using an improved voltage multiplier technique**. *Solid-State Circuits, IEEE Journal of*, **11**(3):374–378, 1976. 120

[99] M. USAMI. **An ultra small RFID chip: mu-chip**. In *Radio Frequency Integrated Circuits (RFIC) Symposium, 2004. Digest of Papers. 2004 IEEE*, pages 241–244, June 2004.

[100] R. BARNETT, S. LAZAR, AND JIN LIU. **Design of multistage rectifiers with low-cost impedance matching for passive RFID tags**. In *Radio Frequency Integrated Circuits (RFIC) Symposium, 2006 IEEE*, page 4, June 2006.

[101] J.-P. CURTY, N. JOEHL, C. DEHOLLAIN, AND M.J. DECLERCQ. **Remotely powered addressable UHF RFID integrated system**. *Solid-State Circuits, IEEE Journal of*, **40**(11):2193 – 2202, nov. 2005. 120

[102] R.E. BARNETT, JIN LIU, AND S. LAZAR. **A RF to dc Voltage Conversion Model for Multi-Stage Rectifiers in UHF RFID Transponders**. *Solid-State Circuits, IEEE Journal of*, **44**(2):354–370, 2009. 120

[103] R.G. HARRISON. **Full nonlinear analysis of detector circuits using Ritz-Galerkin theory**. In *Microwave Symposium Digest, 1992., IEEE MTT-S International*, pages 267–270 vol.1, June 1992. 121

[104] U. KARTHAUS AND M. FISCHER. **Fully integrated passive UHF RFID transponder IC with 16.7- mu;W minimum RF input power**. *IEEE J. Solid-State Circuits*, **38**(10):1602–1608, Oct 2003. 121

[105] G. DE VITA AND G. IANNACCONE. **Ultra low power RF section of a passive microwave RFID transponder in 0.35 mu;m BiCMOS**. In *Circuits and Systems, 2005. ISCAS 2005. IEEE International Symposium on*, pages 5075–5078 Vol. 5, May 2005.

[106] SANTIAGO CAPDEVILA CASCANTE ET AL. **RFID multiantenna systems for wireless communications and sensing**. 121, 125

[107] S. AAZOU AND E.-M. ASSAID. **Schottky diode parameters extraction using two different methods**. In *Microelectronics (ICM), 2009 International Conference on*, pages 240–243, Dec 2009. 124

[108] BEHZAD RAZAVI AND RAZAVI BEHZAD. *RF microelectronics*, **1**. Prentice Hall New Jersey, 1998. 125

[109] UPM. **Rafsec MemoryStick, Wet Inlay, Global UHF C1G2 EPC**. 129, 153

[110] ALI M NIKNEJAD. *Electromagnetics for high-speed analog and digital communication circuits*. Cambridge University Press Cambridge, 2007. 130

[111] J. SHEFER. **Harmonic radar detecting and ranging system for automotive vehicles**, January 14 1975. US Patent RE28,302. 136

[112] H.C. GOMES AND N.B. CARVALHO. **The use of intermodulation distortion for the design of passive RFID**. In *Radar Conference, 2007. EuRAD 2007. European*, pages 377 – 380, oct. 2007. 136

[113] J. SONG, J. SALMI, V. VIIKARI, AND N. PESONEN. **Maximum Likelihood Estimation for Passive Wireless Intermodulation Communication Sensors**. *Sensors Journal, IEEE*, **PP**(99):1–1, 2014. 136

[114] FAN YU, K.G. LYON, AND E.C. KAN. **A Novel Passive RFID Transponder Using Harmonic Generation of Nonlinear Transmission Lines**. *IEEE Trans. Microw. Theory Techn.*, **58**(12):4121–4127, Dec 2010. 136

[115] YUNFEI MA AND E.C. KAN. **Accurate Indoor Ranging by Broadband Harmonic Generation in Passive NLTL Backscatter Tags**. *Microwave Theory and Techniques, IEEE Transactions on*, **62**(5):1249–1261, May 2014. 136, 138

[116] K. RASILAINEN, J. ILVONEN, A. LEHTOVUORI, J. HANNULA, AND V. VIIKARI. **On Design and Evaluation of Harmonic Transponders**. *Antennas and Propagation, IEEE Transactions on*, **PP**(99):1–1, 2014. 136, 139

[117] K. RASILAINEN, J. ILVONEN, AND V. VIIKARI. **Antenna Matching at Harmonic Frequencies to Complex Load Impedance**. *Antennas and Wireless Propagation Letters, IEEE*, **PP**(99):1–1, 2014. 136, 139

[118] F. ALIMENTI, V. PALAZZARI, G. ORECCHINI, G. PINCA, P. MEZZANOTTE, M.M. TENTZERIS, AND L. ROSELLI. **Crossed dipole frequency doubling RFID TAG based on paper substrate and ink-jet printing technology**. In *Microwave Symposium Digest (MTT), 2010 IEEE MTT-S International*, pages 840–842, May 2010. 136

[119] G. ORECCHINI, F. ALIMENTI, V. PALAZZARI, A RIDA, M.M. TENTZERIS, AND L. ROSELLI. **Design and fabrication of ultra-low cost radio frequency identification antennas and tags exploiting paper substrates and inkjet printing technology**. *Microwaves, Antennas Propagation, IET*, **5**(8):993–1001, June 2011. 136

[120] M. VIRILI, G. CASULA, C. MARIOTTI, G. ORECCHINI, F. ALIMENTI, P. COSSEDDU, P. MEZZANOTTE, A BONFIGLIO, AND L. ROSELLI. **7.5-15 MHz organic frequency doubler made with pentacene-based diode and paper substrate**. In *Microwave Symposium (IMS), 2014 IEEE MTT-S International*, pages 1–4, June 2014. 136

[121] N. BORGES CARVALHO, A GEORGIADIS, A COSTANZO, H. ROGIER, A COLLADO, J.A GARCIŤA, S. LUCYSZYN, P. MEZZANOTTE, J. KRACEK, D. MASOTTI, AJ.S. BOAVENTURA, M. DE LAS NIEVES RUIŤZ LAVIN, M. PINUELA, D.C. YATES, P.D. MITCHESON, M. MAZANEK, AND V. PANKRAC. **Wireless Power Transmission: R&D Activities Within Europe**. *IEEE Trans. Microw. Theory Techn.*, **62**(4):1031–1045, April 2014. 136

[122] S. LADAN AND KE WU. **35 GHz harmonic harvesting rectifier for wireless power Transmission**. In *Microwave Symposium (IMS), 2014 IEEE MTT-S International*, pages 1–4, June 2014. 136

[123] ETSI. **Electromagnetic compatibility and Radio spectrum Matters (ERM); Radio Frequency Identification Equipment operating in the band 865 MHz to 868 MHz with power levels up to 2 W; Part 1: Technical requirements and methods of measurement**, EN 302 208-1 V1.2.1 2008. 137

[124] ECC. **Electronic Communications Commite, Compatibility between the mobile service in the band 2500-2690 MHz and the radiodetermination service in the band 2700-2900 MHz**. 137

[125] NTIA-USA. **National Telecommunications and Information Administration 2700-2900 MHz**. 137

[126] G. ANDIA VERA, Y. DUROC, AND S. TEDJINI. **Tag-to-Reader harmonic Link in Passive UHF RFID**. In *Microwave Symposium Digest (MTT), 2014 IEEE MTT-S International*, pages 1–3, Proceedings-June. 2014. 137, 164

[127] L.W. MAYER, R. LANGWIESER, AND A.L. SCHOLTZ. **Evaluation of Passive Carrier-Suppression Techniques for UHF RFID Systems**. In *2009 IEEE MTT-S International Microwave Workshop on Wireless Sensing, Local Positioning and RFID*, Cavtat, Croatia, September 2009. 138

[128] G. LASSER, ROBERT LANGWIESER, AND A.L. SCHOLTZ. **Broadband suppression properties of active leaking carrier cancellers**. In *RFID, 2009 IEEE International Conference on*, pages 208–212, April 2009.

[129] L.W. MAYER AND A.L. SCHOLTZ. **Circularly Polarized Patch Antenna with High Tx / Rx-Separation**. In *IEEE RFID 2009, 2009 IEEE International Conference on RFID*, pages 213–216, Orlando, USA, April 2009. 138

[130] G. ANDIA VERA, Y. DUROC, AND S. TEDJINI. **RFID Test Platform: Nonlinear Characterization**, 2014. 138, 139, 164, 166, 167, 179

[131] S. HEMOUR AND KE WU. **Radio-Frequency Rectifier for Electromagnetic Energy Harvesting: Development Path and Future Outlook**. *Proceedings of the IEEE*, **102**(11):1667–1691, Nov 2014. 139

[132] R. SCHEELER, S. KORHUMMEL, AND Z. POPOVIC. **A Dual-Frequency Ultralow-Power Efficient 0.5-g Rectenna**. *Microwave Magazine, IEEE*, **15**(1):109–114, Jan 2014. 139, 141, 164

[133] P.V. NIKITIN, K. V S RAO, AND LAM S. **UHF RFID Tag Characterization: Overview and State-of-the-Art**. In *Annual Symposium of the Antenna Measurement Techniques Association AMTA*, pages 1–6, 2012. 140

[134] FEDERAL COMMUNICATIONS COMMISSION. **Guidelines for Determining the Effective Radiated Power (ERP) and Equivalent Isotropically Radiated Power (EIRP) of a RF Transmitting System**. 140

[135] ETSI. **Electromagnetic compatibility and Radio spectrum Matters (ERM); Radio Frequency Identification Equipment operating in the band 865 MHz to 868 MHz with power levels up to 2 W.** 140, 159

[136] JIAN LIU. **Dual-band RFID tag antenna using coplanar inverted-F/L structure**. In *RFID-Technology and Applications (RFID-TA), 2010 IEEE International Conference on*, pages 96–99, June 2010. 142, 147, 169

[137] HUCHENG SUN, YONG-XIN GUO, MIAO HE, AND ZHENG ZHONG. **A Dual-Band Rectenna Using Broadband Yagi Antenna Array for Ambient RF Power Harvesting**. *Antennas and Wireless Propagation Letters, IEEE*, **12**:918–921, 2013. 142

[138] RAO R TUMMALA AND ENBENE J RYMASZEWSKI. **Microelectronics packaging handbook, 1989**. *YT Cheng, L. Lin and K. Najafi,ŞLocalized Silicon Fusion and Eutectic Bonding for MEMS Fabrication and Packaging,Ť Journal of MEMS*, pages 3–8, 2000. 154

[139] W. WANG, S. LOU, K. CHUI, AND S. RONG. **Single-Chip UHF RFID reader in 0.18- um CMOS**. In *Custom Integrated Circuits Conference, 2007. CICC '07. IEEE*, pages 111–114, 2007. 159

[140] D. DE DONNO, L. CATARINUCCI, AND L. TARRICONE. **A Battery-Assisted Sensor-Enhanced RFID Tag Enabling Heterogeneous Wireless Sensor Networks**. *Sensors Journal, IEEE*, **14**(4):1048–1055, April 2014. 164

[141] B.S. COOK, R. VYAS, SANGKIL KIM, TRANG THAI, TAORAN LE, A. TRAILLE, H. AUBERT, AND M.M. TENTZERIS. **RFID-Based Sensors for Zero-Power Autonomous Wireless Sensor Networks**. *Sensors Journal, IEEE*, **14**(8):2419–2431, Aug 2014.

[142] A. RAMOS, A. LAZARO, AND D. GIRBAU. **Semi-Passive Time-Domain UWB RFID System**. *Microwave Theory and Techniques, IEEE Transactions on*, **61**(4):1700–1708, April 2013.

[143] A. ATHALYE, V. SAVIC, M. BOLIC, AND P.M. DJURIC. **Novel Semi-Passive RFID System for Indoor Localization**. *Sensors Journal, IEEE*, **13**(2):528–537, Feb 2013. 164

[144] A. GEORGIADIS AND A. COLLADO. **Improving range of passive RFID tags utilizing energy harvesting and high efficiency class-E oscillators**. In *Antennas and Propagation (EUCAP), 2012 6th European Conference on*, pages 3455–3458, March 2012. 164, 172

[145] A. VAZ, A. UBARRETXENA, I. ZALBIDE, D. PARDO, H. SOLAR, A. GARCIA-ALONSO, AND R. BERENGUER. **Full Passive UHF Tag With a Temperature Sensor Suitable for Human Body Temperature Monitoring**. *Circuits and Systems II: Express Briefs, IEEE Transactions on*, **57**(2):95–99, Feb 2010. 164

[146] Z. POPOVIC, E. FALKENSTEIN, AND R. ZANE. **Low-power density wireless powering for battery-less sensors**. In *Radio and Wireless Symposium (RWS), 2013 IEEE*, pages 31–33, Jan 2013. 164

[147] S.D. NAWALE AND N.P. SARAWADE. **RFID vapor sensor: Beyond identification**. In *Sensing Technology (ICST), 2012 Sixth International Conference on*, pages 248–253, Dec 2012. 164

[148] EM-MICROELECTRONIC-MARIN-SA. **EM4325 datasheet.** 167

[149] AVAGO TECHNOLOGIES. **HSMS-286x Series.** 167

[150] S. LADAN, N. GHASSEMI, A. GHIOTTO, AND KE WU. **Highly Efficient Compact Rectenna for Wireless Energy Harvesting Application**. *Microwave Magazine, IEEE*, **14**(1):117–122, Jan 2013. 167

[151] DAT SON NGUYEN, XUAN CHIEN LE, TIEN THONG PHAM, VIET HOA NGUYEN, MAU CHIEN DANG, AND S. TEDJINI. **Novel design of RFID UHF passive tag for wideband applications by direct and contactless chip connection**. In *RFID-Technologies and Applications (RFID-TA), 2012 IEEE International Conference on*, pages 131–136, Nov 2012. 169

[152] JOSHUA GORDONSON TAYLOR W. BARTON AND DAVID J. PERREAULT. **Transmission Line Resistance Compression Networks for Microwave Rectifiers**. In *Microwave Symposium Digest (MTT), 2014 IEEE MTT-S International*, pages 1–3, Jun. 2014. 189

[153] EHSAN YAVARI MEHRAN BABOLI ADITYA SINGH OLGA BORIC-LUBECKE, XIAOMENG GAO AND VICTOR M. LUBECK. **E-Healthcare: Remote Monitoring, Privacy, and Security**. In *Microwave Symposium Digest (MTT), 2014 IEEE MTT-S International*, pages 1–3, Jun. 2014. 189

[154] B. MOHAMED, B. FERGANI, S. TEDJINI, AND E. PERRET. **Simulation and measurements of physical layer parameters for passive UHF RFID tags toward collision detection and canceling**. In *RFID-Technologies and Applications (RFID-TA), 2012 IEEE International Conference on*, pages 383–388, Nov 2012. 189

Publications of the author

Peer-Reviewed journal articles

I **Analysis and exploitation of harmonics in Wireless Power Transfer(H-WPT): Passive UHF RFID Case**
G. Andia Vera, Y. Duroc, S. Tedjini, *Wireless Power Transfer, Cambridge Journals*, **Accepted**, 1-21 (2014).

II **RFID Test Platform: Nonlinear Characterization**
G. Andia Vera, Y. Duroc, S. Tedjini, *IEEE Transactions on Instrumentation and Measurement*, **IEEE EARLY ACCESS ARTICLES**, 1-10 (2014).

III **Analysis of harmonics in UHF RFID signals**
G. Andia Vera, Y. Duroc, S. Tedjini, *IEEE Transactions on Microwave Theory and Techniques*, **vol. 61, no. 6**, 1-10 (2013).

IV **Considerations on the backscattered wireless communication links**
Y. Duroc, G. Andia Vera, *Microwave and Optical Technology Letters*, **vol. 55, no. 3**, 554-559 (2013).

V **Modified RSSI Technique for the Localization of Passive UHF RFID Tags in LOS Channels**
Y. Duroc, G. Andia Vera, JP. Garcia Martin, *International journal of microwave and wireless technologies*, **vol. 5, no. 5**, 645-651 (2013).

VI **Customized RSSI method for passive UHF RFID localization system**
I. Kharrat, Y. Duroc, G. Andia Vera, M. Awad, S. Tedjini, T. Aguili, *Journal of Telecommunications*, **no. 10**, 5-9 (2011).

VII **Rectenna design and optimization using reciprocity theory and harmonic balance analysis for electromagnetic (EM) energy harvesting**
A. Georgiadis, G. Andia Vera, A. Collado, *IEEE Antennas and Wireless Propagation Letters*, **no. 9**, 444-446 (2010).

Application Patent

VIII **RFID communication system**
S. Tedjini, Y. Duroc, G. Andia Vera, C. Loussert, M. Recouly, *WO2014072812*, **Pub. No.: WO2014072812**, International Application No.: PCT/IB2013/002628 (2014).

Book chapter

IX **Towards Autonomous Wireless Sensors: RFID and Energy Harvesting Solutions**
Y. Duroc, G. Andia Vera, *Internet of Things, Challenges and Opportunities*, **Springer International Publishing**, 233-255 (2014).

Peer-Reviewed conference articles

X **Passive UHF RFID Backscattering for Indoor Lighting Control**
G. Andia Vera, S. Nawale, Y. Duroc, S. Tedjini, *IEEE Indicon, 2014*, **Pune-India**, 1-4(December 2014).

XI **Non-linear Electromagnetic Energy Harvesting in Passive UHF RFID**
G. Andia Vera, S. Nawale, Y. Duroc, S. Tedjini, *URSI Kleinheubacher, 2014*, **Miltebnberg-Germany**, 1-4(September 2014).

XII **Optimum Integration of passive UHF RFID Tag-Rectenna in a Single Feed Dual Band Antenna**
G. Andia Vera, S. Nawale, Y. Duroc, S. Tedjini, *General Assembly and Scientific Symposium, 2014 XXXIth URSI* , **Beijing**, 1-4(August 2014).

XIII **Tag-to-Reader Harmonic Link in Passive UHF RFID**
G. Andia Vera, Y. Duroc, S. Tedjini, *IEEE MTT-S International Microwave Symposium Digest (IMS), 2014*, **Tampa**, 1-4(June 2014).

XIV **Redundant Backscattering Modulation from UHF Passive RFID Tags**
G. Andia Vera, Y. Duroc, S. Tedjini, *IEEE MTT-S International Microwave Symposium Digest (IMS), 2013*, **Seattle**, 1-3 (June 2013).

XV **RFID air interface setup for power spectral density analysis**
G. Andia Vera, Y. Duroc, S. Tedjini, *IEEE International Conference on RFID-Technologies and Applications (RFID-TA), 2012*, **Nice**, 193-197 (November 2012).

XVI **Transferts d'énergie rétrodiffusés dans un réseau de tags**
G. Andia Vera, Y. Duroc, *Journées Nationales Microondes*, **Paris**, 1-3 (May 2013).

XVII **Spectre du signal de backscattering des tags RFID UHF passifs**
G. Andia Vera, Y. Duroc, S. Tedjini *Journées Nationales Microondes*, **Paris**, 1-3 (May 2013).

XVIII **Design of a 2.45 GHz rectenna for electromagnetic (EM) energy scavenging**
G. Andia Vera, G. Apostolos, A. Collado, S. Via, *Radio and Wireless Symposium (RWS), 2010 IEEE*, **New Orleans**, 61-64 (January 2010).

UNIVERSITÉ DE GRENOBLE

ANALYSE ET EXPLOITATION DES NON-LINEARITES DANS LES SYSTEMES RFID UHF PASSIFS

Résumé :
Avec le développement des réseaux de capteurs et l'explosion de l'Internet des Objets, de nouveaux dispositifs permettant de taguer les objets sont nécessaires afin de permettre non seulement leur identification mais aussi assurer des communications performantes et offrir de nouvelles fonctionnalités comme la détection, la localisation, la capture d'informations ou encore l'authentification. Cette tendance s'appuie sur la technologie bien établie qu'est la RFID (identification par radiofréquence) et donc l'utilisation d'étiquettes (dit tags) faibles coûts et télé-alimentées. Les travaux présentés dans cette thèse visent à étudier les phénomènes non-linéaires produits lors d'une communication RFID avec pour objectif d'en tirer profit. Pour la première fois à notre connaissance, l'exploitation des non-linéarités des puces RFID est non seulement envisagée mais démontrée à travers deux applications : nouveau canal de communication sur la 3ème harmonique et nouvelles approches de récupération d'énergie. Les contributions sont originales et couvrent de nombreux aspects : procédures de tests et méthodologies de caractérisation, modélisation du comportement non linéaire des tags, et conception de nouveaux types de tags. Les études présentées prouvent les différents concepts développés et ouvrent la voie à de nouveaux champs de recherche aussi bien fondamentaux qu'applicatifs.

Mots-clés : caractérisation et modélisation de circuits non-linéaires, conception d'antennes et de tags, co-simulation RF-circuit, exploitation des fréquences harmoniques, modélisation de tags RFID, récupération d'énergie, systèmes RFID UHF passifs.

ANALYSIS AND EXPLOITATION OF NON-LINEARITIES IN PASSIVE RFID UHF SYSTEMS

Abstract:
Powered by the exploding popularity of the Internet-of-Things, the demand for tagged devices with labels capable to ensure a reliable communication with added functions beyond the identification, such as sensing, location, health-care, and among others is growing rapidly. Certainly this growing is headed by the well-established Radio Frequency Identification (RFID) technology, and the use of wireless low-cost self-powered tags, in other words passive RFID tags, is the most widespread used alternative. The work presented in this thesis aims to study the non-linear phenomena produced in an RFID communication. For the first time to the knowledge of the authors, the exploitation of the RFID chip non-linearities is considered and experimentally demonstrated through two applications: The harmonic communication by meaning of a new communication channel from tag-to-reader at the 3rd harmonic and new approaches for energy harvesting. The contributions are original and cover many aspects such as: characterization methodologies and testing procedures, modeling of the non-linear behavior of tags and design of new types of tags. The studies presented demonstrate the different concepts developed and pave the way for new research fields in fundamental and applied fields.

Keywords: electromagnetic-electric co-simulation, energy harvesting, exploitation of harmonic signals, modeling and characterization of non-linear circuits, modeling of RFID tags, passive UHF RFID system, tag antenna design.